UNIVERSITÉ DU QUÉBEC À TROIS-RIVIÈRES

POLYHYDROXYBUTYRATE-BASED MATERIALS FOR ANTIBACTERIAL AND BIODEGRADABLE APPLICATIONS

THÈSE PRÉSENTÉE
COMME EXIGENCE PARTIELLE DE LA

DOCTORAT EN SCIENCES DE L'ÉNERGIE ET DES MATÉRIAUX

PAR
SAFA LADHARI

FÉVRIER 2025

UNIVERSITÉ DU QUÉBEC À TROIS-RIVIÈRES

DOCTORAT EN SCIENCES DE L'ÉNERGIE ET DES MATÉRIAUX

Direction de recherche:

Phuong Nguyen-Tri, Professor	
Prénom et nom	Directeur de recherche
Alireza Saidi, Ph.D	
Prénom et nom	Codirecteur de recherche

Jury d'évaluation

Prof. **Phuong Nguyen-Tri** (UQTR)	Directeur de thèse, membre
Prénom et nom	Fonction du membre de jury
Prof. **Alireza Saidi** (IRSST, UQTR)	Co-directeur de thèse, membre
Prénom et nom	Fonction du membre de jury
Nhu-Nang Vu, Ph.D (UQTR)	Président
Prénom et nom	Fonction du membre de jury
Prof. **Cyrille Sollogoub** (Cnam de Paris)	Membre externe
Prénom et nom	Fonction du membre de jury
Prof. **Amine Aymen Assadi** (Uni. de Rennes 1)	Membre externe
Prénom et nom	Fonction du membre de jury

Thèse soutenue le 13/02/2025

Résumé

Cette recherche présente une approche innovante pour développer des matériaux antibactériens, antibiofouling et biodégradables avancés en incorporant des nanoparticules photoactives et sensibles à la lumière dans des matrices de biopolymères. La nouveauté de cette étude réside dans la combinaison de fibres électrofilées, de polymères biodégradables et de nanoparticules activées par la lumière (dioxyde de titane dopé à l'argent Ag-TiO_2 et oxyde de zinc ZnO) pour créer des matériaux multifonctionnels qui non seulement présentent d'excellentes propriétés antibactériennes, mais se dégradent aussi efficacement dans l'environnement. Ce travail exploite de manière unique la génération d'espèces réactives de l'oxygène (ROS) sous irradiation lumineuse comme nouveau mécanisme antibactérien, offrant ainsi une alternative durable aux agents antimicrobiens traditionnels.

Le principal avantage des matériaux mis au point dans le cadre de cette recherche réside dans les nanoparticules sensibles à la lumière, qui améliorent considérablement les performances antibactériennes par rapport aux méthodes antimicrobiennes conventionnelles. L'incorporation de nanoparticules Ag-TiO_2 NPs dans des membranes en microfibres de polyhydroxybutyrate (PHB) a démontré une excellente activité antibactérienne, avec des efficacités d'inactivation bactérienne supérieures à 99 % contre *Escherichia coli* et *Staphylococcus epidermidis*, en particulier sous une lumière LED de faible puissance. Cet effet antibactérien induit par la lumière, obtenu par la génération photocatalytique de ROS, représente une nouvelle stratégie très efficace et respectueuse de l'environnement pour la stérilisation des surfaces. Par rapport aux études précédentes, qui s'appuyaient principalement sur des propriétés antibactériennes statiques, ce mécanisme activé par la lumière offre une méthode plus dynamique et plus économe en énergie pour lutter contre la contamination bactérienne, ce qui rend ces matériaux particulièrement adaptés à une utilisation à long terme dans des environnements dynamiques, tels que les dispositifs médicaux et les surfaces environnementales.

De même, la deuxième étude de cette thèse étend l'application des matériaux sensibles à la lumière à l'industrie de l'emballage en incorporant des microparticules d'oxyde de zinc (ZnO MPs) synthétisées de manière écologique dans une matrice de PHB. Ces MPs de ZnO ont également présenté une activité antibactérienne accrue sous lumière LED, montrant des effets antibactériens supérieurs à ceux des NPs de ZnO commerciales. L'inclusion de ZnO microporeux dans les films

de PHB a non seulement renforcé l'inactivation bactérienne, mais a également amélioré les propriétés antibiofouling, empêchant efficacement l'attachement microbien et la formation de biofilms. En outre, ces films ont démontré une excellente biodégradabilité, avec des taux de dégradation atteignant 99 % après seulement 10 semaines dans le sol. Cette approche constitue une solution durable pour réduire la contamination bactérienne dans les matériaux d'emballage, offrant une alternative prometteuse aux films plastiques conventionnels chargés de conservateurs chimiques nocifs. La nouvelle contribution de cette étude est l'utilisation de ZnO synthétisé vert, qui garantit que les matériaux sont à la fois respectueux de l'environnement et très efficaces pour réduire la croissance bactérienne lors de l'exposition à la lumière.

La troisième étude de cette thèse présente un nouveau matériau composite composé de nanofibres de PHB mélangées à de la gélatine (GE) et à des NP d'Ag-TiO_2 photoactives. La combinaison de gélatine et de PHB a amélioré les propriétés mécaniques des membranes électrofilées et a apporté un avantage supplémentaire en matière d'anti-biofouling, en réduisant l'adhésion microbienne. Cette étude est unique en ce sens qu'elle intègre un mélange de biopolymères et de nanoparticules photoactives pour créer une membrane qui est non seulement antibactérienne, mais qui présente également une efficacité de filtration accrue. L'activité antibactérienne de ces membranes, qui ont atteint une inactivation bactérienne de plus de 99 % sous irradiation lumineuse, a démontré l'effet synergique des nanoparticules Ag-TiO_2 et du mécanisme de génération photocatalytique de ROS. En outre, les membranes présentaient des propriétés mécaniques presque deux fois plus solides que les membranes en PHB pur, ce qui les rend adaptées aux applications nécessitant à la fois une durabilité et des performances antimicrobiennes, telles que la filtration médicale et le traitement de l'eau.

Par rapport aux études précédentes, qui se concentraient principalement sur les propriétés antimicrobiennes statiques ou sur les matériaux non sensibles à la lumière, cette recherche offre des avancées significatives en incorporant des mécanismes antimicrobiens activés par la lumière. L'utilisation de nanoparticules photocatalytiques ($AgTiO_2$ et ZnO) sous irradiation lumineuse pour générer des ROS distingue cette étude des matériaux antibactériens traditionnels, car l'effet photocatalytique améliore non seulement la capacité du matériau à désactiver les bactéries, mais offre également un mécanisme d'auto-activation qui ne nécessite pas d'apports externes constants

d'agents chimiques. Ce nouveau mécanisme antibactérien améliore considérablement l'efficacité et la durabilité des matériaux, les rendant plus polyvalents et plus rentables au fil du temps.

En outre, l'une des principales nouveautés de ces travaux est l'intégration de la biodégradabilité et de l'activité antibactérienne. Contrairement aux polymères antimicrobiens conventionnels qui persistent dans l'environnement, contribuant potentiellement à la pollution, les matériaux développés dans cette étude ont été conçus pour se dégrader naturellement, avec des taux de dégradation du sol dépassant 99 % en quelques semaines. Cette biodégradabilité est renforcée par l'activité antibactérienne des nanoparticules, qui favorise également la dégradation microbienne de la matrice polymère. Cette double action antibactérienne et biodégradable constitue un avantage significatif en matière de durabilité environnementale et de sécurité sanitaire.

En conclusion, la recherche présentée dans cette thèse fait progresser de manière significative le développement de matériaux multifonctionnels et durables qui combinent des propriétés antibactériennes, antibiofouling et biodégradables. En intégrant des nanoparticules sensibles à la lumière et en tirant parti de la génération photocatalytique de ROS, cette étude introduit un mécanisme antibactérien novateur, économe en énergie et respectueux de l'environnement. La polyvalence de ces matériaux, associée à leur biodégradabilité, en fait des solutions innovantes pour diverses applications dans les secteurs de la médecine, de l'environnement et de l'emballage, ce qui les distingue des études précédentes qui se concentraient sur des matériaux antimicrobiens statiques.

Abstract

This research presents an innovative approach to developing advanced antibacterial, anti-biofouling, and biodegradable materials by incorporating photoactive and light-sensitive nanoparticles NPs into biopolymer matrices. The novelty of this study lies in the combination of electrospun fibers, biodegradable polymers, and light-activated nanoparticles (silver-doped titanium dioxide Ag-TiO_2 and zinc oxide ZnO) to create multifunctional materials that not only exhibit excellent antibacterial properties but also degrade efficiently in the environment. This work uniquely exploits the generation of reactive oxygen species (ROS) under light irradiation as a novel antibacterial mechanism, thus providing a sustainable alternative to traditional antimicrobial agents. The main advantage of the materials developed in this research lies in the light-sensitive nanoparticles, which significantly improve the antibacterial performance compared to conventional antimicrobial methods. The incorporation of Ag-TiO_2 NPs into polyhydroxybutyrate (PHB) microfiber membranes demonstrated excellent antibacterial activity, with bacterial inactivation efficiencies greater than 99% against *Escherichia coli* and *Staphylococcus epidermidis*, especially under low-power LED light. This light-induced antibacterial effect, achieved by photocatalytic ROS generation, represents a novel, highly efficient, and environmentally friendly strategy for surface sterilization. Compared with previous studies, which mainly relied on static antibacterial properties, this light-activated mechanism offers a more dynamic and energy-efficient method to combat bacterial contamination, making these materials particularly suitable for long-term use in dynamic environments, such as medical devices and environmental surfaces.

Similarly, the second study of this thesis extends the application of light-responsive materials to the packaging industry by incorporating eco-friendly synthesized zinc oxide microparticles (ZnO MPs) into a PHB matrix. These ZnO MPs also exhibited enhanced antibacterial activity under LED light, showing superior antibacterial effects to commercial ZnO NPs. Including microporous ZnO in the PHB films enhanced bacterial inactivation and improved the anti-biofouling properties, effectively preventing microbial attachment and biofilm formation. Furthermore, these films demonstrated excellent biodegradability, with degradation rates reaching 99% after only 10 weeks in soil. This approach provides a sustainable solution to reduce bacterial contamination in packaging materials, offering a promising alternative to conventional plastic films loaded with harmful chemical preservatives. The novel contribution of this study is the use of green synthesized ZnO, which ensures that the materials are both environmentally friendly and highly

effective in reducing bacterial growth upon exposure to light.

The third study of this thesis presents a novel composite material composed of PHB nanofibers blended with gelatin (GE) and photoactive Ag-TiO_2 NPs. The combination of gelatin and PHB improved the mechanical properties of the electrospun membranes and provided an additional anti-biofouling benefit by reducing microbial adhesion. This study uniquely integrates a blend of biopolymers and photoactive nanoparticles to create an antibacterial membrane with increased filtration efficiency. The antibacterial activity of these membranes, which achieved more than 99% bacterial inactivation under light irradiation, demonstrated the synergistic effect of Ag-TiO_2 nanoparticles and the photocatalytic ROS generation mechanism. In addition, the membranes exhibited nearly twice as strong mechanical properties as pure PHB membranes, making them suitable for applications requiring both durability and antimicrobial performance, such as medical filtration and water treatment.

Compared with previous studies, which mainly focused on static antimicrobial properties or non-light-sensitive materials, this research offers significant advances by incorporating light-activated antimicrobial mechanisms. The use of photocatalytic nanoparticles ($AgTiO_2$ and ZnO) under light irradiation to generate ROS distinguishes this study from traditional antibacterial materials, as the photocatalytic effect not only enhances the material's ability to deactivate bacteria but also offers a self-activation mechanism that does not require constant external inputs of chemical agents. This novel antibacterial mechanism significantly improves the efficiency and durability of the materials, making them more versatile and cost-effective over time.

In addition, one of the main novelties of this work is the integration of biodegradability and antibacterial activity. Unlike conventional antimicrobial polymers that persist in the environment, potentially contributing to pollution, the materials developed in this study were designed to degrade naturally, with soil degradation rates exceeding 99% within a few weeks. This biodegradability is enhanced by the antibacterial activity of the nanoparticles, which also promotes microbial degradation of the polymer matrix. This dual antibacterial and biodegradable action constitutes a significant advantage in environmental sustainability and health safety.

In conclusion, the research presented in this thesis significantly advances the development of multifunctional and sustainable materials that combine antibacterial, anti-biofouling, and biodegradable properties. This study introduces a novel, energy-efficient, and environmentally friendly antibacterial mechanism by integrating light-sensitive nanoparticles and using

photocatalytic ROS generation. The versatility of these materials, combined with their biodegradability, makes them innovative solutions for various medical, environmental, and packaging applications, distinguishing them from previous studies that focused on static antimicrobial materials.

Table of content

List of Figures

List of Tables

List of Equations

List of abbreviations

Ag@T	$AgTiO_2$
API	Active Pharmaceutical Component
b-LED	blue LED
CLSM	Confocal Laser Scanning Microscopy
DDSs	Drug Delivery Systems
DLC	Drug Loading Content
DLE	Drug Loading Efficiency
DPE	Disposable protective equipment
DSP	Downstream processing
DTG	Derivative thermogravimetry
E. Coli	*Escherichia coli*
EPS	Extracellular polymeric substance
FDA	Food and Drug Administration
Ge	Gelatin
lcl-	Long Chain Length
mcl-	Medium Chain Length
MPs	Microporous particles
NPs	Nanoparticles
PCL	Poly(ε-caprolactone)
PE	Protective equipment
PGA	Poly (glycolic acid)
PHA	Polyhydroxyalkanoates
PHB	Polyhydroxybutyrate
PHBHHx	Poly(3-hydroxybutyrate-co-3-hydroxyhexanoate)
PHBV	Poly (3-hydroxybutyrate-co-3-hydroxyvalerate)
PHO	Poly[(R)-3-hydroxyoctanoate
PLA	Poly (lactic acid)
PLGA	Poly(lactide-co-glycolide)
p-NDA	p-nitrosodimethylaniline
P4HB	Poly (4-hydroxybutyric acid)

ROS	Reactive oxygen species
S. aureus	*Staphylococcus aureus*
scl-	Short Chain Length
SEM	Scanning electron microscope
S. Epidermidis	*Staphylococcus Epidermidis*
TGA	Thermogravimetric analysis
WCA	Water contact angle
WVP	Water vapor permeability
ZnO	Zinc oxide

Acknowledgments

First and foremost, I would like to express my deepest gratitude to God and my family, whose unwavering love, guidance, and support have been the foundation of all my academic and personal successes. Despite the thousands of kilometers that separate us, they have remained by my side every single day, nurturing my growth with endless care and joy.

I extend my heartfelt thanks to my research supervisor, Professor Phuong Nguyen-Tri, for allowing me to work on this project and guiding me whenever needed. His trust in me—whether in presenting my research at many conferences, participating in major competitions, or supervising trainees- has allowed me to achieve more success and gain more experience than I ever imagined.

I am equally grateful to my co-supervisor Doctor Alireza Saidi, and Doctor Nhu-Nang Vu, for their invaluable advice, encouragement, meticulous corrections, and, most importantly, the knowledge they shared, all of which were essential to the success of my research project.

I would also like to thank Professor Simon Bernabé and Professor Bruno Chabot, with whom I had the privilege of collaborating during my doctoral studies. Working in their laboratories allowed me to acquire knowledge beyond my immediate research field, immerse myself in diverse environments, and expand my professional network.

I am profoundly thankful to my husband, Ghassen Khelifi, whose unwavering love, encouragement, and sacrifices have been my greatest source of strength throughout this journey. His sacrifice to live apart for three years so that I could pursue my PhD speaks volumes about his selflessness and dedication to our shared dreams. Despite the distance, he has been my rock, offering moral support during challenging times and providing financial assistance to ensure I could focus entirely on my research. Above all, his love and partnership have blessed me with the greatest gift—our soon-to-arrive baby—whose presence has already filled my heart with immeasurable joy and renewed purpose. Ghassen, you have made this journey not just possible but extraordinary, and I am endlessly grateful to share this life with you.

I wish to thank my dear friends and colleagues at the Nguyen-Tri lab. Their friendship, shared knowledge, and experiences have been invaluable to me. We have created beautiful memories and shared unforgettable adventures I will always treasure.

I also thank all my colleagues and the staff at the I2E3 institute, who offered assistance whenever I needed it. Special thanks go to kéziah Milette and Isabelle Boulan for always supporting me in the laboratory.

Finally, I am deeply appreciative of the financial support provided by the Institut de recherche Robert-Sauvé en santé et en sécurité du travail (IRSST), the Mitacs Globalink program, the Research Center for High-Performance Polymer and Composite Systems (CREPEC), and the UQTR Foundation, during my PhD studies.

All of you have made this doctoral journey possible; I am forever grateful.

Foreword

The present PhD thesis consists of eight chapters. It is constructed based on a combination of scientific articles whose first author is also the author of this thesis. All the articles have been published at the time of the thesis submission.

The introduction and chapter 2 are partially included in the review article "Recent Development of Polyhydroxyalkanoates (PHA)-Based Materials for Antibacterial Applications: A Review" published by Safa Ladhari, Nhu-Nang Vu, Cédrik Boisvert, Alireza Saidi, and Phuong Nguyen-Tri in ACS Applied Bio Materials, 2023, 3, doi:10.1021/acsabm.3c00078.

Chapter 4 reports the study "Biodegradable polyhydroxybutyrate microfiber membranes decorated with Ag-TiO_2 nanoparticles for enhanced antibacterial and anti-biofouling activities" published by Safa Ladhari, Nhu-Nang Vu, Cédrik Boisvert, Marcos Antonio Polinarski, Camille Venne, Alireza Saidi, Simon Barnabe, and Phuong Nguyen-Tri in Journal of Applied Polymer Science, 2024, 5, doi:10.1002/app.55660.

Chapter 5 reports the study "A green synthesis route of ZnO/polyhydroxybutyrate composites with antibacterial and biodegradable properties" published by Safa Ladhari, Nhu-Nang Vu, Juliette Vallée Bastien, Bich Van Tran, Thi Ha Nguyen, Alireza Saidi, Simon Barnabe, Cyrille Sollogoub, and Phuong Nguyen-Tri in Polymer Engineering and Science, 2024, 12, https://doi.org/10.1002/pen.27055.

Chapter 6 reports the study "Mechanical and antimicrobial properties of green and photoactive $AgTiO_2$/ polyhydroxybutyrate (PHB) electrospun membranes" published by Safa Ladhari, Nhu-Nang Vu; Alireza Saidi, Amine Aymen Assadi, and Phuong Nguyen-Tri and in Polymer Engineering and Science, 2024, 11, https://doi.org/10.1002/pen.27036.

Introduction

This part introduces the necessity of developing new materials for antibacterial and biodegradable applications, a pressing issue today that cannot be overstated. Finding innovative solutions is crucial in the face of increased resistant bacteria and mounting plastic pollution. While materials with antibacterial actions prevent microbes from spreading and secure health and well-being, biodegradable materials offer a sustainable alternative to traditional plastics, reducing environmental impact. It also presents one efficient biodegradable polymeric candidate with an antibacterial nanoparticle agent for antimicrobial applications. Finally, this part highlights the major objectives of the present thesis.

1.1.General Introduction

The global pandemic of COVID-19 caused by SARS-CoV-2 raises awareness to avoid better the microorganism spread. Worldwide demand for antimicrobial materials is rapidly increasing due to the spreading of diseases related to bacteria and viruses. Indeed, contaminated surfaces expand the spread and transmission of epidemics [1]. The extent of these microorganisms occurs through water or air directly and via surface to surface indirectly [2]. Enormous amounts of those microbes can harm human life and are a leading cause of death. Antibacterial coatings are of great research interest as they can either inactivate or destroy these microbes, thereby providing an effective and durable solution [3]. The worldwide antimicrobial coatings market achieved $2.8 billion in 2019 and is supposed to reach $5.4 billion by 2024 [4]. This significant increase in the antimicrobial coatings market is due to the COVID-19 crisis.

Ensuring antibacterial effects with a combination of chemical entities is ground-breaking intent to reduce the transmission of agent-causing diseases. Microbes attached to fabricated surfaces tend to remain alive and proliferate in a humid environment. Meantime, a biofilm is built up by microbial cells, but their number increases on the surface. The biofilm is composed of a polysaccharide pattern with enclosed cells. This biofilm provides nutriments to the microbial cells and enables them to survive under extreme conditions [5]. In addition, microbial biofilms can degenerate practically all inorganic materials [6]. Consequently, the fundamental matters in medicine and material science are the control of microbial growth on artificial surfaces. Sterilization of the surrounding environment is one way to inhibit surface contamination. Hydrogen peroxide, hypochlorite, or other reactive oxygen species (ROS) are the most popular disinfectants. Otherwise, alcohols, quaternary ammonium compounds, silver, or triclosan are also frequently utilized [7]. However, the aseptic state is not permanent, and the regular use of disinfectants can cause severe environmental problems, especially in the case of triclosan [8]. The other way is preventing microbial biofilm growth using antimicrobial surfaces. Corresponding surfaces prevent the adhesion of microbes to the surface by repelling or locally destroying them [9] **(Figure 1.1)**. Such surfaces usually are loaded with antimicrobial biocides, such as antibiotics, antimicrobial ammonium compounds, active chlorine, silver, or triclosan [10]. Even though these surfaces are efficient, their eventually released biocides generate similar stated problems. As an alternative, surfaces that produce biocides via catalyzes, such as electricity, externally applied chemicals, or optical energy, are attractive substitutes [11].

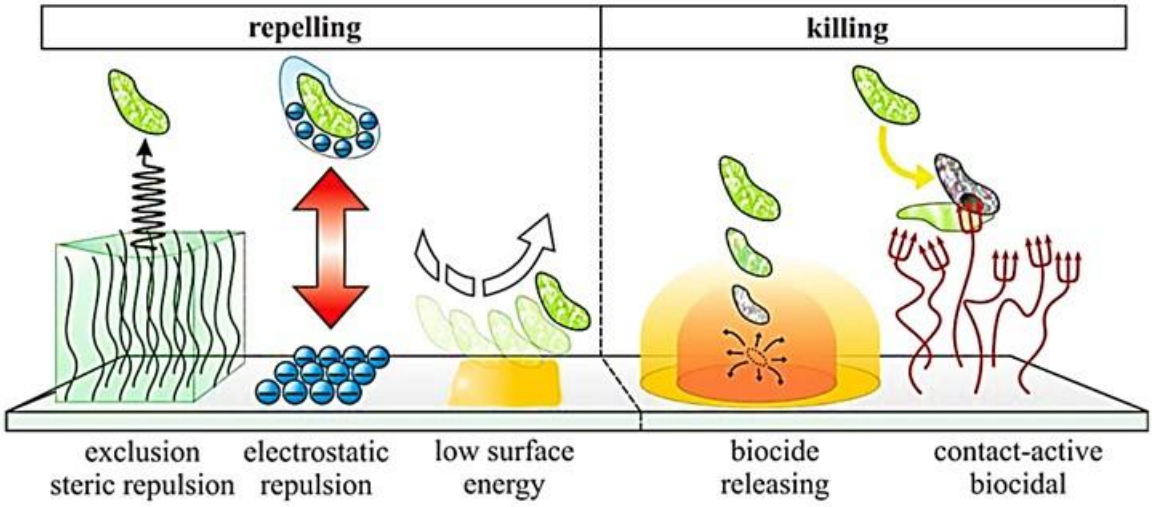

Figure 1.1: General approaches of antimicrobial surfaces [7]

Antimicrobial polymers have been recognized since 1965 [7] when Cornell and Dunraruma stated polymers and copolymers designed from 2-methacryloxytroponones that destroyed bacteria [12]. These polymers have enticed substantial consideration in academic and industrial research [13]. The three main areas of used antimicrobial agents are medical, food, and textiles. Polymeric materials, particularly bio-sourced polymers, are of considerable interest in antimicrobial materials preparation, namely coatings, films, etc. Many propitious antimicrobial polymers have been reported, and the number of Food and Drug Administration FDA-approved antimicrobial polymers has increased drastically in recent decades [7]. Antimicrobial biopolymers have proved to be a promising candidate for exploration and advancement in the field of antibacterial treatment. Poly([R]-3-hydroxyalkanoates) (PHAs), one of the biobased, eco-friendly, and biodegradable polymeric materials synthesized by a variety of bacteria, belongs to the large category of bio-polyesters and are the main candidates used in the biomedical field. They form a large group of biodegradable and biocompatible with the lowest tissue toxicity [14]. PHAs have been applied in slow-release drug delivery, anti-inflammatory, antifungal, antimicrobial, antibiofilm, and virucidal fields depending on the enclosed/conjugated medicinal agent.

Commercial interest is rising due to industrial interest in ‘green’ materials and environmental concerns. As a result, several companies have developed PHA-processable bioplastics for packaging materials. However, PHAs as a biodegradable polymer can substitute petro-plastic polymers in a binding domain needing an ecological solution: « personal protective equipment (PPE) ». PPE, such as face masks, is indispensable in facing the SARS-CoV-2 crisis

and spreading diseases related to bacteria and viruses. Still, the dominant polypropylene-based PPE is deprived of antibacterial/antiviral properties and environmental friendliness and harms the soil and marine ecosystems. Hence, developing biodegradable, antibacterial, and antiviral PHAs PPE for better protection against coronavirus and addressing ecological concerns raised by the piling of COVID-19-related wastes may present an innovative route for research. Hence, our first article inspires the development of reusable and sustainable PEs with significant bioprotective and biodegradable characteristics.

PHAs are becoming increasingly popular due to their attractive properties like biocompatibility, biodegradability, hydrophobicity, etc. On the other hand, these biopolymers also have some disadvantages that limit their competition with synthetic polymers. Therefore, PHAs are being modified to improve their properties for potential applications in diverse sectors to overcome these limitations. Blending different types of PHAs or PHAs with synthetic or other biopolymers has produced innovative biomaterials to broaden their application domain. Nevertheless, copolymerization decreases crystallinity, increases flexibility, and makes more readily processable materials than pure PHAs. They have already been reinforced by blending with other biodegradable polymers, natural particles, and fibers, including nanosized fillers like chitin, chitosan, and cellulose nanowhiskers. Some works studied the reinforcement/filler selection with PHA for antibacterial applications. This method addresses their influence on the material structure and performance, such as mechanical and thermal properties, crystallinity, biodegradation kinetics, etc. However, compatibility is frequently highlighted when blending natural fibers with PHA as a problem that causes mechanical deterioration. Using compatibilizing agents can enhance poor filler-matrix compatibility. Therefore, there is a need for further mechanical performance improvement to enable better load transmission with ideal processing parameters and fillers and antibacterial agent dispersion. Thus, examining the blending effect of Polyhydroxybutyrate (PHB) with gelatin with a comprehensive study of their structure, morphology, thermal, mechanical, and biological properties is the research topic of our third article.

However, the biodegradability rate of PHA-based materials may be negatively impacted by including specific additives (chain extenders) and other biodegradable/non-biodegradable polymers used to improve their qualities. In aerobic and anaerobic settings, the unfavorable effects of antifouling chemicals and non-degradable or hydrophobic plasticizers may inhibit PHA biodegradation. Mixing PHAs with PLA, PBAT, etc. prevents PHAs from degrading in most

environments, except compost, where PLA performs better than PHAs. The addition of natural fibers and fillers can speed up the biodegradation of PHAs depending on the makeup of the fibers, whereas inorganic fillers either impede or completely prevent biodegradation. Improved hydrophilicity and facilitated biodegradation are advantages of natural fibers rich in cellulose and hemicellulose, respectively. On the other hand, the biodegradation of PHAs can be inhibited by fillers with high levels of lignin and low levels of hemicellulose in the cellulose, respectively, because of their complexity and low hydrophilicity. PHA biodegradation has significantly improved thanks to the high hydrophilicity and facilitated biodegradation of starch-based fillers. Additionally, the biodegradation of PHAs can be enhanced beyond starch and natural fillers by combining fillers with proteinaceous materials like Dried Distiller's Grains and soy. Nevertheless, the research on PHA biocomposite biodegradation is severely constrained in maritime environments, where there is a substantial amount of improperly managed plastic trash. Hence, our second article systematically elucidated the role of the antibacterial agent added to PHB materials in biodegradation control.

In addition, research is also required to improve the antibacterial effect through chemical, physical, and biological treatment methods. For example, as discussed in this thesis, applying a plasma treatment to PHA surfaces in different ways, such as etching, cleaning, activation, and cross-linking, can improve wetting qualities, increase the adherence of plasma-deposited coatings, or decrease friction. However, plasma conditions and gas type must be cautiously adjusted to minimize degradation and aging effects because of the different ways in which plasma interacts with the polymer surface. In addition, plasma treatment decreases PHA hydrophobicity and thus enhances the surface coating with antibacterial agents.

Although one of the main drawbacks, delaying the evolution and productivity, is strongly related to the behavior of the NPs detachment from the polymer surface in the presence of fluids, which usually induces their aggregation. On the other hand, PHB's high crystallinity provokes complex migration of antimicrobial nanoparticles from the bulk to the surface of the polymer. Therefore, further additives like plasticizers, lubricants, and surfactants are used for better nanoparticle migration. Suppose PHA-based materials are to be used in the antibacterial domain; in that case, further research will be required into the migratory characteristics of PHA-based films and their probable performance in service.

The greatest challenge to the antimicrobial application of PHA- based materials arises from

the considerable variation of antibacterial agents and their incorporation method, which influence biological efficiency. In addition, as stated in this work, metal-oxide biocides' presence in the electrospinning solution, for example, modifies the spinning solution's conductivity and viscosity, making the production of antimicrobial nanofibers difficult.

This thesis suggests a novel, more efficient antibacterial mechanism produced by reactive oxygen (ROS) generation. Unfortunately, this mechanism has received relatively little attention with PHA-based materials. Thus, this mechanism of antibacterial action is further studied with PHB polymer in this study.

1.2.Objectives of the thesis

Generally, the present thesis aims to prevent bacterial agent contamination and maintain the health and well-being of Canadian and international community members exposed to recent biological substances by sustaining ecological balance and preserving a safer and greener environment.

The first objective is the development of suitable methods for blending antibacterial agents with biodegradable polymer polyhydroxybutyrate (PHB). Three methods are considered: 1) a direct deposition method by coating antibacterial agents onto the electrospun fibrous material after surface modification treatment, 2) dispersing the antibacterial agent in the PHB matrix using a simple casting method to prepare bioactive films and 3) electrospinning blended biodegradable polymer solution loaded with antibacterial agent.

The second objective - the most important objective is to measure the antibacterial activity of the prepared materials. Visible light is used in this thesis to enhance the antibacterial effectiveness, breaking the traditional way of destroying bacteria by contact and providing an innovation in active antibacterial material.

The final objective is the investigation of the biodegradability, stability, and durability of prepared materials.

1.3.Outline of the thesis

Introduction:

This section provides an overview of the thesis, including a general introduction, objectives, and outline.

Chapter 2:

This chapter provides a background of the present thesis by reporting different aspects of polyhydroxyalkanoates PHAs, from their synthesis to potential antibacterial applications. Antibacterial PHAs have been used in different forms, generally as scaffolds for soft and hard tissues and particles for drug delivery or catalyst immobilization. As detailed in this work, nanofibers represent the newest PHAs form used for biological activities. PHAs can be subjected to surface modification and integration with various antibacterial agents to be effectively applied in antibacterial applications. Moreover, the potential fabrication methods of antibacterial PHA materials are thoroughly discussed in this chapter.

Chapter 3:

This chapter details the experimental analysis and methodological approach adopted, as well as the various products used in this work.

Chapter 4:

Chapter 4 reports an ecological preparation of innovative PHB microfiber membranes decorated with hybrid Ag-TiO_2 NPs (Ag@T NPs) using the electrospinning technique coupled with a simple dip-coating process. The introduction of Ag@T NPs enhanced the antibacterial activities of prepared membranes against two bacterial strains, including *Escherichia coli* and *Staphylococcus aureus*, with exposure to low-power commercial LED light. These prepared membranes also displayed strong antibiofouling properties and excellent biodegradability.

Chapter 5:

Chapter 5 reports developing environmentally friendly polymer-based materials with

antibacterial and biodegradable properties, which are crucial for advancing sustainable packaging solutions. Green-synthesized zinc oxide microporous particles (ZnO MPs) were incorporated into the PHB matrix using a straightforward casting method to produce bioactive films. These films exhibit improved antibacterial and anti-biofouling properties due to the homogeneous distribution of micro-sized pores and the effective dispersion of ZnO MPs within the biopolymer. PHB-ZnO (PZ) films promote microbe adhesion, accelerating biofilm biodegradation with fast soil biodegradation rates.

Chapter 6:

Chapter 6 reports the fabrication of hybrid material by blending PHB with gelatin (GE) and incorporating photoactive $AgTiO_2$ nanoparticles. Electrospun membranes exhibit outstanding antibacterial properties, enhanced mechanical strength, and anti-biofouling characteristics. PHB-Ge-$AgTiO_2$ membranes promote microbe adhesion, accelerating biodegradation.

Conclusion and outlook:

This section summarizes all the work completed for the current thesis, including literature reviews and research findings from chapters 4–6.

Chapter 2: Literature Review

In recent decades, bactericidal materials have been considered promising candidates to combat bacterial pathogens. Recently, polyhydroxyalkanoates (PHAs) have been used as green and biodegradable materials in various promising alternative applications, especially in healthcare for antiviral or antiviral purposes. Therefore, the ultimate goal of this chapter is to provide the recent application of this emerging PHA biopolymer material in terms of cutting-edge production technologies and promising antibacterial applications. In addition, special attention was given to collecting scientific information on antibacterial agents that can potentially be incorporated into PHA materials for biological and durable antimicrobial protection.

2.1. Polyhydroxyalkanoate polymers

In recent years, great attention has been paid to biobased and biodegradable polymers due to the accretive demand for sustainable materials [15]. However, fuel-based polymers are the leading cause of resource limitations and ecological issues such as plastic pollution. In specific biomedical uses, the employment of biopolymers is inevitable because of their biocompatibility, non-toxicity, and biodegradation [16]. Among various biopolymers, polylactic acid (PLA) is extensively used as a promising sustainable material. This polymer is produced from potato, corn, and wheat, but the more used source is beet and sugar cane [17]. In this case, the soil is used to "cultivate bio plastique" instead of food. In other words, the development of PLA and all the other biopolymers require extensive exploitation of feedstock, thus posing severe ethical doubts [18]. Overview of some recent analyses, the production and commercialization of PLA are expected to decelerate in the foreseeable future [19]. Recently, Polyhydroxyalkanoates (PHAs) have been recognized as the new generation of bioplastics as their production is based on the microorganism fermentation. They are considered biocompatible and biodegradable [20].

Polyhydroxyalkanoates (PHAs) belong to the polyester family that contains a unique bond of esters, accumulated as energy and carbon reserve with a deficient nitrogen source, and provide necessary energy [21]. PHAs are composed of 3-hydroxy acid monomers [22], as shown in **Table 2.1**. The n value commonly varies between 100 to 30000 [23]. Therefore, it depends on the type of micro-organism in which PHA polymer is produced and the pendant group.

Based on the number of carbon atoms in a monomer, polyhydroxyalkanoates are divided into three groups: Short chain length (scl-PHAs), which contains 3 to 5 carbon atoms; medium chain length (mcl-PHAs), which includes 6 to 14 carbon atoms and long chain length (lcl-PHAs) which have 15 or more than 15 carbon atoms [24]. The molecular weight of PHAs makes them very similar in characteristics to thermoplastic groups. Indeed, their stability, durability, and flexibility are pretty similar [25]. scl-PHAs are mainly close to conventional plastics due to their physical and mechanical properties [26], such as crystallinity and rigidity. mcl-PHAs are amorphous thermoplastics with different degrees of crystallinity and have adhesive and elastomeric properties [27]. The most popular PHAs polymers are listed in **Table 2.1.**

1

Table 2.1: Chemical formula of Poly(3-hydroxyalkanoates) and the correspondant R-groups

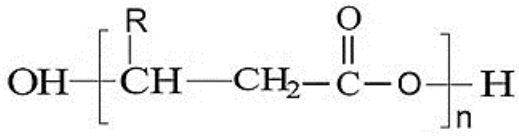

R-Groupe	PHA	Abbreviation
CH_3	Poly(3-hydroxybutyrate)	PHB
C_2H_5	Poly(3-hydroxyvalerate)	PHV
C_3H_7	Poly(3-hydroxyhexanoate)	PHHx
C_5H_{11}	Poly(3-hydroxyoctanoate)	PHO

Using different substrates, various PHAs are synthesized, varying by the length of the side chains. A detailed overview of microbially produced PHAs including biopolymers, microbial strains, and substrate (source), is provided in **Table 2.2**. By changing bacterial strains and carbon sources, the PHA's production may be conceivable to broaden the application domains and reduce production costs.

Table 2.2: Overview of common microbial strains used to produce PHAs

Microbial Strain	Biopolymer	Substrate	Ref.
Aeromonas hydrophila	mcl-PHAs	oleic acid, lauric acid,	[28]
Alcaligenes latus	PHB	soy waste, vinegar waste, milk waste, malt waste, sesame oil	[29]
Bacillus cereus	PHB	ε-caprolactone, glucose, sugar beet molasses	[30]
Bacillus firmus NII 0830	PHB	crude glycerol	[31]
Bacillus megaterium	PHB	date syrup, beet molas	[32]
Bacillus spp.	PHB, PHBV	ε-caprolactone, glucose, alkanoates, soy molasses nutrient broth,	[33]
Burkholderia cepacia	PHB, PHBV	palm kernel oil, palm stearin, palm olein, crude palm oil,	[34]

		sugarbeet molasses, xylose, oleic acid, levulinic acid	
Burkholderia sacchari sp. nov.	PHB, PHBV	arabinose, adonitol, cellobiose, arabitol, fucose, fructose, maltose, lactose, raffinose, melibiose, rhamnose, sucrose, sorbitol, xylitol, trehalose	[35]
Caulobacter crescentus	PHB	glucose, caulobacter medium	[36]
Burkholderia sp. USM (JCM 15050)	PHB	glycerol, Palm oil derivatives, fatty acids,	[37]
Comamonas acidovorans	[P(3HB-co-4HB)]	Glucose and 1,4-butanediol	[38]
Comamonas testosteroni	mcl PHA	sesame oil, coconut oil, castor oil, cottonseed oil, mustard oil, olive oil, groundnut oil,	[39]
Cupriavidus necator	PHB	bagasse hydrolysates	[40]
Cupriavidus necator H16	PHBV	sunflower oil, olive oil, kernel oil, cooking oil, crude palm oil, palm olein, palm kernel oil, coconut oil + sodium propionate	[41]
Cupriavidus necator DSM 545	PHB	waste glycerol	[42]
Escherichia coli mutants	PHB	glycerol, glucose, palm oil, sucrose, ethanol, molasses	[43]
Halomonas boliviensis	PHB	maltose, starch hydolysate, maltohexaose, maltotetraose	[44]
Halomonas hydrothermalis	PHB	seaweed-derived crude levulinic acid (SDCLA)	[45]
Hydrocarbonaclastic bacteria: Ochrobactrum, Achromobacter, and Alcaligenes	PHA	engine oil (SEO)	[46]
Legionella pneumophila	PHB	Nutrient broth	[47]
Massilia albidiflava, M. aerilata, M. aurea, M. brevitalea, M. dura, M. lutea, and M. plicata	PHA	glucose, starch	[48]
Methylocystis sp.	PHB	Methane	[49]
Microlunatus phosphovorus	PHB	Glucose, acetate	[50]
Pseudomonas aeruginosa IFO3924, P. aeruginosa NCIB	mcl PHA	palm oil, waste frying oil, coprah oil	[51]

40045, P. guezennei biovar. Tikehau, and P. stutzeri			
Ralstonia eutropha	PHA	Paddy straw	[52]
Recombinant Cupriavidus necator	P(3HB-co-3HHx)	crude palm oil, palm kernel oil, palm acid oil, palm olein	[53]
Recombinant Escherichia coli	P(3HB-co-3HHx-co-3HO)	Soybean oil	[54]
Recombinant E. coli harboring phaC1 of Pseudomonas sp. LDC-5	PHA	Molasses and sucrose	[55]
Recombinant R. eutropha	P(3HB-co-3HA)	Fructose, soybean oil	[56]
Rhizobium meliloti, R. viciae,	PHB	sucrose, glucose, galactose, trehalose, mannitol, raffinose, xylose, lactose, maltose, dextrose, sugar beet molasses, pyruvate, whey	[57]
Rhodopseudomonas palustris	PHB, PHBV	malate, acetate, fumarate, propionate, succinate, gluconate, malonate, butyrate, citrate, glycerol	[58]
SM-P-1S, SM-P-2S, SM-P-3S, SM-P-4S and SM-P1M, SM-P-2M, SM-P-3M, SM-P4M and SM-P-5M	PHA/PHB	Jatropha biodiesel by-product	[59]
Spirulina platensis (cyanobacterium)	PHB	Carbon dioxide	[60]
Staphylococcus epidermidis	PHB	soy waste, malt, vinegar waste, milk waste, sesame oil	[61]
Wautersia eutropha Mutant	Poly(3-hydroxybutyrate-co-3-hydroxyhexanoate) [P(3HB-co-3HHx)]	palm olein, palm kernel oil, palm acid oil, and crude palm oil	[62]

The chemical and physical properties depend on the monomer component of PHA-forming microbes and their nourishment [63]. Because of their various structural and mechanical properties, PHAs are being employed in many technological fields [64]. Their significant advantages are that they are eco-friendly and do not pollute the environment like conventional plastics. These polymers are mainly entirely biodegradable in soil or marine nature compared with PLA, which is very persistent [65]. Compared with other natural-originated elements (e.g., chitosan and collagen), PHAs

exhibit superior mechanical properties and better thermal stability, ensuring a wide array of manufacturing processes [66]. Nevertheless, the major limitation of utilizing PHA polymers is their high production cost [67].

2.2. Applications of PHA-based materials

PHAs have been widely applied in agriculture, aquaculture, and human health [68]. Their most outstanding economic value results from their biodegradable, biocompatible, and non-toxic nature. In addition, their biodegradable nature eliminates the need to dispose of them after use. PHAs have been advanced in healthcare as drug delivery systems, biocontrol agents, heart valves, surgical sutures, artificial organ reconstruction, artificial skin, and memory enhancers [69]. Their use in the agricultural domain extends from plant protection against challenging operating environments, such as clips, shade nets, and geotextiles [70]. They are additionally employed for making low-cost bags for growing and transporting mulching and seedlings. As conventional plastic nets have a short lifespan and their use generates large amounts of waste [71], replacing them with biopolymers offers an ecological and sustainable solution.

2.2.1. PHAs in medical applications

Biocompatibility is the primary requirement for using synthetic and natural polymers in the biomedical field. In addition, biomaterials should be nontoxic and not release any allergenic degraded components. Besides, they should have a controlled degree of degradation with adequate surface properties. In vitro studies have been extensively investigated to confirm the biocompatibility and the absence of cytotoxicity of PHA materials [72]. Elemental types of fibroblasts [73, 74], osteoblasts [73, 75], chondrocytes [76], keratinocytes [77, 78], hepatocytes [79], or mesenchymal stem cells [77, 80] have been tested. The biocompatibility characteristic of PHA polymers is due to (3-hydroxybutyric acid), which is produced by cell metabolism and exists in the human blood with 0.3–1.3 mM of concentrations [63, 81]. Moreover, the constant local pH value during degradation allows PHAs to be highly compatible with cells and the immune system in comparison with other polymers, such as poly(ε-caprolactone) (PCL), poly(lactic acid) (PLA), poly(lactide-co-glycolide) (PLGA) and poly(glycolic acid) (PGA) [82, 83]. In recent decades, polyhydroxyalkanoates have become very attractive for biomedical applications such as tissue engineering, drug delivery, and conventional medical devices [84] (**Figure 2.1**).

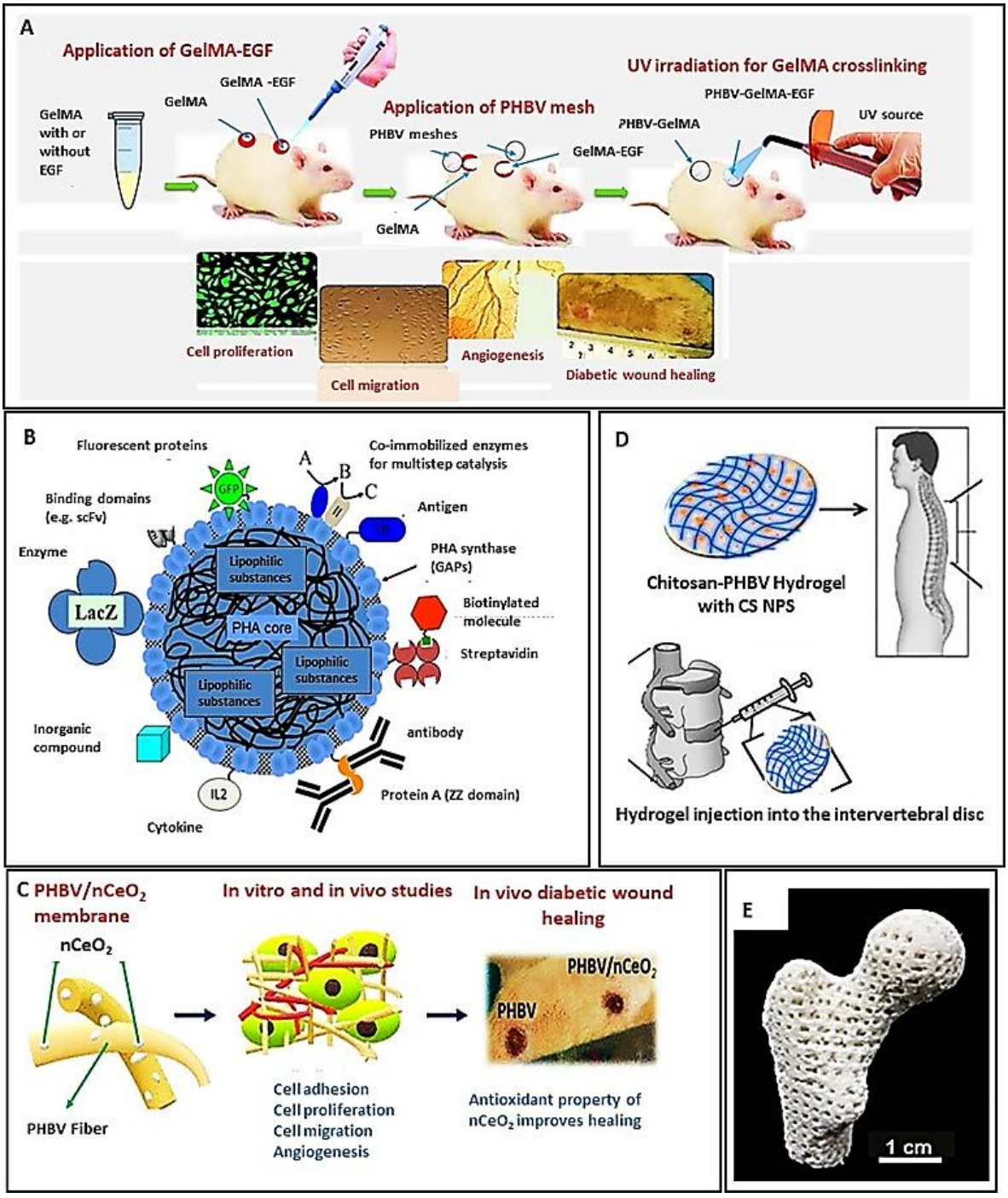

Figure 2.1: Polyhydroxyalkanoates use in biomedical applications. A) GelMA/PHBV hybrid meshes loaded with growth factors for diabetic wound healing [85]. B) PHA–protein assemblies exhibiting biologically active protein-based functions relevant for applications as vaccines or diagnostics [86]. C) PHBV- $nCeO_2$ membranes for cell proliferation and cell adhesion for wound dressings [87]. D) Chondroitin sulfate (CS) nanoparticles-incorporated chitosan–PHBV hydrogels for

nucleus pulposus tissue engineering [88]. E) Sintered Ca-P/PHBV nanocomposite scaffold for bone tissue repair [89].

2.2.2. PHAs in drug delivery systems

Drug delivery systems (DDSs) are created to encapsulate an active pharmaceutical component (API) (a gene, a drug, or a functional agent) and acquire its controlled release at the aimed site. Various parameters could be determined the DDSs effectiveness in capsulizing a molecule, such as drug loading efficiency (DLE) and drug loading content (DLC) [90]. Although many advanced medicines exist today, efficient drug delivery remains challenging [91]. It is due to the first-pass effect in which the drug metabolism tends to reduce the active drug's bioavailability upon reaching its site of action or the systemic circulation [92]. Consecutively, the drug concentration risks being below its therapeutic efficiency, making it ineffective.

Conversely, too high concentration can cause an overdose resulting in toxicity. Therefore, researchers increased their focus on controlled DDSs to guarantee a slow and controlled drug release at a specific dose to ensure maximized intended effects [93]. As a result, for 40 years, controlled DDSs technologies have shown rapid progress from macroscopic to the nanoscopic scale [94].

Plenty of materials, including natural polymers, synthetic polymers, and their blends, have been employed to prepare biomedical materials [95]. Among these materials, biodegradable polymers have captivated particular attention in drug research [96] since the delivery system of biodegradable polymers degrades into compounds that can be ejected from the body. Therefore, there is no following cleanup at the end of treatment [97]. PHAs can be shaped into porous matrices, films, microspheres, microcapsules, and nanoparticles. Drugs can be microencapsulated or entrapped in a PHA homopolymer or copolymer. The microsphere- or microcapsule-based delivery systems have been widely used to deliver several medicines, such as antibiotics, anesthetics, steroids, hormones, anticancer agents, anti-inflammatory agents, and vaccines [98]. In recent years, several reviews documented using PHAs as carriers in biomedicine [99, 100]. They can be shaped on particles, micelles, spheres, vesicles, liposomes, or capsules as medicinal delivery carriers [83].Xiong *et al*. attempted to fabricate a novel model of drug-loaded PHA particles and their constant intracellular release behavior [100]. Moreover, some searchers reported that PHA degradation rarely occurs without the presence of degrading proteins, contrary to other biodegradable polymers such as PLA [101]. For instance, the molecular weight of PHA did not vary at 37 °C in a pH 7.4 phosphate buffer

for over 84 days [101]. Thus, PHA particles can serve as drug vectors that can release drugs only inside the body since drug release from such drug-loaded PHA particles cannot occur without the PHA decomposition [102].

The slow release of anticancer drugs is a significant area of drug delivery. Human PhaP peptide and polypeptide or protein ligands fused to PhaP were advanced [103]. The ligand-PhaP-PHA specific drug delivery system confirmed its effectiveness in vitro and in vivo targeting cancer cells [104].

2.2.3. Tissue engineering

Tissue engineering is a versatile field of research geared toward creating biological tissues by combining cells, biomaterials, and bioactive molecules, intending to repair diseased or damaged organs and tissues [105]. Tissues can be assorted as soft tissues, skin grafts, and vascular or hard tissue substitutes, such as cartilage and bone [106]. To be considered a tissue repairer, the used biomaterial must have two essential features: suitable mechanical properties to support the organ during the new tissue regeneration and improved surface topography to ensure efficient proliferation and cell adhesion [83]. Hence, engineered scaffolds are designed to mimic the spatial distribution, topography thoroughly, and chemical environment matching the original extracellular matrix of the desired tissue to maintain cell growth and differentiation [107]. PHAs are an excellent substitute for tissue engineering due to their good mechanical properties, biocompatibility, degradability, and low tissue toxicity.

PHAs have been exploited for healing and the replacement of soft and hard tissues in biomedical tissue engineering to repair cardiovascular tissues, cartilage, bone marrow, skin, and nerve conduits [108]. For example, the high biocompatibility of Polyhydroxybutyrate (PHB) and Poly (3-hydroxybutyrate-co-3-hydroxyvalerate) (PHBHV) implants was successfully confirmed in animal-model experiments [82]. Furthermore, as mentioned by Shishatskaya *et al.* [109] and Volova *et al.* [110], the biochemical and physiological reactions of rats having implants with PHA sutures were examined in long-term studies. Over one year of monitoring, the animals with PHA threads were in good health and active during the experimental period. Moreover, implanted polymer threads did not severely affect the rats' organisms, as previously stated [110, 111].

Furthermore, Doyle *et al.* [112] revealed that materials based on PHB generated a consistent beneficial bone tissue adaptation response without evidence of an unsuitable chronic inflammatory response after implantation periods of 12 months. Indeed, bone rapidly forms close to the material

and becomes remarkably organized. Furthermore, during the implantation period of the study, the biomaterials did not show any conclusive evidence of an extensive structural breakdown in vivo [111].

Various successful studies using different animal models have demonstrated that PHAs, represented by PHB, poly-4-hydroxybutyrate (P4HB), poly(3-hydroxybutyrate-co-3-hydroxyvalerate) (PHBV), poly-3-hydroxyoctanoate (PHO), and poly(3-hydroxybutyrate-co-3-hydroxyhexanoate) (PHBHHx), have biocompatibility, biodegradability, and thermoprocessibility [111]. Furthermore, to adjust their biocompatibility and mechanical properties depending on end-used applications, PHA can be either blended, modified, or composited with other polymers, enzymes, or even inorganic materials [111]. The modifications to tailor-made PHA for biomedical applications have proved that this category of materials has a reasonable prospect as biological materials.

The economic efficiency of PHAs and their derivates in medical applications are the most studied. However, the PHAs use can be expanded to other health-related issues such as resolving malnutrition, metabolic and neurodegenerative disorders, anti-diabetic agents, etc.

2.2.4. Packaging films

Thanks to increased public awareness about sustainable 'green' packaging, the use of biopolymers over the last few years was amplified [113]. Also, the growth of consumer concern about the environmental and economic features of petrochemical-based materials exploitation raises attention to their substitution by biopolymers. However, the packaging industry still represents the biggest bioplastics market, with about 65 % (1.2 million tonnes) of the total produced bioplastics in 2018 [114]. Replacing petroleum-derived plastics with bioplastics like polyhydroxyalkanoates (PHAs) has attracted attention due to their valuable properties, which are equivalent to conventional polymers. Moreover, bioplastics offer better biodegradability and biocompatibility and have non-toxic behavior [115]. The first traditional applications of PHAs were the packaging materials and coating used in cosmetology and everyday articles, such as bottles, vials, and containers. PHA-based products were also found in household goods and disposable items, including utensils, hygiene products, and compostable bags [116]. Polyhydroxyalkanoates (PHAs) exhibit excellent barrier properties toward oxygen, carbon dioxide, and moisture, thus making them suitable for food packaging [117, 118]. Also, the PHB lamellar structure provides superior gas barrier properties with a vapor permeability of approximately 560 g μm/m^2/day, which is appropriate for

low-end food packaging [117, 119, 120]. However, its applications in the food industry are limited due to its high production cost. Among PHAs, poly(3-hydroxybutyrate) (PHB) and its copolymer with 3-hydroxyvalerate (HV), i.e., poly(3-hydroxybutyrate-co-3-hydroxyvalerate) (PHBV), have too far gained significant attention concerning characterization and industrial-scale production [120]. Several methods improve its economic viability, such as blending with other biopolymers like starch and Polylactic acid (PLA) or fabricating nanocomposite material based on PHAs and other organic or inorganic materials fillers (e.g., cellulose nanowhiskers and carbon nanotubes) [121]. Therefore, incorporating other biopolymers or nanofillers can improve their thermal stability, crystallization behavior, and mechanical properties, which are essential for packaging materials [122].

To enhance the antimicrobial and mechanical properties while maintaining the lowest migration rate to improve the shelf life of poultry items, Zare *et al.* [123] used the leaf extract of Thymus vulgaris to prepare zinc oxide–silver nanocomposites which were incorporated into PHBV-chitosan. These have revealed interesting antimicrobial activity that could replace the conventional petrochemical-based polymers currently used for food packaging poultry items. Another work reported by Castro-Mayorga *et al.* [124] showed that incorporating only 0.04 wt% of Ag NPs into PHBV reduced 56 % oxygen permeability compared to neat PHBV. Moreover, the prepared films showed up to 7 months of antimicrobial activity against eminent foodborne pathogens such as *Listeria monocytogenes* and *Salmonella enterica*. The final results were promising, producing biodegradable composites that could be used as potential films and coatings in active food packaging [125]. **Table 2.3** summarizes several works using polyhydroxyalkanoates-based materials in the packaging sector.

Table 2.3: PHA-based materials for packaging materials

BIOPOLYMERS	ADDITIVES	FABRICATION METHODS AND TREATMENTS	ANTIMICROBIAL TESTS AGAINST	REF.
PHB	ZnO NPs and Bacterial cellulose nanofibers (BC)	Melt compounding technique and zinc oxide (ZnO) nanoparticle plasma coating	*Staphylococcus aureus* and *Escherichia coli*	126
PHB	ZnO NPs	Combination of ultrasonication with the solution casting	*Staphylococcus aureus* and *Escherichia coli*	127

PHB	Lignin NPs	Oil-in-water Pickering emulsion approach	-	[128]
PHB	Graphene nanocomposites	Solution casting technique	-	[129]
PHB	Polylactide (PLA), Poly (ethylene glycol) (PEG)	Blending under shear deformation, Electrospinning	-	[130]
PHB	Cellulose fibers (from 2% to 10%)	Melt processing	-	[131]
PHBV	Aloe-emodin (AE)	Photoactivation of aloe-emodin under blue light (400 nm–500 nm)	*Escherichia coli*	[132]
PHBV	Salmonella Enteritidis bacteriophage Felix O1, polyvinyl alcohol (PVOH)	Casting and electrospinning	*S. Enteritidis H40499 SDE*	[133]
PHBV	ZnO NPs	(1) direct melt-mixing, (2) melt-mixing of preincorporated ZnO into PHBV fiber mats made by electrospinning, and (3) coating of the annealed electrospun PHBV/ZnO fiber mats over compression molded PHBV	*L. monocytogenes*	[134]
PHBV	1 wt% Fe doped ZnO (NPs)	i) PLA films were obtained by hot-pressed ii) Nanofibers based on PHBV/ZnO/Fex were deposited onto PLA films by the electrospinning process	*Pseudomonas aeruginosa (ATCC-27853)*	[135]
PHBV	Graphene oxide-zinc oxide (rGO-ZnO)	Melt extrusion	*Escherichia coli*	[136]
PHBV	AgNPs	Melt blending process	*Salmonella enterica* and *Listeria monocytogenes*	[137]

PHBV	Multi-walled carbon nanotubes (MWCNTs)	solution casting	-	[138]
PHBV	Cellulose nanocrystals (CNCs), Gelatin (GE), agar (AG), xanthan gum (XG), gum arabic (GA), Glycerol plasticizer	Electrospinning process, interfiber coalescence process	-	[139]
PHBV	Thermoplastic polyurethane (TPU)	Melt blending, compression molding	-	[140]
PHBV	Poly (butylene succinate) (PBS)	Melt mixing	-	[141]
PHBV	Coffee Silverskin (CS), acetyl tributyl citrate (ATBC)	Melt extrusion technique, injection molding	-	[142]
PHBV	Glycerol	Solvent casting method	-	[143]
PHBV	Ceiba pentandra bark fibers	Solvent casting technique	*S. aureus* and *E. coli*	[144]
PHBHV	Kraft lignin	Melt compounding, thermoforming	-	[145]
PHBV/PBAT	Nanoclay	Compression molding and cast film extrusion	-	[146]
PHBHHX	Organo-modified montmorillonite clay (OMMT) nanocomposites	Melt blending, solvent-casting, and compression molding	-	[147]
PHBHHX	Graphene oxide (GO) nanocomposites	Solvent casting method	*E. coli* and *B. cepacia* (Gram negative), *S. aureus* and *B. subtilis* (Gram positive)	[148]
PHB/PCL	Organo-clays (Cloisite® 30 B and 10A)	Nisin activation, Compression molding at 175 °C	*Lactobacillus plantarum CRL691*	[149]
PHB/PCL	Cellulose nanocrystals	1) solvent casting followed by 2) melt compounding and finally	-	[150]

		3) thermocompressing process		
PHA /CHITOSAN	Cinnamaldehyde (Ci)	Poiseuille flow principle, Molding PHA/CS composite scaffolds	*Staphylococcus aureus* and *Escherichia coli*	[151]
PHB / PLA	Tributyrin (TB)	Compression molding	-	[152]
PHB / PLA	-	Cast solution methodology	-	[153]
PHB / PLA	Poly (ethylene glycol) (PEG) and acetyl (tributyl citrate) (ATBC)	Melt blending and compression molding	-	[154]
PBAT/PHB	Babassu	Flat-die extrusion	-	[155]

PBAT: Poly (butylene adipate-co-terephthalate)

2.3. Fabrication approaches of PHA-based materials with antibacterial functionality

As bacterial infections are one of the major causes of chronic diseases, antibacterial materials are urgently needed. The nanofibers have a large surface area and are well-suited for incorporating antibacterial agents. As previously described, the antibacterial character is crucial for materials used in medical fields such as drug delivery and tissue engineering or the packaging domain, especially for food packaging. In literature, antibacterial PHA materials are used as scaffolds for soft and hard tissues and particles for drug delivery or catalyst immobilization. However, a few studies report the fabrication of antibacterial PHA fibers. Therefore, this section focuses on different fabrication methods to produce PHA polymeric fibers that can be used as antibacterial materials.

Polymeric nanofibers loaded with drug vectors of antibiotics destructive to the growth of bacteria have recently enticed the attention of scientists. Various studies reviewed nanofibers' tunable and intrinsic structure, properties, and components, providing sustained drug deliveries [156, 157]. The nanofibers can suppress the growth of bacteria due to their topographic characteristics [158]. Nanofibrous structures have various inherent properties, making them exceptionally functional for antimicrobial applications [156, 159]. Indeed, they have a large surface area-to-volume ratio as well as interconnecting and tiny interstitial space due to their small size, making them more beneficial than their wholesale form [158]. Furthermore, their high surface area can advance the hemostasis of

wounded tissues and fluid absorption [160]. The nanofibers are also effective at targeted drug delivery [161].

The porosity of nanofibers (60–90%) significantly influences their performance [158, 162], as it provides a high surface and wetting permeability. Successively, it affects vascularization, cell proliferation, and mechanical stability [163]. Moreover, their interconnected nanopores, coupled with exceptional surface reactivity, surface energy, and high electric and thermal conductivities, can inhibit the penetration of microbes [164]. These facts confirm that nanofibers are potentially advantageous as antimicrobial materials [158, 165]. In general, the significant applications of polymer nanofibers cope with various rising health, energy, and environmental challenges. Several techniques have been stated to produce submicron nanofibers, such as electrospinning [166], flash spinning [167], melt-blowing [168], multi-component spinning [168], template synthesis [169], nanolithography [157] and self-assembly [170]. To judge the efficiency of these techniques, an overall consideration of suitable polymers, possible fiber assembly, production cost, and production rate [157] are determined. Among the methods deployed for the manufacture of nanofibers, electrospinning is one of the most popular ones.

2.3.1. Electrospinning

Electrospinning has been created since the 1930s. However, it was widely recognized in the mid-1990s when the term electrospinning was conceived [171]. As a result, several natural and synthetic polymers have been effectively electrospun [172]. This technique gained popularity due to its simplicity, cost-effectiveness, and admissibility. It applies to mostly synthetic polymers and numerous natural polymers (e.g., carbohydrates and proteins).

The electrospinning process is considerably documented in the literature [72, 173]. As shown in **Figure 2.2**, an electrospinning system includes a high-voltage source, polymer pump, nozzle with a needle, a grounded collector, and preferably an air conditioning unit. While a sufficiently high voltage is applied, the polymer solution is pressed through a metal needle via the syringe pump. Thus, a potential difference is generated between the needle and the collector. The electric field drives the polymer jet as the solvent evaporates, and electrospun fibers are collected [174, 175]. Numerous parameters impact the morphology of the obtained fibers, mainly the applied voltage polarity [176], the flow rate of the polymer [177], the distance between the needle tip and the collector [175], the polymer solution characteristics [177], and environmental conditions such humidity and

temperature during the electrospinning process [178, 179]. Furthermore, an advanced spinning needle system can generate innovative electrospun fibers with unconventional shapes like core-shell [180], twisted, hollow, or multilayer structures [178].

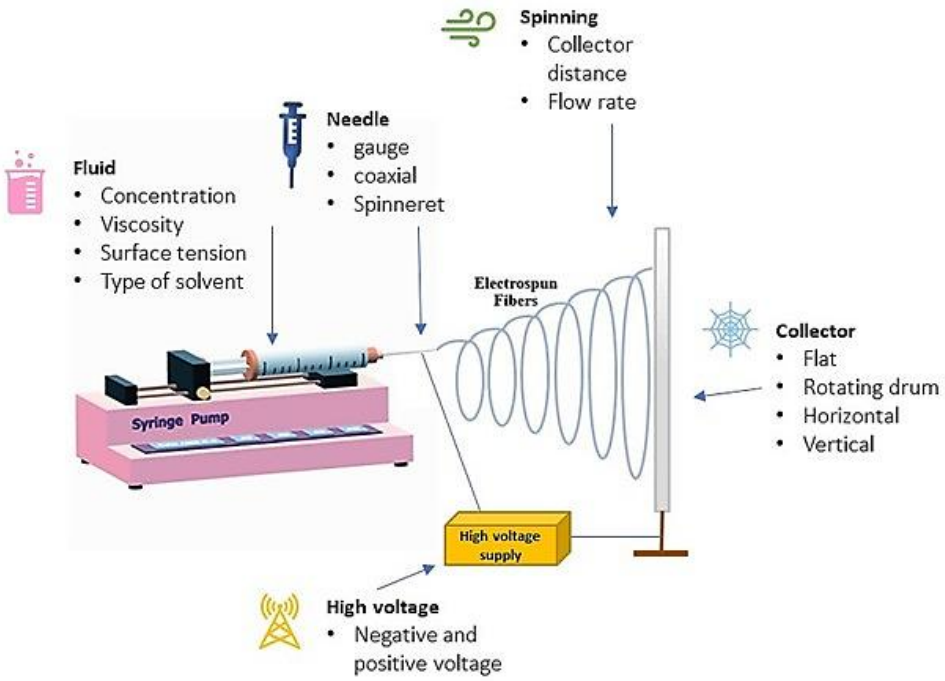

Figure 2.2: Schematic illustration of electrospinning technique [181]

Electrospinning studies using PHAs were not conducted until quite recently [182]. The first published studies reported the usage of this technique to produce super microfibers from poly-3-hydroxybutyrate and copolymers of 3-hydroxybutyrate with 3-hydroxyvalerate were performed in 2006 [183]. Previously, P(3HB-co-3HV) copolymers were mainly reported in electrospinning studies. Sombatmankhong *et al.* [183, 184] and Tong *et al.* [185] investigated the effects of the electrospinning conditions on the properties of electrospun fibers produced from P(3HB-co-3HV). They further evaluated the possible potential of mats and ultrafine fibers as cell scaffolds and the effects of the process parameters on the morphology and mechanical behaviors of fibers and fibrous scaffolds.

Similarly, depending on the type and the molecular weight of the used polymer, Ying *et al.* [186] compared three types of electrospun PHA scaffolds – P(3HB), P(3HB-co-3HHx), and P(3HB-co-4HB) – and reported their morphology, their diameter of the fibers and their mechanical properties (such as Young's modulus). The substantial contribution of nanofibers is the prevention of infection or bacterial growth. Several works have been performed in recent years in assembling antibacterial nanofibers loaded with various biocides or antibiotics [187]. Generally, the antibacterial

effect is provided by a biocide incorporated in the fibers. It can include i) blending the active drug in the polymer solution before electrospinning, ii) enclosing the active agent in the core of the fiber using coaxial electrospinning, iii) encapsulating the antibiotics in nanostructures before dispersing them in the electrospinning solution, iv) post-treatment of the fiber after electrospinning, so the precursor converts to its active form or v) attachment of the effective substance onto the fiber surface **(Figure 2.3)** [187].

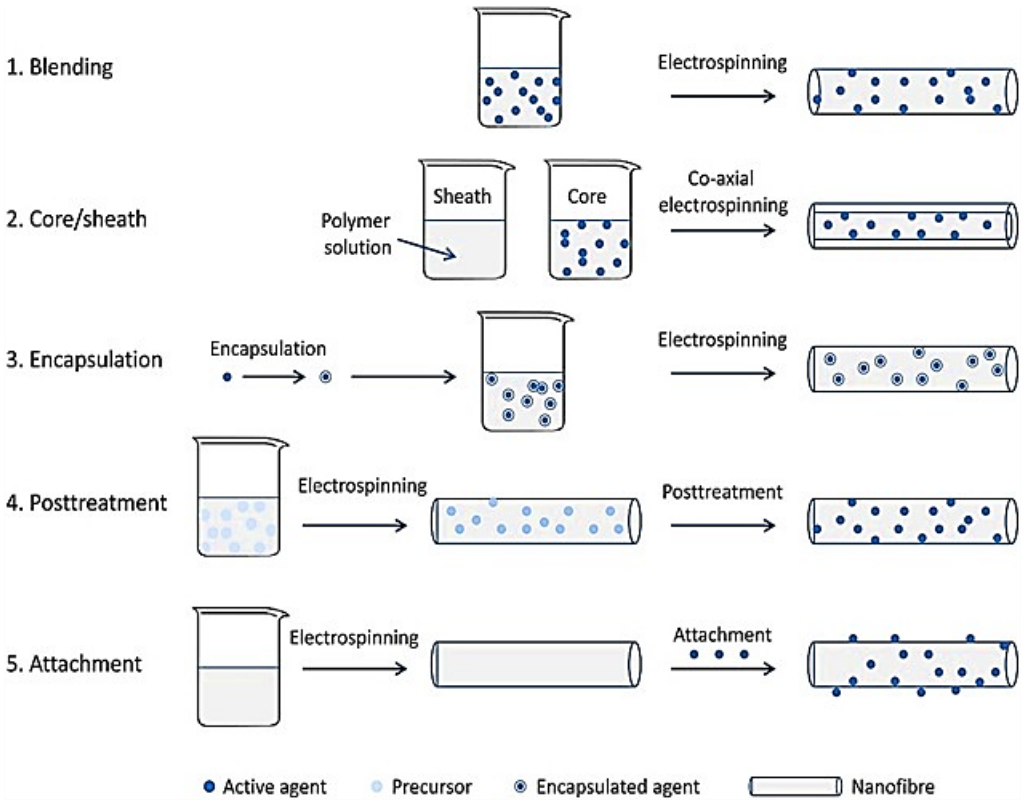

Figure 2.3: Different strategies of incorporating biocides into electrospun nanofibers: 1. blending the active drug in the polymer solution before electrospinning, 2. enclosing the active agent in the core of the fiber using coaxial electrospinning, 3. encapsulating the antibiotics in nanostructures prior dispersing them in the electrospinning solution, 4. post-treatment of the fiber after electrospinning, so the precursor converts to its active form, 5. attachment of the effective substance onto the fiber surface [187].

Diverse remarkable active agents have been documented, including antibiotics, chlorhexidine, triclosan, biguanides, QACs, metal oxide, and Ag NPs [187]. Adding biocides to the electrospinning solution is technologically the most straightforward approach for treating nanofibers compared to subsequent post-treatment. However, the presence of biocides modifies the

spinning solution conductivity and viscosity, thus affecting the morphology and diameter of nanofibers. In recent years, the novel core/shell technology with coaxial electrospinning for the preparation of nanofibers was exhibited as suitable for biocides in the core of fibers [187, 188]. Furthermore, the surface of nanofibers can be modified and functionalized via coating with antibacterial substrates. These modifications can further improve the nanofibers' topography and promote specific interactions between nanofibers and bacteria [158, 189]. Many electrospun fibrous membranes have been fabricated as antimicrobial materials, such as nylon, ultrafine polyacrylonitrile, and polyethylene oxide nanofibers [190, 191]. However, a few fibrous membranes from biopolymers have been studied so far. Despite this, a recent tendency toward nontoxic, sustainable eco-materials has emerged in innovative textile manufacturing techniques. Cellulose, starch, polylactide (PLA), PHAs, and polyhydroxybutyrate (PHB) are the most considered biodegradable biopolymers. PLA and PHB are the most advantageous as they are extracted from sustainable materials [191, 192]. However, due to their low elongation properties and high brittleness, these neat polymers are restrictive. Fernandes *et al.* [193] produced electrospun meshes of poly(hydroxybutyrate) (PHB) and poly(hydroxybutyrate)/poly(ethylene oxide) (PHB/PEO). They used chlorhexidine (CHX) as an antibacterial agent for drug delivery systems. It was concluded that exceeding 5 wt% of CHX concentrations, the electrospinning operation was unstable because of added charges by the drug into the polymer solution and the poor polymer entanglement. However, for 1 wt% CHX, PHB/PEO-1%CHX displayed a high antibacterial reduction rate of 100 % and 99.69 % against *E. coli* and *S. aureus*, respectively.

As a member of the polyhydroxyalkanoates family, PHB has received considerable attention for several medical applications because of its advantageous properties, such as good biocompatibility, nontoxic degradation products, and excellent mechanical strength compared to other polymers in different fields, including tissue engineering. For example, PHB was used as alloy scaffolds coated with ceramic-based stands to improve degradation rate, hydrophobicity, and brittleness [194]. In addition, PHB electrospun fibers were used in various medical applications, as described in **Figure 2.4.**

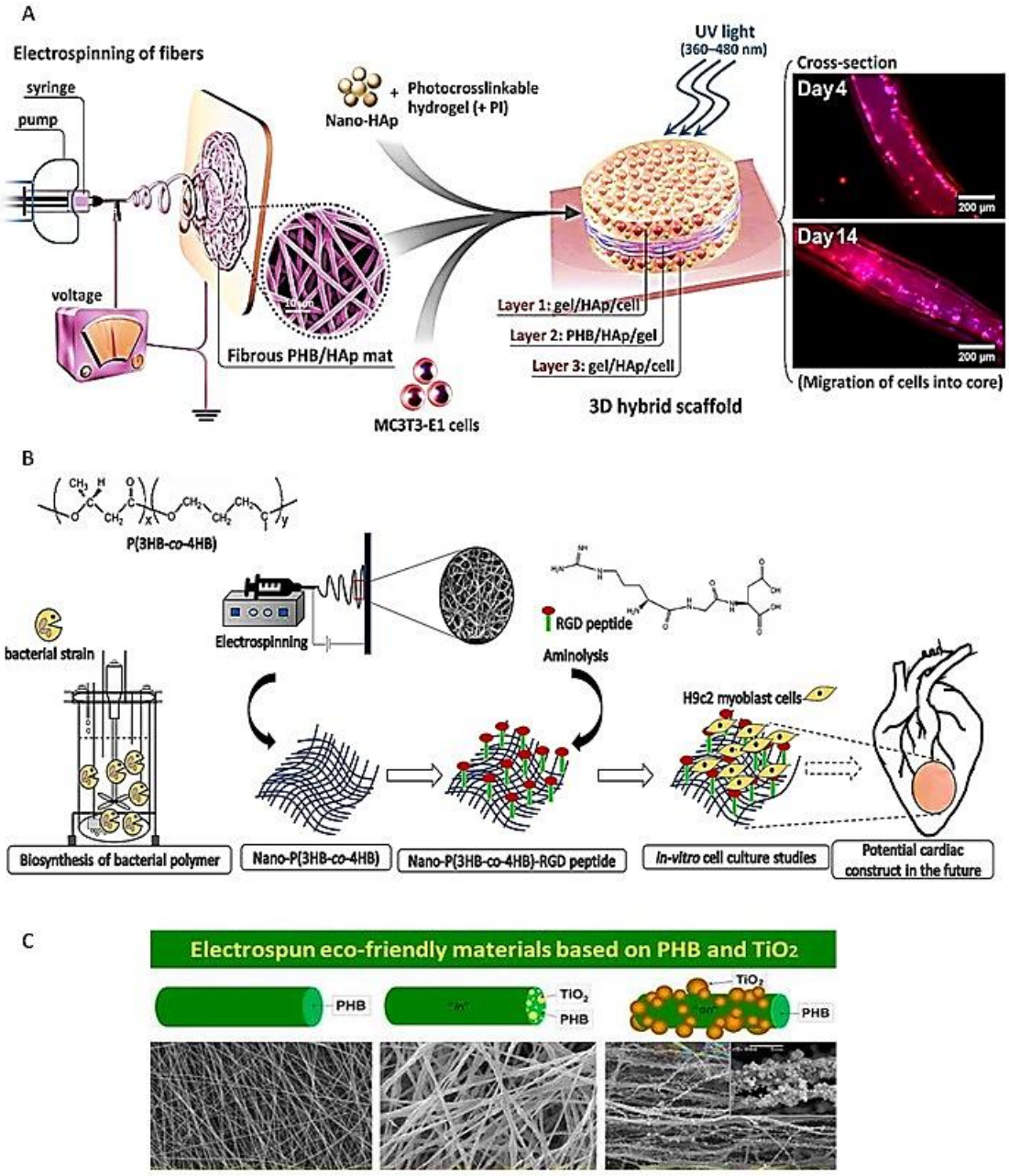

Figure 2.4: Electrospinning of antibacterial fibers. A) PHB electrospun mat, hydroxyapatite (HAp), and protein-based hydrogel combined in a single tri-layered scaffold for tissue engineering scaffold in vivo [195]. B) nano-P(3HB-co-4HB)-RGD scaffold fabrication as a potential future application for building cardiac tissue [196]. C) Antibacterial PHB electrospun fibers with TiO2 NPs [197].

Electrospinning technology allows micron and nano fibers to simulate the extracellular substrate (ECM) of biodegradable polymers and proteins in a single scaffold and evaluate their

ability to treat diabetic wounds. Sanhueza *et al.* [198] used PHB and gelatin to make microns and nanofibers, respectively. After 1, 3, and 7 days, all scaffolds showed excellent fibroblast vitality and adhesion. Electrospun PHB proved to be a suitable scaffold for treating more complex tissue regeneration comprising drug delivery of different polarities to improve skin wound healing.

However, the electrospinning technique is not ready for the large-scale industrial production of antimicrobial fibers that the market demands. Furthermore, the fabrication process of nanofibers with complex morphologies, such as multiaxial fibers and/or multicomponent, still has some difficulties relating to large-scale feasibility. Therefore, further studies are required to facilitate the entrapment mechanism and fabrication process.

2.3.2. Casting method

Different methods exist to develop active antimicrobial materials. In general, migratory and non-migratory techniques were proposed for this purpose [199, 200]. In the migratory system, the antimicrobial agents are released from the polymeric matrix to the surface, and, in the other case, the active elements are linked to the polymer material [201]. For example, using a solution casting technique, zinc oxide (ZnO) NPs, which are effective UV hinders, were loaded with PHB [202]. Díez-Pascual et Díez-Vicente [202] have successfully prepared novel PHB/ZnO biodegradable nanocomposites using a primary solution casting method. The resulting nanocomposites increased antimicrobial activity against *E. coli* and *S. aureus* by increasing ZnO concentration. In a similar study [203], ZnO NPs were also used to reinforce (3-hydroxybutyrate-co-3-hydroxyvalerate) (PHBV) via the solution casting technique. As a result, the optimum balance between barrier, mechanical, migration, and antibacterial properties was obtained at a critical ZnO concentration of 4.0 wt % against 5.0 wt % in their previously stated study. However, the antibacterial effect of PHBV/ZnO films was proved more efficient against *E. coli* than against *S. aureus*.

In most previous methods stated so far, significant amounts of solvents such as chloroform are used to prepare PHB antimicrobial membranes, which may cause health problems and/or environmental issues. Moreover, a large amount of metal nanoparticles is used in the whole PHB matrix, which generates the same effect when attached only to the surface. However, antibacterial agents on the surface proved to be more efficient [201]. PHB's high crystallinity provokes complex migration of antimicrobial nanoparticles from the bulk to the surface of the polymer. Further additives like plasticizers, lubricants, and surfactants are used for better nanoparticle migration. In

this case, surface modification is urgently required to enhance the attachment of antibacterial agents to the PHB matrix. Various surface modification exists, such as physical, wet chemical, corona, ultraviolet, annealing, and patterning treatments [204]. Otherwise, PHB surface treatment with plasma presents an innovative eco-friendly method to obtain antimicrobial activity without significantly changing bulk characteristics.

2.3.3. Modification of electrospun nanofiber membranes with plasma treatment

In recent years, plasma technology has emerged as a new surface modification treatment due to its simplicity and green character. This technique generates ionized gas consisting of negative and positive charges, including ions, electrons, radicals, UV photons, and excited molecules **(Figure 2.5)**. The plasma qualities and the surface effects are determined by several parameters, such as the substrate properties, the gas introduced, and the treatment condition (pressure, power, and exposure time) [205]. Preliminary studies reported the use of plasma with electrospun nanofiber membranes [206, 207]. However, few reports have stated the effect of plasma in enhancing the antibacterial activity and release efficiency of electrospun nanofibers. For instance, Cui *et al.* [207] studied the effects of plasma exposure time and operation power with poly (ethylene oxide) (PEO) electrospun nanofibers containing Beta-cyclodextrin (β-CD) and tea tree oil (TTO) as antibacterial agents. They demonstrated that the antibacterial effects were in a good correlation with the intensity of the plasma under high plasma power. It might be explained by the fact that plasma treatment enhances the release rate of nanofibers' biocomponents and also generates reactive ingredients such as ions, photons, atoms, free electrons, and free radicals [208].

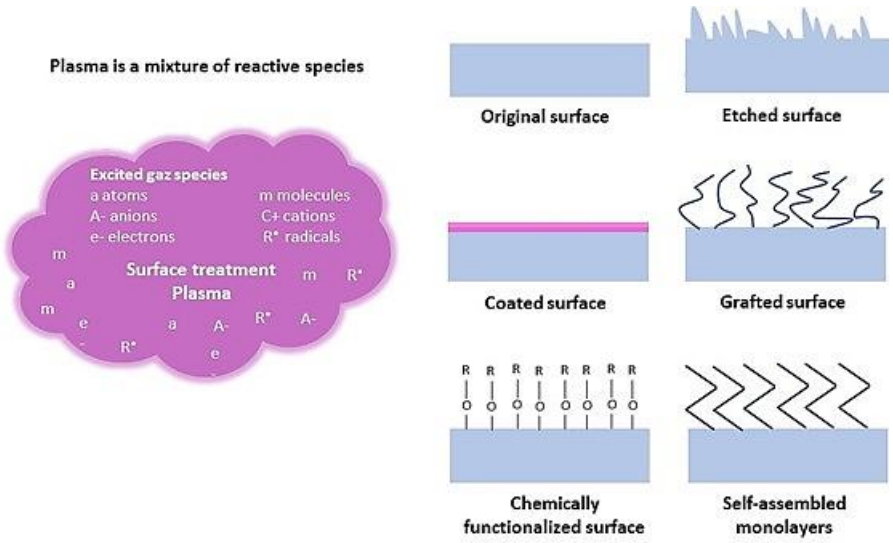

Figure 2.5: Potential surface modifications with plasma treatment.

Some researchers documented the plasma treatment of PHA electrospun nanofibers to enhance their antibacterial effect. For example, PHB modified with bacterial cellulose nanofibers was treated by a plasma or ZnO nanoparticle plasma coating [201]. Higher antibacterial activity was observed after the plasma treatment and total inhibition of *S. aureus* growth after ZnO nanoparticle plasma coating. Moreover, the plasma treatment did not alter the nanocomposites' crystallinity, thermal stability, and melting behavior. In another study, PHB was plasma-activated and silver-coated to be used in packaging [209]. The plasma-modified PHB fabric immersed in Ag nanoparticle solutions showed an enhancement of antibacterial efficiency against *E. coli*.

The effect of low-pressure plasma treatment in the surface modification of PHB by polymerization, grafting, or functionalization in medical fields, such as increasing cell adhesion and proliferation for scaffolding, was early documented [210]. Indeed, low-pressure plasma treatments were mainly exploited to enhance cell compatibility [211] by improving the surface hydrophilicity of PHB/PHBV films. However, low-pressure plasma processes have limitations due to the complicated installations and high costs inherent to vacuum technology [201].

Different methods of manufacturing sequential or simultaneous deposition of fibers and/or nanoparticles [212, 213] have been optimized to introduce antibacterial material. In this context, over fiber morphology, antibacterial agent loading highly affects the release curve [213]. However, constant rate release is strictly conditionally limited by the polarity of the polymer, the drugs (i.e., they must be similar), and the solubility of the antibacterial agent in the polymer solution.

2.4. Integration of PHA-based nanofibers with antibacterial agents

The intrinsic antimicrobial action and mechanism of nanofibers alone have not been extensively examined. Some nanofiber properties are responsible for bacterial adhesion **(Figure 2.6 A)**: (1) Fiber porosity (nanoscale) leads to early biofilm formation, allowing bacterial cells to attach to highly porous nanofibers; (2) Nanofibers with positively charged surfaces also attract the negatively charged surfaces of bacterial cells; (3) The rough surface of the nanofibers also provides a larger contact area for bacterial cell attachment; (4) The diameter of fibers (smaller than the size of bacteria) allows for changes in the conformation of bacterial cells. The surface wettability of nanofibers has an essential role in the bacterial attachment; (5) Hydrophobic bacterial cells adhere to hydrophobic nanofibers' surfaces due to hydrophobic interactions [214].

Among antimicrobial nanofibers most well documented, chitosan nanofibers are almost the only natural polymer with intrinsic antimicrobial properties [215, 216]. Therefore, the antimicrobial activity against *E. coli*, *S. aureus*, *S. typhimurium,* and *L. innocua* is implied to be granted by the protonated amino groups of chitosan nanofibers. However, an antimicrobial test conducted by Shahini Shams Abadi *et al.* [216] of chitosan nanofibers with *Clostridium difficile* assumed that the destruction of protein synthesis is not responsible for the antibacterial action of chitosan nanofibers. The consequence is that nanofibers alone cannot kill bacteria [158]. Therefore, functionalization with antimicrobial agents is requisite to ensure an antibacterial effect.

The bactericidal effect of functionalized nanofibers depends on the primary material used, its morphology, and its surface chemistry [188, 217]. In addition, functionalized nanofibers display enhanced cell membrane penetration and improved potential to regulate cellular interaction [218, 219]. However, their exact antimicrobial mechanism is still unknown in the literature, and several assumptions from earlier investigations vary as a function of the additional antibacterial component used [220, 221].

Theoretically, it has been reported that the antimicrobial mechanisms of antimicrobial agents include cytoplasmic membrane disintegrations that alter the structure and morphology of microbial cells [200], leading to the leakage of proteinaceous intracellular components and respiration inhibition. Subsequently, the ATPase enzyme activities are restrained, responsible for nutrient transport across the microbial cytoplasmic membrane, energy production, and structural component synthesis in the microorganism [200] **(Figure 2.6 B)**.

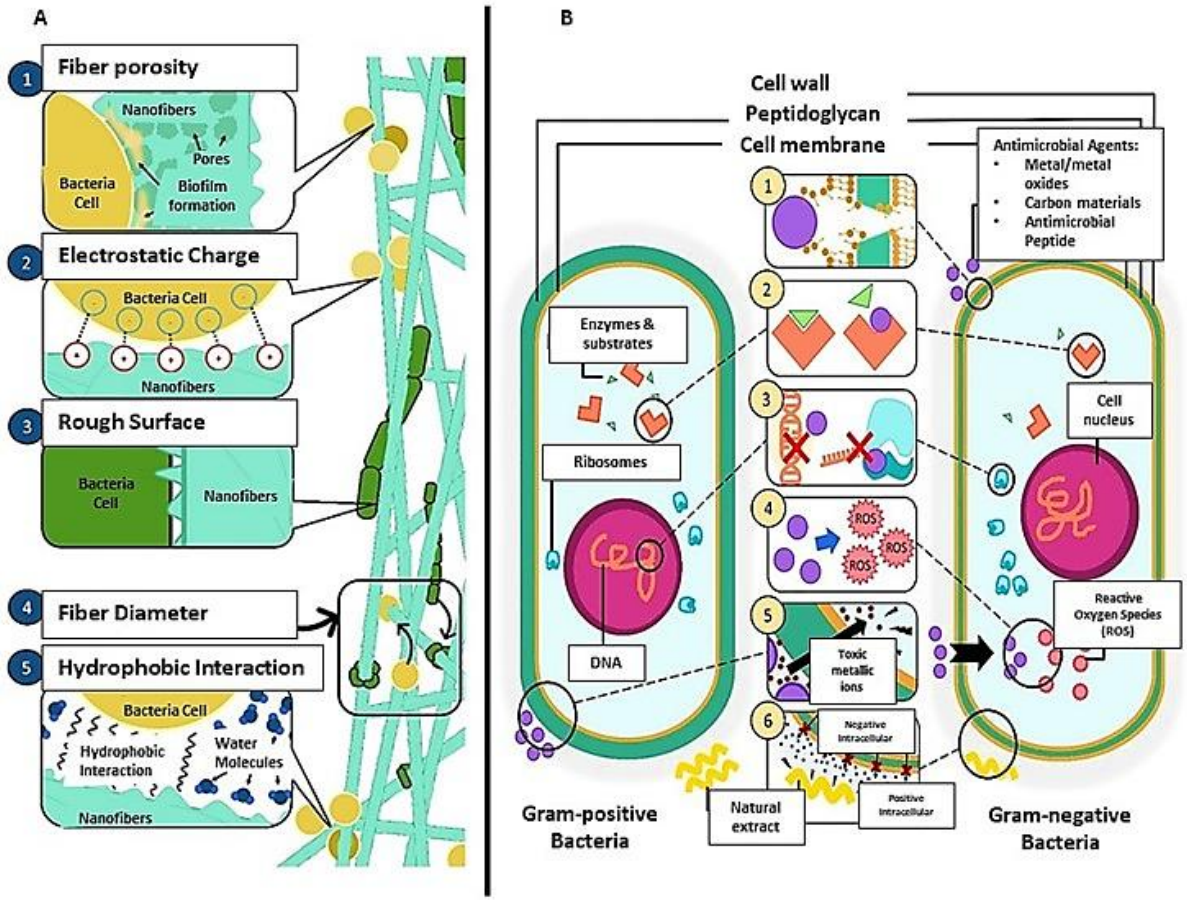

Figure 2.6: Bacterial interaction with fibers: A) Illustration of bacterial adhesion on nanofibers. B) Illustration of different mechanisms of action by antimicrobial agents incorporated in nanofibers on bacteria cells via (1) disruption of the cell membrane/cell wall. (2) Inhibition of cellular metabolic pathways. (3) Inhibition of DNA and gene expression. (4) Instigation of cellular oxidative stress. (5) Metal-based nanomaterial toxification. (6) Cellular hyperpolarization [214].

The therapeutical action of antibacterial treatment consists of cell wall synthesis inhibition, interference with essential proteins, and disruption of the DNA reproduction mechanism. However, in many cases, bacteria have successfully transformed and enhanced their ability to resist the bacterial destruction mechanism [220], known as antibacterial resistance. Although, it was recognized for over 50 years and is a significant cause of increased morbidity, mortality, and healthcare costs [222]. The primary antibacterial resistance mode of action is destroying the antibiotic target. Moreover, bacteria can over-product enzymes such as aminoglycosides and β-lactamases to destroy antibiotics [220].

Additionally, to escape from the antibiotics, mostly limited to the extracellular area, several pathogens like *Chlamydophila pneumonia* remain inside the cellular compartments of the host cells [223]. Alternatively, nanomaterials can be an excellent substitute to overcome antibiotic-resistance action due to their unique physio-chemical characteristics, enabling them to establish a novel antibacterial mechanism. Indeed, nanomaterials can attach and destroy bacterial membranes, leading to the cytoplasmic components discharging [218, 224]. Subsequently, once they penetrate the bacterial membrane, nanomaterials can bind to intracellular constituents such as DNA, enzymes, and ribosomes to destroy the conventional cellular mechanism **(Figure 2.6 B)**.

2.4.1. PHA-based nanofibers integrated with metal (metal oxide) nanoparticles

Metal and metal oxide nanoparticles are recognized to penetrate the bacterial membrane and destroy cellular activities. Ag ions are released from nanofibers to adhere to the bacterial membrane, destroy it, and cause the leakage of intracellular materials. In addition, Ag ions interact with DNA and intracellular proteins by penetrating the bacterial cells and causing their inactivation. Nevertheless, Ag ions can bind to amino groups of DNA nucleotides and break their hydrogen bonds, which disturbs the DNA base pairing [9].

Apart from these mechanisms, Ag species can attack bacteria through the generation of reactive oxygen species (ROS), such as hydroxyl radicals ($OH^{\bullet}$), oxygen superoxide radicals ($O_2^{\bullet-}$), and hydrogen peroxide (H_2O_2) [9, 214]. The over-production of ROS species will generate severe oxidative tension that causes bacterial cell membrane damage, protein synthesis disruption, and DNA-specific site destruction, eventually resulting in cell lysis [225, 226]. Recently, metal NPs such as gold and silver, added to metal oxide NPs such as iron oxide, zinc oxide, copper oxide, and titanium dioxide, have been extensively reviewed for their antimicrobial applications [227, 228]**.** In addition, composite materials involving nanofibers and metal nanoparticles are well documented with convincing evidence of antimicrobial activity [229]**.**

2.4.2. PHAs with silver nanoparticles

Due to their excellent thermal stability and antimicrobial properties, Ag NPs have been one of the most documented nanomaterials. The most standard approach to preparing antimicrobial polymeric films has been directly blending the nanometal with the matrix [230] and solvent casting

[231, 232], as previously described. Nevertheless, synthesizing stable NPs in the polymer solution remains the main challenge, as their antimicrobial efficiency depends on the agglomeration state and size distribution [233]. In addition, the effects of Ag NPs on health and environment [234] evoke an increasing interest, mainly when these NPs are used in biomedicine or pharmaceutical applications. In these cases, the cytotoxicity properties become particularly important. Latest investigations pointed out that detached NPs may penetrate cells of living organisms, possibly leading to cell damage [235]. In this context, Składanowski *et al.* [236] confirmed that Ag NPs could be safely used as an antibacterial agent after being proved harmless for eukaryotic cells. Salama *et al.* concluded a similar outcome [237]. Also, Chairuangkitti *et al.* [238] demonstrated that if Ag load concentrations are below 25 ppm, they do not affect the ROS generation of human lung carcinoma (A549) cells or the cell viability. At all events, Ag NPs are very unlikely to be released from polymeric films that do not highly plasticize or dissolve in the contact media [124].

Regarding incorporating Ag NPs into submicron polymer fibers, only a few studies have been reported, such as poly-(L-lactide) [239], ethylene vinyl alcohol [240], poly(ε-caprolactone) [241], polyacrylonitrile [242], or polypropylene [243]. Furthermore, few studies about the preparation of Ag NPs and polyhydroxybutyrate electrospun fibers [244]. For example, Castro-Mayorga *et al.* [124] used the electrospinning coating technique to develop active PHA–Ag NPs with bactericidal efficiency against *Salmonella enterica*. Similarly, PHB–Ag NPs composite was synthesized by Jayakumar *et al.* [200]. The nanocomposite was stable, polydisperse, and exhibited high antimicrobial resistance against *E. Coli* and *Pseudomonas sp.* Moreover, the PHB polymer maintained its original structure after adding Ag NPs. A more complex study was conducted by Yu *et al.* [232], whose synthesized poly(3-hydroxybutyrate-co-3-hydroxyvalerate) (PHBV) and cellulose nanocrystals/Ag (CNC-Ag) nanohybrids. They concluded that the homogeneously dispersed CNC-Ag was considered bifunctional reinforcement as it improved the mechanical, thermal, and antibacterial properties of PHBV. However, despite the actual progress, the application of these materials specially in food legislation is still restrained.

2.4.3. PHAs with Titanium dioxide

Titanium dioxide (TiO_2) received particular attention, as a nanofiller, due to its inert, nontoxic, and eco-friendly properties [245]. Also, it is inexpensive material with good accessibility and thermal and environmental stability [246]. Furthermore, due to its photocatalytic activity, it has a

high potential action against different micro-organisms [247]. TiO_2 is an inorganic material collected from various natural ores containing rutile, ilmenite, leucoxene, and anatase. It is mainly utilized in solar energy conversion [248], UV detection, photoelectrochemical activity [249], and photocatalysis [250], and it offers a promising solution for water or wastewater treatment [251]. It has significant advantages over metals (commonly Ag)-based systems [252] and chemical (H_2O_2, NO) [253]. Moreover, polymeric nanocomposites containing TiO_2 are eco-friendly and exert biocidal effects with non-contact action. Thus, no potential risk of nanoparticle release, which can cause unpredictable effects on human health, is observed [254].

Matsunaga *et al.* [255] were the first to discover the antimicrobial effect of photocatalytic TiO_2. The antimicrobial effectiveness of the photocatalytic oxidation under UV irradiation was evaluated against different microorganisms such as yeast (*Saccharomyces cerevisiae*), green algae (*Chlorella vulgaris*), Gram-positive bacteria (*Lactobacillus acidophilus*) and Gram-negative bacteria (*Escherichia coli*). Afterward, numerous studies on photocatalytic disinfection have been extensively performed on various microorganisms such as fungi, viruses, and many species of bacteria [256]. The antibacterial activity of TiO_2 is induced by UV light irradiation, which activates this material to generate charge carriers, including electrons and holes. These charge carriers then reduce atmospheric oxygen and/or oxidize water molecules, producing ROS that participates in antimicrobial activities [257, 258]. Some studies have proposed that the photo-oxidation of coenzyme A, derived from pantothenic acid and considered influential in respiration and many other biochemical reactions of microbial cells, will inhibit cell respiration and cause cell death [257]. Other studies have demonstrated that the cell membrane leading to lipid peroxidation is the elementary site to be invaded by (ROS) species [257, 259]. Cell damage and further oxidative attack of intracellular constituents inevitably cause cell death. In general, TiO_2 is three times more efficient in disinfection than chlorine and one and a half times more than ozone [258, 260]. The antibacterial efficiency of TiO_2 can be significantly improved in the case of the presence of TiO_2 in nanometric form. TiO_2 NPs presented high-toxic behavior against *P. aeruginosa* and *Escherichia coli* after photoactivation [261]. The peptidoglycan content and cell configuration of the microorganism control the degree of toxicity [228]. Gram-negative bacteria (*E. coli*) were more vulnerable to TiO_2 NPs than Gram-positive microorganisms (*S. aureus* and *E. faecalis*), which were more susceptible than the fungi *Aspergillus niger* and *C. Albicans* [262]. It is assumed that different cell walls are the reason for this phenomenon. The bacterial cells of Gram-negative bacteria, such as *E. coli*, are covered with a layer of peptidoglycans (~8 nm thick) and lipopolysaccharides (1-3 μm thick) [263]. This disposition may

advance the entry of ions released from the NPS into the cell. Conversely, Gram-positive bacteria such as *S. aureus* have a much thicker peptidoglycan layer than Gram-negative bacteria, extending over 80 nm with teichuronic and teichoic acids covalently attached [264] **(Figure 2.7)**. The destruction of the cell wall, which occurs from the physical interaction between the NPs and the cell wall, is more damaging to Gram-negative bacteria due to the lack of the thick layer of peptidoglycan found in Gram-positive bacteria that could potentially serve as a shielding layer [225].

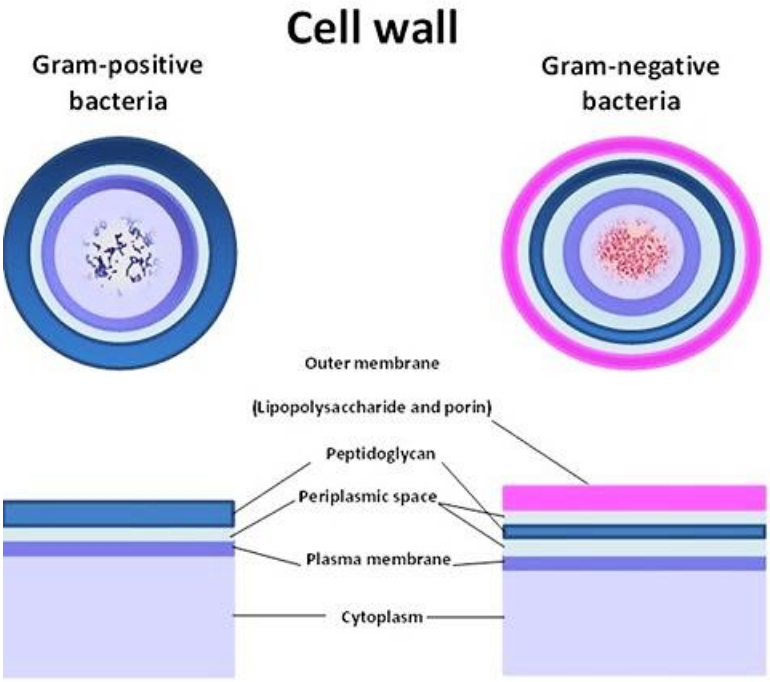

Figure 2.7: Gram-negative and Gram-positive comparison of the bacterial cell wall structure.

Several studies have reported using TiO_2-organic hybrid materials in different biomedical fields [265]. A recent scientific trend is using the electrospinning technique to produce multi-mats with nano-TiO_2NPs with an antibacterial activity which can be potentially applied in tissue engineering using in vitro approaches. In this regard, PVA/nano-TiO_2 composite fibers have been prepared by Lee *et al.* [266], which exhibited excellent antibacterial activity against *K. pneumonia* and *S. aureus.*

However, there are scarce studies evaluating the antibacterial activity of TiO_2 NPs with PHA fibers. Korina *et al.* have [267] effectively developed a novel recyclable hybrid fibrous material designed for water and air purification from organic pollutants. The studied material consists of magnetic poly(3-hydroxybutyrate)-based core-shell fibers decorated with (TiO_2) which displayed excellent stability in the presence of a model organic pollutant and kept almost all its photocatalytic

activity after three uses under UV irradiation. Another study combined three techniques: electrospinning, electrospraying, and impregnation to prepare PHB/nanoTiO_2/chitosan oligomers (COS) fibrous materials [268]. The designed hybrid biomaterials presented a significant biocidal effect against *E. Coli* and effectively killed the bacterium.

Additionally, it was demonstrated that PHB/TiO_2 fibrous materials could be used as scaffolds for tissue engineering and regenerative medicine as the content of TiO_2 NPs (5–10%) did not affect the proliferation of different cell lines [269]. The antibacterial activity against *E. Coli* was also confirmed using PHB–TiO_2 composite film with ameliorated photocatalytic sterilization action over time in a further study by Yew *et al.* [270]. Titanium dioxide (TiO_2) antibacterial effectiveness can be enhanced by adding Ag to create a double-antibacterial hybrid agent.

2.4.4. PHAs with hybrid nanoparticles

Nowadays, antibiotic resistance is one of the most severe threats to global health, food security, and development. Indeed, antibiotic resistance is reaching dangerously high levels in all regions worldwide. New resistance mechanisms are emerging and spreading, compromising our ability to treat common infectious diseases. The unrestrained and inappropriate usage of antimicrobial drugs results in more threatening mutated strains that develop antimicrobial resistance, defined as the ability of microorganisms to defend themselves against the biocidal action of antimicrobials [271]. Thus, the hybridization and combination of bactericidal nanoparticles would constitute an effective new technique to combat these resistant bacteria [272]. Different entities are combined to form a nano-component with unique, desirable characteristics not provided by their correspondents when used individually. Some researchers have realized that the antibacterial efficiency of ZnO NPs against Gram-positive bacteria (e.g., *S. aureus)* is better than that against Gram-negative bacteria (e.g., *E. Coli)*. When combining ZnO NPs and AgNPs, the nanohybrid materials show a more evident antibacterial effect and a reduced cytotoxicity level [273]. Additionally, the hybridization of Ag NPs with Fe_3O_4 NPs (or MnO_2 NPs) could increase the ionization rate and thus ameliorate the antibacterial activity. Nonetheless, the ROS generation rate was also enhanced when the semiconductor oxides such as TiO_2 or ZnO were combined with noble metals such as Au or Ag, thus enhancing the biological activity [272].

Few data were found in the literature concerning the preparation of antibacterial polymer fibers issued from renewable sources with hybrid NPs. The standard method consists of

electrospraying metal oxide (MgO, TiO_2, or Al_2O_3) suspensions, generally stabilized with surfactants, onto premade nanofibers [274]. The major drawback of this method is the low concentration of the antibacterial agents in the suspensions used for electrospraying (0.6 wt%) [275]. Based on this method combined with the impregnation technique, Korina *et al.* [275] developed a novel hybrid fibrous material from biodegradable PHB, chitosan oligomers, and TiO_2, which can be used in different fields such as tissue engineering and regenerative medicine, as well as in air and water purification from organic pollutants. In another study, Gouvêa *et al.* [136] prepared a hybrid material of PHBV with graphene oxide-zinc oxide (rGO-ZnO) recommended for active food packaging because of effective antibacterial property against *E. Coli*.

2.5. Summary and outlook

PHAs have unique characteristics, making them suitable for several applications, such as medical and packaging. In addition, they present a promising alternative to petroleum-derived plastic products as a degradable biopolymer. In this chapter, PHA-based materials proved to be an emerging biodegradable polymeric family for antibacterial applications. The polymer characteristics and production were first discussed. Therefore, this study was conducted to better document the actual state of knowledge on PHA biopolymers by reviewing the existing technologies currently used for production. In addition, particular attention was paid to collecting scientific information on antibacterial agents that can potentially be integrated into PHA material for biological and sustained antimicrobial protection. This chapter discussed the critical role of nanomaterials in ensuring antibacterial effectiveness. Integrating PHAs with various antibacterial agents presents a significant challenge as their type and incorporation method highly influence the biological efficiency and final properties of the PHA material. The bactericidal effects of PHA-based materials are related to the morphology, the physical characteristics of PHA-based materials, and the antimicrobial agents added to the structure. Further studies are required to deeply understand the interactions of these antimicrobial nanomaterials with the target bacteria, as bacteria are complex microorganisms that can rapidly customize to their surroundings to survive. Similarly, as surface modification of PHA-based materials can enhance the surface coating with antibacterial agents, plasma treatment should be cautiously adjusted to minimize degradation, as detailed in this work.

The commercial upscaling of PHA-based materials is limited due to the high cost of the feed, the lack of industrial production facilities, and their chemical and physical characteristics. Based on the knowledge gathered and discussions on the current gaps in studies, the efforts still to be made and the strategies to be adapted were proposed. Finally, using biodegradable, antibacterial materials to face coronavirus spread and to address environmental issues brought on by the accumulation of COVID-19-related trash can be achieved using promising PHA materials, as proposed in this work.

Finally, the development of PHB and hybrid antibacterial agents for antimicrobial applications has remained considerable challenges and unique aspects that are still unexplored. These features encourage studies presented in chapters 4-6 of this thesis.

Chapter 3: Materials and Methods

This chapter summarizes the materials and methodology adopted in this thesis. However, they are detailed in the scientific papers included in Chapters 4 to 6.

3.1. Materials

Pellets of poly(3-hydroxybutyrate) (PHB) with a weight-average molecular mass (M_w) of 550 kg/mol and a polydispersity index (PI) of 1.2 were acquired from Goodfellow (Huntingdon, England). Commercial ZnO NPs, ranging in size from 10 to 30 nm in powder form, were supplied by SkySpring Nanomaterials. Thermo Scientific (United States) and Alfa Aesar (Mississauga, United States) provided the chloroform (purity ≥99.8%) and dichloromethane (purity ≥99.8%), which were used to dissolve PHB, respectively. For biological tests, *Escherichia Coli (ATCC 11229)* and *Staphylococcus epidermidis (ATCC 12228)* were purchased from Cedarlane (Southern Ontario, Canada). Bactotryptic soy broth (TSB) and tryptic soy agar (TSA) were also supplied by Sigma Aldrich. For bacteria cell fixation, we purchased glutaraldehyde 5% from Sigma Aldrich and Sodium Cacodylate buffer (0.2 M, pH 7.4) from Fisher Scientific. The Live/Dead Bacterial Viability Kits (L7012) was purchased from Thermofisher Scientific. Demineralized water was used in this work, and all chemicals were used without further purification.

3.2. Methods

3.2.1. Synthesis of $AgTiO_2$ hybrid nanoparticles

The process developed by our group for the synthesis of $AgTiO_2$ NPs consists of two primary steps: the preparation of TiO_2 NPs and the photodeposition of Ag NPs. In the presence of H_2O_2, a water-soluble titanium peroxo complex was formed by the hydrolysis of titanium (IV) iso-propoxide. This complex was obtained by dehydrating the solution and subsequently calcining it at 400°C for 4 hours to produce TiO_2 NPs. The NPs were dispersed in a 10% ethanol solution that contained $AgNO_3$ (Ag amounts account for 6% (wt) of the TiO_2). The solution was subsequently exposed to UV light (100W) for 45 minutes. NPs were deposited on the surface of TiO_2 NPs, which were activated by the illumination to reduce Ag^+ to Ag^0.

3.2.2. Green synthesis of ZnO microporous particles

ZnO MPs are synthesized using a process devised by our group. In particular, a double-necked round-bottom flask containing a mixture of ethanol and Melaleuca Cajuputi essential oil (65 mL, v/v = 1.5/5) was filled with an optimal amount of $Zn(NO_3)2.6H_2O$. At 80°C, the mixture was refluxed while being stirred. The condenser was removed after an hour, and the mixture was swirled for two more hours at the same temperature until a precipitate formed and the color

darkened. After quickly adding 5 ml of deionized water and stirring the mixture for 15 minutes, it was allowed to cool to room temperature. ZnO MPs were obtained by centrifuging the precipitate and repeatedly washing it with a 95% ethanol solution.

3.2.3. Electrospinning PHB fibers

The electrospinning process was performed using laboratory-built equipment, including a high-voltage direct current (DC) source with a working range of approximately 0-25 kV (Figure SI2). A syringe pump propelled the polymer spinning solution through the needle's positively charged tip. The collector, a plexiglass substrate with a flat aluminum foil, acquired a negative charge. Each new electrospun membrane was placed on a new aluminum sheet. To ensure total solvent evaporation, PHB membranes were kept in a vacuum oven for 24 hours in the air and 10 hours at 40 degrees.

3.2.4. Methodology

The methodology adopted in this thesis is summarized in **Figure 3.1**.

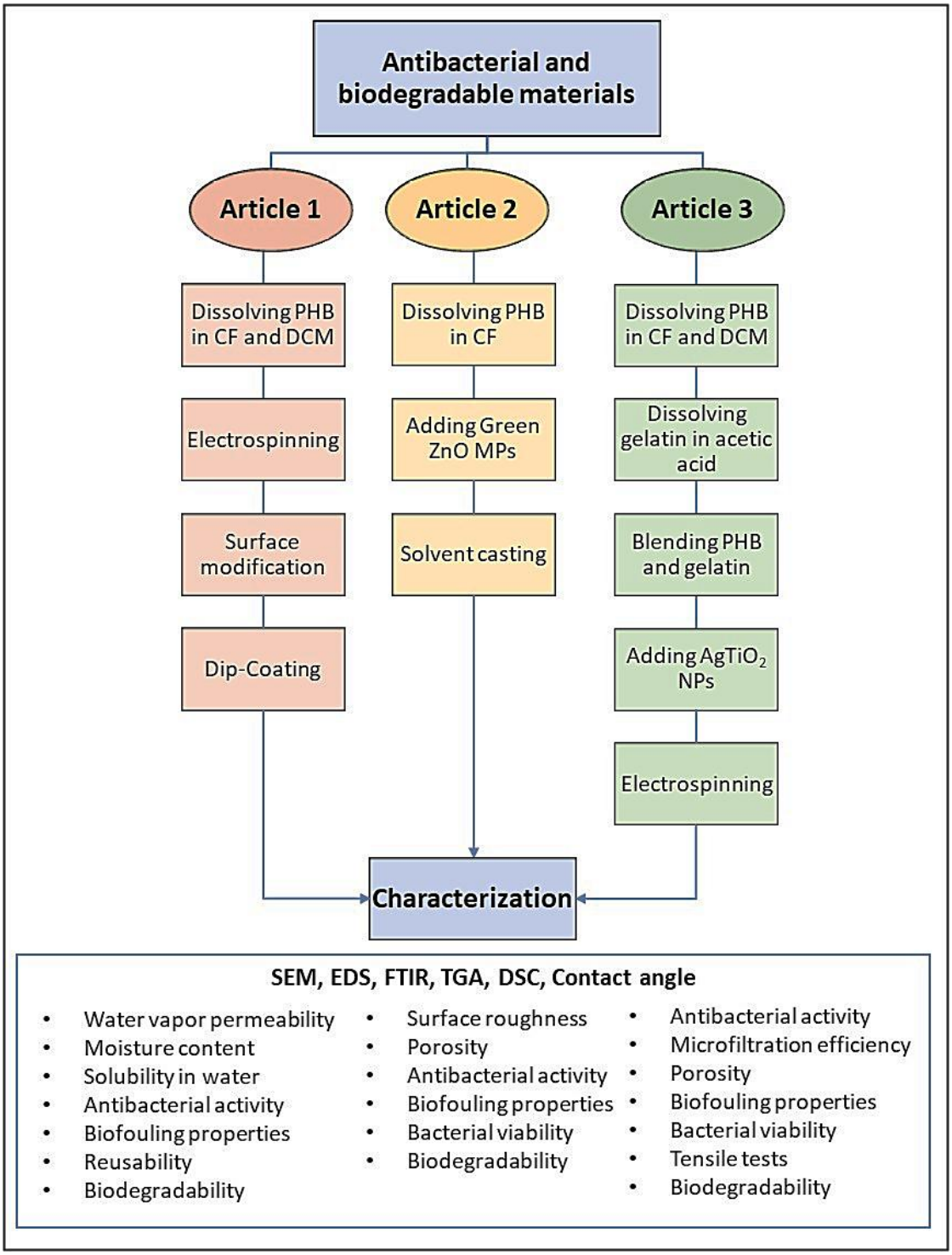

Figure 3.1: Summary diagram of the methodology adopted in this thesis

Chapter 4: Biodegradable polyhydroxybutyrate microfiber membranes decorated with photoactive Ag-TiO_2 nanoparticles for enhanced antibacterial and anti-biofouling activities

Safa Ladhari[a,b], Nhu-Nang Vu[a,b], Cédrik Boisvert[a,b], Marcos Antonio Polinarski[a,b], Camille Venne[a,b], Alireza Saidi[a,b,c], Simon Barnabe[a], Phuong Nguyen-tri[a,b]*

[a] *Department of Chemistry, Biochemistry, and Physics, Université du Québec à Trois-Rivières (UQTR), 3351 Boulevard des Forges, Trois-Rivières, Québec, G8Z 4M3, Canada*

[b] *Laboratory of Advanced Materials for Energy and Environment, Université du Québec à Trois-Rivières (UQTR), 3351 Boulevard des Forges, Trois-Rivières, Québec, G8Z 4M3, Canada*

[c] *Institut de Recherche Robert-Sauvé en Santé et Sécurité du Travail (IRSST), 505 Boulevard de Maisonneuve Ouest, Montréal, QC H3A 3C2, Canada*

*Email: phuong.nguyen-tri@uqtr.ca

Published in *Journal of Applied Polymer Science*, 2024, 5, doi:10.1002/app.55660.

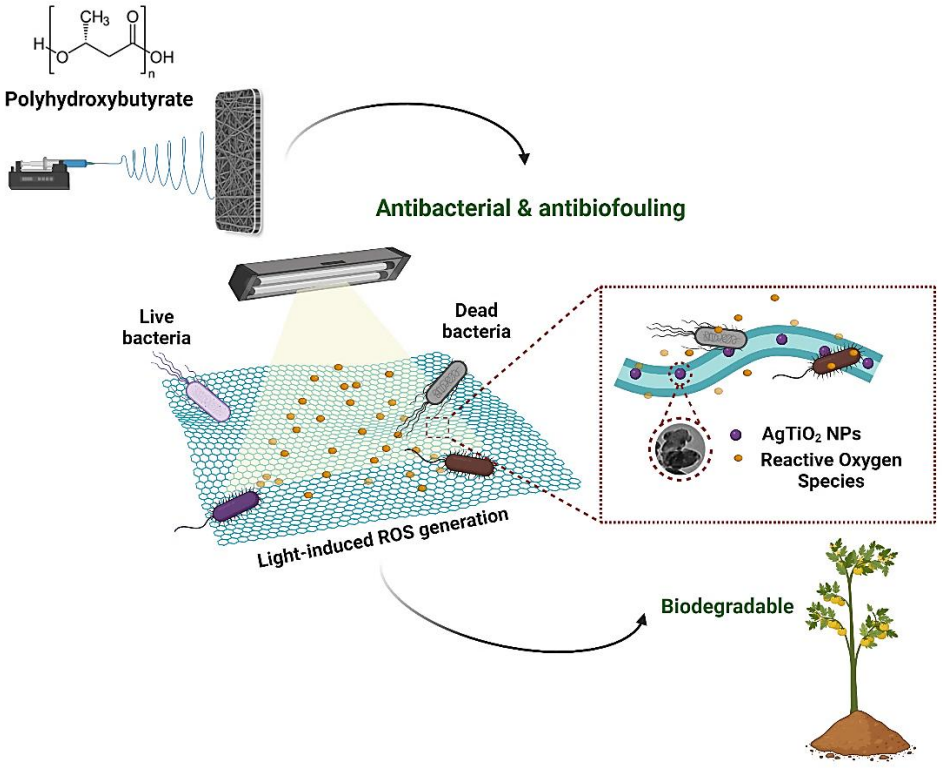

Résumé

Le développement de matériaux avancés dotés d'activités antibactériennes et antifouling offre une solution de protection adéquate contre la contamination bactérienne de surface - une cause courante d'infection menaçant la santé humaine. Les travaux actuels portent sur la préparation de membranes en microfibres de polyhydroxybutyrate (PHB) décorées de nanoparticules d'Ag-TiO_2 photoactives en utilisant l'électrofilage couplé à des méthodes de revêtement par immersion. La décoration de nanoparticules d'Ag-TiO_2 améliore fortement les propriétés antibactériennes des membranes préparées, en particulier sous illumination lumineuse, grâce à leur activité photocatalytique. L'échantillon le plus performant présente une efficacité antibactérienne puissante supérieure à 99 % contre *Escherichia coli* et *Staphylococcus epidermidis* après trois heures et une heure d'exposition à une lumière LED commerciale de faible puissance, respectivement. Les échantillons préparés présentent également une excellente réutilisabilité avec une diminution insignifiante de l'activité antibactérienne après trois cycles (<2% de perte d'efficacité antibactérienne). En outre, ces échantillons empêchent efficacement le colmatage bactérien grâce à leurs puissantes propriétés antibactériennes. Notamment, malgré le fort effet antibactérien, les nanoparticules Ag-TiO_2 décorées favorisent l'adhésion des micro-organismes, accélérant la biodégradation des microfibres de PHB. Par conséquent, les membranes en microfibres préparées avec des nanoparticules décorées présentent une biodégradabilité comparable à celle des membranes non décorées, avec des taux de dégradation du sol atteignant presque 99 % après seulement six semaines.

Abstract

Developing advanced materials with antibacterial and antifouling activities offers an adequate protection solution against surface bacterial contamination – a common cause of infection threatening human health. The current work reports the preparation of polyhydroxybutyrate (PHB) microfiber membranes decorated with photoactive Ag-TiO_2 nanoparticles using electrospinning coupled with dip-coating methods. The decoration of Ag-TiO_2 nanoparticles strongly enhances the antibacterial properties of prepared membranes, particularly under light illumination, thanks to their photocatalytic activity. The best-performing sample exhibits potent antibacterial efficiency exceeding 99% against *Escherichia coli* and *Staphylococcus epidermidis* after three hours and one hour of exposure to low-power commercial LED light, respectively. The prepared samples also display excellent reusability with an insignificant antibacterial activity decrease after three cycles (<2% loss in antibacterial efficiency). Furthermore, these samples effectively prevent bacterial fouling due to their potent antibacterial properties. Notably, despite the strong antibacterial effect, decorated Ag-TiO_2 nanoparticles promote the adhesion of microorganisms, accelerating the biodegradation of PHB microfibers. As a result, the prepared microfiber membranes with nanoparticle decoration exhibit biodegradability comparable to the non-decorated membrane, with the soil degradation rates reaching almost 99% after only six weeks.

4.1. Introduction

Protective equipment (PE), including face masks, protective suits, and shields, effectively reduces the risk of respiratory infectious diseases transmitted primarily through aerosol droplets. However, the actual PE can merely provide physical obstruction or electrostatic rejection of pathogens [1]. In addition, live infectious pathogens on the contaminated PE surface can lead to cross-contamination after reuse and even disposal. Communicable diseases include illnesses caused by bacteria, viruses, fungi, and other microorganisms. The new generation of PE should provide better antimicrobial protection that inhibits the transmission of pathogens and be reusable or disposable as required. With the growing threat of infectious diseases, developing new and improved PEs is essential to guarantee the highest level of safety.

Medicine, food, and textiles are the primary industries where antimicrobial agents are used. Different antimicrobial materials exist, such as coatings, membranes, ceramics, and plastics [2]. Polymeric materials, particularly biobased polymers, are attracting increasing attention from the scientific community for investigation and development in antibacterial applications. One of the main options considered is Poly([R]-3-hydroxyalkanoates) (PHAs), a large family of bio-polyesters produced instinctively by bacteria demonstrating biocompatibility and biodegradability [3]. Depending on the medicinal substance incorporated or conjugated, the application of PHAs has improved in controlled-release medication delivery, anti-inflammatory, antifungal, antimicrobial, anti-biomembrane, and virucidal fields [3].

Compared to non-biodegradable polymers, biodegradable polymers offer a significant advantage in terms of sustainability. As they can be naturally decomposed with microbes and added back to the soil to improve it, their usage can lower the labor costs of removal, stabilize the environment, and lengthen the lifespan of landfills. Moreover, through microbiological, enzymatic, and hydrolytic processing, they can be transformed back into functional oligomers for other applications. The simplest poly (3-hydroxy alkanoates) family member is the semi-crystalline thermoplastic biopolyester known as poly (3-hydroxybutyrate, or PHB). This polymer has similar properties to conventional plastics, but it is a renewable, biocompatible, and linear thermoplastic with low oxygen and water permeability, which provides attractive barrier properties compared to other polyesters [3]. Moreover, it exhibits superior renewability, biodegradability, and biocompatibility compared to other biodegradable aliphatic polyesters (such as polylactic acid PLA and polycaprolactone PCL) [4]. These characteristics make PHB ideal for various applications. PHB

membranes have been extensively produced using the electrospinning technique. This method can produce materials by creating ultrafine fibers, forming a dense, highly porous structure. These materials are ideal for applications such as filters, face masks, and other similar protective gear that offer excellent barrier properties against pathogens, chemical substances, and other hazardous materials [3]. The major limitation of PHB is that it does not possess intrinsically antibacterial, antifungal, or antioxidant capabilities.

Interest in creating potent antibacterial properties for polymeric materials by incorporating metal-based nanoparticles (NPs) have received considerable attention in recent years. Metal-based NPs can induce various antibacterial mechanisms, leading to strong antibacterial potency against a wide range of bacteria [5]. In addition, the nanometric size and large surface area facilitate their incorporation onto various types of surfaces to form antibacterial coatings (e.g., fibers, and films), which are potential for fabricating PE [6, 7]. Among various developed NPs, Ag NPs have been extensively employed for biological applications due to their potent antibacterial activity at lower concentrations and their being non-toxic and non-allergic. Several types of Ag NPs have been administered by the US Food and Drug Administration (FDA) for commercial use [8]. Notably, owing to the surface plasmonic resonance (SPR) effect, Ag NPs can generate charge carriers like electrons (e^-) and holes (h^+), which trigger redox reactions, producing reactive oxygen species – strong antibacterial agents [9]. More interestingly, depositing these NPs on TiO_2 NPs induces a hybrid composite nanostructure that effectively promotes the separation of charge carriers to enhance the production of Reactive Oxygen Species (ROS), resulting in excellent antibacterial activity [10, 11]. For these reasons, incorporating hybrid Ag-TiO_2 NPs into polymeric materials could generate efficient and stable antibacterial performance based on the photoactive effect of these NPs. To date, submicron polymer fibers composed of vinyl alcohol [12], poly-(L-lactide) [13], or poly(ε-caprolactone) [14] and PHB [15, 16], incorporated with Ag NPs have been widely developed for antibacterial applications. However, reports on the fabrication of electrospun fibers incorporated with $AgTiO_2$ NPs and assessment of their antibacterial activity have still been limited.

The work herein reports an ecological preparation of innovative PHB microfiber membranes decorated with hybrid Ag-TiO_2 NPs (Ag@T NPs) using the electrospinning technique coupled with a simple dip-coating process. The introduction of Ag@T NPs enhanced the antibacterial activities of prepared membranes against two bacterial strains, including Escherichia coli and Staphylococcus aureus. These prepared membranes also displayed strong antifouling

properties and excellent biodegradability. The current work could inspire the development of reusable and sustainable PEs with significant bioprotective and biodegradable characteristics.

4.2. Materials and methods

4.2.1. Materials

Poly(3-hydroxybutyrate) (PHB) with a weight-average molecular mass (Mw) of 550 Kg/mol and polydispersity index (PI) of 1.2 was purchased in pellet form from Goodfellow (Huntingdon, England). Dichloromethane (purity ≥99.8%) and chloroform (purity ≥99.8%), used to dissolve PHB, were supplied by Alfa Aesar (Mississauga, United States) and Thermo Scientific (United States), respectively. For biological tests, Escherichia Coli (ATCC 11229) and Staphylococcus epidermidis (ATCC 12228) were purchased from Cedarlane (Southern Ontario, Canada). Additionally, tryptic soy agar (TSA) and bactotryptic soy broth (TSB) were provided by Sigma Aldrich. Ag@T NPs (Figure SI1) are prepared following the process developed by our group, which is summarized in Supporting Information.

4.2.2. Preparation of $AgTiO_2$-Based Coatings on PHB electrospun membranes

PHB pellets were dissolved in a (1:1) chloroform/dichloromethane co-solvent and stirred for 24 hours by heating at 60 °C using a reflux condenser before the next steps. The final polymer solution of (1,4 g; 7% by w/v) PHB was spilled into a syringe with a metallic needle to prepare fiber membranes. The electrospinning technique was achieved with a laboratory-built device containing a high-voltage direct current (DC) source with a working range of about 0-25 kV) **(Figure SI2)**. A syringe pump drove the polymer spinning solution through the needle's tip positively charged. The collector, a plexiglass substrate covered by a flat aluminum foil, received the negative charge. Each new electrospun membrane was collected on a new aluminum sheet. Table SI1 describes the electrospinning process conditions. To ensure solvent evaporation, PHB membranes were left in a vacuum oven for 24h in air and 10h at 40°C.

Surface activation of PHB membranes was performed under oxygen plasma at radiofrequency electromagnetic radiation (RF) of 80W for 2 minutes using PE-50 Venus Plasma Etcher. After the plasma treatment, these membranes were coated with Ag@T NPs using Ossila Dip Coater L2006A1-UK. In detail, plasma-treated PHB membranes were immersed in the suspension of Ag@T NPs (0,06 mg/mL) at room temperature (23°C) for 30 minutes at a constant speed of 20 mm/s and extracted with a controlled withdrawal speed of 10 mm/min. This dip-coating

was repeated 2-3 times to increase the deposition of Ag@T NPs. Between each time, PHB membranes were air-dried for 30 minutes. After the dip-coating, treated membranes were air-dried for 24 h **(Figure 4.1)**. Obtained PHB membranes were named PATx, where x is the number of dip-coating cycles.

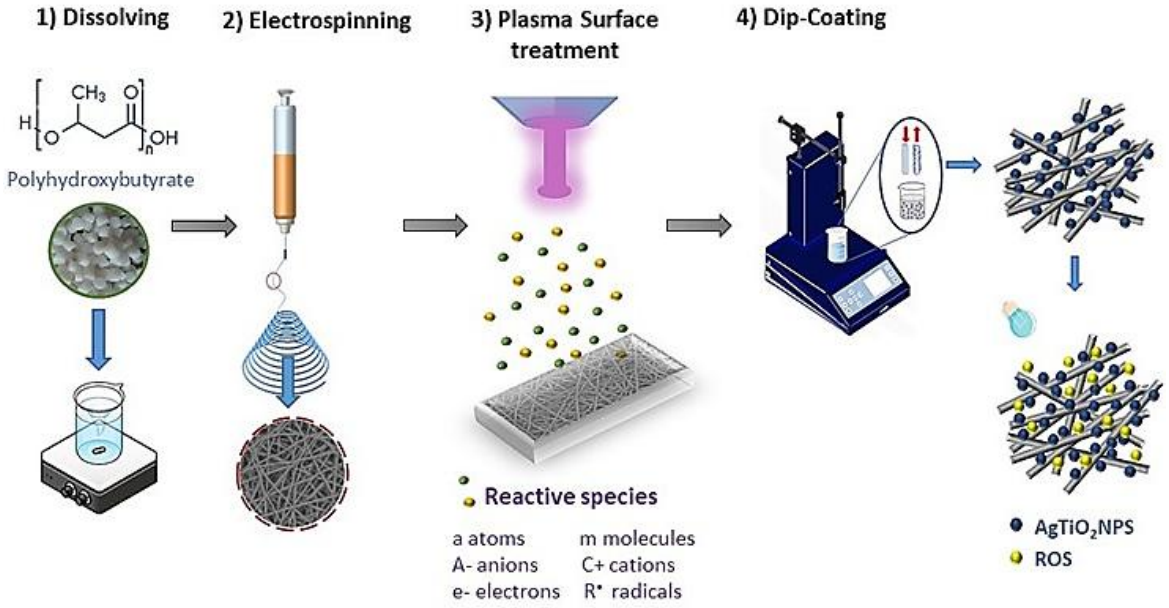

Figure 4.1: Different PHB-Ag@T membrane preparation steps.

4.2.3. Characterization

Morphological analysis of prepared PHB electrospun fibers was examined using a scanning electron microscope (SEM) (JEOL-JSM 5500). PHB samples were cut into 1 cm × 1 cm pieces mounted on aluminium stumps, and a thin coating of (around 2–20 nm) was applied for 15 seconds. The structural interaction of PHB membranes was studied by Attenuated Total Reflectance-Fourier transform infrared spectroscopy FTIR, ATR mode using an infrared spectrophotometer (FTS 45). The membrane membranes were attached to the sample holder, and the recorded spectra were measured over a wavenumber starting from 400 to 4000 cm^{-1} at room temperature. The surface wettability of prepared PHB membranes was established using the Surface Energy (Theta Flex optical tensiometer by Attension) to measure the water contact angle (WCA). The 5.0 ± 0.2 µL volume water drop was deposited on a 4 cm^2 PHB membrane by automatic pipetting. The grammage and thickness of membrane membranes were investigated according to the reported method [17]. First, according to ISO 536:1995, the membranes' mass-to-area ratio (g/m^2) was used to determine their grammage. Then, the thickness (µm) was measured using a micrometer (TMI,

model 549E, Amityville, New York, USA) following ISO 534:2011., with ten random measurements being tested. Thermogravimetric analysis (TGA) tests in a nitrogen atmosphere with a 20 mL/min gas flow rate were realized using a Perkin Elmer TGA (Perkin Elmer Instruments, USA) to test the control and treated membranes' mass loss and derivative mass loss. PHB membranes were heated at 10°C/min from 30 to 600°C.

4.2.3.1. Water vapor permeability (WVP), moisture content, and solubility in water

Water vapor permeability (WVP) (g.mm/h. m^2.Pa) of the prepared PHB membranes was determined using a simple method reported previously [18]. Initially, 4 cm^2 of treated membranes were placed to seal the heads of glass bottles filled with distilled water (10 mL). After that, these bottles were set in the desiccator containing silica gel lumps to determine their weight loss as a function of time and were weighed every two hours until they created a steady state. The following equation was used to determine the WVP of the PHB membranes:

$$WVP = (S \times d) \div (A \times \Delta P) \qquad \text{Equation 4.1}$$

where S (g/h) is the weight loss slope vs. time, d (m) is the membrane thickness, and A (m^2) is the permeation area. The water vapor pressure differential across the membranes is represented by ΔP, which equals 2.33×10^3 Pa, assuming that the relative humidity on the silica gel is negligible.

4.2.3.2. Antibacterial activity and reusability study

The antibacterial efficacy of prepared PHB membranes was evaluated against *S. epidermidis* and *E. coli* using an agar plate test, following the procedure reported previously [19]. Before starting the test, all materials and equipment were sterilized under UV light for 30 minutes. The prepared samples (2 cm x 2 cm), including non-treated PHB membranes and PHB membranes treated with Ag@T NPs, were placed in wells (Inner diameter = 3.5 cm, Dept = 1.7 cm) of the 6-well plate. Next, two wells were dropped with 100 µL bacterial suspension ($1.5\ 10^5$ CFU mL), followed by adding 1 mL of physiological saline to all wells. The 6-well plate was then placed under the white light irradiation produced by the LED-L16 Photoreactor (4,8 mW/cm^2 of intensity, Luzchem Inc.). After specific irradiation periods, 2 mL of physiological saline was added to each

well, and 100 µL of the combined solution was spread onto agar plates, followed by a 24-hour incubation period at 37°C. The average of three replicates is used to report the results. The antibacterial activity of these samples was also performed in a similar procedure but in the dark.

For reusability tests, treated membranes were rinsed after the antibacterial tests with deionized water and dried overnight at room temperature for subsequent antibacterial tests. Before starting each new antibacterial test, the membranes were sterilized with UV light. Then, the following tests were carried out. The reusability test against *E. coli* was performed for 3 hours of treatment, while it was one hour against *S. epidermidis*.

4.2.3.3. Biofouling tests

To evaluate bacterial adhesion and biomembrane formation onto the treated PHB membranes, they were dipped into tubes containing 100 µL of bacteria culture (10^8 cells/mL) and 2 ml of TSB. The resulting tubes were incubated at 37 °C for five days. Afterward, samples were washed three times with distilled water to remove detached cells. First, the cells were immobilized in the specimens for 1 hour using 5% (v/v) formaldehyde in a sodium cacodylate buffer (0.2 M, pH 7.4) at room temperature in preparation for SEM analysis. After multiple washes with sodium cacodylate buffer, they underwent sequential treatments with 25, 50, 70, 90, and 100% ethanol concentrations to dehydrate. Finally, the samples were sputter-coated with gold membrane and analyzed with a scanning electron microscope (JEOL-JSM 5500).

4.2.3.4. Biodegradability

A soil burial degradation test was performed, as reported by Kumar et al. [20]. The membranes of 4 cm^2 were buried in a rectangular container containing natural soil (from UQTR University Campus, Canada). The membranes were buried at a depth of 8 cm from the surface. The temperature was 23 °C, and the relative humidity was around 40%. At predetermined intervals of 2 weeks, the samples were removed from the soil, cleaned thoroughly with deionized water, and then dried for 24 hours at 50°C in an oven. Finally, the membrane samples were weighed to determine the weight loss using the equation 4.2:

$$\text{Weight loss (\%)} = (W_{initial} - W_{final}) \div W_{initial} \times 100 \qquad \text{Equation 4.2}$$

Where $W_{initial}$ is the initial mass, W_{final} is the final mass (after burial and drying) at a predetermined time t.

4.3. Results and discussions

4.3.1. Membrane characterizations

The main electrospinning parameters, including solution and apparatus parameters, were carefully adjusted to avoid creating solid particles generated by electrospraying, a combination of fibers and particles (electrospraying/electrospinning effect), or beaded fibers **(Table SI 4.1)**.

Figures 4.2 (a, c, d, e, and f) show SEM images of PHB randomly oriented microfibers with an average fiber diameter of 1,19 ± 0,24 µm. The increased immersion into the suspension of Ag@T NPs resulted in more significant loading with antibacterial agents, as seen in the SEM images of the treated samples in **Figures 4.2 (b, c, and d)**. Additionally, it can be seen that Ag@T NPs are gathered in agglomerated clusters. The treatment of PHB membranes with oxygen plasma led to a slight change in the microfibers' physical structure, as reported [21]. As seen in **Figure 4.2 e**, the plasma process caused etching and a slight diameter reduction of the fibers. Even though plasma modification has been employed extensively over the past ten years, it can still add originality and difference to the field of fiber surface engineering if the modification parameters are appropriately regulated. Generally, the plasma treatment initiates only the surface modification, affecting a depth range of several hundred Å to 10 µm without altering the material's natural properties [22]. Although, a severe fiber etching and diameter reduction could be observed at harsh plasma conditions, resulting in fiber rupture at higher voltages or a more prolonged treatment time. In fact, for plasma treatment exceeding 3 min, an extreme fiber degradation resulting in fiber rupture was detected **(Figure 4.2 f)**.

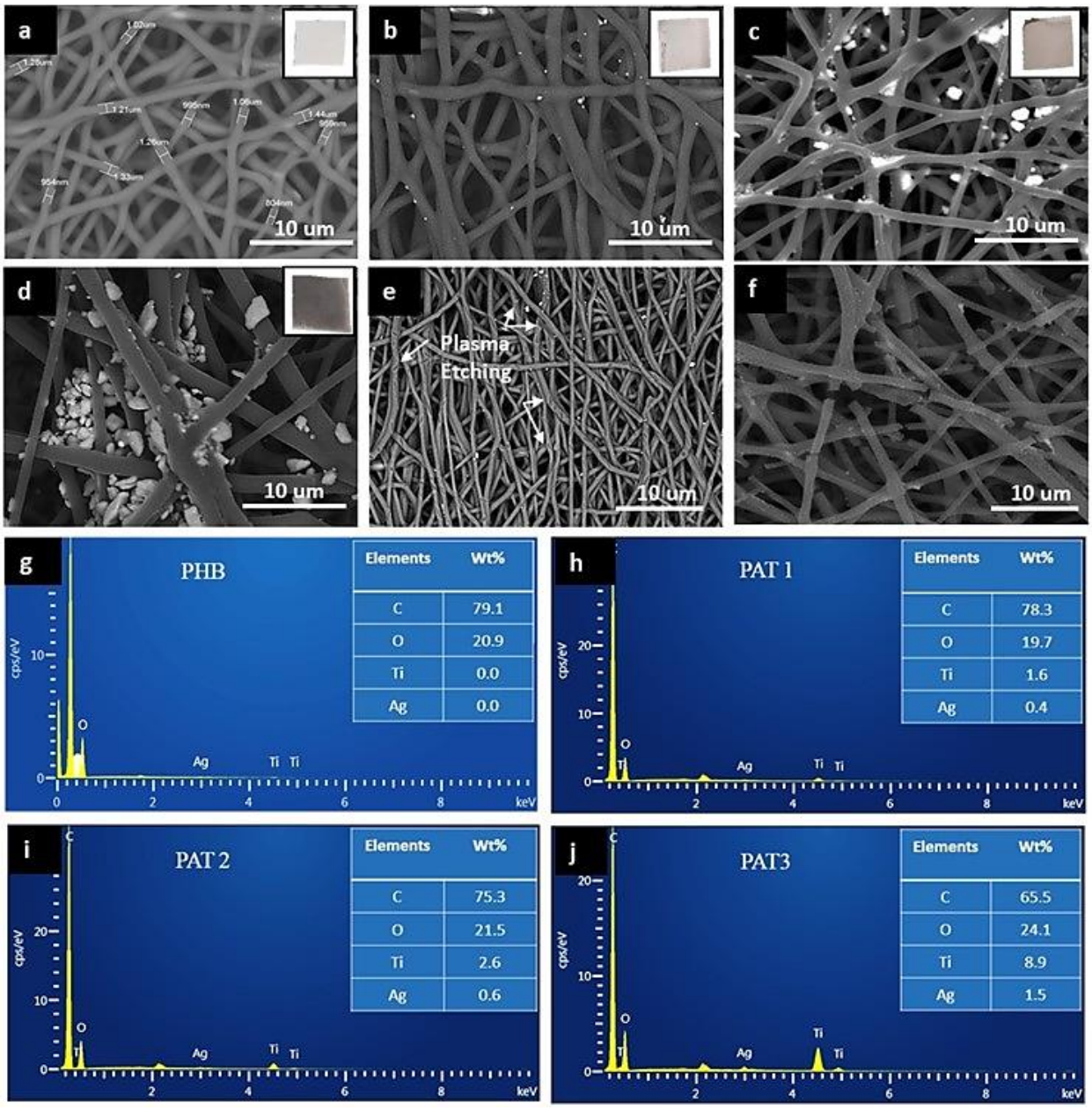

Figure 4.2: SEM images of electrospun membranes: (a) unmodified PHB fibers, (b) PAT1, (c) PAT2, and (d) PAT3, (e) Mild surface etching of PAT1 fibers, (f) extreme PAT1 fiber degradation after 4min of plasma treatment, RF 80W, EDX tabulated data of: (g) unmodified PHB fibers, (h) PAT1, (i) PAT2, and (j) PAT3 membranes.

The chemical composition of treated PHB was evaluated using the EDX technique, as presented in **Figures 4.2 (g, h, i, and j)**. The analysis of these spectra indicates the existence of different amounts of titanium, oxygen, carbon, and silver elements. The titanium and silver content values increase in membranes with the number of dip-coating.

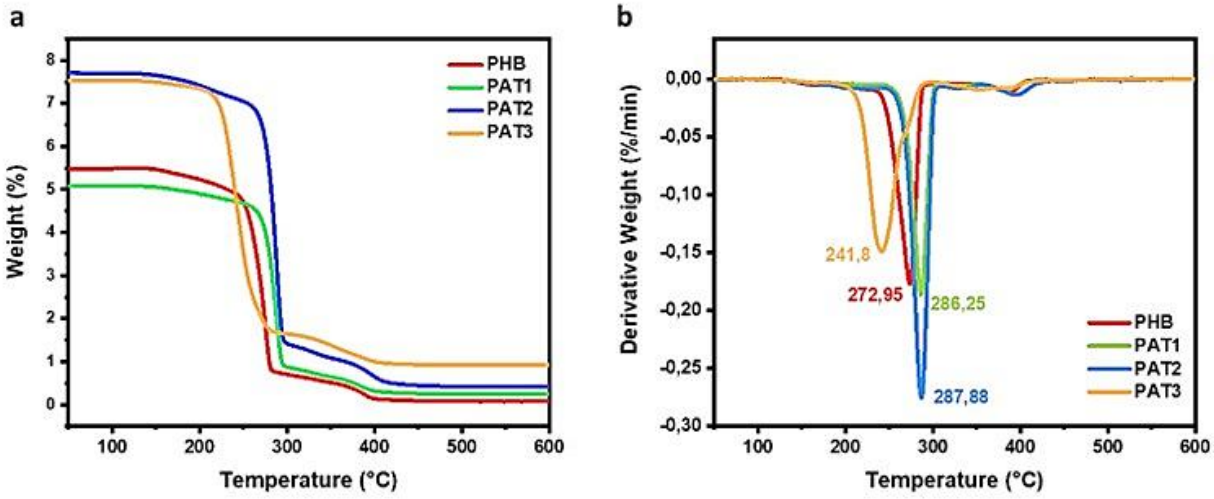

Figure 4.3: (a) TGA and (b) Derivative thermogravimetry (DTG) curves of PHB, PAT1, PAT2, and PAT3

To ascertain the ideal processing temperature, the membranes' shelf life, their capacity for recycling, and the best way of disposal, thermal degradations of untreated PHB and dip-coated membranes were studied by TGA and DTG analysis. **Figures 4.3 a and b** display curves in weight loss due to controlled heating (versus temperature) for untreated PHB and dip-coated membranes. The onset degradation temperature (T_{onset}) at which thermal degradation starts, the temperature at the maximum degradation rate (T_{max}), the temperature at which thermal degradation is complete (T_{endset}), and the residue at 500°C (R) are summarized in **Table 4.1**.

Table 4.1: Thermal parameters obtained from thermogravimetric analysis.

Designation	***Decomposition temperature (°C)***			***Residual weight (%) at 500 °C***
	T_{onset}	**T_{max}**	**T_{endset}**	
PHB	260.34	272.95	387.33	0.07
PAT1	273.70	286.25	388.82	0.25
PAT2	274.60	287.88	394.25	0.41
PAT3	223.43	241.80	395.85	0.93

As was observed in **Figure 4.3**, the thermal degradation mechanism of electrospun membranes involves two degradation stages. In the first stage, ranging between 100º-200ºC, PHB membranes degraded according to a random scission kinetic model, but eventually, low molecular weight compound function caused auto-acceleration of pyrolysis [23, 24]. In the second stage, severe

degradation of olefinic and carboxylic acid compounds, such as crotonic acid and different oligomers, followed by the production of their degraded products through the random chain scission reaction, which involved a six-member ring transition and a b-CH cis-elimination response. Then, the free carboxylic acid of the 3-hydroxybutyric acid unit released proton acid (H^+), which acts as an electrophile and increases with the rise of the low molecular weight degradation products. Thus, the chain scission reaction of PHB molecules may be accelerated with degradation time [24].

The TGA analysis examined the effect of Ag@T NPs on the thermal degradation behaviors of PHB membranes with increased Ag@T NPs concentrations. The starting temperature of thermal decomposition rises with the increase in Ag@T NPs content expressed by T_{onset} **(Table 4.1)**, indicating that the degradation temperature of PHB samples strongly depends on the amount of Ag@T NPs. As described by Abe [24], metal ions like Ag^{2+} are known to be Lewis acids, and they act as electrophiles. By removing the β -hydrogen, the Lewis acid interacts with carboxyl groups to enable the production of the double bond found in the crotonyl unit. Therefore, in the presence of metal compounds like Ag^{2+}, a chain scission reaction of PHB molecules was enhanced. Moreover, as Moon et al. [23] reported, TiO_2 nanofillers boost the heat transfer characteristics from the heat source toward the inside of the polymer. For these reasons, the thermal degradation of PHB increased, as is the case for PAT3. Regarding low Ag@T NP concentrations, PAT1 and PAT2 exhibit higher thermal stability. Finally, it should be highlighted that no degradation occurred under 200 °C. PAT membranes are thermally stable and do not risk thermal degradation.

The unmodified PHB membrane is a hydrophobic material with a surface contact angle of 145.7° [25-27]. The plasma modification of the PHB membrane surface (RF 80W and 2 min), used as the first step of the modification process, induced a sharp decrease in the original contact angle, and the surface became utterly hydrophilic (contact angle < 30°) **(Figure 4.4 a)**. Plasma treatment can form new chemical groups that are naturally hydrophilic, like carboxylic acid (-COOH) groups, on the polymer surface by bond-breaking reactions [28]. For plasma treatment exceeding 3 min **(Figure 4.4 a)**, notable damage to the PHB membrane was observed, as shown in **Figure 4.2 f**. Then, the plasma-activated samples were used as substrates for consequent coating with antibacterial agents by dip-coating into the dispersion of Ag@T NPs. The influence of increasing Ag@T NPs concentrations on the wettability of plasma-modified membranes is introduced in **Figure 4.4 b**. With the increasing immersion of the plasma-treated membrane into the dispersion

of Ag@T NPs, the contact angle of the coated surfaces decreases for PAT1 and PAT2. This effect corresponds to the formation of discontinuous metal clusters on the polymer surface. The contact angles of the coated surface were determined to be 126.9° and 122.3° for PAT1 and PAT2, respectively. For PAT3, the WCA of the coated surfaces remarkably decreases to 37.92°. This effect corresponds to the formation of metal clusters agglomeration on the polymer surface (as observed in **Figure 4.2 d**), which could leave free hydrogen bonds produced by plasma treatment to be linked to water drop.

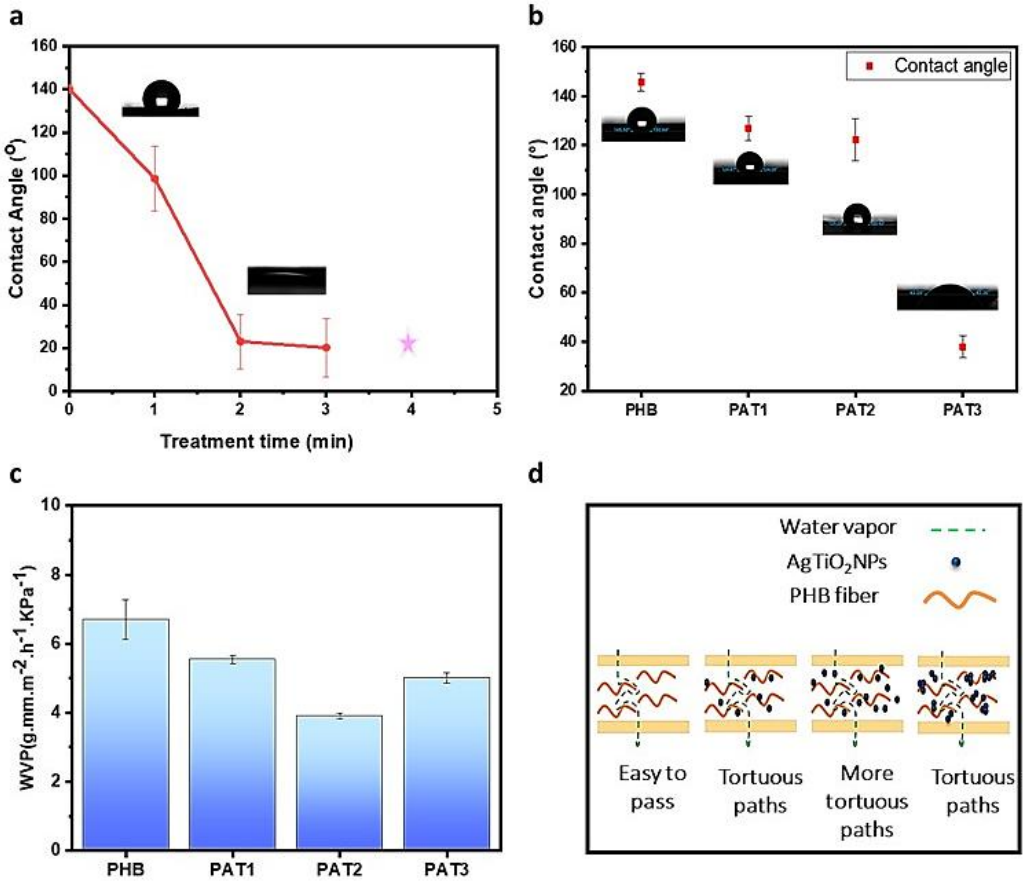

Figure 4.4: (a) WCA of untreated PHB membrane varying the plasma-treatment time, (b) WCA of untreated PHB and dip-coated membranes, (c) water vapor permeability (WVP) of membranes, and (d) schematic diagram of water vapor transmission.

Water vapor permeability (WVP) is an important parameter to evaluate the barrier ability of membranes to water molecules, generally referred to as the breathability parameter. An optimal WVP value for personal protective equipment is needed as it influences wearing comfort. Several parameters, such as chemical structure, molecular weight, size, etc., affect the membrane matrix's

moisture content and molecules' mobility [29]. In this current study, all the membranes depict WVP values between 1 and 10 g.mm/h. m^2. Pa, indicating that they are semi-permeable materials. As observed in **Figure 4.4 c**, with the addition of Ag@T NPs in PHB membranes, the WPV decreases. In addition, the WVPs of the plasma-treated membranes dip-coated with Ag@T NPs are smaller than that of the untreated PHB membrane without the antibacterial nanoparticles. For both PAT1 and PAT2, their WVP values gradually decrease with the increase in the Ag@T concentration. This reduction is reportedly due to the formation of hydrogen bonding between plasma treated PHB membrane and Ag@T NPs, which decreases the water affinity of coated membranes. These interactions may decrease the polymeric matrix's free volume and create a denser matrix, reducing the rate at which water molecules diffuse through the electrospun membrane [30]. In agreement with our findings, increasing gallnut extract from 2.5 to 50 wt% decreased the WVP of sodium alginate membranes [31]. The same results were found when increasing Chinese hawthorn extract from 2 to 4 wt% into chitosan-gelatin blend membranes [32]. As depicted in **Figure 4.4 e**, adding Ag@T NPs filled the inter-fiber voids. Subsequently, it provided more tortuous paths for the water vapor to pass through [31, 33], thus decreasing the WVP value. However, the WVP value of PAT3 is slightly higher than that of PAT2, considering many more nanoparticles aggregated in the PHB matrix. It was assumed that agglomerating particles may have forced the polymer chains apart, creating a wider passageway for the water molecules. Despite the slight increase, the WVP value remained lower than the untreated PHB membrane, as explained similarly in Ref [34].

4.3.2. Antibacterial activity and reusability potential of the prepared microfibers

The antibacterial properties of untreated and treated PHB fibers against *E. coli* and *S. epidermidis* were determined using agar plate tests. **Figures 4.5 a and b** show the antibacterial properties against *E. coli*, and **Figures 4.5 c** and d show the antibacterial properties against *S. epidermidis*. Untreated PHB exhibited less antibacterial activity than treated membranes against both strains. **Figure SI 4.5** shows almost no colonies on samples PAT2 and PAT3. Furthermore, the colonies' number of bacteria is reduced from PAT1 to PAT3, with significant bacterial development suppression with PAT2 and PAT3 samples. This indicates that decorating Ag@T NPs on PHB fibers increases the antibacterial activity of electrospun membranes. Moreover, using Ag@T NPs on a nanometric scale produces larger surface areas, which could accelerate the damage and wrinkling of bacterial cell walls [35]. Moreover, when exposed to visible light, Ag@T NPs can generate (ROS) via oxidation-reduction reactions, and these include hydroxyl radicals (•OH) and

superoxide radicals ($O_2^{\bullet-}$). ROS are highly oxidative molecules that can rupture bacterial cell membranes and damage biomolecules, contributing to cell death [36].

The Ag@T NPs content was the main factor influencing the antibacterial activity of membranes. The treated PHB membranes demonstrated efficient bacterial death against *E. Coli* under the 3 hours light irradiation condition while only 1-hour light irradiation condition against *S. epidermidis*. This difference in antibacterial impact between Gram-positive and Gram-negative bacteria is mainly caused by variations in their cell wall structures, as previously reported by Siripatrawan and Vitchayakitti [37]. The peptidoglycan and acidic polysaccharides (teichoic acids) that make up the exterior cell wall of gram-positive bacteria have many pores that may facilitate the adherence or penetration of bioactive molecules into the cell. Moreover, gram-negative bacteria have an additional outer membrane, in addition to their cell membrane, made of proteins, lipids, and lipopolysaccharide that may serve as a barrier to the entry of bioactive chemicals into the cell [31, 38]. Kundrat et al. [39] also reported a difference in bacterial efficiency between gram-negative and gram-positive bacteria when incorporating levofloxacin into PHB electrospun meshes.

Furthermore, the bacterial survivability was evaluated using light irradiation. In the absence of light, the antibacterial activity of PHB membranes was only affected by the content of Ag@T NPs. The resulting PHB-Ag@T displayed light-enhanced and time-dependent antibacterial activity against *E. coli* and *S. epidermidis*. The best antibacterial effect was found for PAT2 and PAT3 against *E. coli* after 3 hours of treatment, with 98.59% and 99.60%, respectively, in the dark and 99.49% and 99.98% under the light. On the other hand, bacterial tests against *S. epidermidis* showed more effective antibacterial efficiency after only 1 hour for PAT2 and PAT3, with 97.03% and 99.90% %, respectively, in the dark and 99.5% and 99.95%, respectively, under the light. In fact, Ag@T NPs may produce ROS during light irradiation. ROS are proven to cause oxidative stress, which may deteriorate bacterial membrane integrity and, as a result, present more significant antibacterial activity [40]. A rapid test was performed to confirm the formation of hydroxyl radicals ($OH\cdot$), the most potent oxidant among the ROS species [41], using the p-nitrosodimethylaniline (p-NDA) – one of the selective scavengers of these radicals [42]. The procedure of this test was illustrated and detailed in SI. As seen in **Figure SI 4.3**, the concentration of p-NDA was considerably decreased after contact with PAT membranes. Moreover, this decrease is much higher than that induced by the untreated PHB membrane. This result reveals the effective formation of

OH· due to the photocatalysis triggered by incorporated Ag@T NPs, which led to the high antibacterial activity of treated membranes under light irradiation.

Also worth noting is that the plasma treatment has little effect on antibacterial efficacity, as Slepička et al. [43] reported, stating that plasma activation did not affect Gram-negative bacteria of *E. coli* and had a moderate impact on the inhibition of bacterial growth of *S. epidermidis*. Overall, PHB-Ag@T membranes showed good antimicrobial efficacy against both gram bacteria, indicating their good potential as an antibacterial material.

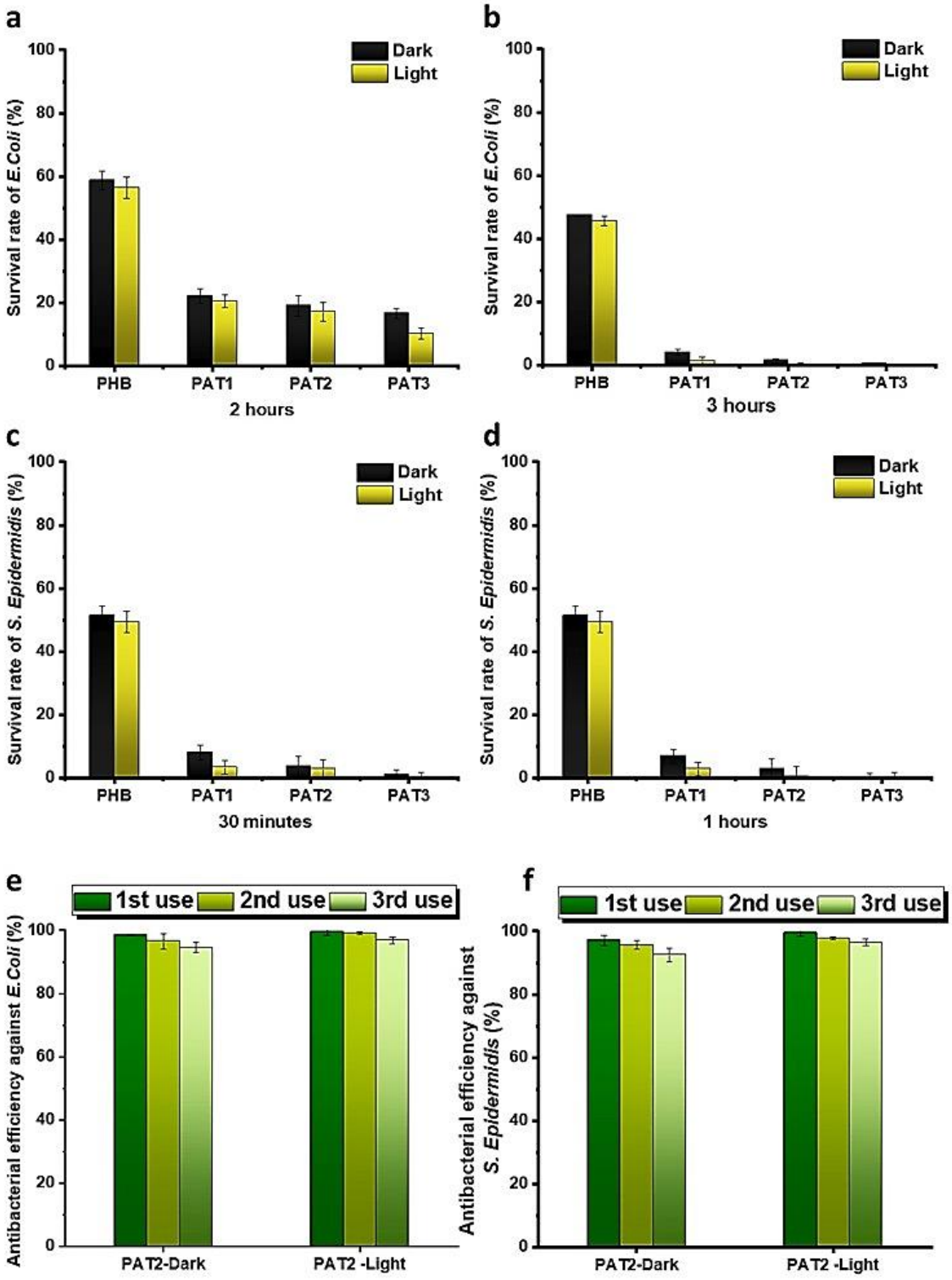

Figure 4.5: (a) survival rate (%) of *E. Coli* by different membranes for 2 hours of treatment in dark and light conditions, (b) survival rate (%) of *E. Coli* by different membranes for 3 hours of treatment in the dark and light conditions, (c) survival rate (%) of *S. Epidermidis* by different

membranes for 30 minutes treatment in the dark and light conditions, (d) survival rate (%) of *S. Epidermidis* by different membranes for 1-hour treatment in the dark and light conditions, (e) Reusability performance of treated PAT2 under light and dark conditions for three following antibacterial tests against *E. Coli*, (f) Reusability performance of treated PAT2 under light and dark conditions for three following antibacterial tests against *S. Epidermidis*

The reusability of nanofibrous membranes is a critical aspect of antibacterial efficiency, as it is an essential issue for long-term use in practical applications and economic improvement, especially on an industrial scale. Thus, multiple antibacterial tests were carried out to evaluate the performance of the treated PHB membranes. **Figures 4.5 e and f** show the antibacterial properties of PAT2 membranes are slightly reduced after three subsequent antibacterial measurements.

On the other hand, PAT2 and PAT3 show the best antibacterial stability after three successive tests, especially under light, with 96.77% and 97.09% against *E. Coli* and 96.42% and 97.89%, respectively, against *S. Epidermidis* **(Figure 4.6)**. Nevertheless, the results demonstrate that the treated PHB electrospun membranes can be reused several times without significant loss of antibacterial efficacity. This is, therefore, opening meaningful opportunities for industrial applications. Furthermore, it presents a promising new nonwoven material that can be used in reusable and antibacterial protective equipment for improving protection against the transmission of infectious diseases.

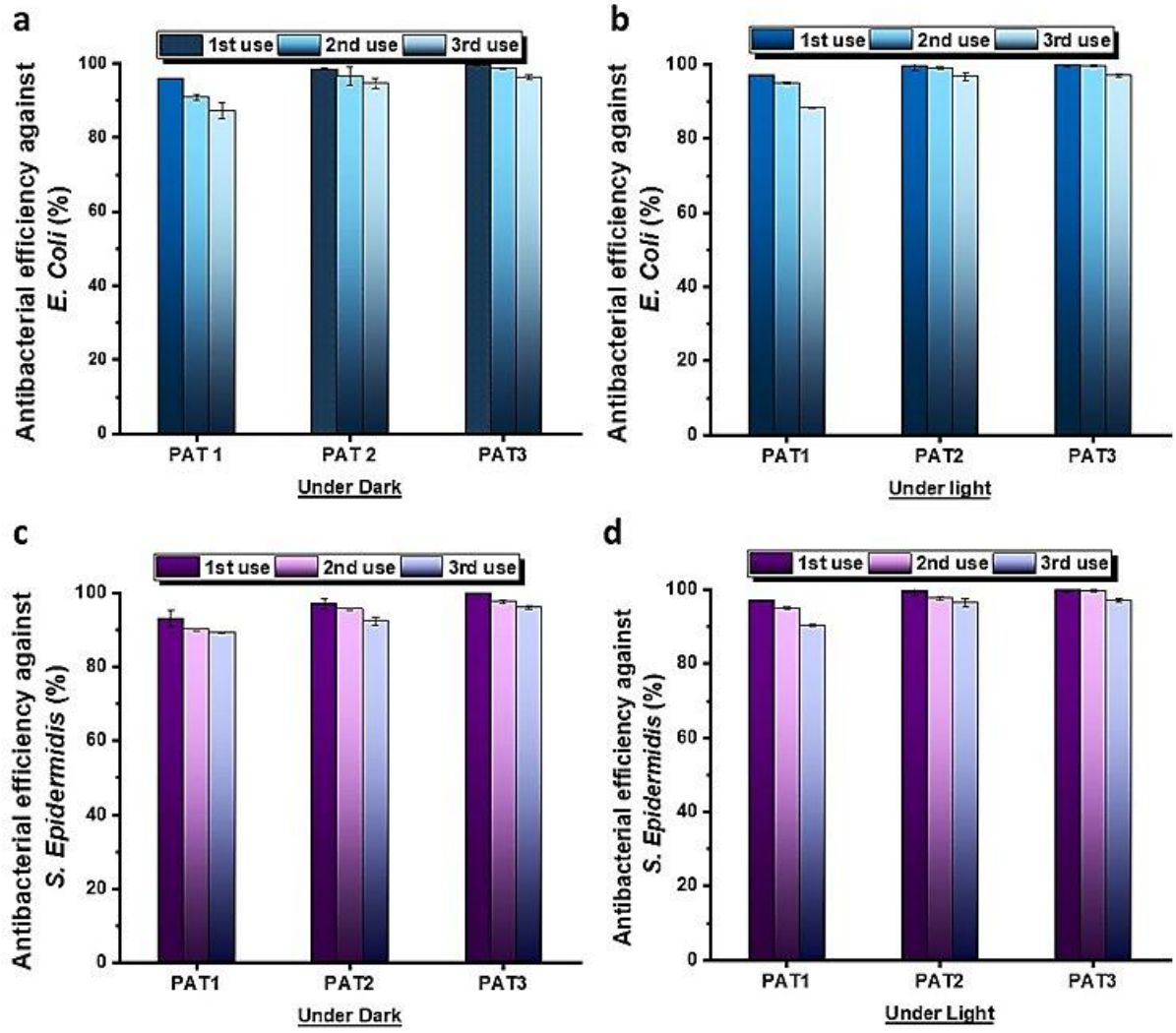

Figure 4.6: (a) Reusability performance of treated PAT1, PAT2, and PAT3 under dark conditions for three following antibacterial tests against *E. Coli*, (b) Reusability performance of treated PAT1, PAT2, and PAT3 under light conditions for three following antibacterial tests against *E. Coli*, (c) Reusability performance of treated PAT1, PAT2, and PAT3 under dark conditions for three following antibacterial tests against *S. Epidermidis*, (d) Reusability performance of treated PAT1, PAT2, and PAT3 under dark conditions for three following antibacterial tests against *S. Epidermidis*.

4.3.3. Anti-Biofouling performance of PHB-Ag@T membranes

Biomembranes are created on the membrane surfaces due to the colonization and proliferation of biologically active organisms, known as biofouling. It reduces membrane efficiency and the lifespan of the membranes. **Figure 4.7** shows that bacterial adhesion of the two

bacteria strains, *E. Coli* and *S. Epidermidis*, is extreme on untreated PHB membranes surface. However, many bacteria do not entirely cover all membrane samples, and severe biomembrane cannot be formed. Compared to untreated PHB membranes, the number of bacteria adhering to PAT1, PAT2, and PAT3 surfaces is relatively low. Furthermore, the bacterial adhesions on the PAT surface effectively diminished with the increase of Ag@T content, while that of PAT2 is slightly higher than that of PAT3. The above result demonstrates that the antibacterial NPs could enhance the membrane resistance to bacterial adhesion. Furthermore, it was visible that coating PHB membranes with Ag@T NPs effectively strengthened the anti-biofouling performance of the membrane.

In fact, two surface modification techniques to reduce the biofouling potential of polymer membranes exist [44]. The first strategy uses an anti-adhesion method to reduce membrane biofouling. For example, hydrophilic substances, polyelectrolytes, or surface modification might lessen bacterial adhesion to polymer membrane surfaces. The second technique, which uses biocides to prevent membrane biofouling, is the antibacterial strategy. Antibacterial agents are integrated into membranes to efficiently destroy microorganisms on the membrane surfaces. In our study, the first technique, plasma surface modification and coating with Ag@T NPs, has little effect on anti-biofouling performance as PAT1 and PAT2 presented a hydrophobic surface (contact angle > 90°). In contrast, PAT3 only showed a hydrophilic surface. This situation revealed that the membrane anti-biofouling performance varied with hydrophilicity due to the influence of plasma treatment and Ag@T NPs loading, forming a hydrated shell to prevent bacterial adhesion. On the other hand, the second approach, using antibacterial agents, so far substantially strengthened the anti-biofouling property. PHB-Ag@T membranes imparted intense anti-biofouling activities. Ag@T NPs formed a protected shell, avoiding resisting protein and bacteria from approaching the PHB membrane.

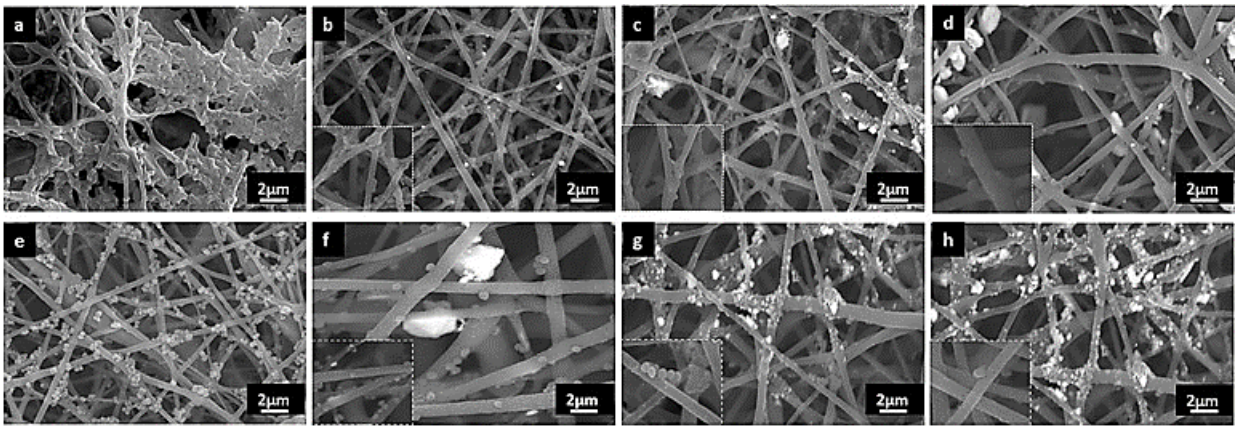

Figure 4.7: SEM photographs of the bacterial adherence on: (a) untreated PHB membrane in contact with *E. Coli*, (b) PAT1 membrane in contact with *E. Coli*, (c) PAT2 membrane in contact with *E. Coli*, (d) PAT3 membrane in contact with *E. Coli*, (e) untreated PHB membrane in contact with *S. Epidermidis*, (f) PAT1 membrane in contact with *S. Epidermidis*, (g) PAT2 membrane in contact with *S. Epidermidis*, (h) PAT3 membrane in contact with *S. Epidermidis*

4.3.4. Biodegradability of prepared antibacterial membranes

The biodegradability of untreated and treated PHB membranes was investigated using soil burial. **Figure 4.8 a** shows the images of the membrane samples before and after the soil burial test, and the corresponding weight loss percentage is shown in **Figure 4.8 b**. The weight loss of the PHB membrane is an obvious indicator of the biodegradation process in the soil due to the presence of moisture and microorganisms. As can be observed from Figure 8a, treated membranes started large cracks on the surface of treated PHB membranes beginning in the second week. At the same time, no considerable damage can be observed on the surface of the untreated PHB membrane. In addition, as shown in Figure 8b, the weight loss percentage of the PHB-Ag@T NPs is dependent on the Ag@T content. Interestingly, increasing Ag@T NPs content led to a higher degradation of PHB membranes. Overall, the weight loss of all PHB membranes was 50% after 5 weeks of soil burial, reaching almost 99% after only 6 weeks. The fast degradation noticed within the 5th week can be explained by the notable increase in microorganism number in the soil, as described by Altaee et al. [45]. With longer incubation times, the microbial population grew, which accelerated the degradation of the polymeric membranes. The depolymerase enzymes in the soil bacteria can hydrolyze PHB polymer, using the resulting metabolic breakdown products as a source of energy and nutrition. All common plastics are, in theory, primarily biodegradable, but because

of their sluggish breakdown, they are not considered biodegradable. Recent developments suggest that (PHAs) are an excellent alternative to traditional plastics because of their biocompatible and biodegradable characteristics.

Figures 4.8 c and d show the PHB membrane's surface after degradation. It unmistakably denotes a non-rank surface with pores, grooves, cavities, extended items like fungal hyphae, spherical objects like bacteria, and apparent ruptures of most nanofibers. Also, it was clear that the PHB membranes' fiber diameters degraded around 500 nm. This indicates that the fibers got thinner after degradation than their corresponding fibers before soil burial.

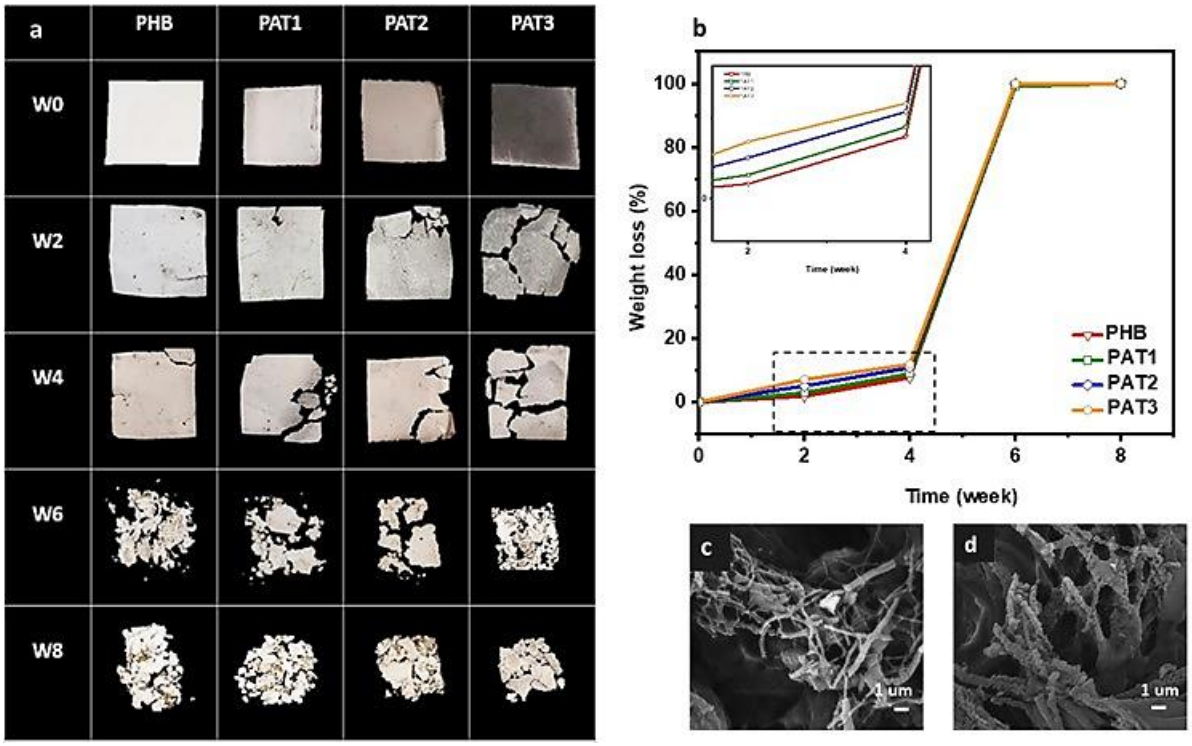

Figure 4.8: (a) Soil burial test of untreated and treated PHB membranes after 2, 4, 6, and 8 weeks, (b) Weight loss of untreated and treated PHB membranes after 2, 4, 6, and 8 weeks, (c) SEM micrographs for PHB membrane after 6 weeks of soil burial and (d) SEM micrographs for PHB membrane after 8 weeks of soil burial

This notable degradation of nanofibers could be due to the high porosity level, large surface area, and three-dimensional structure, which made it possible for a more significant number of microorganisms to adhere to the polymeric sheets [45]. In addition, the following factors, including increased aggregation and the development of large cavities by Ag@T NPs on the membrane

surface, as described previously, may impact the improvement in biodegradability. This reason agrees with the reported results of some research groups [18, 46]. Similarly, the literature demonstrated that adding SiO_2 NPs, halloysite nanotubes, and TiO_2 NPs somehow boosted the bio-sustainability rates of membranes [46-48]. Indeed, Zan et al. [49] synthesized a photodegradable polystyrene-TiO_2 nanocomposite membrane. They noticed that TiO_2 nanoparticles significantly accelerated the photocatalytic degradation of polystyrene material. On the other hand, the membrane composition and several variables involving the amount and type of microorganisms present, the degrading circumstances (i.e., oxygen, humidity, pH, and temperature), the amount of pollutants, and the soil characteristics affect the weight loss (e.g., particle size distribution in the soil) [18, 50]. Finally, the results indicate that the electrospun membranes are biodegradable, and it is possible to blend PHB with Ag@T NPs to improve their biodegradability.

In this work, when compared to the non-decorated membrane, the produced microfiber membranes with Ag@T NPs PAT2 and PAT3 show good antibacterial activity and biodegradability. The results show that increasing the dip coating number of PHB membranes strongly influenced their antibacterial activity and their anti-biofouling properties. The presence of Ag@T NPs did not prevent the biodegradation process of the coated fiber, even at the highest concentration. Unlike other studies, adding antibacterial agents can slow or halt biodegradation [51]. This work studies a more sustainable, environmentally friendly environment with a minor environmental impact. Bio-based and biodegradable bioplastics PHB can offer features similar to traditional plastics while yielding additional benefits due to their reduced carbon footprint. To minimize waste management issues and environmental contamination, interest in competitive antibacterial and biodegradable materials is developing. PHA materials are the primary resource used in most engineering application domains to replace conventional plastic consumption [52].

4.4. Conclusion

This work presents a new approach for fabricating PHB membranes via electrospinning, plasma surface modification, and dip-coating with hybrid antibacterial nanoparticles. The antibacterial coating was successfully achieved after the plasma treatment as the membrane's surface was converted to hydrophilic materials, which revealed the potential to serve as a platform for developing antibacterial materials. Furthermore, the antibacterial results showcased a highly efficient antibacterial effect of daylight treatment for 3h and 30 min against *E. Coli* and *S. Epidermidis*, respectively. Herein, the resulting PHB-Ag@T displayed light-enhanced and time-

dependent antibacterial activity against bacteria. On the other hand, the PHB-Ag@T membranes showed good reusability (up to 3 times) and rapid biodegradation (6 weeks). Moreover, the biofouling test demonstrated that the introduction of Ag@T NPs effectively prevented bacterial fouling on the surface of prepared PHB membranes. The anti-biofouling properties of the PHB-Ag@T were more significant than those of the non-decorated PHB membrane. Our results demonstrated that the PAT microfibers could enhance the anti-biofouling characteristic of the membrane through both anti-adhesive and antibacterial surface properties.

Overall, considering the characterizations' results, PAT2 displayed the best performance, such as thermal and physical stability, with an excellent antibacterial efficiency of 99,50% against *E. Coli* and *S. Epidermidis* under LED light and good anti-biofouling performance. This work is anticipated to offer a technique to create antibacterial and biodegradable functional materials for PE advances.

4.5. Author contributions

Safa Ladhari: Conceptualization (lead); formal analysis (lead); investigation (equal); methodology (equal); writing – original draft (lead). Nhu-Nang Vu: Validation (equal); writing – review and editing (equal). Cédrik Boisvert: Investigation (supporting); methodology (supporting). Marcos Antonio Polinarski: Investigation (supporting). Camille Venne: Investigation (supporting). Alireza Saidi: Funding acquisition (supporting); writing – review and editing (supporting). Simon Barnabe: Funding acquisition (supporting). Phuong Nguyen-Tri: Conceptualization (lead); funding acquisition (lead); investigation (lead); project administration (lead); resources (lead); supervision (lead); writing – review and editing (lead).

Acknowledgment

Regards to Natural Sciences and Engineering Research Council of Canada (NSERC), l'Institut de recherche Robert-Sauvé en santé et en sécurité du travail (IRSST), Canada and le Centre de Recherche sur les Systèmes Polymères et Composites à Haute Performance (CREPEC) to financial support of this work.

Data availability statement

Data is not available due to commercial restrictions.

4.6. References

[1] C. Venne, N.-N. Vu, S. Ladhari, A. Saidi, S. Barnabe, P. Nguyen-Tri, One-pot preparation of superhydrophobic polydimethylsiloxane-coated cotton via water/oil/water emulsion approach for enhanced resistance to chemical and bacterial adhesion, Progress in Organic Coatings, 174 (2023) 107249.

[2] S. Mahira, A. Jain, W. Khan, A.J. Domb, Antimicrobial Materials—An Overview, in: A.J. Domb, K.R. Kunduru, S. Farah (Eds.) Antimicrobial Materials for Biomedical Applications, The Royal Society of Chemistry, 2019, pp. 0.

[3] S. Ladhari, N.-N. Vu, C. Boisvert, A. Saidi, P. Nguyen-Tri, Recent Development of Polyhydroxyalkanoates (PHA)-Based Materials for Antibacterial Applications: A Review, ACS Applied Bio Materials, (2023).

[4] P. Basnett, B. Lukasiewicz, E. Marcello, H.K. Gura, J.C. Knowles, I. Roy, Production of a novel medium chain length poly(3-hydroxyalkanoate) using unprocessed biodiesel waste and its evaluation as a tissue engineering scaffold, Microb Biotechnol, 10 (2017) 1384-1399.

[5] N.-N. Vu, C. Venne, S. Ladhari, A. Saidi, L. Moskovchenko, T.T. Lai, Y. Xiao, S. Barnabe, B. Barbeau, P. Nguyen-Tri, Rapid Assessment of Biological Activity of Ag-Based Antiviral Coatings for the Treatment of Textile Fabrics Used in Protective Equipment Against Coronavirus, ACS Applied Bio Materials, 5 (2022) 3405-3417.

[6] R. Pandimurugan, S. Thambidurai, UV protection and antibacterial properties of seaweed capped ZnO nanoparticles coated cotton fabrics, International Journal of Biological Macromolecules, 105 (2017) 788-795.

[7] M. Salat, P. Petkova, J. Hoyo, I. Perelshtein, A. Gedanken, T. Tzanov, Durable antimicrobial cotton textiles coated sonochemically with ZnO nanoparticles embedded in an in-situ enzymatically generated bioadhesive, Carbohydrate Polymers, 189 (2018) 198-203.

[8] K. Dunn, V. Edwards-Jones, The role of Acticoat™ with nanocrystalline silver in the management of burns, Burns, 30 (2004) S1-S9.

[9] H. Yu, Y. Peng, Y. Yang, Z.-Y. Li, Plasmon-enhanced light–matter interactions and applications, npj Computational Materials, 5 (2019) 45.

[10] J. Gamage McEvoy, Z. Zhang, Antimicrobial and photocatalytic disinfection mechanisms in silver-modified photocatalysts under dark and light conditions, Journal of Photochemistry and Photobiology C: Photochemistry Reviews, 19 (2014) 62-75.

[11] G. Yang, H. Yin, W. Liu, Y. Yang, Q. Zou, L. Luo, H. Li, Y. Huo, H. Li, Synergistic Ag/TiO2-N photocatalytic system and its enhanced antibacterial activity towards Acinetobacter baumannii, Applied Catalysis B: Environmental, 224 (2018) 175-182.

[12] A. Martínez-Abad, G. Sánchez, J.M. Lagarón, M.J. Ocio, Influence of speciation in the release profiles and antimicrobial performance of electrospun ethylene vinyl alcohol copolymer (EVOH) fibers containing ionic silver ions and silver nanoparticles, Colloid and Polymer Science, 291 (2012) 1381-1392.

[13] B.S. Munteanu, Z. Aytac, G.M. Pricope, T. Uyar, C. Vasile, Polylactic acid (PLA)/Silver-NP/VitaminE bionanocomposite electrospun nanofibers with antibacterial and antioxidant activity, Journal of Nanoparticle Research, 16 (2014) 1-12.

[14] H.J. Jeon, J.S. Kim, T.G. Kim, J.-H. Kim, W.R. Yu, J.H. Youk, Preparation of poly(ε-caprolactone)-based polyurethane nanofibers containing silver nanoparticles, Applied Surface Science, 254 (2008) 5886-5890.

[15] W.-P. Chae, Z.-C. Xing, Y.J. Kim, H.-S. Sang, M.-w. Huh, I.K. Kang, Fabrication and Biocompatibility of Rutin-containing PHBV Nanofibrous Scaffolds, Polymer-korea, 35 (2011) 210-215.

[16] M. Min, Y.Y. Shi, X.X. Chen, J. Shi, H. Ma, H.L. Huang, L. Wang, Preparation and Characteristics of Electrospun Silver-Containing PHBV Ultrafine Fiber, Applied Mechanics and Materials, 548-549 (2014) 34 - 37.

[17] Â. Luís, F. Domingues, A. Ramos, Production of Hydrophobic Zein-Based Films Bioinspired by The Lotus Leaf Surface: Characterization and Bioactive Properties, Microorganisms, 7 (2019).

[18] N. Janani, E.N. Zare, F. Salimi, P. Makvandi, Antibacterial tragacanth gum-based nanocomposite films carrying ascorbic acid antioxidant for bioactive food packaging, Carbohydrate Polymers, 247 (2020) 116678.

[19] K. Ma, T. Zhe, F. Li, Y. Zhang, M. Yu, R. Li, L. Wang, Sustainable films containing AIE-active berberine-based nanoparticles: A promising antibacterial food packaging, Food Hydrocolloids, 123 (2022) 107147.

[20] D. Kumar, P. Kumar, J. Pandey, Binary grafted chitosan film: Synthesis, characterization, antibacterial activity and prospects for food packaging, International Journal of Biological Macromolecules, 115 (2018) 341-348.

[21] M. Mohammadalipour, M. Asadolahi, Z. Mohammadalipour, T. Behzad, S. Karbasi, Plasma surface modification of electrospun polyhydroxybutyrate (PHB) nanofibers to investigate their

performance in bone tissue engineering, International Journal of Biological Macromolecules, 230 (2023) 123167.

[22] C.-K. Chang, H.-M.D. Wang, J.C.-W. Lan, Investigation and Characterization of Plasma-Treated Poly(3-hydroxybutyrate) and Poly(3-hydroxybutyrate-co-3-hydroxyvalerate) Biopolymers for an In Vitro Cellular Study of Mouse Adipose-Derived Stem Cells, Polymers, 10 (2018) 355.

[23] J. Moon, U. Jung, B. Jung, J. Park, Improvement of Heat Transfer Properties through TiO2 Nanosphere Monolayer Embedded Polymers as Thermal Interface Materials, Applied Sciences, 12 (2022) 1348.

[24] H. Abe, Thermal Degradation of Environmentally Degradable Poly(hydroxyalkanoic acid)s, Macromolecular Bioscience, 6 (2006) 469-486.

[25] D. Daranarong, R.T.H. Chan, N.S. Wanandy, R. Molloy, W. Punyodom, L.J.R. Foster, Electrospun Polyhydroxybutyrate and Poly(L-lactide-co-ε-caprolactone) Composites as Nanofibrous Scaffolds, BioMed Research International, 2014 (2014) 741408.

[26] G. Ma, D. Yang, K. Wang, J. Han, S. Ding, G. Song, J. Nie, Organic-soluble chitosan/polyhydroxybutyrate ultrafine fibers as skin regeneration prepared by electrospinning, Journal of Applied Polymer Science, 118 (2010) 3619-3624.

[27] M.P. Arrieta, J. López, D. López, J.M. Kenny, L. Peponi, Development of flexible materials based on plasticized electrospun PLA–PHB blends: Structural, thermal, mechanical and disintegration properties, European Polymer Journal, 73 (2015) 433-446.

[28] T. Jacobs, R. Morent, N. De Geyter, P. Dubruel, C. Leys, Plasma Surface Modification of Biomedical Polymers: Influence on Cell-Material Interaction, Plasma Chemistry and Plasma Processing, 32 (2012).

[29] F.S. Mostafavi, R. Kadkhodaee, B. Emadzadeh, A. Koocheki, Preparation and characterization of tragacanth–locust bean gum edible blend films, Carbohydrate Polymers, 139 (2016) 20-27.

[30] C.M. Bitencourt, C.S. Fávaro-Trindade, P.J.A. Sobral, R.A. Carvalho, Gelatin-based films additivated with curcuma ethanol extract: Antioxidant activity and physical properties of films, Food Hydrocolloids, 40 (2014) 145-152.

[31] H. Aloui, A.R. Deshmukh, C. Khomlaem, B.S. Kim, Novel composite films based on sodium alginate and gallnut extract with enhanced antioxidant, antimicrobial, barrier and mechanical properties, Food Hydrocolloids, 113 (2021) 106508.

[32] J. Kan, J. Liu, H. Yong, Y. Liu, Y. Qin, J. Liu, Development of active packaging based on chitosan-gelatin blend films functionalized with Chinese hawthorn (Crataegus pinnatifida) fruit extract, International Journal of Biological Macromolecules, 140 (2019) 384-392.

[33] N. Follain, S. Belbekhouche, J. Bras, G. Siqueira, S. Marais, A. Dufresne, Water transport properties of bio-nanocomposites reinforced by Luffa cylindrica cellulose nanocrystals, Journal of Membrane Science, 427 (2013) 218-229.

[34] R. Priyadarshi, H.-J. Kim, J.-W. Rhim, Effect of sulfur nanoparticles on properties of alginate-based films for active food packaging applications, Food Hydrocolloids, 110 (2021) 106155.

[35] G. Guan, L. Zhang, J. Zhu, H. Wu, W. Li, Q. Sun, Antibacterial properties and mechanism of biopolymer-based films functionalized by CuO/ZnO nanoparticles against Escherichia coli and Staphylococcus aureus, Journal of Hazardous Materials, 402 (2021) 123542.

[36] W.-C. Lin, C.-N. Chen, T.-T. Tseng, M.-H. Wei, J.H. Hsieh, W.J. Tseng, Micellar layer-by-layer synthesis of TiO2/Ag hybrid particles for bactericidal and photocatalytic activities, Journal of the European Ceramic Society, 30 (2010) 2849-2857.

[37] U. Siripatrawan, W. Vitchayakitti, Improving functional properties of chitosan films as active food packaging by incorporating with propolis, Food Hydrocolloids, 61 (2016) 695-702.

[38] R.M. Epand, C. Walker, R.F. Epand, N.A. Magarvey, Molecular mechanisms of membrane targeting antibiotics, Biochimica et Biophysica Acta (BBA) - Biomembranes, 1858 (2016) 980-987.

[39] V. Kundrat, N. Cernekova, A. Kovalcik, V. Enev, I. Marova, Drug Release Kinetics of Electrospun PHB Meshes, Materials, 12 (2019) 1924.

[40] S. Bhattacharyya, S.R. Ali, M. Venkateswarulu, P. Howlader, E. Zangrando, M. De, P.S. Mukherjee, Self-assembled Pd12 coordination cage as photoregulated oxidase-like nanozyme, Journal of the American Chemical Society, 142 (2020) 18981-18989.

[41] C. Fabrice, Chemical Basis of Reactive Oxygen Species Reactivity and Involvement in Neurodegenerative Diseases, Int J Mol Sci, 20 (2019).

[42] S. Mortazavian, E.R. Bandala, J.-H. Bae, D. Chun, J. Moon, Assessment of p-nitroso dimethylaniline (pNDA) suitability as a hydroxyl radical probe: Investigating bleaching mechanism using immobilized zero-valent iron nanoparticles, Chemical Engineering Journal, 385 (2020) 123748.

[43] P. Slepička, Z. Malá, S. Rimpelová, V. Švorčík, Antibacterial properties of modified biodegradable PHB non-woven fabric, Mater Sci Eng C Mater Biol Appl, 65 (2016) 364-368.

[44] J.-A. Park, S.-B. Kim, Anti-biofouling enhancement of a polycarbonate membrane with functionalized poly(vinyl alcohol) electrospun nanofibers: Permeation flux, biofilm formation, contact, and regeneration tests, Journal of Membrane Science, 540 (2017) 192-199.

[45] N. Altaee, G.A. El-Hiti, A. Fahdil, K. Sudesh, E. Yousif, Biodegradation of different formulations of polyhydroxybutyrate films in soil, Springerplus, 5 (2016) 762.

[46] Z. Hejri, A.A. Seifkordi, A. Ahmadpour, S.M. Zebarjad, A. Maskooki, Biodegradable starch/poly (vinyl alcohol) film reinforced with titanium dioxide nanoparticles, International Journal of Minerals, Metallurgy, and Materials, 20 (2013) 1001-1011.

[47] Z.W. Abdullah, Y. Dong, Biodegradable and water resistant poly (vinyl) alcohol (PVA)/starch (ST)/glycerol (GL)/halloysite nanotube (HNT) nanocomposite films for sustainable food packaging, Frontiers in materials, 6 (2019) 58.

[48] S. Tang, P. Zou, H. Xiong, H. Tang, Effect of nano-SiO2 on the performance of starch/polyvinyl alcohol blend films, Carbohydrate polymers, 72 (2008) 521-526.

[49] L. Zan, L. Tian, Z. Liu, Z. Peng, A new polystyrene–TiO2 nanocomposite film and its photocatalytic degradation, Applied Catalysis A: General, 264 (2004) 237-242.

[50] I. Korbag, S. Mohamed Saleh, Studies on mechanical and biodegradability properties of PVA/lignin blend films, International Journal of Environmental Studies, 73 (2016) 18-24.

[51] H. Zhang, X. Zhang, Y. Zhao, X. Wang, Y. Cheng, X. Zeng, Fabrication of biodegradable materials with antibacterial and high-strength properties from wheat straw fibers, Industrial Crops and Products, 208 (2024) 117925.

[52] G. Coppola, M.T. Gaudio, C.G. Lopresto, V. Calabro, S. Curcio, S. Chakraborty, Bioplastic from Renewable Biomass: A Facile Solution for a Greener Environment, Earth Systems and Environment, 5 (2021) 231-251.

4.9. Supporting Information

Synthesis of $AgTiO_2$ hybrid nanoparticles

The synthesis of $AgTiO_2$ NPs follows the process developed by our group, including two main steps: preparation of TiO_2 NPs and the photodeposition of Ag NPs. Titanium (IV) iso-propoxide was hydrolyzed in the presence of H_2O_2 to form a water-soluble titanium peroxo complex. This complex was acquired by drying the obtained solution before calcined at 400°C for 4 h to form TiO_2 NPs. These NPs were dispersed in ethanol solution (10%) containing $AgNO_3$ (Ag amount accounts for 6% (wt) of the TiO_2), which was then illuminated under UV light (100W) for 45 minutes. The illumination activated TiO_2 NPs to reduce Ag^+ to Ag^0 in the form of NPs deposited on their surface. **Figure SI4.1** shows a TEM image of obtained $AgTiO_2$ NPs.

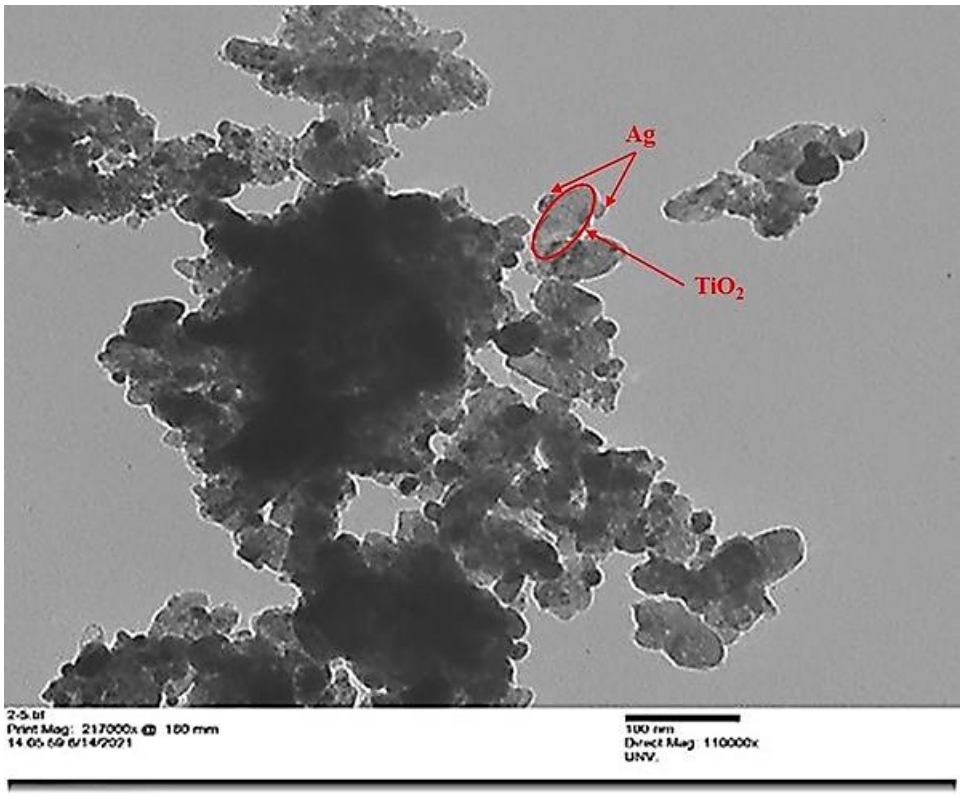

Figure SI. 4.1: TEM image of $AgTiO_2$ NPs. The result is extracted from our progressing article.

Table SI. 4.1: Setting conditions for PHB electrospinning solution

Applied voltage (DC)	**13 kV**
Internal Needle diameter	0,9 mm
Distance from the needle tip and the collector	12 cm
Supply flow rate	0.5 mL/min
Average temperature	23°C

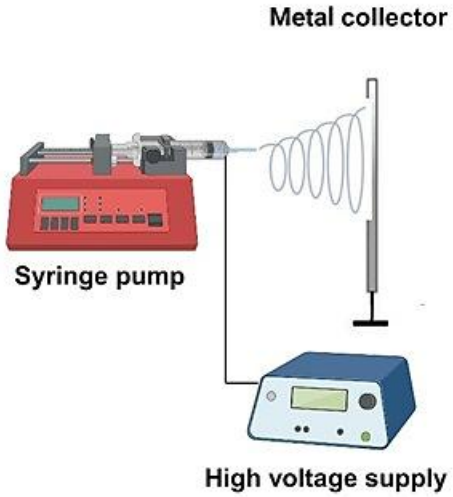

Figure SI. 4.2: Electrospinning equipment

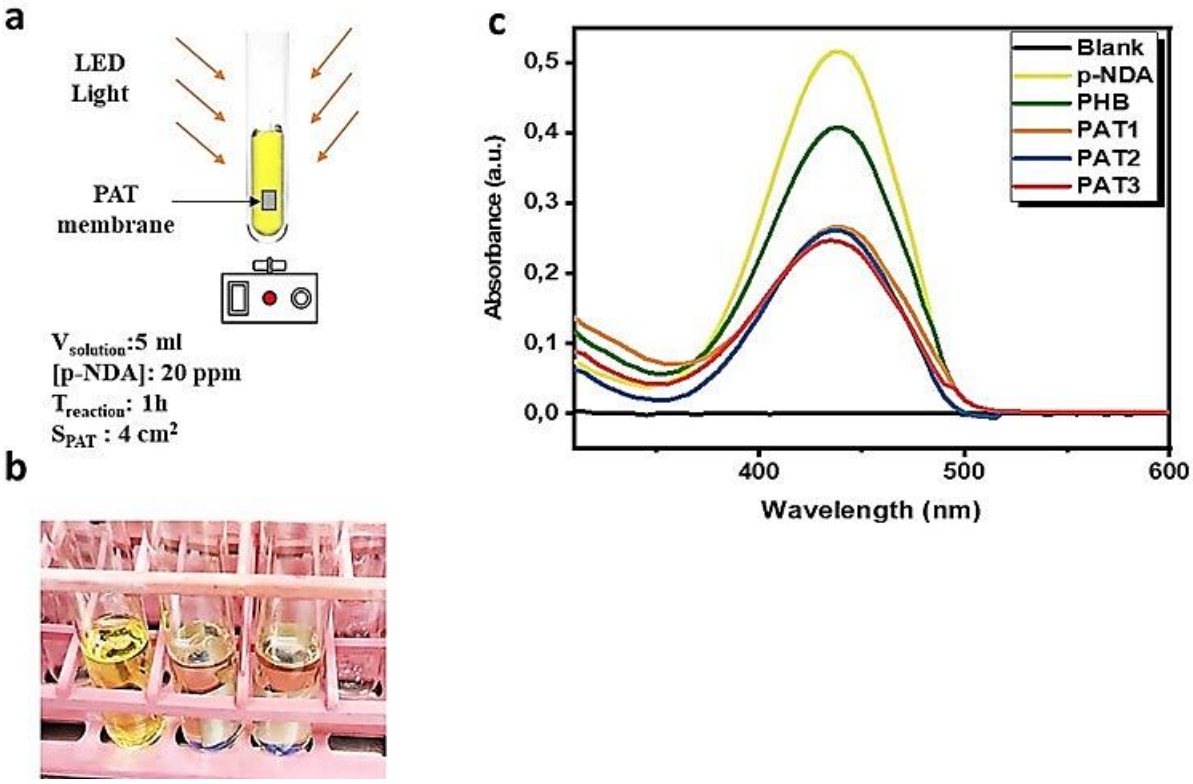

Figure SI. 4.3: Generation of hydroxyl radicals (OH·) by bleaching p-nitroso dimethylaniline (p-NDA) using UV light. (a) (p-NDA) bleaching experiment conditions, (b) Photograph of (p-NDA) bleaching in the presence of PAT2, and (c) UV-Vis absorption spectra of p-NDA with PAT membranes.

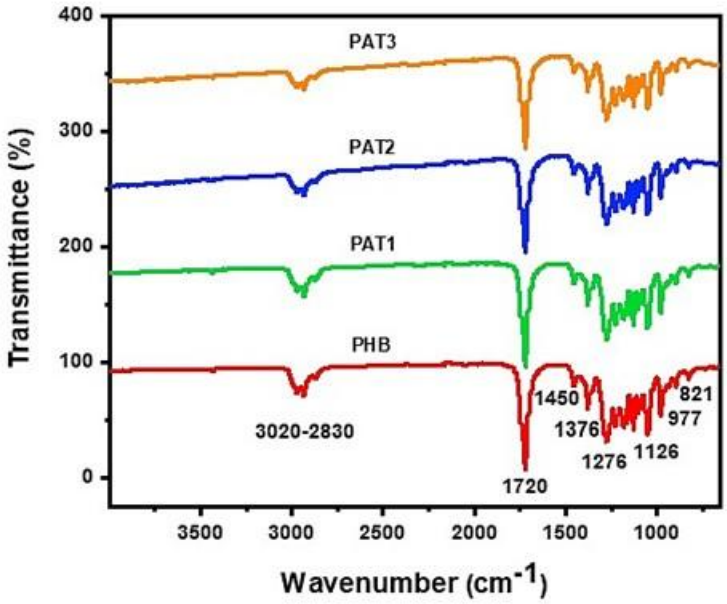

Figure SI. 4.4: ATR-FTIR spectra of PHB membranes.

Figure SI4.4 shows the FTIR spectra of the untreated PHB and samples treated with plasma and dip-coated with suspensions of Ag@T NPs. The ATR spectrum of treated membranes displays no difference from that of the untreated PHB membrane. All the spectra show a broad peak at 3430 cm^{-1}, which is characteristic of hydrogen-bonded O–H absorption. The FT-IR spectrum of all membranes presents peaks in 3020–2830 cm^{-1}, indicating the presence of methyl and methylene groups. The strong band indicates the carbonyl stretching of an ester group at 1720 cm^{-1}. The bands indicate methyl groups stretching symmetrically and asymmetrically at 1450 and 1376 cm^{-1}. The aliphatic ester group vibrations (in the crystalline and amorphous phases) are represented by the bands at 1276, 1226, and 1126 cm^{-1} in FTIR spectra. Furthermore, the dip-coated membranes with Ag@T NPs did not confirm distinctive peaks of $AgTiO_2$. It suggests that the antibacterial NPs were possibly adsorbed on the surface of the electrospun fiber and were little incorporated inside the meshes. Finally, ATR-FTIR spectroscopic, coupled with SEM and EDX analysis, verified the existence of Ag@T NPs in PHB electrospun membranes.

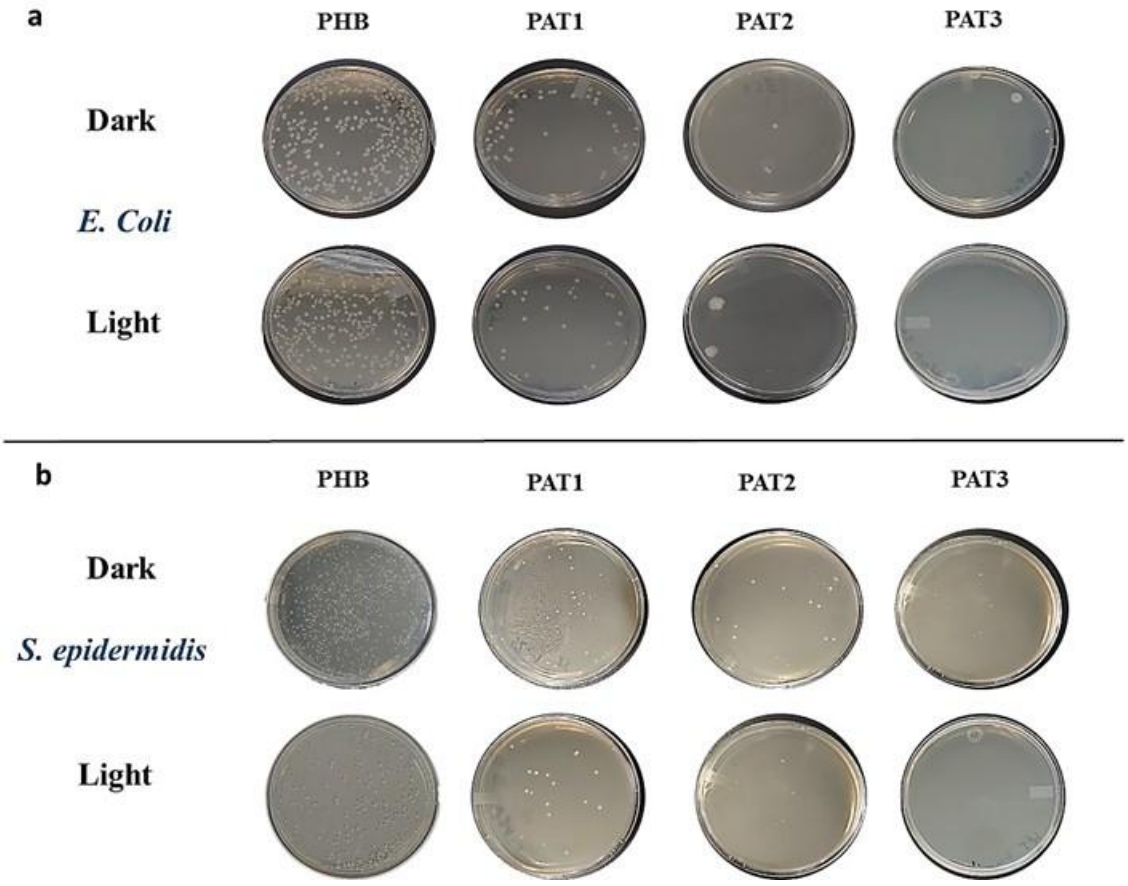

Figure SI. 4.5: (a) Photographs of plate count of untreated PHB, PAT1, PAT2, and PAT3 under dark and light conditions against *E. Coli*, (b) Photographs of plate count of untreated PHB, PAT1, PAT2, and PAT3 under dark and light conditions against *S. Epidermidis*.

Chapter 5: A green synthesis route of ZnO/polyhydroxybutyrate composites with antibacterial and biodegradable properties

Safa Ladhari[a, b], Nhu-Nang Vu[a,b], Juliette Vallée Bastien[a,b], Bich Van Tran[a,b], Thi Ha Nguyen[a,b], Alireza Saidi[a,b,c], Simon Barnabe[a], Cyrille Sollogoub [d], Phuong Nguyen-tri[a,b]*

[a] *Department of Chemistry, Biochemistry, and Physics, Université du Québec à Trois-Rivières (UQTR), 3351 Boulevard des Forges, Trois-Rivières, Québec, G8Z 4M3, Canada*

[b] *Laboratory of Advanced Materials for Energy and Environment, Université du Québec à Trois-Rivières (UQTR), 3351 Boulevard des Forges, Trois-Rivières, Québec, G8Z 4M3, Canada*

[c] *Institut de Recherche Robert-Sauvé en Santé et Sécurité du Travail (IRSST), 505 Boulevard de Maisonneuve Ouest, Montréal, QC H3A 3C2, Canada*

d Laboratoire PIMM, CNRS, Arts etMétiers Institute of Technology, Cnam,HESAM Universite, Paris, France

*Email: phuong.nguyen-tri@uqtr.ca

Published in *Polymer Engineering and Science*, 2024, 12, doi:10.1002/pen.27055.

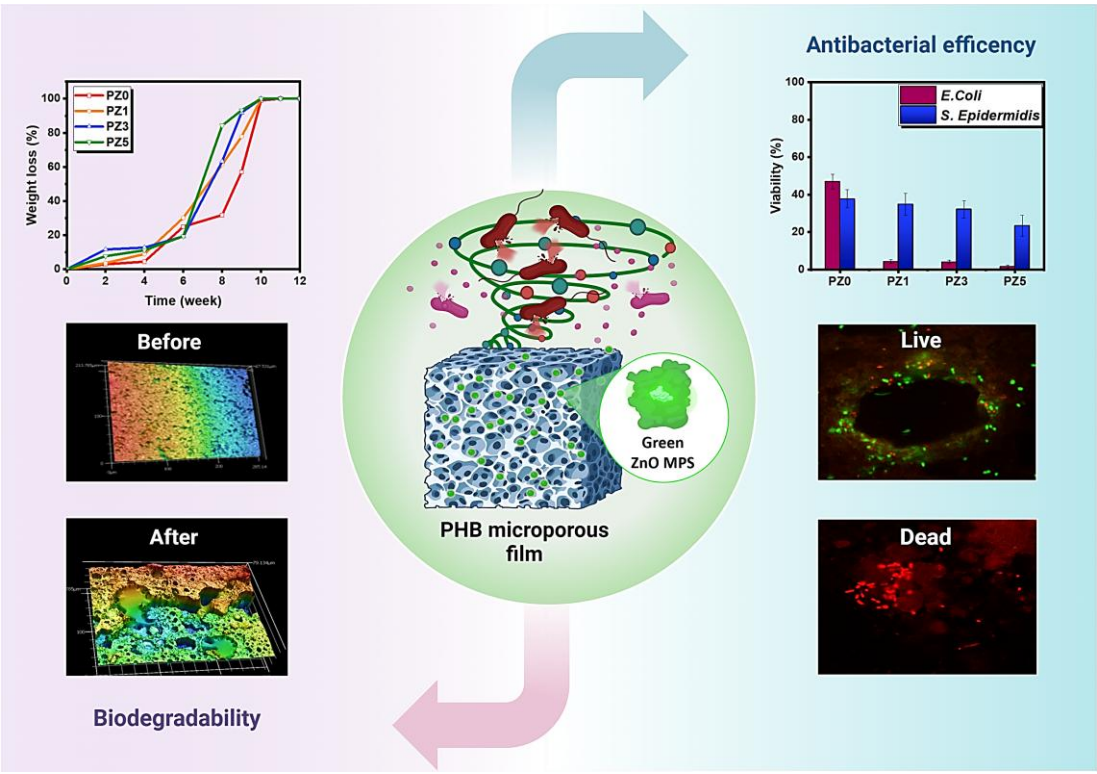

Résumé

Le développement de matériaux à base de polymères respectueux de l'environnement, dotés de propriétés antibactériennes et biodégradables, apporte des avantages significatifs à l'industrie de l'emballage. Dans le présent travail, des particules microporeuses d'oxyde de zinc (ZnO MPs) synthétisées de manière écologique sont dispersées dans la matrice de poly(3-hydroxybutyrate) (PHB) à l'aide d'une méthode de coulée simple afin de préparer des films bioactifs aux propriétés antibactériennes et anti-fouling. Les films obtenus présentent une morphologie microporeuse avec une dispersion uniforme des particules de ZnO dans la matrice polymère. L'incorporation de particules de ZnO synthétisées par ume méthode verte (3 % en poids) dans des films de PHB entraîne une puissante activité antibactérienne, notamment sous lumière LED, avec des efficacités d'inactivation bactérienne de 97,5 % et 76,2 % contre *E. coli* et *S. epidermidis*, respectivement, après 90 minutes d'irradiation lumineuse. Cette activité antibactérienne est supérieure à celle induite par des films chargés de la même quantité de nanoparticules de ZnO commerciales. En outre, la puissante activité antibactérienne permet aux films préparés de mieux lutter contre la contamination biologique et la formation de biofilms à leur surface. Notamment, l'incorporation de ZnO MPs améliore l'adhésion des microbes, accélérant la biodégradation des films développés, avec des taux de biodégradation du sol atteignant 99% en 10 semaines. Le présent travail offre une approche simple et rentable pour produire des composites prometteurs avec une durée de conservation prolongée et la capacité de réduire la contamination bactérienne pour les applications de l'industrie de l'emballage.

Abstract

The development of environmentally friendly polymer-based materials with antibacterial and biodegradable properties is bringing significant benefits to the packaging industry. In the present work, green-synthesized zinc oxide microporous particles (ZnO MPs) are dispersed in the poly(3-hydroxybutyrate) (PHB) matrix using a simple casting method to prepare bioactive films with improved antibacterial and anti-biofouling properties. The resultant films display a microporous morphology with a uniform dispersion of ZnO MPs within the polymeric matrix. The incorporation of green-synthesized ZnO MPs (3% wt) into PHB films leads to potent antibacterial activity, notably under LED light, with bacterial inactivation efficiencies of 97.5% and 76.2% against *E. coli* and *S. epidermidis*, respectively, after 90 minutes of light irradiation. This antibacterial activity is superior to that induced by films loaded with the same amount of commercial ZnO nanoparticles. Furthermore, the potent antibacterial activity gives rise to improved anti-biofouling for prepared films, in which the biofilm formation on their surface is effectively eliminated. Notably, the ZnO MP incorporation improves the microbe adhesion, accelerating the biodegradation of developed films, with soil biodegradation rates reaching 99% in 10 weeks. The present work offers a simple and cost-effective approach to producing promising composites with prolonged shelf-life and the capability of reducing bacterial contamination for packaging industry applications.

5.1. Introduction

Antimicrobial activity is one of the most essential functional features of packaging materials, as they risk being contaminated by bacteria and fungi [1]. These microorganisms' surface adhesion and contamination can cause health and hygiene issues [2-4]. Meanwhile, with its withdrawal from petroleum-based plastics, biodegradable packaging helps to foster a circular economy, wherein the materials eventually return to nature without harming it [5].

Because of their excellent mechanical qualities, thermal stability, and ability to act as effective barriers to carbon dioxide, oxygen, and aromatic chemicals, synthetic petrochemical-based polymers have been in greater demand as packaging materials. The primary factors influencing the selection of synthetic polymers based on petrochemicals as packaging materials are their widespread availability and comparatively low cost. The drawback of synthetic petrochemical-based polymers is that, despite their widespread use in packaging materials, their poor biodegradability makes them a significant source of trash after use. The major amount of extremely harmful emissions, problems with composting, and changes in the carbon dioxide cycle are the main causes of this environmental threat [6]. Furthermore, because of socioeconomic limitations and technical difficulties, discarded packaging plastics are rarely recycled in many nations, resulting in a significant amount of used plastic material either dumped in landfills or added to the litter surrounding the environment, which ultimately strains and stresses the balance of the environment. As a result, this phenomenon has drawn the interest of numerous researchers working to create active, sustainable packaging materials. Thus, in addition to shelf-life, cost, and protection, the packaging design should consider user-friendliness and environmental sustainability.

Therefore, examining packaging materials made of naturally degradable polymers has drawn more attention. This is an essential movement towards a greener, more sustainable world. Among biodegradable biomaterials, polyhydroxyalkanoates (PHAs) attracted particular attention. PHAs are thermoplastic, biocompatible, and biodegradable microbial polymers of hydroxy-derived fatty acids in biological medium [7]. Due to their characteristics, they are very promising for various antibacterial applications, including drug delivery systems, patches for wound healing, implantable medical devices, tissue engineering cell scaffolds, etc. [8]. PHAs are represented by polymers with different monomer units and a range of physicochemical characteristics, such as highly crystalline thermoplastic materials or rubber-like elastomers [9]. Poly(3-hydroxybutyrate) (PHB), the first PHA

found in the 1920s [10], represents the most explored microbial polyesters because of their thermoplastic behavior and mechanical qualities suited for load-bearing applications. Specifically, PHB is known as an environmentally friendly polymer because of its excellent biodegradability. Nonetheless, the major limitation of this material is its weak antimicrobial activity. Therefore, improving antimicrobial properties is critical to make PHB suitable for packaging applications.

However, when making antimicrobial and biodegradable films, there appears to be a greater risk that incorporating an antimicrobial agent will destroy the film polymer's biodegradability, a prominent feature and significant advantage of bioplastic from an environmental standpoint. As a result, achieving antimicrobial activity while maintaining the material's biodegradability remains a considerable issue, requiring important consideration when choosing an antibacterial agent and its concentration.

As PHB's main weakness is its lack of inherent antimicrobial properties, metal-based particles have gained attention due to their potential to enhance the antibacterial properties of polymeric materials [11]. Recently, metal nanoparticles (NPs) such as silver and gold and metal oxide NPs such as zinc, iron, copper, and titanium dioxide have been intensively studied for antibacterial applications [12-14]. In our recent study [15], we reported the preparation of PHB microfiber membranes decorated with photoactive $AgTiO_2$ NPs with advanced antibacterial and anti-biofouling activities. Because of their photocatalytic activity, $AgTiO_2$ NPs significantly improved the antibacterial properties of produced membranes, especially when exposed to light. The top-performing sample, exposed to low-power commercial LED light for three hours and one hour, respectively, showed strong antibacterial efficacy, surpassing 99% against *Escherichia coli* and *Staphylococcus epidermidis*. Furthermore, these samples successfully avoid bacterial biofouling because of their strong antibacterial qualities.

Among various developed metal oxide particles, zinc oxide (ZnO) has been extensively employed for biological applications due to its low toxicity and being ecologically benign [16-18]. It is frequently used in dermatological products such as lotions, ointments, and creams [8]. ZnO also possesses antimicrobial qualities in both microscale and nanoscale compositions [9]. The ZnO antibacterial mechanism is based on the well-established paradigm of induced reactive oxygen species (ROS) generation and oxidative damage inside bacterial cells [19].

Díez-Pascual [20] prepared biodegradable nanocomposites via solution casting technique by adding ZnO NPs to bacterial polyester poly(3-hydroxybutyrate-co-3-hydroxyvalerate) (PHBV). The resulting PHBV/ZnO films demonstrated antibacterial activity against human pathogen

bacteria, more substantially affecting *E. Coli* than *S. aureus*. In another similar study [21], ZnO NPs were incorporated in electrospun poly (3-hydroxybutyrate-co-3-hydroxyvalerate) (PHBV)/polyethylene oxide (PEO) microfibers for antibacterial, antibiofilm for wound dressing application. The composites showed antibacterial action against pathogenic bacteria that cause wound infections, with more significant effects on S. *aureus* than *P. aeruginosa* at higher ZnO concentrations. At a concentration of 5wt% ZnO NPs, antibiofilm activity was more vigorous against *S. aureus* and *P. aeruginosa* compared to 1 and 3 wt% ZnO NPs.

Traditional approaches for creating ZnO particles involve various physical and chemical techniques. Chemical techniques are the most commonly used, including liquid ultrasonication, sol-gel, and electrochemical reactions [22-24]. These processes necessitate high vacuum and energy and may involve using hazardous chemical reagents while producing products with low biocompatibility [25]. The issues with physical and chemical processes can be resolved using green synthesis to create sustainable ZnO MPs. Furthermore, as the green synthesis process needs plant extracts, it doesn't require any hazardous chemicals to act as reducing or oxidizing agents [26]. One of the most environmentally friendly, non-toxic, biocompatible, and cleanest ways to produce antibacterial agents is through green synthesis, which uses plant extracts [27-28]. The primary ingredient in plant extracts, polyol, stabilizes the creation of metallic nanoparticles and functions as a chelating and capping agent for prompt nanoparticle synthesis [29]. The goal of green practices is to minimize or get rid of hazardous materials. For these reasons, incorporating green-synthesized ZnO NPs into PHB materials could generate effective antibacterial action.

In this work, we develop an eco-friendly polymer-based material for packaging applications. Green-synthesized zinc oxide microporous particles (ZnO MPs) are effectively loaded into a poly(3-hydroxybutyrate) (PHB) matrix using a simple casting technique without additional surfactants. The PZ biofilms showed improved antibacterial and anti-biofouling properties due to the uniform dispersion of micropores and the efficient dispersal of ZnO MPs. When exposed to light due to the photocatalytic activity of ZnO MPs, the films are more effective at killing bacteria than commercial antibacterial agents. Although the PZ films promote microbe attachment, they also accelerate biofilm biodegradation, resulting in up to 99% soil biodegradation rates over ten weeks. Our findings mainly aim to provide an excellent simple antibacterial material using green ZnO MPs to inhibit bacterial growth and biofilm formation, demonstrating the possibility of low-cost PHB-ZnO films for packaging applications.

5.2. Results and Discussion

5.2.1. Morphological structure of porous films

Scanning electron microscope (SEM) images acquired at various magnifications were used to record surface images and cross-sections of neat PHB and ZnO MPs added films (PZ0, PZ1, PZ3, and PZ5). **(Figure 5.1)** revealed a homogenous distribution of irregular, micro-sized pores, nearly spherical, across the entire surface of the film. **(Figure 5. 1. b3**) shows that the pores were only generated on the top surface of the PHB film, while the bottom surface was almost smooth and devoid of any apparent porosity. This was proposed to be caused by the pore generation mechanism shown in **(Figure 5.2)**, where pores were left behind during the drying process when agitation-formed chloroform microbubbles and trapped air moved toward the surface. The kinetics of highly viscous polymer solution settling down at the bottom surface and migration of partially diluted polymer solution accompanied by microbubbles toward the top surface must be quick enough for pore-forming during the drying stage. The addition of ZnO MPs (3 and 5 %) produced bulkies with irregular surfaces and aggregates at the bottom of the films, as shown in **(Figures 5.1. c3 and d3**)

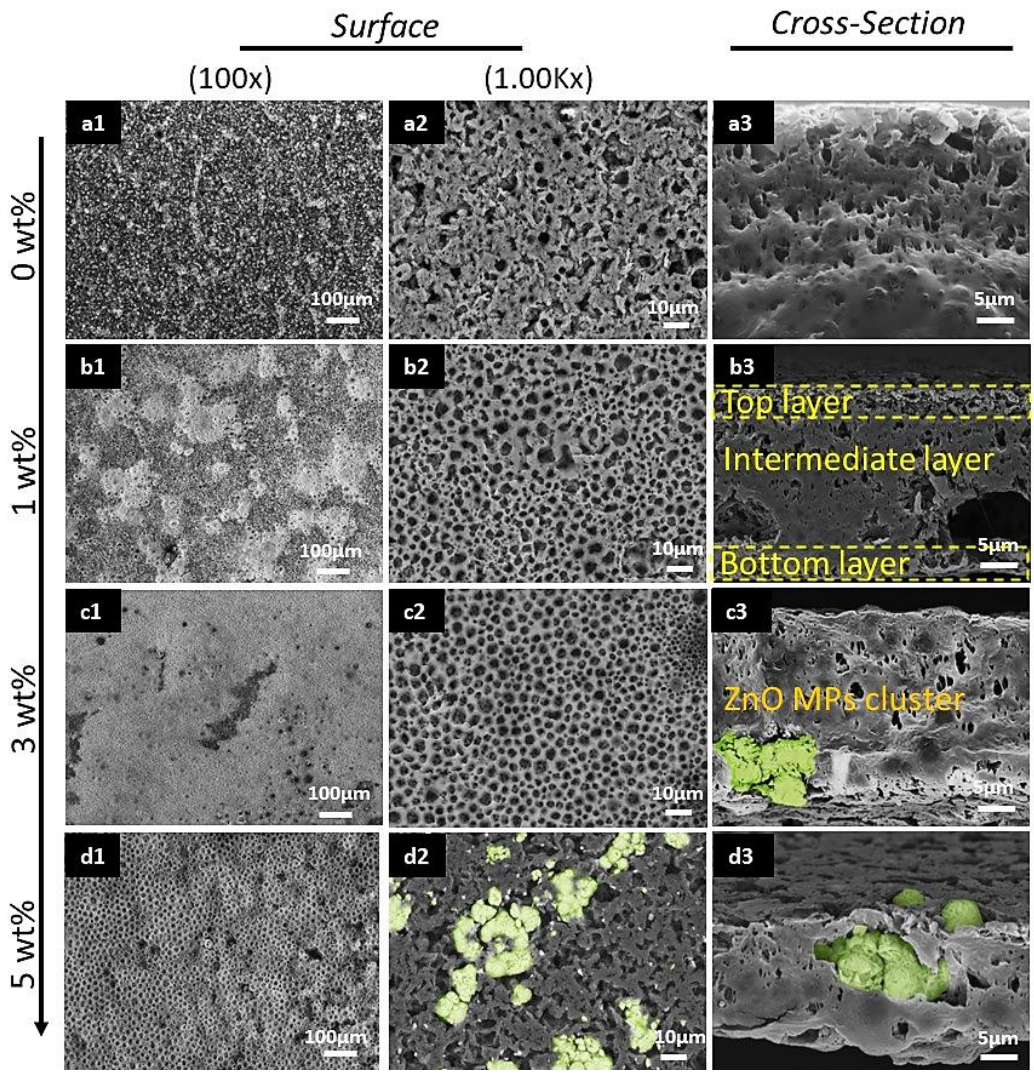

Figure 5.1: SEM images of 1) the surface of the film (100x), 2) the surface of the film (1.00Kx), and 3) cross-sectional (500x), a) PZ0; b) PZ1; c) PZ3; and d) PZ5.

PZ films, with 0,5 ± 0,01 mm of thickness, have a cross-sectional structure of three layers. A dense polymer intermediate layer is formed between the solution-air interface (the top layer) and above the solution-glass contact (the bottom layer). The pore size in the intermediate layer is comparatively smaller than the average in the top layer. This portion of the solution rapidly becomes more viscous due to the quick evaporation of solvent from the top layer, which also stops polymer-lean nuclei from forming and growing [30]. However, the casting parameters, such as the casting film thickness and exposure duration in air, significantly impact the membrane properties regarding pore size and total porosity. Therefore, due to the addition of different concentrations of ZnO MPs, the PHB films may have distinct pore properties.

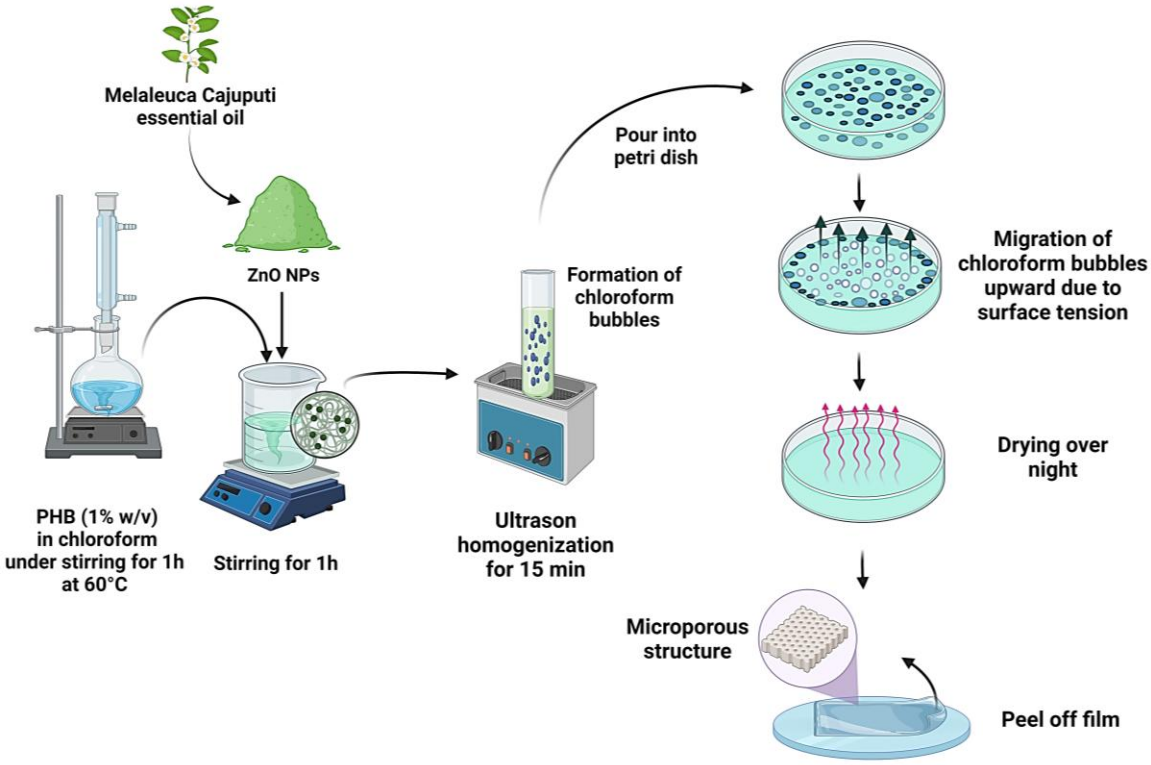

Figure 5.2: Different steps of PZ microporous film preparation.

The particles in the mixture containing 1wt % ZnO MPs **(Figure 5.3 b)** are dispersed uniformly and without clumping together with a narrow-size distribution. In contrast to the sample with a lower filler level, the particle dispersion is less uniform at 3 wt % and 5 wt % loading **(Figures 5.3 c and d)**. The ability of ZnO MPs's surface hydroxyl groups to establish hydrogen bonds with other nanoparticles increases the tendency for aggregation [31]. This can lead to the flocculation of the fillers and the development of tiny clusters, which are consistent with SEM results.

Energy-dispersive X-ray spectroscopy (EDS) images and mapping of ZnO MPs were performed further to examine the formation of ZnO tiny cluster structures, as shown in **Figure 5.3**. The analysis of PZ spectra indicates the existence of different amounts of zinc, oxygen, and carbon elements. The zinc content values were higher at 5 wt% with PZ5. **Figure 5.3** presents the selective area of the PZ films, revealing the presence of ZnO MP (Zn as a blue color) along with O (green color) and C (red color). Elemental analysis also confirmed the ZnO cluster structure with PZ3 and PZ5 films.

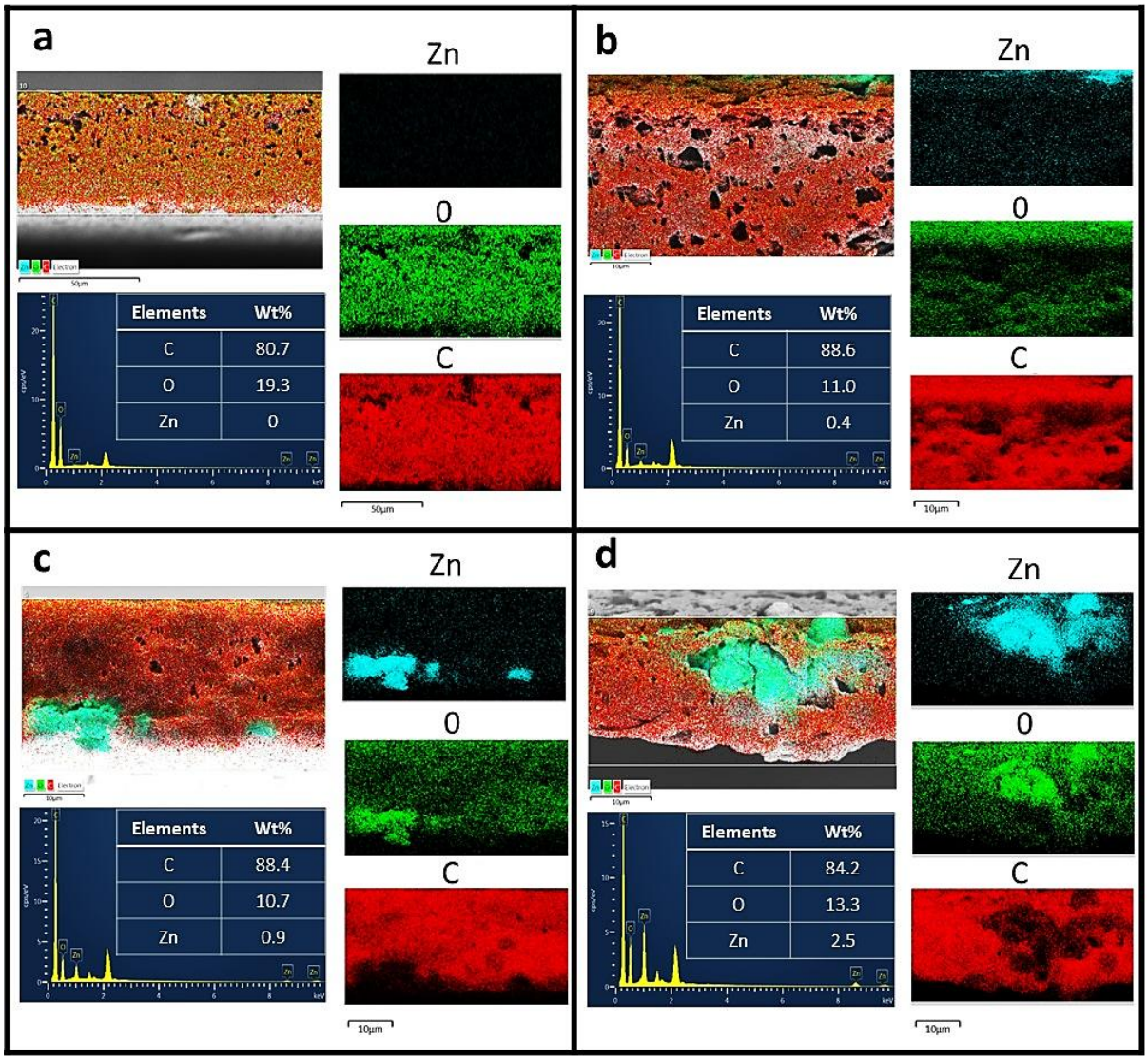

Figure 5.3: Mapping and EDX tabulated data of a) PZ0, b) PZ1, c) PZ3, and d) PZ5.

Overall, statistical analysis shows that at low concentrations, ZnO MPs disperse in PHB as single particles; at the more significant loading examined, ZnO MPs disperse as single particles and tiny clusters. Most importantly, ZnO MPs dispersion within the biopolymer was accomplished without the requirement for coupling agents or surfactants, which shortened, simplified, and reduced the cost of fabricating these bioactive materials.

The FT-IR spectra of PZ films and ZnO MPs are presented in **(Figure SI5.1)** to analyze the interactions between PHB polymer and ZnO MPs. ZnO's spectrum exhibits a broad band in the 3650-3000 cm^{-1} range, attributed to the surface stretching of the nanoparticle's hydrogen-bonded (-OH) groups. Further, an intense band is found at 1400 cm^{-1} that corresponds to C-H bending

vibration in methyl (CH_3) and methylene (CH_2) groups. On the other hand, a noticeable band is seen at 1720 cm^{-1} in PZ0 due to the ester group C=O stretching [32]. C–O–C stretching vibrations are represented by bands in the 1280–1097 cm^{-1} range, while C–H stretching bands are associated with bands at approximately 2900 cm^{-1}. The O–C–H in-plane bending is located at 1380 cm^{-1}, while the CH_3 asymmetric bending is visible at 1457 cm^{-1}. The distinct bands of PHB and ZnO are more visible in the PZ3 and PZ5 spectra than in PZ1. The signal attributed to hydroxyl stretching appears to be broadened in the samples with 3 and 5 weight percent loading, and it is centered at around 3435 cm^{-1}. Ultimately, the presence of ZnO MPs in PHB film was confirmed by ATR-FTIR spectroscopy coupled with SEM and EDX examination.

Figure 5.4 a gives the statistical characteristics for the surfaces estimated by roughness analysis of the 3D laser confocal microscope (LCM) images. The study found that the film's surface roughness gradually increased with increased ZnO MPs content. The influence of the ZnO MPs content in the membrane was also observed in the surface pores. The image analysis software package ImageJ was utilized to get quantitative evaluations of porosity percentages (**Figures 5.3 b and c)**.

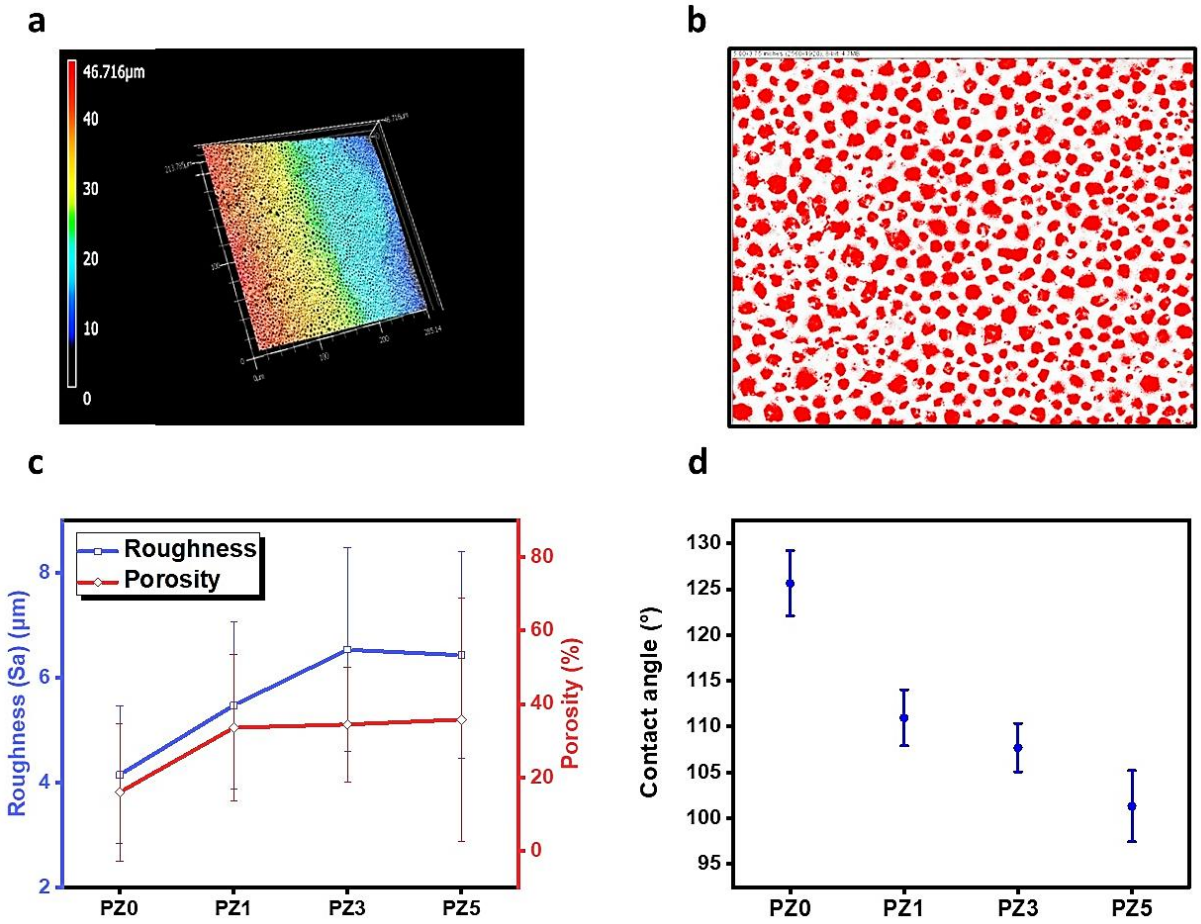

Figure 5.4: a) Confocal profiler 3D image of PZ3 surface, b) Image analysis using ImageJ for percentage area (porosity) measurement estimation of PZ3, c) Surface roughness (Sa) and the porosity of PZ films, and d) Contact angle of PZ films.

The pores were masked with red color on a white backdrop **(Figure 5.4 b).** The surface pores, with an almost circular shape with 2,3 ± 0,52 µm of average diameter, were more noticeable than those in ZnO MPs-free films **(Figure 5.4 c)**. Also, the average porosity of PZ1, PZ3, and PZ5 was almost identical. Particles incorporated in the polymeric material (whether aggregates, agglomerates, or non-aggregated nanoparticles) impact the polymer's porosity [33].

Incorporating ZnO MPs into PHB films via the simple casting method increases porosity and roughness due to several critical processes during film formation. PHB typically forms a smooth, compact film when cast from a solution as the solvent evaporates and the polymer chains align and settle homogeneously. However, the introduction of ZnO MPs disrupts this process. First, the mapping results show that ZnO particles are insoluble in PHB and remain solid inclusions

within the polymer matrix. These particles aggregate or cluster during casting, preventing the polymer chains from packing uniformly. As the solvent evaporates, the ZnO MPs act as nucleation sites, leading to localized variations in the polymer's packing density. The polymer chains are less densely packed in areas around these particles, forming voids or pores. These voids increase the overall porosity of the film, as the polymer does not fill the spaces around the particles. Second, the presence of ZnO MPs affects the film's surface morphology. Since the particles do not dissolve and remain embedded in the polymer matrix, they cause localized disruptions on the film's surface. As a result, the film surface becomes more irregular, with a rougher texture. Surface roughness is mainly determined by the size, shape, and distribution of ZnO particles, as more significant or poorly dispersed particles lead to greater surface unevenness. In contrast, smaller, more uniformly distributed particles might produce finer roughness. Additionally, the casting method, which involves the slow evaporation of the solvent, might not allow the polymer chains to fully relax and reconfigure around the ZnO MPs. This slower process can enhance surface roughness formation and increase porosity compared to faster evaporation methods, potentially leading to more uniform film structures. In conclusion, the ZnO MPs disrupt the normal film-forming process of PHB, increasing both porosity and surface roughness due to the incomplete integration of the particles into the polymer matrix and their effect on the polymer's microstructure during film formation.

The decrease in water contact angle **(Figure 5.4 d)** following the addition of ZnO MPs to the PHB polymer solution can be attributed to several interconnected factors influencing the surface properties of the PZ film. First, because of their size and distribution, ZnO MPs are primarily responsible for surface roughness in the polymer matrix. The observed hydrophobicity is decreased due to the increased roughness, increasing the surface area with which water molecules can interact. Second, ZnO MPs' potential polar surface groups, such as hydroxyl groups, may raise the composite's surface energy, increasing wetting behavior and fostering a stronger affinity for water molecules.

5.2.2. Antibacterial activity

Figure 5.5 displays the outcomes of the antibacterial activity. First, the antibacterial effect observed in PHB films without ZnO MPs can be attributed to the intrinsic properties of the PHB polymer. PHB's natural hydrophobicity has the potential to damage bacterial cell membranes upon contact [4], leading to the death of the cells. These intrinsic properties contribute to its ability to inhibit bacterial growth, demonstrating that PHB alone has an inherent antibacterial potential even

though its antibacterial efficacy is not as strong as that of PHB loaded with ZnO MPs. Moreover, it was found that antibacterial activity was more effective against *E. coli* than against *S. epidermidis*, regardless of the amount of ZnO MPs component in the film matrix. PHB films loaded with ZnO MPs obtained sufficient antibacterial activity with bacterial reduction superior to 95% against *E. coli*. This activity rose marginally when the ZnO MPs content was increased from 1wt% to 5wt% in PHB samples. This could indicate that it has a bacteriostatic effect on *E. Coli*. However, despite the ZnO MPs concentration, a slight bacterial decrease against *S. epidermidis* was seen for all investigated samples **(Figure 5.5 a)**. This was unexpected because it is usually accepted that ZnO MPs are more efficient against Gram-positive bacteria than against Gram-negative bacteria [34-37]. However, our finding follows Malis D. et al. [1], which reported that gram-negative bacteria were more sensitive to ZnO MPs than gram-positive bacteria. The bacterial reductions caused by PZ3 and PZ5 are very similar to those obtained for the PZ1, marking the excellent antimicrobial activity of ZnO MPs even at lower concentrations. The antibacterial activity against *E. Coli* drastically increased when ZnO MPs were included in the film matrix. This was not the case against *S. epidermidis,* where there was a slight enhancement with progressively increasing ZnO MPs content, reaching a maximum antibacterial efficacy of 76.5% for PZ5 **(Figure 5.5 a)**. The disparity in antibacterial activity of ZnO microparticles (MPs) against Gram-positive and Gram-negative bacteria can be related to various factors influencing antibacterial test results. Changes in the interaction mechanisms of ZnO MPs with bacterial cells can explain the difference in susceptibility between Gram-positive and Gram-negative bacteria [38]. These findings coincide with several earlier findings [1]. It is claimed that variations in the cell walls' structure play an important role. It is commonly known that Gram-positive bacteria are less vulnerable to the membrane damage caused by ZnO MPs because their cell walls include peptidoglycan that is substantially thicker than that of Gram-negative bacteria. Moreover, Applerot et al. [39] demonstrated that *E. Coli* showed a greater vulnerability to ZnO MPs than *S. aureus*. The difference in the internal antioxidant content, such as carotenoid pigments, and the presence of detoxifying solid agents, like antioxidant enzymes, could be a further reason.

Several variables could account for this, including ZnO MPs' particle size and surface area, significantly impacting their antibacterial activity. Smaller ZnO particles have a higher surface area and are more likely to penetrate bacterial cell walls, potentially providing easier access to gram-negative bacteria's weaker peptidoglycan layer and increasing their sensitivity. Second, ZnO MPs' synthesis technique and shape can affect their dispersion, aggregation, and surface charge,

influencing their interactions with bacterial membranes. Well-dispersed ZnO particles are more likely to produce ROS, which can harm bacterial cells. Furthermore, bacterial strain changes and test conditions (medium composition, pH, and temperature) can influence the observed antibacterial activity, as various strains of bacteria may have varying degrees of resistance to ZnO. Notably, despite their protective outer membranes, gram-negative bacteria may be more vulnerable to oxidative stress and ROS production caused by ZnO particles, potentially leading to more potent antibacterial effects. Finally, the aggregation status of ZnO particles during the test could be significant, as aggregated particles have a smaller surface area and are less effective at penetrating bacterial membranes or producing ROS, resulting in less antibacterial action. In conclusion, while gram-positive bacteria are typically more sensitive to ZnO MPs, these factors—particle characteristics, bacterial strain, and environmental conditions—can cause variations, and in some cases, gram-negative bacteria may exhibit higher sensitivity, as demonstrated by our findings.

Furthermore, it is commonly recognized that ZnO with higher concentrations and smaller sizes may have superior bactericidal effects [40]. Numerous studies have examined the mechanism of ZnO's light-induced antibacterial action. It is thought to be related to ROS generation [41], zinc ion dissolution [42], and internalization of NPs, which ultimately results in cell death [43]. ROS is thought to be the primary mechanism among them. This study examined the antibacterial activity of PHB loaded with ZnO MPs in the presence and absence of visible light.

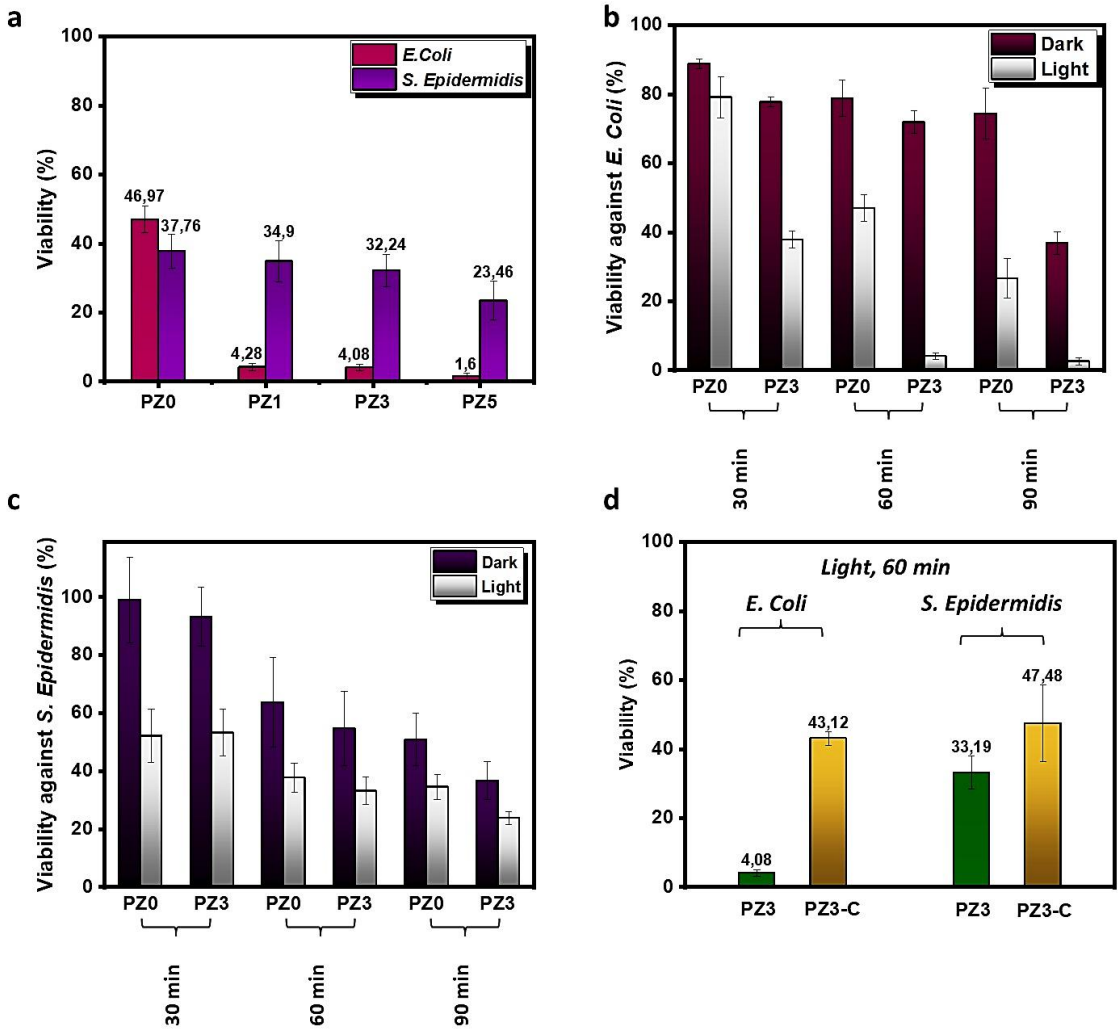

Figure 5.5: a) survival rate (%) of *E. Coli* and *S. epidermidis* by different PHB films for 60 min at visible light; b) survival rate (%) of *E. Coli* by PZ0 and PZ3 I dark and light conditions for 30, 60, and 90 min at visible light; c) survival rate (%) of *S. epidermidis* by PZ0 and PZ3 in dark and light conditions for 30, 60, and 90 min; and d) survival rate (%) of *E. Coli* and *S. epidermidis* by different PZ3 and PZ3-C films for 60 min at visible light.

As 3wt% ZnO MPs content exhibited the optimum antibacterial activity, PZ3 was chosen for further antibacterial characterization. **(Figures 5.5 b, c and 6d)** shows better antibacterial activity with increased time radiation under visible light. The resulting PZ3 films displayed light-enhanced and time-dependent antibacterial activity against *E. coli* and *S. epidermidis*. The best antibacterial effect was found for PZ3 against *E. coli* after 60 and 90 min of treatment, with 96% and 97.5%, respectively. On the other hand, bacterial tests against *S. epidermidis* of PZ3 showed

less effective antibacterial efficiency after 90 min with 76.2%.

Accordingly, ZnO particle size, crystal structure, and environmental factors significantly impact the mechanism underlying the antibacterial action of ZnO MPs. It is important to note that the antibacterial activity of ZnO MPs is thought to be primarily due to Zn^{2+} cations. Zn^{2+} cations can penetrate bacterial cells and inhibit their action. The photocatalytic treatment of metallic oxide particles for sterilization using light as a substitute for chemical or thermal methods to prevent the growth of undesired microbes has garnered heightened interest in various fields such as medicine, food and agriculture, water treatment, and hygiene practices [44]. UV radiation is widely employed to deactivate harmful and spoilage microorganisms, such as fungi and yeasts [45]. Nevertheless, its efficacy in diminishing the quantity of microbes is restricted, primarily because of its limited ability to permeate through non-transparent liquids and solids. In addition, exposure to excessive amounts of UV light might harm the human skin and eyes [46]. Considering these drawbacks and supported by the advancement and affordability of light-emitting diodes (LED), the use of LED technology in the visible light range (400–760 nm) has been emphasized [47]. Preliminary research indicates that LED therapies are efficacious in deactivating harmful germs, including Gram-positive, Gram-negative, and mycobacteria. More precisely, the blue LED (b-LED) with a wavelength range of 400-470 nm appears to possess inherent antibacterial characteristics due to natural photosensitizing chromophores in disease-causing microorganisms [48]. However, limited research studies have studied the application of LED technology in the visible light range (420 -780 nm) for antibacterial properties. In line with previous findings, one potential explanation for the biological impact of ZnO MPs under LED visible light is the existence of b-LED, which is associated with photochemical reactions that occur when photoreceptor molecules absorb light of a specific wavelength. Light absorption in the visible light spectrum, specifically between 400 and 500 nm wavelengths, can produce reactive oxygen species (ROS). The physiological effect of incomplete reduction of molecular oxygen is the creation of reactive oxygen species (ROS), which include superoxide anions (O_2^-), hydrogen peroxide (H_2O_2), extremely reactive hydroxyl radicals (OH°), and hydroxide ions (OH^-) [49]. These ROS are harmful to bacteria and responsible for the potent antimicrobial effect. Excessive ROS generation can damage bacterial cell membranes, impair protein synthesis, and destroy particular DNA sites, leading to cell lysis [50]. ROS demonstrated antibacterial properties against *S. aureus* and *Escherichia coli* [51], supporting the notion of utilizing ROS species formation for antimicrobial oxidative treatment. However, ROS is believed to have a secondary role. Nevertheless, previous research suggests that a b-LED light appears effective in

attenuating gram-negative bacteria compared to positive gram bacteria [44], which aligns with our results. Our findings indicate that exposure to b-LED irradiation leads to a partial deactivation of bacteria, although it is not enough to eradicate the microorganisms. In conclusion, the presence of b-LED, together with the bactericidal efficacy of ZnO MPs, makes this a promising, innovative approach for antibacterial efficiency. Therefore, the photocatalytic antibacterial mechanism's confirmation of green ZnO MPs needs to be further verified by experimental analysis.

To compare the antibacterial effectiveness of our green synthesized ZnO MPs with commercial ones, the antimicrobial activities of PZ3 and PZ3-C were measured under 60 min of light irradiation. As seen in **(Figure 5d),** PZ3, loaded with a green antibacterial agent, is 10.5 times better than PZ3-C against *E. Coli* and 1.4 times against *S. epidermidis,* making them environmentally friendly and a sustainable replacement for commercial antibacterial agents. Moreover, in contrast with PZ3, which showed a significantly better antibacterial efficiency against *E. Coli* than *S. Epidermidis*, PZ3-C antibacterial activity didn't considerably differ from gram-negative to gram-positive bacteria. However, both ZnO tend to be more destructive to gram-negative than gram-positive bacteria. This difference in susceptibility is primarily due to the structural characteristics of their cell walls. Gram-negative bacteria possess an outer membrane that may render them more vulnerable to specific antimicrobial agents. The lipopolysaccharide layer in gram-negative bacteria can also facilitate the uptake of Zn^{2+} cations, allowing them to exert their toxic effects more effectively. In contrast, Gram-positive bacteria have a thicker peptidoglycan layer that provides more structural integrity and can act as a barrier to some antimicrobial agents. However, the effectiveness can vary based on specific strains and environmental conditions. While both types can be affected, *E. coli* was more susceptible to the antimicrobial effects of Zn MPs in this work.

The antibacterial efficacy of ZnO-loaded materials has been evaluated in many research, although the findings appear to vary. **Table 5.1** compares the antibacterial efficiency of various antibacterial materials loaded with ZnO as an antibacterial agent from the literature to our PZ films against bacteria.

Table 5.1: Different ZnO-loaded materials and their antibacterial efficiency against bacteria

Matrix/Polymers description	**Testing method**	**Antibacterial efficiency**	**Reference**

PHB/ZnO NPs, solution casting technique	survival ratio	97% growth inhibition for *E. coli* and 94% for *S. aureus* with 10.0 wt % ZnO loading	[52]	Stronger inhibiting effect against Gram-negative than Gram-positive
Our study, PHB/ZnO MPs, solution casting technique	survival ratio with light irradiation	97,5% growth inhibition for *E. coli* and 76.2% for *S. epidermidis* with 3.0 wt % ZnO loading		
PLA/ZnO NPs, melt-extrusion composite	Log reduction in 24 h (CFU/mL)	6.67 for *K. pneumoniae* and 4.3 for *S. aureus* with 3 wt% ZnO loading	[53]	
PLA/ZnO NPs, solvent cast on paper surface	Log reduction in 24 h (CFU/mL)with light irradiation	3.55 for *E. coli* and 1.68 for *S. aureus* with 1 wt% ZnO loading	[54]	
Nanofibrillated Cellulose (NFC)/ZnO NPs, coating on a paper surface	Log reduction in 24 h (CFU/mL)	3.8 for *K. pneumoniae* and 1.6 for *S. aureus* with 1.37 wt% ZnO loading	[55]	
Calcium alginate/ZnO NPs, solution casting technique	Agar diffusion method	A larger inhibitory zone diameter was detected on the agar plate of *S. aureus* compared to that of *S. typhimurium*	[56]	Stronger inhibiting effect against Gram-positive than Gram-negative
Gelatin/ZnO NPs,	Shaking flask	More potent	[57]	

solvent casting method	method	inhibitory action against *L. monocytogenes* compared to *E. coli*	
Polyethylene/ZnO NPs	monitoring the evolution of Optical Density over time till 24 h	More pronounced inhibitory impact against *B. subtilis* compared to *E. aerogenes*.	[58]

As reported previously, ZnO showed inconsistent results of the antimicrobial activities against gram-negative and gram-positive, which agrees with the results reported in this study.

Thus, synthesizing green ZnO MPs can lower ecological disturbances and exert less influence on humans than synthetic chemical agents. Also, the bio-active PHB materials, loaded with green-synthesized agents, are claimed to be effective in minimizing the side effects and less efficient in creating antibiotic resistance, a global concern worldwide. In addition, these synthesized agents are economical as they can be made from extra green renewable resources with eco-friendly processes. To summarize, green-synthesized ZnO MPs are way ahead of synthetic chemical agents for a healthier environment and population. Overall, the findings show promising results for creating bioactive materials to prevent microbiological contamination, which is particularly important for packing applications.

5.2.3. Biofilm analysis and bacterial viability assay

Biofilms have a significant clinical impact on chronic and persistent infections by decreasing the effectiveness of antibacterial agents [59]. To visualize the inhibitory effect of ZnO MPs on the biofilm of the tested microbes, the SEM showed the disappearance of the accumulation of biofilm microbial cells on the PHB surface loaded with ZnO MPs for *E. Coli*. Similarly, for *S. epidermidis*, there were no or some separated cells on the PZ film surface **(Figure 5.6)**.

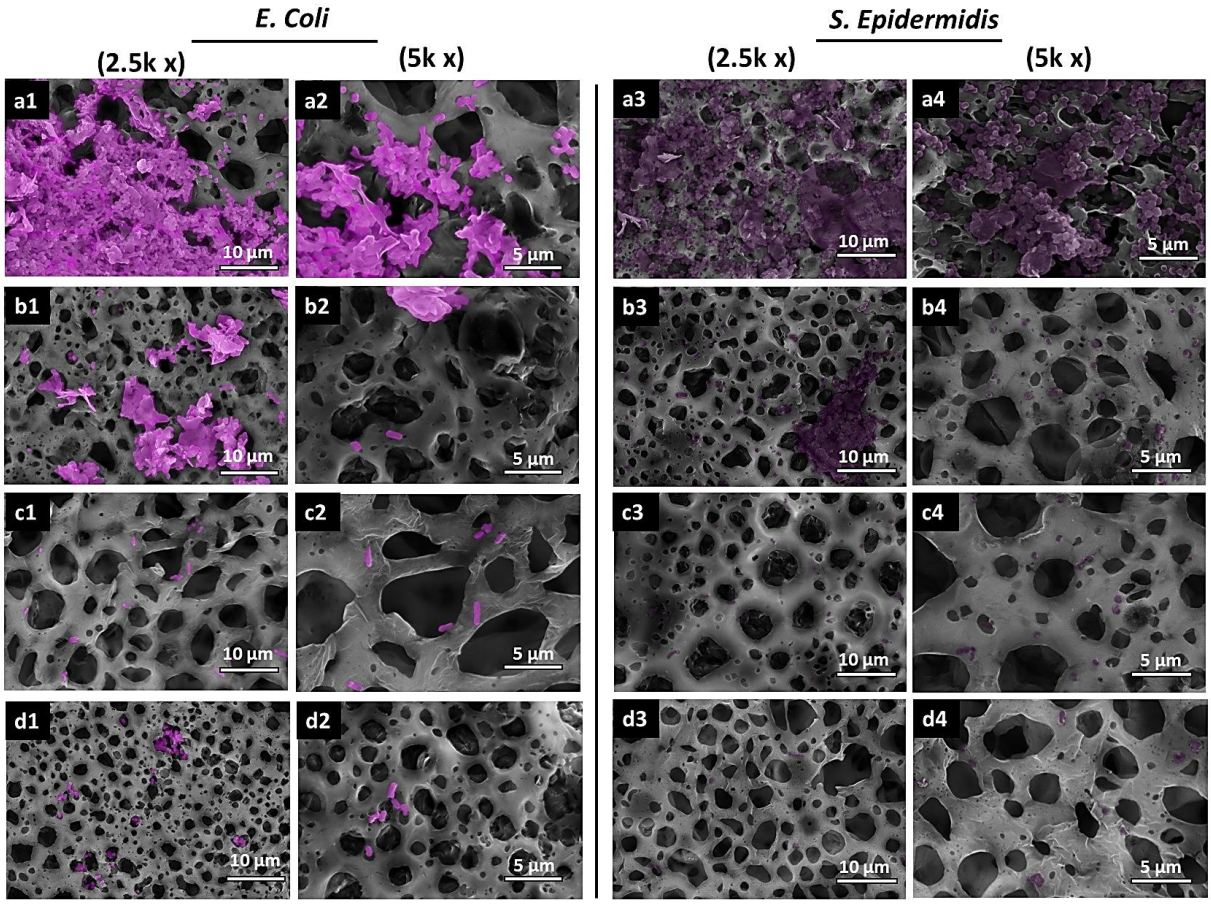

Figure 5.6: SEM images of bacterial adherence on a) PZ0, b) PZ1, c) PZ3, and d) PZ5; 1) the surface of the film (2.5Kx) in contact with *E. Coli*; 2) the surface of the film (5Kx) in contact with *E. Coli*; 3) the surface of the film (2.5Kx) in contact with *S. epidermidis;* and 4) the surface of the film (5Kx) in contact with *S. epidermidis*.

In **(Figure 5.6 a)**, it was visible that bacterial adhesion on the PHB film surface was extreme. The SEM micrographs show that bacteria colonized a large, neat PHB film surface, developing a compact system where each cell supports the adjacent ones, creating aligned cells. Agglomeration of bacterial cell colonies is also found around the pores, forming various layers of extracellular polymeric substance (EPS). Multiple studies of biofilm formation were examined in porous media [60]. Biofilm development in porous materials influences porosity and permeability, leading to clogging membranes [61]. Compared to PZ0, the ZnO MPs significantly decreased the number of biofilm-producing cells, causing a noticeable cellular shape contraction and fewer apparent colonization regions. The EPS was lost, and the cytoplasmic content was released, reducing the cells to single layers. This demonstrates that the ZnO MPs significantly reduce the

biofilm and eradicate the sessile microcolonies. Moreover, the bacterial adhesions on the PZ films effectively diminished with the increase in ZnO MPs content. PZ3 and PZ5 showed no susceptibility to bacteria colonization, indicating that ZnO-incorporated PHB films favor the antibacterial properties.

CLSM images of bacteria on PZ films are presented in **Figure 5.7**, showing live bacterial cells (green emission) and damaged cells (red emission) (contact time = 30 min) to evaluate the antibiofilm efficacy and bacterial viability. Live/Dead BacLight staining may cause bacterial cells that have been injured to become red due to penetration into their cell membranes [62]. The green bacterial cell population was larger on PZ0 than on the ZnO-charged films (**Figures 5.7 a1 and b1),** indicating that gram-negative and positive bacteria were alive. In contrast, visual examination showed that most bacteria in PZ3 were dead. This finding was more noticeable in PZ5. The PZ films showed a dispersed appearance, a significant drop in the number of cells, and a substantial reduction in biofilm. When the ZnO MPs content increased, the bacterial cells turned red, signifying that they had been destroyed.

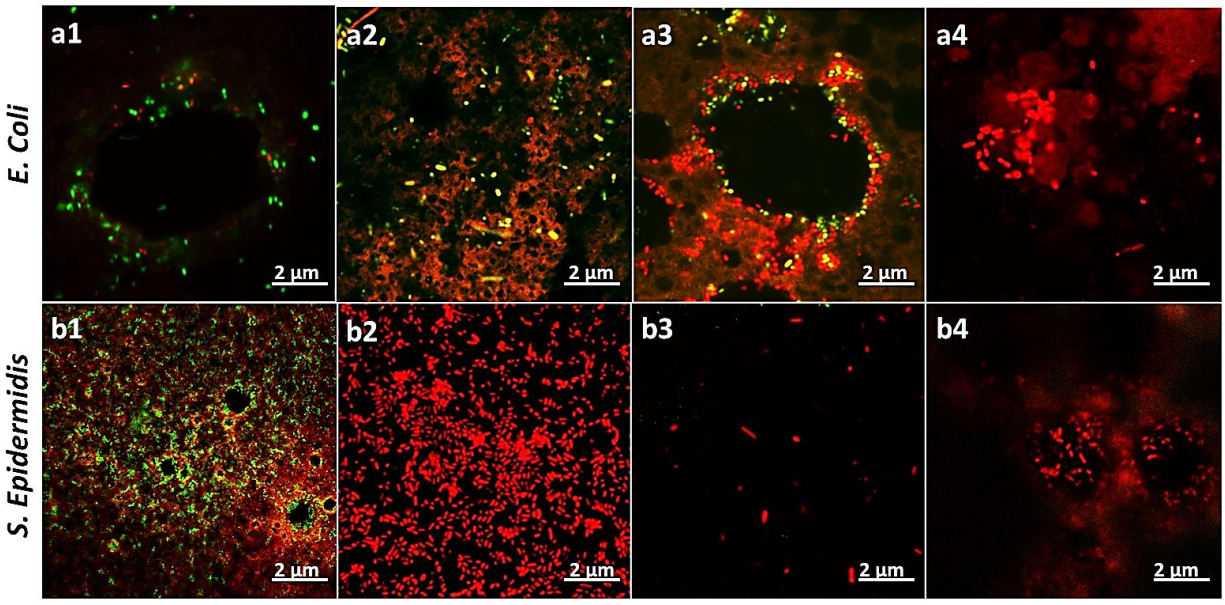

Figure 5.7: Confocal laser scanning microscopy of bacterial biofilms after 18h of growth of a) *E. Coli* and b) *S. epidermidis* adhered on the surface of 1) PZ0, 2) PZ1, 3) PZ3, and 4) PZ5.

This study presents novel data showing that biosynthesized ZnO MPs could broadly antagonize the growth of gram-negative and gram-positive bacteria. Thus, according to our research, PZ films effectively prevent biofilm formation, which may be used in health and food

preservation.

5.2.4. Biodegradation analysis

Studies on biodegradation provide new approaches to non-biodegradable polymers' extended natural life cycle. Utilizing microbes is an environmentally friendly approach because it speeds up the breakdown of materials and could promote the creation of new compounds for commercial use [63]. Because of the moisture and the presence of microorganisms in the soil, the weight loss of polymeric films is a clear indicator of the biodegradation process. The creation of a layer of biofilm—a layer made up of bacteria and their polysaccharides—on the polymer surface is evidence that the microorganisms are growing and using the polymer surface as food throughout the biodegradation process [64]. Polymer properties, including crystallinity, tacticity, molecular weight, organism type, functional group type, and pre-treatment type, are among the various parameters influencing biodegradation [65].

As revealed by **(Figures 5.8 a, b, and c)**, treated membranes started large cracks on the surface from week 4. However, it can be seen that the degradation of PZ films was a little faster than that of uncharged films **(Figure 5.8 d)**. In addition, starting from week 6, the film's weight loss percentage depends on the ZnO MPs content. Increasing ZnO MPs content led to faster degradation. The apparent changes in the surface morphology of polymeric films were detected using 3D LCM and SEM **(Figures 5.8 c and e)**. **(Figure 5.8 e)** displays the SEM micrographs of PZ3 films after degradation, which validated several surface alterations in the polymer surface. It was observed that inert spherical items had degraded. The analysis also indicated the presence of microcracks and the detection of fungal hyphae inside the material**.** Previous studies also reported that fungi could adhere to the plastic surface [66].

After ten weeks, PHB and ZnO-Charged films were discovered to be deteriorated. A link was seen between the physical changes in surface morphology and the weight loss percentage. It was observed that this association grew each week. The antibacterial materials had degraded entirely in ten weeks, and 100% of the weight had been lost. According to Ryan et al. [51], the process of biodegradation consists of the following steps: (i) microbe attachment to the polymer surface initiating the hydrolysis, (ii) microorganism growth using the polymer as a carbon source leading to surface erosion, (iii) polymer primary degradation provoked by moisture-induced cracking, and (iv) polymer final degradation. Moreover, the presence and size of membrane pores significantly influence biodegradation. Larger pores allow better microbial access, leading to more pronounced

enzymatic activity. As degradation progresses, biofilms form within the pores, potentially clogging smaller ones. Continuous microbial activity weakens the membrane structure, causing cracks, pore enlargement, and fragmentation **(Figure 5.8 b)**. The biodegradation process corroborates our study, where it is evident that the PZ3 film thickness decreased progressively during degradation **(Figure 5.8 c)**.

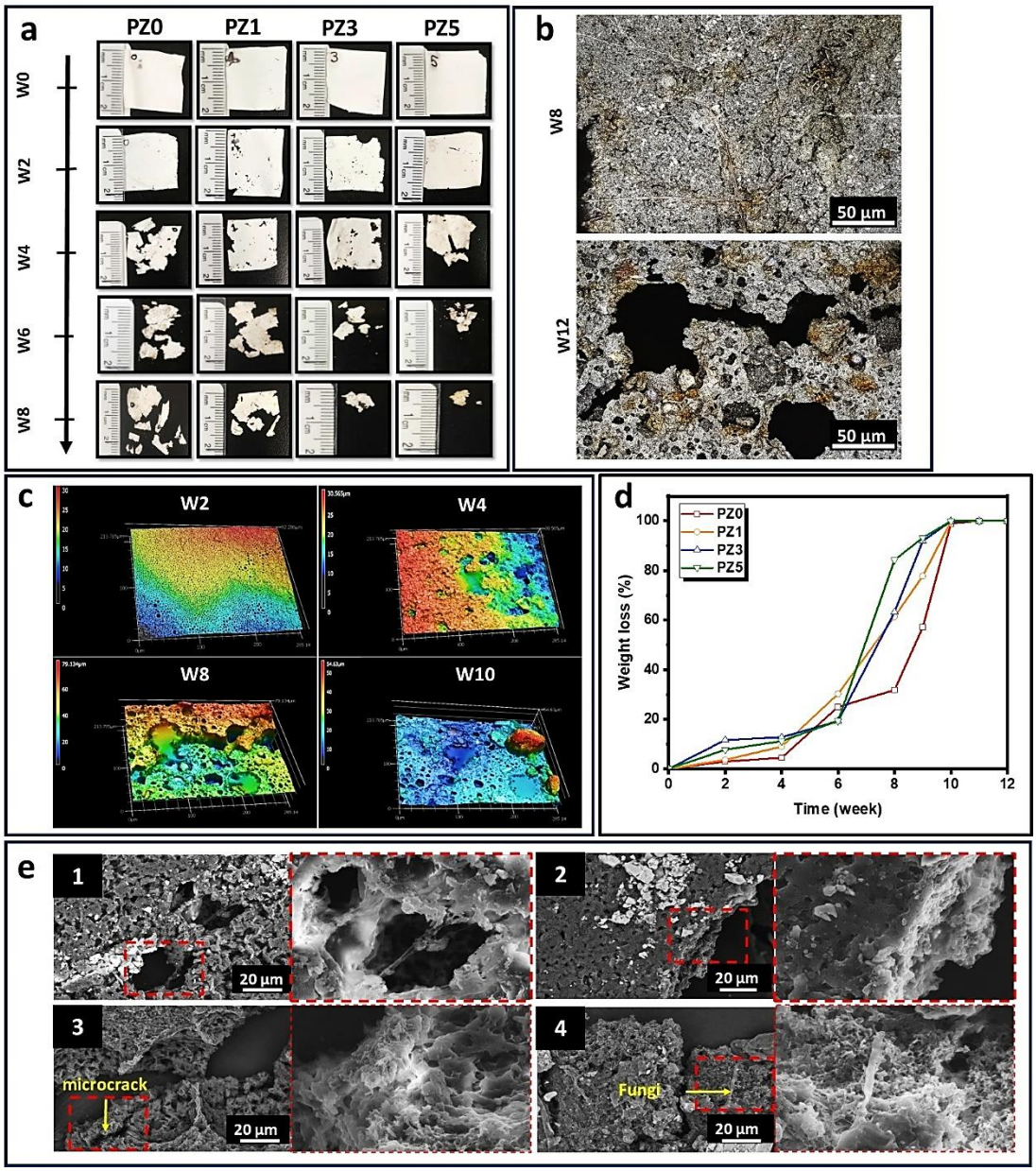

Figure 5.8: a) Photographs of PZ films after soil burial test, b) LCM images of PZ3 after eight and twelve weeks of burial test, c) 3D LCM images of PZ3 after two, four, eight, and ten weeks of soil burial, d) Weight loss of PHB and PZ films after two, four, six, eight, ten, and twelve weeks, and e) SEM micrographs of PZ3 after 1) two weeks, 2) four weeks, 3) six weeks, and 4) eight

weeks of soil burial.

Overall, their increased roughness and decreased hydrophobicity significantly affect the antibacterial activity and biodegradability of PHB-ZnO films. Because of its reduced hydrophobicity, ZnO MPs may be more effective in rupturing bacterial membranes and causing cell death due to the improvement in bacterial adherence, enabling closer contact between bacteria and the film surface [67]. Simultaneously, ZnO MPs' increased surface roughness makes more surface area available for microbial colonization, which speeds up microbial adhesion and biofilm formation. However, as previously discussed, the CLSM analysis confirmed the effective antibacterial efficiency of ZnO MPs as the bacterial biofilm developed onto the PZ films was mainly destroyed. Even though higher surface roughness facilitates biofilm development and early microbial adhesion, it also encourages microbial enzymatic breakdown of the PHB matrix, which may hasten the biodegradation process. Nonetheless, ZnO MPs influence biodegradation rates; their size, concentration, and surface characteristics determine whether they impede or promote microbial activity. These multiple interactions highlight the importance of surface properties in influencing the antibacterial efficacy and ecological fate of PHB-ZnO films, which is vital for improving their performance in packaging and environmental applications.

Finally, the primary outcome of this study is that the ZnO MPs content did not negatively impact the biodegradation characteristics of the antibacterial materials. In conclusion, bioplastics are one of the most cutting-edge biobased and biodegradable materials. More research is also hoped to produce a biomaterial for packaging applications that is strong antibacterial but environmentally friendly.

5.3. Experimental section

5.3.1. Materials

The PHB used is a 5 mm granule with a molecular weight of 550 Kg/mol supplied by Good Fellow. Chloroform purchased from Thermos Scientific was used to dissolve the polymer. Two types of ZnO MPs were used for the antibacterial effect: 1) Commercial ZnO NPs, ranging in size from 10 to 30 nm in powder form, supplied by SkySpring Nanomaterials, and 2) Green ZnO MPs synthesized by our group using Allium schoenoprasum and Melaleuca Cajuputi essential oil, subject of a forthcoming publication **(Figure SI5.2)**. For biological tests, *Staphylococcus epidermidis* (ATCC 12228) and *Escherichia Coli* (ATCC 11229) were purchased from Cedarlane

(Southern Ontario, Canada). Glutaraldehyde 5% from Sigma Aldrich and Sodium Cacodylate buffer (0.2 M, pH 7.4) from Fisher Scientific were used for bacteria cell fixation. The Live/Dead Bacterial Viability Kits (L7012) was purchased from Thermofisher Scientific.

5.3.2. Fabrication of PHB active films

The environmentally friendly and sustainable films were fabricated using conventional solution casting. The polymer solution was prepared by dissolving PHB (1% w/v) in Chloroform under stirring for 1 h at 60 °C until complete dissolution using a reflux condenser. The antibacterial agent was incorporated in PHB film by adding ZnO MPs into casting liquid at 1, 3, and 5 % (w/v) concentrations and named PZ1, PZ 3, and PZ5, respectively. Casting liquid with ZnO MPs was mixed thoroughly under stirring for 60 minutes and kept in a sonic bath for 15 minutes to eliminate trapped air bubbles. The degassed casting solution was transferred to a 9 cm glass petri dish and permitted to dry for 24h at 23°C. The dried films were then peeled off for further analysis. A neat film was also prepared without ZnO MPs and named the PZ0 film. The antibacterial activity of the green ZnO MPs was compared with those of commercial ZnO MPs at 3 % (v/v) concentration. The film with commercial ZnO MPs was named PZ3-C.

5.3.3. Characterization Techniques

The pore morphology and layer structure of the PHB films were investigated using a (JEOL-JSM 5500) scanning electron microscope (SEM) operating at a voltage of 15 kV to examine the surface morphology of the films. Samples were cut in 1 cm^2, mounted on aluminum stumps, and then coated with a gold cover layer (~ 5 nm) for 15 seconds to prevent charging effects. For cross-section analysis, a sharp, high-quality razor blade is used to make a single, clean cut through the film, minimizing mechanical stress that might distort the polymeric structure. To prepare, we carefully place the membrane onto a flat, clean surface to ensure stability. Next, in one smooth, controlled motion, we used the razor blade to create the cross-section by applying minimal pressure. The cut section is then carefully mounted onto an SEM sample holder. The imaging was conducted at an optimized working distance at various magnifications to capture detailed surface and cross-sectional morphologies. ImageJ processing techniques were used to analyze pore size distribution. X-ray spectrometer (SEM-EDX) line mapping analysis was utilized to ascertain the elemental content of ZnO MPs. The film's surface roughness was assessed using a laser confocal microscope (VK-X1000 3D laser confocal microscope). High-resolution 3D images can be

obtained to evaluate and characterize the surface before and after biodegradation. Small samples cut from the active films were examined at a room temperature of 23 ± 1 °C without prior treatment. FT-IR spectra of the attenuated total reflectance were obtained using an (FTS 45) fitted with a Universal ATR sampling attachment (diamond crystal) to study the structural interaction between the PHB matrix and ZnO MPs. For every sample, scans were obtained within the 4000 to 400 cm^{-1} wavelength range. The sample was pressed against the diamond crystal to ensure optimal contact and background spectra were recorded. The resulting spectra were analyzed for characteristic functional groups, with particular attention given to shifts in absorption bands that indicate interactions between the PHB and ZnO MPs. The surface wettability of PZ films was determined using the Surface Energy (Theta Flex optical tensiometer by Attension) to measure the water contact angle (WCA). A 5.0 ± 0.2 µL water drop was placed on 4 cm2 PZ films using automatic pipetting.

5.3.4. Antibacterial Activity

Two test organisms were used to evaluate the antibacterial activity of the films: Gram-negative *Escherichia coli* (ATCC 11229) and Gram-positive *Staphylococcus epidermidis* (ATCC 12228). using a simple method reported previously [15]. The survival ratio (SR) was determined by applying the following formula:

$$SR = (N/No) \times 100) \qquad \text{Equation 5.1}$$

N and N_o represent the average number of bacteria on the control untreated PHB and PZ films, respectively. The average of the three replicates is used to provide findings.

5.3.5. Anti-biofouling test

To measure bacterial adherence and biofilm formation on the active films, 1 x 1 cm samples were dipped in 1 mL of bacterial culture (10^6 cells/mL). The bacterial tubes were cultured at 37°C for eighteen hours without stirring. After removing the bacterial culture, the films underwent three rounds of rinsing with distilled water to eliminate unattached cells. Next, samples were scanned using (SEM), and Confocal Laser Scanning Microscopy (CLSM) was used to track living and dead bacteria.

The cells were initially immobilized for SEM analysis into the specimens using 5% (v/v) glutaraldehyde diluted in 0.2 M sodium cacodylate buffer (pH 7.4) for one hour at room temperature. Following two rounds of washing with sodium cacodylate buffer, samples were

progressively treated with 25%, 50%, 70%, 90%, and 100% ethanol to dehydrate them. After being sputter-coated with a gold film, the film samples were scanned using (SEM) microscope at an accelerating voltage of 10 kV.

CLSM analysis involved uniformly applying 200 µL of 1:1 SYTO 9: Propidium Iodide (PI) dyes in 3 mL of PBS to the surface of each sample. At room temperature, incubation was done in the dark for 15-30 minutes. The green fluorescence (SYTO 9, all cells) was excited at 488 nm and emitted at 575 nm. Red fluorescence (PI, dead cells) was excited at 552 nm and emitted at 620 nm.

5.3.6. Biodegradation of the films

Biodegradation of the neat and active films was carried out using a soil burial test. The 4 cm^2 films were buried in a rectangular container containing natural soil at 23°C and the relative humidity at 40%. The membranes were buried 8 cm below the surface. At two-week intervals, the samples were withdrawn from the soil, carefully cleaned with deionized water, and dried in an oven for 24 hours at 50°C. Finally, the PZ samples were weighed to calculate their weight reduction [15].

5.4. Conclusion

In this study, a new sustainable bio-material was developed. We prepared a ZnO MPs-charged PHB porous film to explore its antibacterial and anti-biofouling performance and biodegradability. This study demonstrates a simple solvent-casting approach for creating porous polymer films using a single chloroform solvent. Microbubbles are generated after thorough mixing, leaving behind pores through solvent evaporation during the drying stage. The microstructure of the PZ films was analyzed to find critical morphological and antibacterial properties. Our findings reveal that ZnO MPs can potentially eliminate individual bacterial cells and significantly reduce biofilm formation. The PZ films demonstrated antibacterial activity against pathogenic bacteria, which was enhanced by increasing ZnO MPs concentration and light exposition. The effect on *E. coli* was consistently more substantial than that on *S. epidermidis*. 3 wt% of green synthesized ZnO MPs was the best composition regarding antibacterial and anti-biofouling properties. Compared to films loaded with commercial ZnO NPs, PZ films exhibits a better ability to deactivate and destroy pathogenic bacteria. Moreover, the role of ZnO MPs in biodegradation control was systematically elucidated with 99% soil biodegradation rates in ten weeks. Our study offers new strategies for practical antibacterial and biodegradable materials.

These biofilms with antimicrobial properties are a fascinating substitute for artificial plastic packaging materials. They help reduce the growth of contaminating bacteria and prolong the shelf life. They are especially appropriate for usage in disposable and packaging applications such as laminating films, blister packages, overwraps, disposable flatware, cups, and utensils for food and beverages. Environmentally, biodegradable packaging will significantly mitigate pollution and ecological degradation by breaking down more quickly in natural environments, thus reducing landfill accumulation and the persistence of microplastics, which pose severe risks to wildlife and ecosystems and thus reduce the ecological footprint of the packaging industry. Although, research is required to improve the antibacterial effect. For example, converting ZnO MPs into nanoparticles will offer several advantages over their microscale counterparts, primarily due to their increased surface area-to-volume ratio, enhanced reactivity, and improved interaction with bacterial cells by penetrating bacterial membranes more easily and disrupting cellular functions more effectively. This heightened activity often leads to lower concentrations required for effective bacterial inhibition, reducing the potential for toxicity and environmental impact. Additionally, nanoscale antibacterial agents can be engineered to release their active components in a controlled manner, providing prolonged antibacterial effects and minimizing the risk of resistance development.

Funding Sources

Regards to Natural Sciences and Engineering Research Council of Canada (NSERC), l'Institut de recherche Robert-Sauvé en santé et en sécurité du travail (IRSST), Canada and le Centre de Recherche sur les Systèmes Polymères et Composites à Haute Performance (CREPEC) to financial support of this work.

5.5. References

[1] D. Malis, B. Jeršek, B. Tomšič, D. Štular, B. Golja, G. Kapun, B. Simončič, Antibacterial Activity and Biodegradation of Cellulose Fiber Blends with Incorporated ZnO, Materials (Basel), 12 (2019).

[2] J. Szostak-Kotowa, Biodeterioration of textiles, International Biodeterioration & Biodegradation, 53 (2004) 165-170.

[3] N.-N. Vu, C. Venne, S. Ladhari, A. Saidi, L. Moskovchenko, T.T. Lai, Y. Xiao, S. Barnabe, B. Barbeau, P. Nguyen-Tri, Rapid Assessment of Biological Activity of Ag-Based Antiviral Coatings for the Treatment of Textile Fabrics Used in Protective Equipment Against Coronavirus, ACS

Applied Bio Materials, 5 (2022) 3405-3417.

[4] C. Venne, N.-N. Vu, S. Ladhari, A. Saidi, S. Barnabe, P. Nguyen-Tri, One-pot preparation of superhydrophobic polydimethylsiloxane-coated cotton via water/oil/water emulsion approach for enhanced resistance to chemical and bacterial adhesion, Progress in Organic Coatings, 174 (2023) 107249.

[5] T. Gasti, S. Dixit, O.J. D'Souza, V.D. Hiremani, S.K. Vootla, S.P. Masti, R.B. Chougale, R.B. Malabadi, Smart biodegradable films based on chitosan/methylcellulose containing Phyllanthus reticulatus anthocyanin for monitoring the freshness of fish fillet, International Journal of Biological Macromolecules, 187 (2021) 451-461.

[6] S.H. Kamarudin, M. Rayung, F. Abu, S. Ahmad, F. Fadil, A.A. Karim, M.N. Norizan, N. Sarifuddin, M.S.Z. Mat Desa, M.S. Mohd Basri, H. Samsudin, L.C. Abdullah, A Review on Antimicrobial Packaging from Biodegradable Polymer Composites, Polymers (Basel), 14 (2022).

[7] G. Satchanska, S. Davidova, P.D. Petrov, Natural and Synthetic Polymers for Biomedical and Environmental Applications, Polymers, 16 (2024) 1159.

[8] S. Ladhari, N.-N. Vu, C. Boisvert, A. Saidi, P. Nguyen-Tri, Recent Development of Polyhydroxyalkanoates (PHA)-Based Materials for Antibacterial Applications: A Review, ACS applied bio materials, 6 (2023).

[9] A.N. Boyandin, L.M. Dvoinina, A.G. Sukovatyi, A.A. Sukhanova, Production of Porous Films Based on Biodegradable Polyesters by the Casting Solution Technique Using a Co-Soluble Porogen (Camphor), Polymers, 12 (2020) 1950.

[10] D. Puppi, G. Pecorini, C. Federica, Biomedical Processing of Polyhydroxyalkanoates, Bioengineering, 6 (2019).

[11] R. Pemmada, X. Zhu, M. Dash, Y. Zhou, S. Ramakrishna, X. Peng, V. Thomas, S. Jain, H.S. Nanda, Science-Based Strategies of Antiviral Coatings with Viricidal Properties for the COVID-19 Like Pandemics, Materials (Basel), 13 (2020) 4041.

[12] A.M. Grumezescu, Engineering of Nanobiomaterials: Applications of Nanobiomaterials, 2016.

[13] A. Khezerlou, M. Alizadeh-Sani, M. Azizi-Lalabadi, A. Ehsani, Nanoparticles and their antimicrobial properties against pathogens including bacteria, fungi, parasites and viruses, Microbial pathogenesis, 123 (2018) 505-526.

[14] K.P. Miller, L. Wang, B.C. Benicewicz, A.W. Decho, Inorganic Nanoparticles Engineered to Attack Bacteria, ChemInform, 46 (2015).

[15] S. Ladhari, N.-N. Vu, C. Boisvert, M.A. Polinarski, C. Venne, A. Saidi, S. Barnabe, P. Nguyen-Tri, Biodegradable polyhydroxybutyrate microfiber membranes decorated with photoactive Ag-TiO2 nanoparticles for enhanced antibacterial and anti-biofouling activities, Journal of Applied Polymer Science, n/a (2024) e55660.

[16] K.M. Rao, M. Suneetha, S. Zo, K.H. Duck, S.S. Han, One-pot synthesis of ZnO nanobelt-like structures in hyaluronan hydrogels for wound dressing applications, Carbohydrate Polymers, 223 (2019) 115124.

[17] K.M. Rao, M. Suneetha, G.T. Park, A.G. Babu, S.S. Han, Hemostatic, biocompatible, and antibacterial non-animal fungal mushroom-based carboxymethyl chitosan-ZnO nanocomposite for wound-healing applications, International Journal of Biological Macromolecules, 155 (2020) 71-80.

[18] K.M. Rao, D. Yeo, E. Kim, K.S.V.K. Rao, M.R.G.S. Chandra, S.S. Han, Xanthan gum and chitosan polyelectrolyte hydrogels with self-reinforcement of Zn+2 for wound dressing applications, Colloids and Surfaces A: Physicochemical and Engineering Aspects, 699 (2024) 134550.

[19] G. Applerot, A. Lipovsky, R. Dror, N. Perkas, Y. Nitzan, R. Lubart, A. Gedanken, Enhanced Antibacterial Activity of Nanocrystalline ZnO Due to Increased ROS-Mediated Cell Injury, Advanced Functional Materials, 19 (2009) 842-852.

[20] A.M. Díez-Pascual, A.L. Díez-Vicente, ZnO-reinforced poly(3-hydroxybutyrate-co-3-hydroxyvalerate) bionanocomposites with antimicrobial function for food packaging, ACS Appl Mater Interfaces, 6 (2014) 9822-9834.

[21] P. Mahamuni-Badiger, P. Patil, P. Patel, D.M. Dhanavade, M. Badiger, Y. Marathe, R. Bohara, Electrospun poly (3-hydroxybutyrate-co-3-hydroxyvalerate) / Polyethylene oxide (PEO) microfibers reinforced with ZnO nanoparticles for antibacterial and antibiofilm wound dressing applications, New Journal of Chemistry, 44 (2020).

[22] V.-S. Mănoiu, A. Aloman, Obtaining silver nanoparticles by sonochemical methods, UPB Sci. Bull. Ser. B, 72 (2010) 179.

[23] J.N. Hasnidawani, H.N. Azlina, H. Norita, N.N. Bonnia, S. Ratim, E.S. Ali, Synthesis of ZnO Nanostructures Using Sol-Gel Method, Procedia Chemistry, 19 (2016) 211-216.

[24] V. Anand, V.C. Srivastava, Zinc oxide nanoparticles synthesis by electrochemical method: Optimization of parameters for maximization of productivity and characterization, Journal of Alloys and Compounds, 636 (2015) 288-292.

[25] K. Vithiya, S. Sen, Biosynthesis of nanoparticles, International Journal of Pharmaceutical Sciences and Research, 2 (2011) 2781.

[26] E. Ismail, A. Diallo, M. Khenfouch, S.M. Dhlamini, M. Maaza, RuO2 nanoparticles by a novel green process via Aspalathus linearis natural extract & their water splitting response, Journal of Alloys and Compounds, 662 (2016) 283-289.

[27] M. Vinoth, R. Suriyaprabha, S. Arunmetha, A. Karthik, S. Karthik, P. Paramasivam, P. Prabu, P. Manivasakan, K. Saminathan, V. Rajendran, Synthesis of Nothapodytes Nimmoniana Leaf Nanoparticles for Antireflective and Self-Cleaning Applications, Synthesis and Reactivity in Inorganic, Metal-Organic, and Nano-Metal Chemistry, 46 (2016) 1445-1449.

[28] M. Pattanayak, P. Nayak, Ecofriendly green synthesis of iron nanoparticles from various plants and spices extract, International Journal of Plant, Animal and Environmental Sciences, 3 (2013) 68-78.

[29] M.H. Koupaei, B. Shareghi, A.A. Saboury, F. Davar, A. Semnani, M. Evini, Green synthesis of zinc oxide nanoparticles and their effect on the stability and activity of proteinase K, RSC Advances, 6 (2016) 42313-42323.

[30] K.M.Z. Hossain, R.M. Felfel, P.S. Ogbilikana, D. Thakker, D.M. Grant, C.A. Scotchford, I. Ahmed, Single Solvent-Based Film Casting Method for the Production of Porous Polymer Films, Macromolecular Materials and Engineering, 303 (2018) 1700628.

[31] A.M. Díez-Pascual, A.L. Díez-Vicente, Poly(3-hydroxybutyrate)/ZnO Bionanocomposites with Improved Mechanical, Barrier and Antibacterial Properties, Int J Mol Sci, 15 (2014) 10950-10973.

[32] A.K. Misra, M.S. Thakur, P. Srinivas, N.G. Karanth, Screening of poly-β-hydroxybutyrate-producing microorganisms using Fourier transform infrared spectroscopy, Biotechnology Letters, 22 (2000) 1217-1219.

[33] Y. Dzyazko, Y. Volfkovich, O. Perlova, L. Ponomaryova, N. Perlova, E. Kolomiets, Effect of Porosity on Ion Transport Through Polymers and Polymer-Based Composites Containing Inorganic Nanoparticles (Review), in: O. Fesenko, L. Yatsenko (Eds.) Nanophotonics, Nanooptics, Nanobiotechnology, and Their Applications, Springer International Publishing, Cham, 2019, pp. 235-253.

[34] S. Karthik, P. Siva, K.S. Balu, R. Suriyaprabha, V. Rajendran, M. Maaza, Acalypha indica–mediated green synthesis of ZnO nanostructures under differential thermal treatment: Effect on textile coating, hydrophobicity, UV resistance, and antibacterial activity, Advanced Powder

Technology, 28 (2017) 3184-3194.

[35] A. Fouda, S. El-Din Hassan, S.S. Salem, T.I. Shaheen, In-Vitro cytotoxicity, antibacterial, and UV protection properties of the biosynthesized Zinc oxide nanoparticles for medical textile applications, Microbial Pathogenesis, 125 (2018) 252-261.

[36] D.A.R. Souza, M. Gusatti, R.Z. Ternus, M.A. Fiori, H.G. Riella, In Situ Growth of ZnO Nanostructures on Cotton Fabric by Solochemical Process for Antibacterial Purposes, Journal of Nanomaterials, 2018 (2018) 9082191.

[37] M. Fiedot, I. Maliszewska, O. Rac-Rumijowska, P. Suchorska-Woźniak, A. Lewińska, H. Teterycz, The Relationship between the Mechanism of Zinc Oxide Crystallization and Its Antimicrobial Properties for the Surface Modification of Surgical Meshes, Materials (Basel), 10 (2017).

[38] R. Brayner, R. Ferrari-Iliou, N. Brivois, S. Djediat, M.F. Benedetti, F. Fiévet, Toxicological Impact Studies Based on Escherichia coli Bacteria in Ultrafine ZnO Nanoparticles Colloidal Medium, Nano Letters, 6 (2006) 866-870.

[39] G. Applerot, N. Perkas, G. Amirian, O. Girshevitz, A. Gedanken, Coating of glass with ZnO via ultrasonic irradiation and a study of its antibacterial properties, Applied Surface Science, 256 (2009) S3-S8.

[40] V. Lakshmi Prasanna, R. Vijayaraghavan, Insight into the Mechanism of Antibacterial Activity of ZnO: Surface Defects Mediated Reactive Oxygen Species Even in the Dark, Langmuir, 31 (2015) 9155-9162.

[41] S. Jiang, K. Lin, M. Cai, ZnO Nanomaterials: Current Advancements in Antibacterial Mechanisms and Applications, Front Chem, 8 (2020) 580.

[42] Z.T. Untracht, A. Ozcan, S. Santra, E.H. Kang, SDS-PAGE for Monitoring the Dissolution of Zinc Oxide Bactericidal Nanoparticles (Zinkicide) in Aqueous Solutions, ACS Omega, 5 (2020) 1402-1407.

[43] N. Zubair, K. Akhtar, Morphology controlled synthesis of ZnO nanoparticles for in-vitro evaluation of antibacterial activity, Transactions of Nonferrous Metals Society of China, 30 (2020) 1605-1614.

[44] C. Lawrence, S. Waechter, B.W. Alsanius, Blue Light Inhibits E. coli, but Decisive Parameters Remain Hidden in the Dark: Systematic Review and Meta-Analysis, Front Microbiol, 13 (2022) 867865.

[45] M. Begum, A.D. Hocking, D. Miskelly, Inactivation of food spoilage fungi by ultra violet

(UVC) irradiation, International Journal of Food Microbiology, 129 (2009) 74-77.
[46] J.-E. Hyun, S.-Y. Lee, Antibacterial effect and mechanisms of action of 460–470 nm light-emitting diode against Listeria monocytogenes and Pseudomonas fluorescens on the surface of packaged sliced cheese, Food Microbiology, 86 (2020) 103314.
[47] G.Y. Lui, D. Roser, R. Corkish, N.J. Ashbolt, R. Stuetz, Point-of-use water disinfection using ultraviolet and visible light-emitting diodes, Sci Total Environ, 553 (2016) 626-635.
[48] M. Grinholc, A. Rodziewicz, K. Forys, A. Rapacka-Zdonczyk, A. Kawiak, A. Domachowska, G. Golunski, C. Wolz, L. Mesak, K. Becker, K.P. Bielawski, Fine-tuning recA expression in Staphylococcus aureus for antimicrobial photoinactivation: importance of photo-induced DNA damage in the photoinactivation mechanism, Appl Microbiol Biotechnol, 99 (2015) 9161-9176.
[49] W. Dröge, Free radicals in the physiological control of cell function, Physiol Rev, 82 (2002) 47-95.
[50] P. Chairuangkitti, S. Lawanprasert, S. Roytrakul, S. Aueviriyavit, D. Phummiratch, K. Kulthong, P. Chanvorachote, R. Maniratanachote, Silver nanoparticles induce toxicity in A549 cells via ROS-dependent and ROS-independent pathways, Toxicology in Vitro, 27 (2013) 330-338.
[51] S. Alfei, G.C. Schito, A.M. Schito, G. Zuccari, Reactive Oxygen Species (ROS)-Mediated Antibacterial Oxidative Therapies: Available Methods to Generate ROS and a Novel Option Proposal, Int J Mol Sci, 25 (2024).
[52] A.M. Díez-Pascual, A.L. Díez-Vicente, Poly(3-hydroxybutyrate)/ZnO bionanocomposites with improved mechanical, barrier and antibacterial properties, Int J Mol Sci, 2014, pp. 10950-10973.
[53] M. Murariu, A. Doumbia, L. Bonnaud, A.L. Dechief, Y. Paint, M. Ferreira, C. Campagne, E. Devaux, P. Dubois, High-Performance Polylactide/ZnO Nanocomposites Designed for Films and Fibers with Special End-Use Properties, Biomacromolecules, 12 (2011) 1762-1771.
[54] H. Zhang, M. Hortal, M. Jordá-Beneyto, E. Rosa, M. Lara-Lledo, I. Lorente, ZnO-PLA nanocomposite coated paper for antimicrobial packaging application, LWT, 78 (2017) 250-257.
[55] N.C.T. Martins, C.S.R. Freire, C.P. Neto, A.J.D. Silvestre, J. Causio, G. Baldi, P. Sadocco, T. Trindade, Antibacterial paper based on composite coatings of nanofibrillated cellulose and ZnO, Colloids and Surfaces A: Physicochemical and Engineering Aspects, 417 (2013) 111-119.
[56] A. Akbar, A.K. Anal, Zinc oxide nanoparticles loaded active packaging, a challenge study against Salmonella typhimurium and Staphylococcus aureus in ready-to-eat poultry meat, Food

Control, 38 (2014) 88-95.

[57] S. Shankar, X. Teng, G. Li, J.-W. Rhim, Preparation, characterization, and antimicrobial activity of gelatin/ZnO nanocomposite films, Food Hydrocolloids, 45 (2015) 264-271.

[58] H. Esmailzadeh, P. Sangpour, F. Shahraz, J. Hejazi, R. Khaksar, Effect of nanocomposite packaging containing ZnO on growth of Bacillus subtilis and Enterobacter aerogenes, Materials Science and Engineering: C, 58 (2016) 1058-1063.

[59] Q. Wei, L.Z. Ma, Biofilm matrix and its regulation in Pseudomonas aeruginosa, Int J Mol Sci, 14 (2013) 20983-21005.

[60] M. Carrel, V.L. Morales, M.A. Beltran, N. Derlon, R. Kaufmann, E. Morgenroth, M. Holzner, Biofilms in 3D porous media: Delineating the influence of the pore network geometry, flow and mass transfer on biofilm development, Water Research, 134 (2018) 280-291.

[61] E. Garg, A. Varma, M.S. Smitha, Biofilms in Porous Media, in: M.P. Shah (Ed.) Modern Approaches in Waste Bioremediation: Environmental Microbiology, Springer International Publishing, Cham, 2023, pp. 365-375.

[62] J.-A. Park, S.-B. Kim, Anti-biofouling enhancement of a polycarbonate membrane with functionalized poly(vinyl alcohol) electrospun nanofibers: Permeation flux, biofilm formation, contact, and regeneration tests, Journal of Membrane Science, 540 (2017) 192-199.

[63] A. Almeida, J. Pontes, G. Alvarenga, H. Finocchio, T. Fill, The sustainable cycle of a new cacao-based bioplastic: from manufacturing to exploitable biodegradation products, RSC Advances, 11 (2021) 29976-29985.

[64] A. Arkatkar, J. Arutchelvi, M. Sudhakar, S. Bhaduri, P.V. Uppara, M. Doble, Approaches to enhance the biodegradation of polyolefins, The Open Environmental Engineering Journal, 2 (2009).

[65] A. Muthukumar, S. Veerappapillai, Biodegradation of plastics–a brief review, Int. J. Pharm. Sci. Rev. Res, 31 (2015) 204-209.

[66] A.C.d.A. Almeida, J.G.d.M. Pontes, G.R. Alvarenga, H. Finocchio, T.P. Fill, The sustainable cycle of a new cacao-based bioplastic: from manufacturing to exploitable biodegradation products, RSC Advances, 11 (2021) 29976-29985.

[67] K. Yamauchi, Y. Yao, T. Ochiai, M. Sakai, Y. Kubota, G. Yamauchi, Antibacterial Activity of Hydrophobic Composite Materials Containing a Visible-Light-Sensitive Photocatalyst, Journal of Nanotechnology, 2011 (2011) 380979.

5.6. Supporting Information

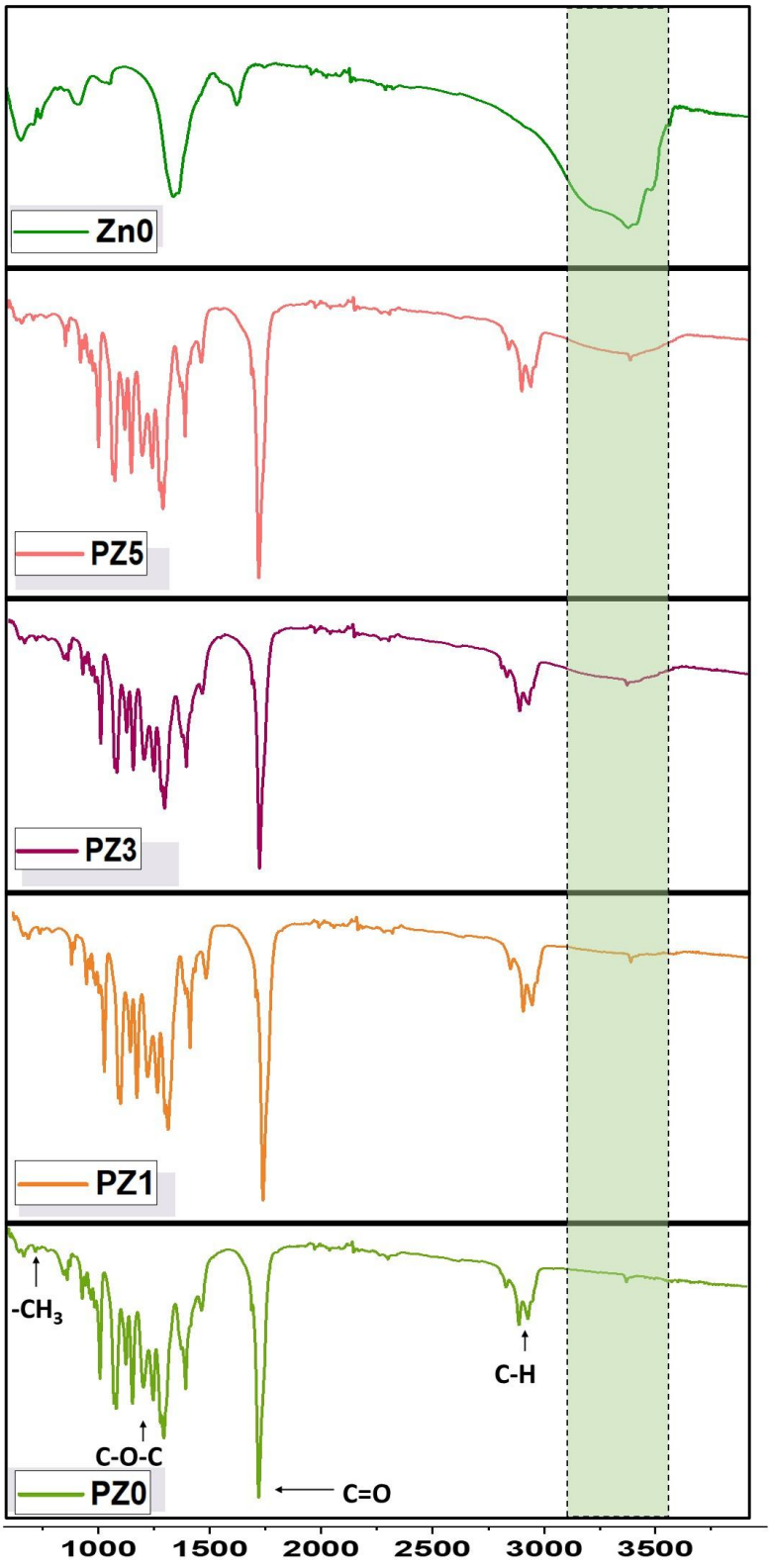

Figure SI. 5.1: ATR-FTIR spectra of PZ films and ZnO MPs

Green synthesis of ZnO microporous particles

The synthesis of ZnO MPs follows a procedure developed by our group. Specifically, an optimized amount of $Zn(NO_3)_2.6H_2O$ was added to the double-necked round-bottomed flask containing a mixture of *Melaleuca cajuputi* essential oil and ethanol (65 mL, v/v = 1.5/5). The mixture was refluxed at 80°C with stirring. After 1h, the condenser was removed, and the mixture was stirred for a further 2h at the same temperature until the color darkened and a precipitate appeared. 5 ml deionized water was quickly added to the mixture, which was stirred for 15 minutes before being cooled to room temperature. The precipitate was collected by centrifugation and washed several times with ethanol solution (95%) before heating to 200°C to obtain ZnO MPs.

It is worth noting that the *Melaleuca cajuputi* essential oil is rich in terpenoids, such as eucalyptol and terpineol. During the reaction, these compounds complex with Zn^{2+} to form Zn^{2+}-terpenoid complex, which subsequently underwent hydrolysis with the addition of water, producing hydroxyl nitrate compounds of Zn [1]. These compounds then decomposed to ZnO particles during the heating step [2].

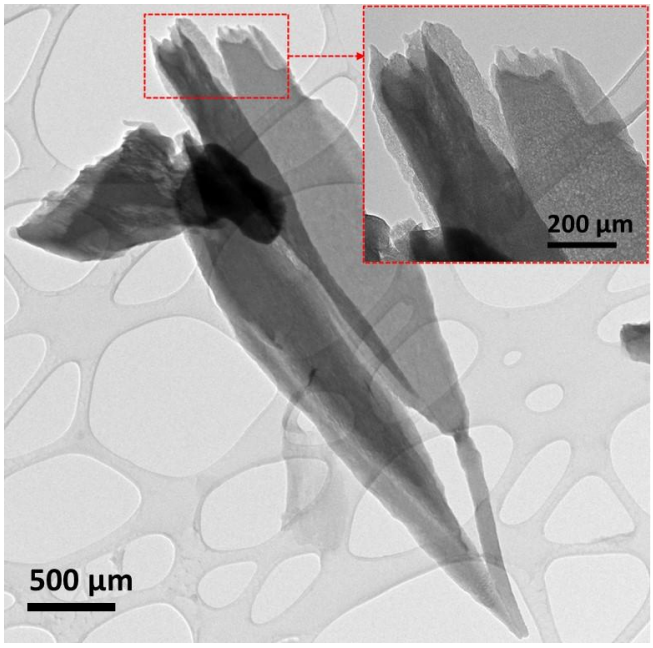

Figure SI. 5.2: TEM image of ZnO microporous particles selected from our unpublished article.

References

[1] Z. Obeizi, H. Benbouzid, S. Ouchenane, D. Yılmaz, M. Culha, M. Bououdina, Biosynthesis of Zinc oxide nanoparticles from essential oil of Eucalyptus globulus with antimicrobial and anti-biofilm activities, Materials Today Communications, 25 (2020) 101553.

[2] T. Biswick, W. Jones, A. Pacuła, E. Serwicka, J. Podobinski, The role of anhydrous zinc nitrate in the thermal decomposition of the zinc hydroxy nitrates Zn5(OH)8(NO3)2·2H2O and ZnOHNO3·H2O, Journal of Solid State Chemistry, 180 (2007) 1171-1179.

Chapter 6: Mechanical and antimicrobial properties of green and photoactive $AgTiO_2$/ polyhydroxybutyrate (PHB) electrospun membranes

Safa Ladhari [a,b], Nhu-Nang Vu [a,b], Alireza Saidi [b,c], Amine Aymen Assadi [d], Phuong Nguyen-Tri [a,b*]

[a] *Department of Chemistry, Biochemistry, and Physics, Université du Québec à Trois-Rivières (UQTR), 3351 Boulevard des Forges, Trois-Rivières, Québec, G8Z 4M3, Canada*

[b] *Laboratory of Advanced Materials for Energy and Environment, Université du Québec à Trois-Rivières (UQTR), 3351 Boulevard des Forges, Trois-Rivières, Québec, G8Z 4M3, Canada*

[c] *Institut de Recherche Robert-Sauvé en Santé et Sécurité du Travail (IRSST), 505 Boulevard de Maisonneuve Ouest, Montréal, QC H3A 3C2, Canada*

d College of Engineering, Imam Mohammad Ibn Saud Islamic University,IMSIU, Riyadh, Saudi Arabia

*Email: phuong.nguyen-tri@uqtr.ca

Published in *Polymer Engineering and Science*, 2024, 11, https://doi.org/10.1002/pen.27036.

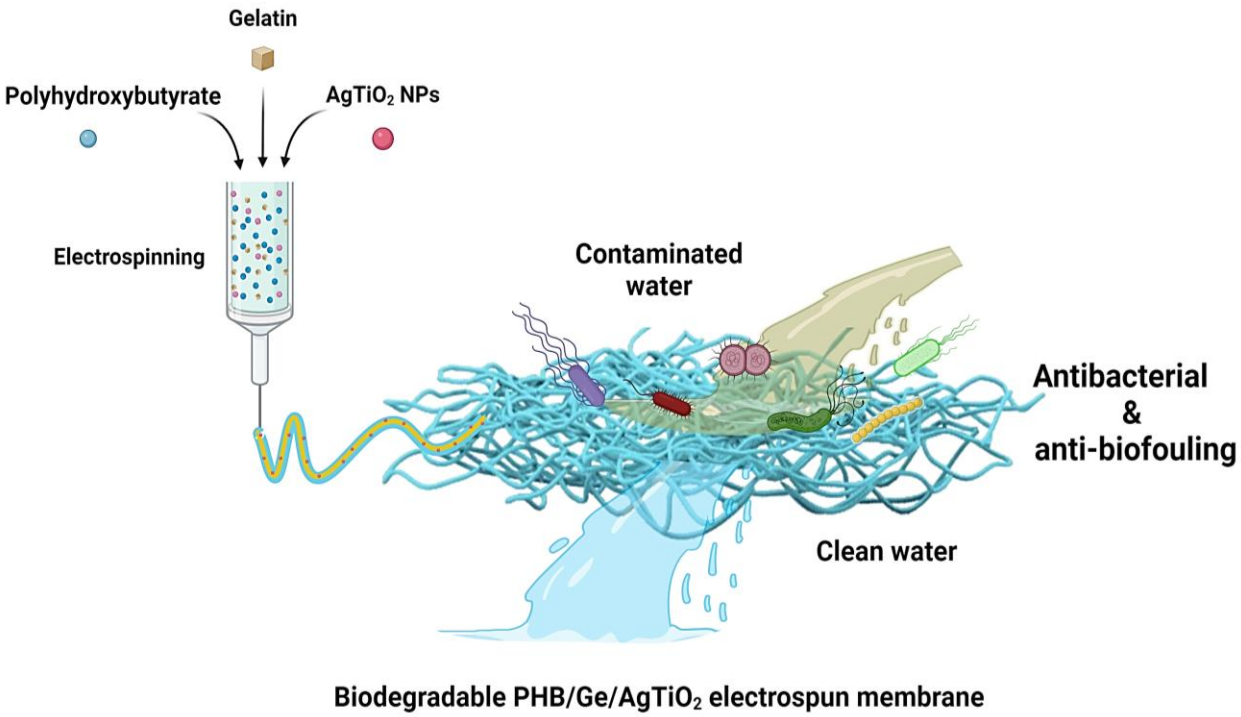

Résumé

L'augmentation des microbes résistants aux antibiotiques et les préoccupations concernant les déchets non biodégradables soulignent le besoin de matériaux innovants avec des fonctionnalités intégrées qui répondent à ces problèmes critiques. Dans cette étude, nous avons synthétisé des nanofibres électrofilées de polyhydroxybutyrate (PHB) mélangées à de la gélatine (GE) et chargées de nanoparticules photoactives d'$AgTiO_2$ aux propriétés mécaniques et biologiques améliorées. Les tests biologiques ont révélé une excellente activité antibactérienne de la membrane préparée, avec une efficacité supérieure à 99 % contre *Escherichia coli* et 95 % contre *Staphylococcus epidermidis* après 90 et 60 minutes d'exposition à des lampes LED commerciales de faible puissance, respectivement. Des études de filtration utilisant une cellule en acier inoxydable sans issue révèlent que les deux bactéries sont éliminées (> 99 % après un cycle de filtration). Les résultats du test de viabilité ont montré que le mélange de PHB et de gélatine améliore les propriétés anti-bio-fouling de la membrane. Les membranes ont également été caractérisées à l'aide des techniques de cartographie SEM et EDX pour l'analyse morphologique et élémentaire, DSC et TGA pour évaluer les propriétés thermiques et la cristallinité, et FTIR pour confirmer la structure chimique. En outre, les membranes électrofilées ont présenté des propriétés mécaniques améliorées avec l'ajout de gélatine. L'échantillon PHB/GE/3wt% $AgTiO_2$ a montré une résistance à la traction 2,2 fois supérieure et un module de Young 1,89 fois supérieur à celui des membranes PHB. Enfin, la dégradation des membranes PHB/GE/$AgTiO_2$ s'est produite progressivement en seulement 8 semaines, démontrant la nature verte et durable des membranes.

Abstract

The rise of antibiotic-resistant microbes and concerns over non-biodegradable waste highlight the need for innovative materials with integrated functionalities that address these critical issues. In this study, we synthesized polyhydroxybutyrate (PHB) electrospun nanofibers blended with gelatin (GE) and loaded with photoactive $AgTiO_2$ nanoparticles with improved mechanical and biological properties. Biological tests revealed excellent antibacterial activity of the prepared membrane, with efficiency exceeding 99% against *Escherichia coli* and 95% against *Staphylococcus epidermidis* after 90 and 60 minutes of exposure to low-power commercial LED lights, respectively. Filtration studies using a dead-end stainless-steel cell reveal that both bacteria are eliminated (> 99% after one filtration cycle). Results of the viability test showed that blending PHB with gelatin improves the membrane's anti-biofouling properties. The membranes were also characterized using SEM and EDX mapping techniques for morphological and elemental analysis, DSC and TGA to evaluate thermal properties and crystallinity, and FTIR to confirm chemical structure. Moreover, the electrospun membranes exhibited enhanced mechanical properties with the addition of gelatin. PHB/GE/3wt% $AgTiO_2$ sample showed 2,2 times better tensile strength and 1,89 times improved Young's modulus compared to PHB membranes. Finally, the breakdown of PHB/GE/$AgTiO_2$ membranes occurred progressively over only 8 weeks, showing the membranes' green and sustainable nature.

6.1. Introduction

Clinical or other healthcare equipment, a hospital-acquired infection, often known as nosocomial, is an infection contracted when obtaining medical treatment [1]. Bacterial infections are collected in surgical operating rooms, clinics, hospitals, and diagnostic labs. Microbes in large quantities can be harmful to humans and cause death [2,3]. Combining chemical entities to achieve antibacterial effects is an innovative method for minimizing the spread of infectious pathogens. Microbes adhered to manufactured surfaces tend to survive and multiply in a humid environment. Meanwhile, microbial cells form a biofilm, which grows in number on the surface. The biofilm consists of polysaccharides and encapsulated cells, nourishing microbial cells and allowing them to endure harsh environments [4]. Controlling microbial development on artificial surfaces is a crucial focus of health and material science. Sterilizing the surrounding environment can prevent surface infection. The most often used disinfectants include hydrogen peroxide, hypochlorite, and reactive oxygen species (ROS). Other often-used chemicals include alcohols, quaternary ammonium compounds, silver, and triclosan [5]. Regular use of disinfectants, particularly triclosan, can lead to significant environmental issues, as the aseptic state is temporary [6]. Another option is to use antimicrobial surfaces to avoid bacteria biofilm formation. Corresponding surfaces reject or kill microorganisms, preventing adhesion [7]. Using antibacterial materials to prevent bacterial contamination in some medical areas is one of the most promising methods for managing pathogenic bacteria [8]. As antibiotics lose efficacy, resulting in treatment failure, infectious diseases become more difficult to treat [9,10]. Various prominent antimicrobial compounds, such as carbon nanotubes, metallic oxide nanoparticles, metal-organic frameworks (MOF), and anti-biofilm gel, have evolved as substitutes for antibiotics to stop bacterial resistance [11,12].

The current drive to discover novel antimicrobial products with unique properties, such as the capacity to combat bacteria resistant to multiple drugs, makes it imperative to enhance the productive techniques for creating nanostructured materials with antibacterial qualities for human health and environmental fields. Specifically, the characteristics of electrospun nanofibers, like their diameter, alignment, high porosity, high surface area to volume, linked pores, controlling the release of active compounds, and increasing the dispersion of nano-additives into biopolymer matrices can be engineered to kill bacteria [13-15]. Poly(3-hydroxybutyrate) (PHB), the simplest member of the poly (3-hydroxy alkanoates) family, is one of the most studied microbial polyesters due to its thermoplastic behavior and mechanical properties that make it suitable for drug-loading

applications. Furthermore, it has better renewability, biodegradability, and biocompatibility than other aliphatic polyesters (such as polylactic acid PLA and polycaprolactone PCL) [12,16]. However, the surface hydrophobicity of materials based on PHB is one of its drawbacks. Regarding biomedical applications, PHB's hydrophobic properties influence its regulated biodegradation and effective interactions with biological media and cells [17,18]. Furthermore, due to its high crystallinity, PHB is stiff and brittle [19], resulting in poor mechanical characteristics and a limited extension at the break, limiting its applicability. Another barrier to the successful use of these polymers is their production costs, determined mainly by the costs of the beginning feedstocks. Since the discovery of PHB, researchers have tackled these challenges, and numerous ways to improve the polymer's processability and reduce brittleness have been developed. Blending with other bio-based polymers provides a diverse way to modify polymer characteristics while maintaining biodegradability [20], specifically gelatin. Gelatin is a biodegradable, biocompatible polymer that is hydrophilic and non-antigenic. It also demonstrates plasticity, and due to the qualities mentioned, it is frequently used in several biomedical applications [21]. In addition to being non-toxic and biodegradable, gelatin, derived from collagen, is commonly chosen as a biofunctionalization agent because of its bioaffinity to bio-cells and its lack of antigenicity [22]. The literature states that gelatin reduces the intermolecular interactions that hold PHB structures together [23]. Hence, electrospinning of blend PHB/gelatin will mitigate potential issues by overcoming the limitations of individual polymers, resulting in a novel biomaterial with high biocompatibility and better mechanical and physical/chemical qualities. Nonetheless, although this blended material presents improved properties, it still lacks antibacterial activity. As a result, enhancing antibacterial characteristics is crucial to make PHB/Ge appropriate for antimicrobial and biodegradable applications.

In recent years, nanotechnology has presented numerous chances to control compounds at the nanoscale, transforming them into potential antibacterial agents. Nanomaterials can disrupt bacterial membranes, form holes and pits on cell walls, generate reactive oxygen species (ROS), bind to sulfhydryl groups of metabolic enzymes, inhibit respiratory activity, and integrate with DNA [24]. This prevents microorganisms from developing resistance against them and would be more effective than antibiotics at inhibiting bacterial resistance. As a result, nanomaterials are particularly effective at killing multi-drug-resistant bacteria strains. In particular, photocatalysts, such as titanium dioxide (TiO_2)-based nanomaterials, have been developed and altered to improve their photocatalytic antibacterial performance in antibacterial research [25]. UV light can activate TiO_2 photocatalytic activity, which then goes through electron transfer processes and produces

photogenerated electron holes. Consequently, many reactive oxygen species (ROS) are produced, including hydroxyl ($HO\cdot$) and superoxide radical (O_2^-), which then interact with biological molecules such as proteins, macromolecules, DNA, and phospholipids in the cellular membrane to cause bacteria cell death. It has been discovered that the antibacterial activity of TiO_2 can be enhanced through assembly with functional nanomaterials, which also helps to separate charges and maximizes their use in visible light for a variety of practical applications. Silver nanoparticles (Ag NPs) are a class of functional nanomaterials well-known for their antibacterial properties. They have been applied extensively in the biomedical area to eradicate germs [26,27]. Ag exhibits antibacterial action without light activation, in contrast to TiO_2. Due to these factors, the photoactive impact of hybrid Ag-TiO_2 NPs, when added to polymeric materials, may produce effective and consistent antibacterial activity. In our recent study [28], Ag-TiO_2 hybrid NPs decorating an electrospun PHB microfiber membranes were found to improve their antibacterial characteristics, especially when exposed to low-power commercial LED light, where the best-performing sample demonstrated over 99% antibacterial efficacy against *Escherichia coli* and *Staphylococcus epidermidis*. In another study, Rodríguez-Tobías used PHB to create nanofibers by the mixing and electrospinning-electrospray methods while using the same concentration of ZnO NPs [29]. The former had an antibacterial efficiency value of 3.20 ± 0.15, while the latter had only 1.20-1.40. Although nanofibers generated utilizing the electrospinning-electrospray approach did not show the expected enhanced antibacterial characteristics. Thus, the antibacterial effectiveness against *E. coli* and *S. aureus* depended on the elaboration technique. The design of ZnO-embedded PHB fibers was more suitable for bactericidal effects.

PHB/gelatin composite scaffolds have been investigated in hybrid PHB-based materials for regenerative tissue and controlled drug release in medical applications [30,31]. They show decreased hydrophobicity, reduced burst effect, and more regulated drug release, but studies of their antibacterial properties have not yet been investigated. In addition, attempts to create hybrid antibacterial materials using PHB, gelatin, and $AgTiO_2$ NPs have been still limited. Thus, this work focuses on the fabrication of hybrid PHB membranes doped with both gelatin and $AgTiO_2$ NPs and a thorough examination of their structure, morphology, thermal and biological properties, and biodegradability as potential materials for various biomedical applications.

Herein, PHB is produced and blended with gelatin, loaded with hybrid Ag-TiO_2 NPs, and optimized for antibacterial activity against *E. coli* and *S. epidermidis*. SEM, FTIR, DSC, and TGA were used to characterize the electrospun nanofibers. The contact angle is determined using the

drop method to determine the wettability of the nanofibers. Furthermore, the antibacterial activity, microfiltration, and cell viability of the functionalized nanofibers' efficiency are assessed. These produced membranes also exhibited excellent antifouling capabilities and high biodegradability. Our studies primarily seek to create an efficient, simple antibacterial material that employs hybrid Ag-TiO_2 NPs to suppress bacterial growth and biofilm formation, demonstrating the feasibility of low-cost biodegradable PHB/Ge membranes and a comprehensive study of their structure, morphology, thermal, mechanical, and biological properties. With such high antibacterial properties, enhanced mechanical strength, effective antibiofilm formation, and biodegradability, these membranes could be considered in biomedical applications, water filtration, and environmental protection.

6.2. Materials and Methods

6.2.1. Materials

The polymer Poly(3-hydroxybutyrate) (PHB) was acquired in the form of pellets from Goodfellow (Huntingdon, England). It has a weight-average molecular mass (M_w) of 550 Kg/mol and a polydispersity index (PI) 1,2. Gelatin was purchased in granular form from Fisher Scientific (New Jersey, USA). Dichloromethane with a purity of at least 99.8% and chloroform with a purity of at least 99.8% were provided by Alfa Aesar (Mississauga, United States) and Thermo Scientific (United States), respectively. These solvents were used to dissolve PHB. Acetic acid was used to dissolve gelatin. The biological assays utilized *Escherichia Coli* (ATCC 11229) and *Staphylococcus Epidermidis* (ATCC 12228) obtained from Cedarlane in Southern Ontario, Canada. In addition, the bacteria cell fixation process involved using Glutaraldehyde 5% obtained from Sigma Aldrich and Sodium Cacodylate buffer (0.2 M, pH 7.4) purchased from Fisher Scientific. The Live/Dead Bacterial Viability Kits (L7012) were acquired from Thermofisher Scientific. $AgTiO_2$ NPs synthesis is summarized in our previous published research [28].

6.2.2. Preparation of PHB/Ge/$AgTiO_2$ complex electrospun microfibers

PHB pellets (1,4 g; 7% w/v) were dissolved in a co-solvent of chloroform/dichloromethane (1:1) and heated to 60°C using a reflux condenser for 24 hours. Meanwhile, Ge powder (0,2 g; 2% w/v) was dissolved in acetic acid by heating at 70°C for 30 minutes. The two polymer solutions were left to cool down at room temperature. 7 ml of PHB solution was gradually mixed with 2 ml gelatin solution while stirring gently. Then, $AgTiO_2$ NPs were added to the mixture. The final

solution was maintained at a consistent temperature at room temperature and agitation for 15 minutes, as sudden changes can cause phase separation. The mixture was injected into a syringe using a metallic needle to create fiber membranes. The electrospinning procedure was performed using a custom-made laboratory instrument with a high-voltage direct current (DC) source capable of generating voltages ranging from 0 to 25 kV. The electrospinning process was carried out with the following parameters: applied voltage 13 kV, average temperature 23°C, average relative humidity 30%, distance between needle tip and collector 12 cm, needle diameter 0.9 mm, and feed rate 0.5 mL/min. To ensure the evaporation of the total solvents, PHB membranes were put in a vacuum oven for 24 hours at room temperature and 10 hours at 40°C. Obtained PHB/Gelatin membranes were named PGx, where x is the wt% of $AgTiO_2$ NPs added to the blended polymer solution. Control bio-based samples, PHB with 0%$AgTiO_2$ NPs and 4%$AgTiO_2$ NPs, P0 and P4, respectively, are examined to determine the role of gelatin in the antibacterial effect and bacterial adhesion.

6.2.3. Characterizations

The scanning electron microscope (JEOL-JSM 5500), SEM, was used to analyze the surface morphologies of the electrospun fibers both before and after the addition of $AgTiO_2$ NPs. Briefly, a small portion of a microfiber sample was vacuum coated with gold after being attached to a brass stub with double adhesive tape. The specimens were examined with a magnification of 2500 times. The elemental composition of $AgTiO_2$ NPs was determined using an X-ray spectrometer (SEM-EDX) line mapping analysis. The average diameter of each sample was determined by measuring the diameters of 100 randomly selected nanofibers using ImageJ Software. This software was also used to measure the electrospun membranes' porosities. SEM images of the membranes were first acquired at high magnification, ensuring clear resolution of individual pores, and then they were imported into ImageJ. At least 10 regions of each image were analyzed to obtain statistically reliable results, and measurements were repeated across 3 SEM images from different membrane areas. The average pore size was then calculated and analyzed for consistency. The membrane surface was evaluated using a high-resolution 3D laser confocal microscope (VK-X1000 3D laser confocal microscope). The nanofiber samples were analyzed using FTIR to identify their functional groups within a 500–4000 cm^{-1} spectral range using an FTS 45 instrument equipped with a Universal ATR sample adapter with a diamond crystal. The wettability of the nanofibers utilizing the Surface Energy (Theta Flex optical tensiometer

manufactured by Attension) was gauged by measuring the contact angle of water using the drop method. In this procedure, deionized water was placed on the surfaces of the membranes. The measurements were conducted three times for each sample, and the mean contact angle was calculated. A Perkin Elmer thermogravimetric analysis TGA (Perkin Elmer Instruments, USA) was employed with a gas flow rate of 20 mL/min and a 10 °C/min heating rate in a nitrogen atmosphere. Differential scanning calorimetry (DSC) studies were conducted on a (TA Waters D.S.C. 25, dynamic) in a nitrogen atmosphere. An axial tensile testing equipment was used to measure the mechanical properties of the PG membranes. Before measurements, samples were preconditioned for 24 hours at 50% relative humidity. The specimen was divided into 30 × 15 mm pieces and affixed between two clamps. Tensile strength refers to the highest force a test specimen creates before rupture. The measurement was conducted on an Instron 4201 universal testing instrument with a 500 N load cell and a 10 mm/min crosshead speed. The length of the gauge was continuously measured until the sample failed at room temperature. The measurements were conducted five times for each sample. As reported, the electrospun membranes were subjected to biodegradation by a soil burial test [28]. The samples were extracted from the soil every two weeks, meticulously washed with deionized water, and subsequently subjected to a 24-hour drying process in an oven set at 50°C to determine their weight decrease.

6.2.4. Antibacterial performance

6.2.4.1. Bacterial reduction assays

Gram-positive *Staphylococcus epidermidis* (ATCC 12228) and Gram-negative *Escherichia coli* (ATCC 11229) were the two test organisms used for assessing the antibacterial activity of the membranes, applying a straightforward technique previously described [28]. First, all the (2 x 2 cm) samples were sterilized with UV light for 30 minutes, then they were put in a 6-well plate. Next, 100 µL bacterial solution (1.5×10^5 CFU/mL) and 1 mL of physiological saline were added to all wells. The 6-well plate was then exposed to white light irradiation provided by the LED-L16 Photoreactor (4,8 mW/cm^2 intensity, Luzchem Inc). After appropriate irradiation times, 2 mL of physiological saline was added to each well, and 100 µL of the combined solution was dispersed on agar plates. Finally, the well plates were incubated at 37°C for 24 hours. The average of three replicates for each sample is given for the results. The following formula was used to calculate the survival ratio (SR):

$$SR = \frac{A}{A0} X\ 100\ \% \qquad \text{Equation 6.1}$$

The average number of microorganisms on the control untreated and antibacterial membranes is denoted by A and A_0, respectively. The findings are derived from the average of the three replicates.

6.2.4.2. Microfiltration analysis

The microfiltration performance was evaluated using a dead-end stainless-steel filtration unit (HP4750 from Sterlitech, U.S.A.) with a total surface area of 14.6 cm^2, as reported in [32]. Before conducting studies, electrospun membranes were sterilized using UV light for 10 minutes, while the filter unit was autoclaved at 120°C for 15 minutes. Before filtering, the specimens were moistened and compressed at a pressure of 69 kPa for 10 minutes. This process ensured a consistent water flow, and all the pores were fully open. Next, 10 ml of liquid bacterial cultures containing (10^4 cells/ml) was passed through the specimens at room temperature at a pressure of 69 kPa. The bacterial concentration decrease following each filtration was assessed using the pour plate technique and quantified using the Log reduction value (LRV, eq. 6.2) and the microfiltration efficiency (eq. 6.3). Every microfiltration test was repeated three times.

$$LRV = Log\ A - Log\ B \qquad \text{Equation 6.2}$$

A 1-log reduction signifies the deactivation of 90% of the bacteria. Consequently, the quantity of bacteria is decreased by a factor of 10. Similarly, a 2-log drop represents a 99% decrease, indicating a reduction of germs by a factor of 100, and so forth.

$$Microfiltration\ efficiency = \frac{A - B}{A} X\ 100\ \% \qquad \text{Equation 6.3}$$

A and B represent the feed and filtrate bacteria concentrations, measured in CFU/mL.

6.2.5. Antibiofouling tests

To assess bacterial adherence and biofilm formation on the specimen, 1 mL volume of bacterial culture containing 10^6 cells/mL was applied to the surface of the samples in a 6-well polystyrene culture plate, and then they were incubated for 18 hours at 37 °C without agitation. Subsequently, the bacteria culture was extracted, and the samples were washed three times with

distilled water to eliminate nonadherent cells. The samples were further examined using Scanning Electron Microscopy (SEM) to capture images, while Confocal Laser Scanning Microscopy (CLSM) was used to monitor both living and dead bacteria. For SEM analysis, the bacterial cells were initially fixed in the samples at room temperature for 1 hour using a 5% (v/v) glutaraldehyde in a 0.2 M sodium cacodylate buffer. After being washed twice with sodium cacodylate buffer, the samples were gradually dehydrated with 25%, 50%, 70%, 90%, and 100% ethanol. Finally, the samples were scanned with a SEM microscope at a voltage of 10 kV.

The assay to determine the viability of bacteria cells was conducted using the LIVE/DEAD L7012 Kit. The staining solutions were made following the manufacturer's directions. In summary, two dyes, SYTO 9 and Propidium iodide dyes, were utilized for staining. The components (A and B) were thoroughly combined in a microfuge tube at a 1:1 ratio. Subsequently, 6 µl of the pre-mixed staining solution was introduced into 2 ml sterile 0.85% sodium chloride solution (NaCl). Subsequently, the microfiber sample was submerged in 200 µL of the staining solution for 30 min at 37 °C in dark conditions. The staining was eliminated, and the sample was washed once with a 0.85% NaCl solution and seen using CLSM. The filters employed are FITC, which has an excitation range of 480–500 nm, and Propidium iodide, which has an excitation range of 550–650 nm.

6.3. Results and discussion

6.3.1. Morphological screening of the electrospun membranes

SEM studied the influence of adding gelatin and $AgTiO_2$ NPs on the electrospun membrane's morphology, structure, and properties. The electrospinning conditions (applied field, inner needle diameter, and flow rate) were kept constant for the different experiments. The surface morphologies of the electrospun samples **(Figure 6.1)** reveal the production of homogenous, uniform, and bead-free fibers. P0 shows a well-distributed surface with a primarily open pore network, while blended PHB/Ge membranes show a straightened pore arrangement. The size-distribution histograms demonstrate that the diameter distribution of the fibers is in the micron range, with P0 and P4 fibers, and in the nano range with the blend PHB/Ge fibers. The average fiber size of pure PHB is about 1.3 µm, possibly because PHB has a higher molecular weight **(Figure 6.1 B)**. The combined PHB/Ge fibers are thinner than the pure PHB fibers; their average diameter is around 786.5 nm ± 221 nm **(Figures 6.1 D, F, G, and K).** The decreased diameter of electrospun fibers compared to the neat PHB sample could be attributed to the addition of gelatin,

which reduced the viscosity of the spinning solution [33]. The gelatin was added at a low concentration, so the solution was less viscous, mainly when dissolved in acetic acid [34,35]. Electrospinning often produces finer fibers because lower solution viscosity influences the jet's stretching and thinning as it moves from the needle to the collector. Moreover, histogram analyses revealed a reduction in the diameters of PHB/Ge fibers upon the introduction of $AgTiO_2$ NPs. The fibers' diameters dropped from 969 nm of PG0 to 512 nm of PG4 as the concentration of $AgTiO_2$ NPs increased. The decrease in nanofiber diameter could be attributed to an elevated electric field resulting from a higher charge density and the conductivity of the electrospinning fluid during the operation. The higher the charge density, the smoother and thinner the resulting fibers due to increased jet-whipping instability [36]. The charge density of the solution increased according to the concentration of $AgTiO_2$ NPs in the mixed polymer solution compared to the neat PHB solution. Consequently, thinner fibers were generated. It is hypothesized that this phenomenon can be explained by the increased concentration of repulsive charges resulting from residual ions and charges produced on the NPs when a voltage bias is applied. This promotes the formation of consistent and thinner fiber structures, which have a greater ratio of surface area to volume [37]. An additional cause of diameter reduction in PHB/Ge nanofibers is enhanced electrical conductivity when adding NPs [38]. However, PG5 showed an increase in fiber diameter. Our investigation demonstrated comparable findings with previous research [23], in which the incorporation of 5% w/v $AgTiO_2$ NPs led to increased fiber diameters, indicating successful integration of $AgTiO_2$ NPs with the PG nanofibers. Furthermore, the accumulation of $AgTiO_2$ NPs during the electrospinning procedure can also result in the extensive dispersion of nanofibers of diverse dimensions [39]. Meanwhile, the agglomeration of $AgTiO_2$ NPs was detected within the PG5 fibers. The distribution of $AgTiO_2$ NPs within the PG fibers was examined using energy dispersive spectroscopy EDS **(Figure 6.1 G)**. The distribution of $AgTiO_2$ components in agglomeration clusters indicates that $AgTiO_2$ was effectively loaded into the PG fibers through electrospinning. However, due to their low concentration in the PG matrix, $AgTiO_2$ NPs did not significantly appear on the surfaces of the PG3, PG4, and P4 fibers. Moreover, considering the SEM sensitivity depth of up to 3 nm, the $AgTiO_2$ NPs were located within the polymer fibers at a more significant depth than the SEM study's sensitivity.

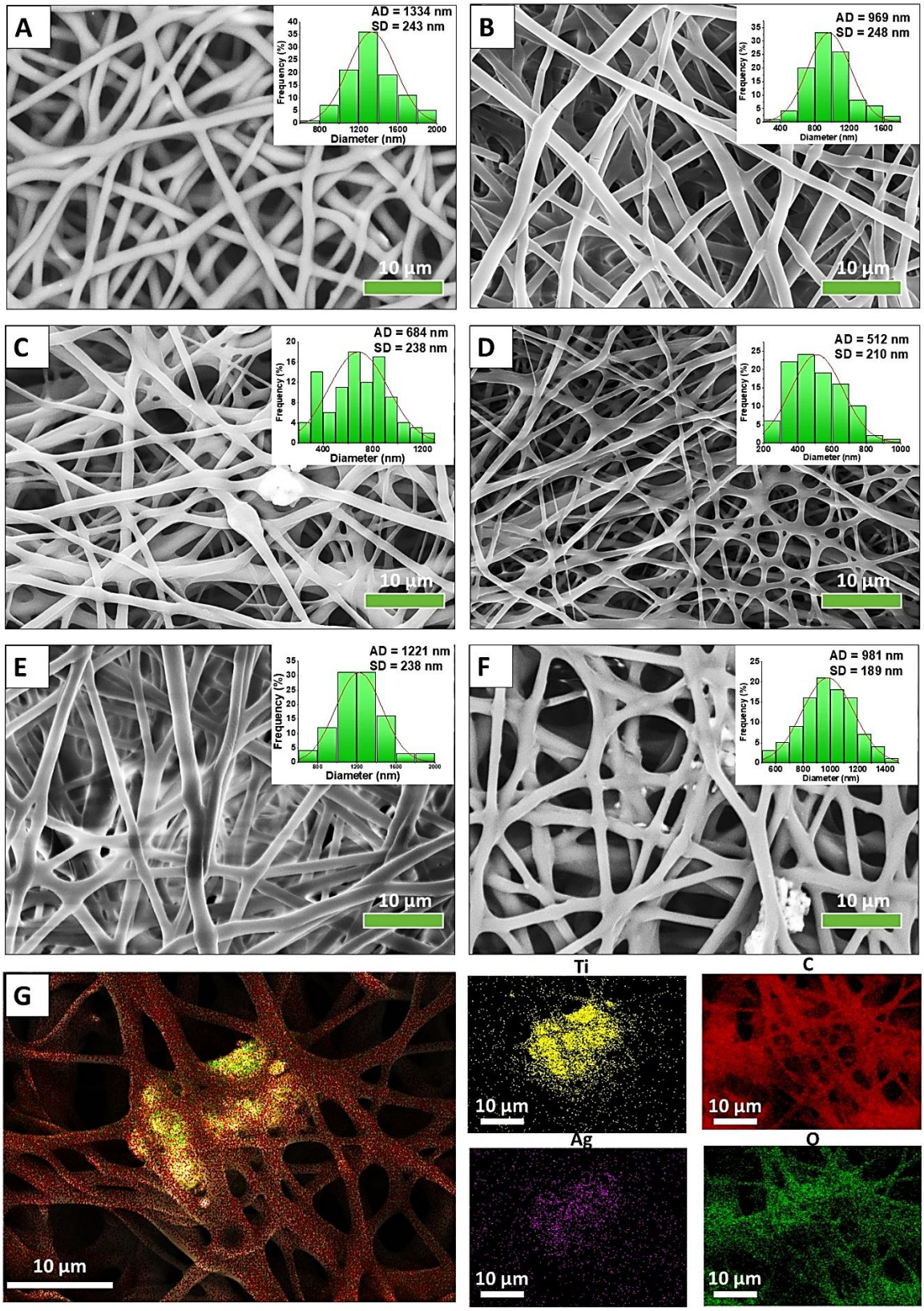

Figure 6.1: SEM images and histograms of the fiber diameter distribution of A) P0, B) PG0, C)

PG3, D) PG4, E) P4, and F g) PG5 fibers. Each histogram was plotted with 100 fibers measured. G) Energy Dispersive Spectroscopy (EDS) mapping of PG5.

6.3.2. Composition and physical-chemical analysis

The water contact angle (WCA) measurements **(Figure 6.2 A)** were used to examine the wettability of the electrospun nanofibers. The PG nanofibers exhibited a decreased hydrophobicity, showing a high level of wettability attributed to the presence of gelatin and $AgTiO_2$ NPs. The enhanced water-attracting properties of the nanofibers were primarily caused by the addition of gelatin and $AgTiO_2$ NPs, which contain -COOH and -OH groups by forming more hydrogen bonds. This resulted in the PG nanofibers having a strong affinity for water compared to pure PHB, which is naturally water-repellent with a water contact angle of 143,7 ± 6°. The water contact angle of P4 was measured to be 127,2 ± 1° **(Figure SI 6.2)**, slightly lower than the pure PHB. This angle is attributed to the presence of $AgTiO_2$ NPs. Hence, gelatin can adjust the hydrophobicity of PHB to achieve the unique needs of different applications. Studies have shown that hydrophilic surfaces are less prone to biofouling than hydrophobic surfaces [40]. As the hydrophobicity of a material's surface rises, hydrophobic organic molecules, like bacteria, are attracted to it, causing surface contamination. Hydrophilic materials typically have better antifouling properties [41,42]. Surface-associated proteins, such as carboxylates and phosphate groups of teichoic acids of the peptidoglycan layer in Gram-positives and fimbriae in Gram-negatives bacteria, have been shown to contribute to hydrophobicity in bacterial cells significantly [43]. This suggests that PG/$AgTiO_2$ NPs composite films have the potential to be effective anti-bifouling materials for antibacterial application.

FTIR analyses were conducted on the electrospun membranes to determine the structural modifications due to PHB blending with gelatin. PG3, PG4, and PG5 had similar IR spectra. **Figure 6.2 B** displays the blended fibers' FTIR spectra of P0, PG, and gelatin. No discernible solvent peaks were observed, indicating that the solvent had evaporated entirely throughout the electrospinning process. Peaks that are related to gelatin and PHB were found to overlap. Three areas in the spectra 3,600–2,300 cm^{-1} (Amide A) (N-H stretch), 1,656–1,644 cm^{-1} (Amide I) (C=O stretch), and 1,560–1,335 cm^{-1} (Amide II) (C-N stretch) can be used to establish the presence of gelatin in the sample [44]. Amides A, I, and II bands were slightly visible in the PG electrospun spectra, and their intensity lightly increased as the gelatin was added compared to P0. The spectrum demonstrates the FTIR's

sensitivity and capacity to detect gelatin peaks even when blended at low concentration. The presence of an amide group verifies the existence of gelatin in nanofibers formed during polymer blending and electrospinning. Amide groups in gelatin can establish hydrogen bonds with water molecules. Thus, gelatin enhanced the hydrophilicity of the resulting PG membrane, as described earlier. The gelatin bands were attenuated due to shrinkage within the fiber blends and higher PHB-nanofiber exposure. As previously stated [31], PHB-nanofibers supported Ge-nanofibers. Comparable results were observed in an FTIR investigation for fibers made by combining PHB and Ge polymers. In addition, the FTIR spectra exhibited a prominent peak at 1720 cm^{-1}, indicating the stretching vibration of the ester (C=O) bond. This peak is exclusive to PHB and is associated with the conformation of the polymer backbone [45].

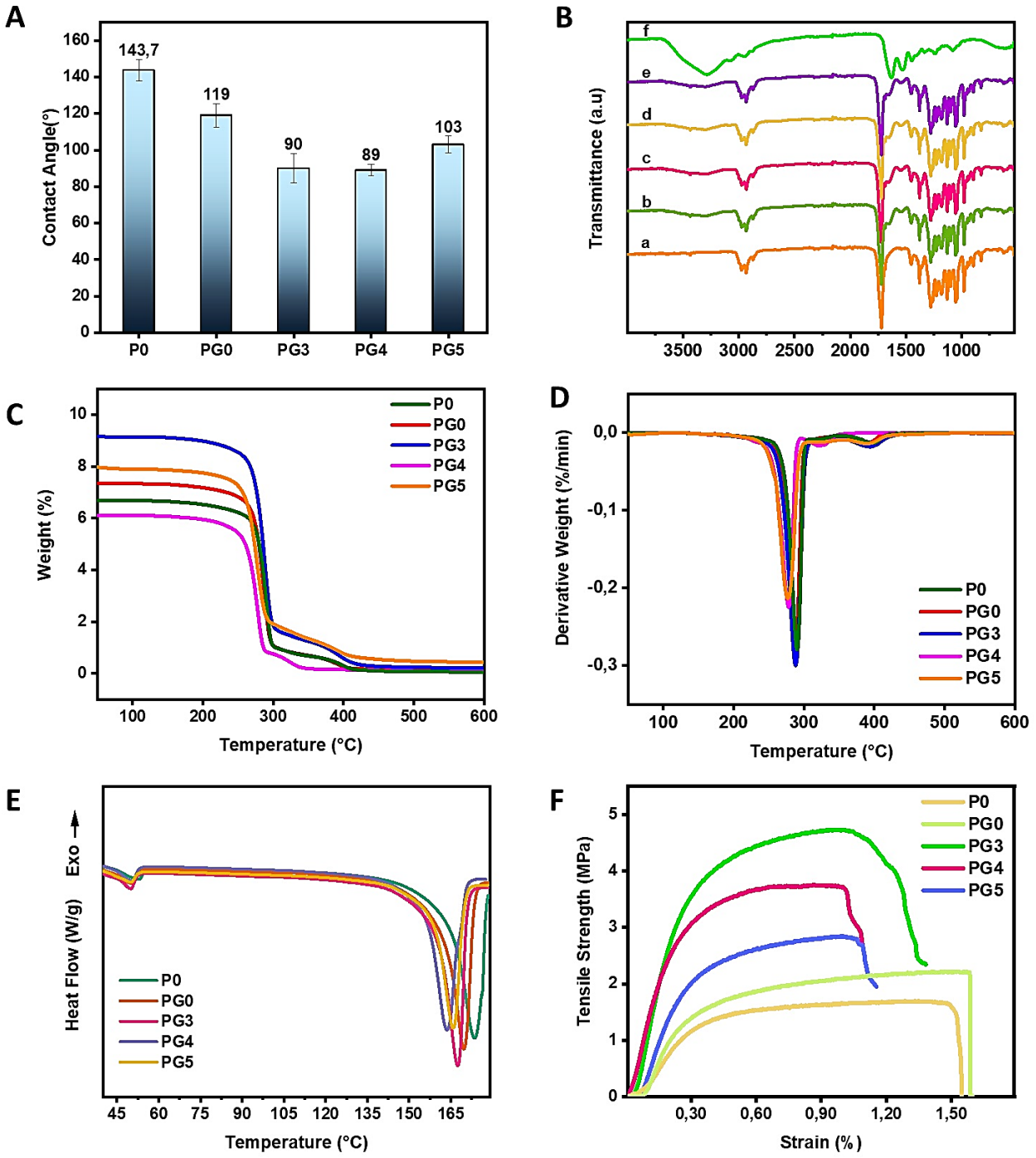

Figure 6.2: A) WCA of P0, PG, and P4 membranes; B) FTIR spectra of a) P0, b) PG0, c) PG3, d) PG4, e) PG5 and f) gelatin; C) TGA curves; D) Derivative thermogravimetry (DTG) curves, E) DSC curves; and F) Stress-strain curves of P0 and PG membranes.

Studying the crystallization and melting behavior of PG membranes is crucial due to its impact on the crystalline structure and the macroscopic properties of the materials. The thermal characteristics

of the electrospun membranes were assessed using a TGA and DSC combined testing analysis **(Figures 6.2 C, D, and E)**. The thermal parameters derived from these analyses are collected in **Table 6.1**. The thermal stabilities of PGO, PG3, PG4, and PG5 were diminished compared to the PO fibers, possibly due to the addition of gelatin. The gelatin enhanced the surface wettability of the PG nanofibers, resulting in a larger area for water adsorption and a decrease in its thermal stability [46]. The thermal stability of PG nanofibers was also affected by the incorporation of $AgTiO_2$ NPs. The initial temperature at which thermal degradation occurs decreases as the amount of $AgTiO_2$ NPs increases, as indicated by the T_{onset} value **(Table 6.1)**. As previously reported, TiO_2 nanofillers improve heat transmission properties from the heat source to the inside of the polymer, increasing the thermal deterioration of PHB [47].

The DSC curves were produced for P0 and PG nanofibers. The pure PHB membrane exhibits a distinct endothermic peak at 173.5 °C, corresponding to the polymer's melting point [48]. Including gelatin in PG reduces the melting temperature, which decreases to 169-165 °C compared to the P0 sample. According to reports, PHB and Ge are thermodynamically immiscible polymers. Consequently, phase separation occurs during electrospinning, developing a core-shell structure composed of PHB (core) and gelatin (shell) [49]. Because gelatin has a polyelectrolyte (polyampholyte) character, it tends to move towards the outer layer of the PHB/gelatin solution jet due to electrostatic repulsion, forming a shell layer [50]. Thus, the variations in the melting temperature could be linked to the core-shell composition of the fibers, which in turn impacts the passage of heat from the gelatin layer to the PHB core. The crystallinity of pure PHB membrane aligns with the information provided in the literature [23]. The combination of PHB and gelatin, as well as PHB, gelatin, and $AgTiO_2$ NPs, reduced crystallinity. This tendency can be attributed to the development of a thin gelatinous layer (shell), which hinders the crystallization of PHB (confinement effect). Adding $AgTiO_2$ NPs to the polymer matrix also induces a reduction in the crystallinity of PHB. $AgTiO_2$ NPs act as nucleating agents and disrupt the crystalline lattice of PHB.

The tensile properties of P0 and PG membranes were tested to measure their durability and elasticity. A tensile stress-strain curve for electrospun samples was generated, and Young's modulus, the tensile strength, and the strain break were estimated from the curve. **Figure 6.2 F** depicts the elastic deformation of electrospun nanofibers. As the deformation progressed, the sample hit the yield stage or elastic limit, and the material was deformed beyond recovery. Tensile strength is the maximum stress value (y-axis), whereas strain break is the maximum strain point

(x-axis), as determined by the curve. The functionalized nanofibers' Young's modulus was calculated using the stress-strain curve's starting slope or gradient. The findings are summarized in **Table 6.2**. Including gelatin with PHB nanofibers improved the samples' tensile strength and modulus while lowering their elongation percentage. Similar findings were discovered when adding gelatin to polycaprolactone microfibers [51]. It could be because, when stretched, the gelatin nanofibers' stress on PHB nanofibers is somewhat distributed, improving the composite scaffolds' tolerance and minimizing their deformation. Gelatin creates a stiffer polymer matrix that may enhance mechanical performance.

Table 6.1: Thermal properties of P0 and PG electrospun materials

Sample	Decomposition temperatures [a]			Residue [a] (%)	Cold crystallization temperature, T_{cc}[b] (°C)	Heat of cold crystallization, ΔH_{cc}[b] (J g^{-1})	Melting temperature, T_m[b] (°C)	Heat of melting, ΔH_m[b] (J g^{-1})	Degree of crystallinity, X_c[c] (%)
	T_{onset}	T_{max}	T_{endset}						
P0	262,3	290,3	409,9	0,22	52,8	3,2	173,5	68,3	44,65
PG0	261,1	286,4	399,8	0,23	49,9	4,3	169,7	69,1	31,07
PG3	257,6	287,3	413,3	0,24	50	4,4	167,4	69	30,97
PG4	251,4	278,8	368,1	0,26	51	4,6	163,7	65,7	29,27
PG5	243,8	277,1	407	0,47	50,2	4	165,5	54,8	24,37

[a] were determined from TGA analysis.

[b] T_g, T_{cc}, ΔH_{cc}, T_m, and ΔH_m were determined from the second heating curve using DSC analysis. The peak maximum was designated as T_m. The values of ΔH_m and ΔH_{cc} were obtained by analyzing the endothermic melting and exothermic cold crystallization peaks, respectively.

[c] was calculated using Eq. (6.4) (SI).

Additionally, the reinforcing impact of $AgTiO_2$ NPs may contribute to the improved mechanical properties observed. Tensile strength increased with $AgTiO_2$ NPs inclusion into the PHB-Ge matrix, suggesting that $AgTiO_2$ NPs may play a role in efficient stress transfer across the polymer matrix. These nanoparticles may exert a strengthening impact due to their actions as fillers, which allow them to distribute stress more uniformly throughout the matrix, enhancing mechanical performance. The highest tensile stress was obtained in the PG3 samples and then PG4, reaching 4,7 MPa and 3,74 MPA, respectively. Previous research on reinforcing electrospun fibers shows that low concentrations of nanoparticles enhance mechanical characteristics. Meanwhile, agglomerations can also cause fibers to become less mechanically strong by forming structures resembling defects [52], as observed with PG4 and PG5. Increased $AgTiO_2$ NPs content causes fiber agglomeration and exposure of nanoparticles, resulting in decreased tensile strength and brittleness [53]. Samadian et al. [54] stated that adding nanohydroxyapatite to cellulose/gelatin nanofibrous films reduced their tensile strength from 3.01 MPa to 2.68 MPa at weight ratios ranging from 12.5 to 50%.

Table 6.2: Mechanical Properties of P0 and PG electrospun materials

	Youngs Modulus (MPa)	**Tensile Strength (MPa)**	**Strain Break (%)**
P0	62.12 ± 2,31	1,47 ± 0,3	15,48 ± 1,16
PG0	89.86 ± 8,62	1,23 ± 0,26	15,87 ± 0,8
PG3	179,01 ± 13,30	4,70 ± 0,27	13,43 ± 1,03
PG4	126,68 ± 13,58	3,74 ± 0,32	11,23 ± 2,26
PG5	117,07 ± 0,72	2,85 ±0,77	11,14 ± 1,82

6.3.3. Antibacterial response

6.3.3.1. Quantitative antimicrobial assay

The plate-counting assay was used to assess the antibacterial efficacy of the nanofibers against *E. coli* and *S. epidermidis*, with PG0 nanofibers serving as control samples. P0 and P4 were examined to study the effect of gelatin on the antibacterial activity. The studies were conducted in light conditions as our previous work confirmed that $AgTiO_2$ NPs displayed enhanced antibacterial activity under low-power commercial LED light [28]. Antibacterial efficiency, represented as a percentage, demonstrates the absence of viable colonies on the electrospun mats after 90 minutes for *E. coli* and 60 minutes for *S. epidermidis.* The results are shown in **Figure 6.3**.

The P0 and PG0 nanofibers lacked antibacterial efficacy against both bacteria strains. After incubation with PG nanofibers, a limited amount of *E. coli* colonies were identified on the agar plate, although no *S. epidermidis* colonies grew. Furthermore, the number of bacteria in the colonies decreases from PG0 to PG5, and bacterial development is significantly suppressed with PG4 and PG5. This suggests that $AgTiO_2$ NPs induce the antibacterial activity of electrospun membranes. Furthermore, employing $AgTiO_2$ NPs on a nanometric scale results in larger surface areas, which may expedite the destruction and wrinkling of bacterial cell walls [55]. Moreover, when exposed to visible light, $AgTiO_2$ NPs can create ROS through oxidation-reduction processes, including hydroxyl radicals ($^{\bullet}OH$) and superoxide radicals ($O_2^{\bullet}$). ROS are highly oxidative chemicals that can tear bacterial cell membranes and destroy biomolecules, resulting in cell death [56]. $AgTiO_2$ NPs content was the key factor impacting the antibacterial activity of membranes. In addition, as expected, blending PHB with gelatin decreases the T_g and the crystallinity of the polymeric membrane, resulting in increased $AgTiO_2$ NPs release. The gradual release of $AgTiO_2$ NPs from PG electrospun nanofibers increases their ability to kill bacteria by slowly releasing antimicrobial agents over time. The PHB and gelatin mixture controls the NP's release rate and ensures a long-lasting antibacterial effect, which is more effective than burst release. As a biocompatible material, gelatin makes the nanofibers more compatible with biological systems. This enhances the antibacterial activity by promoting the interaction between $AgTiO_2$ NPs and the bacterial cells.

Nonetheless, PG nanofibers were more successful in killing the Gram-positive bacteria *S. epidermidis* than the Gram-negative bacterium *E. coli*. As previously reported, the difference in antibacterial impact between Gram-positive and Gram-negative bacteria is primarily due to changes in their cell wall architectures [57]. Gram-positive bacteria's outer cell wall comprises peptidoglycan and acidic polysaccharides (teichoic acids), which include many holes that may allow the adhesion or penetration of antibacterial agents into the cell. Furthermore, gram-negative bacteria have an outer membrane composed of proteins, lipids, and lipopolysaccharides, which may act as a barrier to the entry of bioactive compounds into the cell [58]. The antibacterial activity of the PG fibrous membrane showed strong antibacterial effects due to the sustained antibacterial action of $AgTiO_2$ NPs against Gram-positive and Gram-negative bacteria.

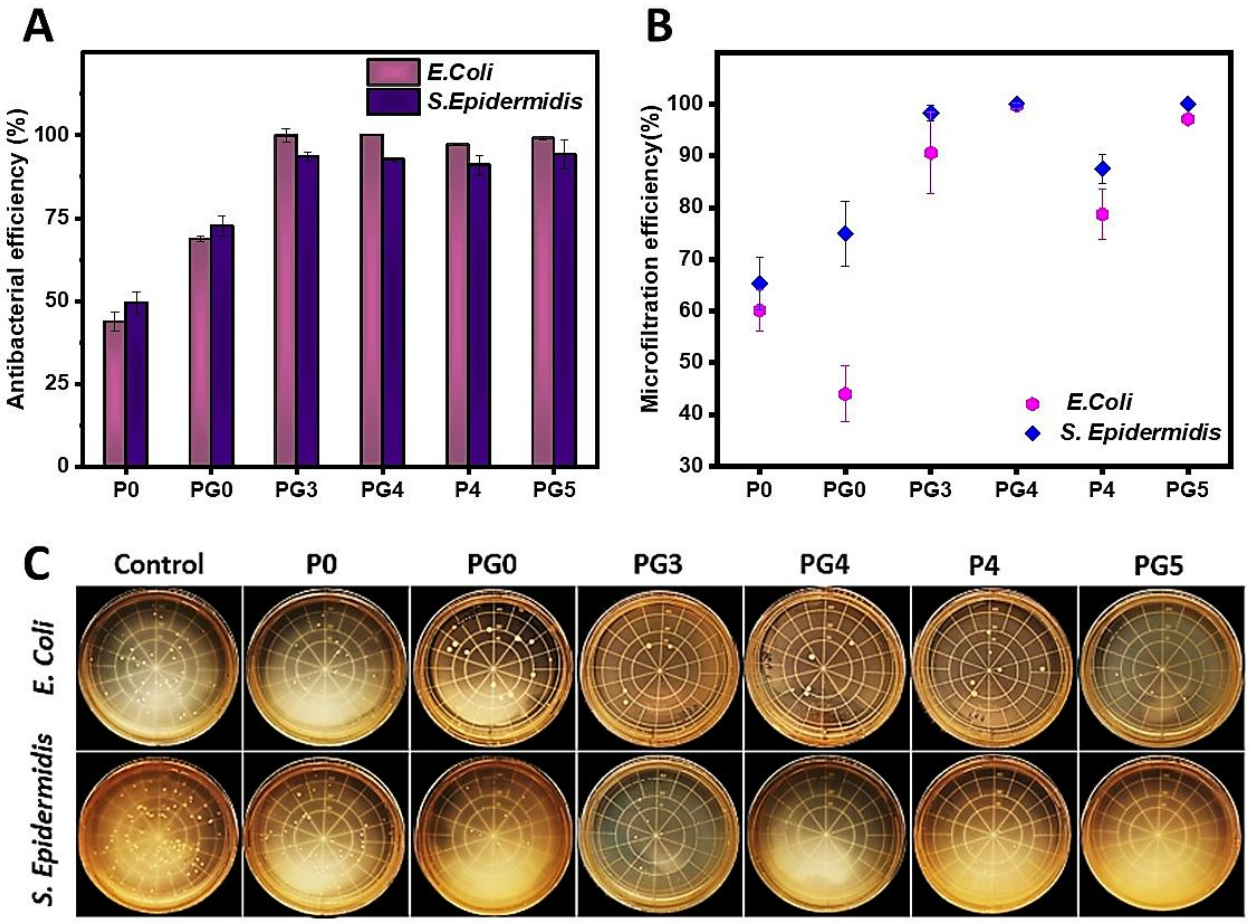

Figure 6.3: A) Antibacterial activity of P0, PG, and P4 membranes against *E. coli* after 90 minutes of light illumination and against *S. epidermidis* after 60 minutes of light illumination, B) Microfiltration efficiency of P0, PG, and P4 membranes against *E. coli* and *S. Epidermidis*, and C) Photographs of agar plates after microfiltration of *E. coli and S. Epidermidis* with the P0, PG, and P4 membranes.

6.3.3.2. Microfiltration action

The nanofibrous membranes' filtration ability was challenged using a representative waterborne bacterium, *E. coli* and *S. Epidermidis*. **Table 6.3** displays the bio-based specimens' efficiency in eliminating both bacteria. After one filtration cycle, PG3, PG4, and PG5 retained >95% of the cells related to a 1-log decrease value **(Figures 6.3 B and C)**. The microfiltration process depends on a size exclusion mechanism, so the pore diameter of the membranes is correlated with the microfiltration efficiency. The quantitative assessments of pore average size were obtained using the image analysis software program ImageJ. The samples with the lowest

pore size diameter provided the best retention rate. Given their average pore diameter of 126 nm, which was the lowest among the other specimens examined, except P4, it was unsurprising that the PG4 and PG5 nanofibers showed the highest retention rates.

Table 6.3: Microfiltration efficiency and pore average diameter of electrospun membranes

	LRV		**Microfiltration efficiency (%)**		**Pore average diameter (nm)**
	E. coli	***S. Epidermidis***	***E. coli***	***S. Epidermidis***	
P0	0,57 ± 0,07	0,59 ± 0,09	60,13 ± 4,04	65,33 ± 5,06	528 ± 1,61
PG0	0,39 ± 0,06	0,60 ± 0,21	43,98 ± 5,40	75,00 ± 10,26	223 ± 1,05
PG3	1,03 ± 0,87	1,76 ± 0,12	90,58 ± 7,79	98,26 ± 1,59	129 ± 0,74
PG4	2,72 ± 0,00	1,98 ± 0,00	99,71 ± 0,50	100,00 ± 0,00	126 ± 0,52
P4	0,85 ± 0,10	0,90 ± 0,10	78,70 ± 4,94	87,50 ± 2,76	120 ± 0,89
PG5	1,54 ± 0,04	1,76 ± 0,00	97,10 ± 0,25	100,00 ± 0,00	126 ± 1,33

These results also fit rather well with the diameters stated in the literature of bacterial cells for *E. coli*; the average bacterial cell size is 1-2 µm in length and 0.5 µm in width, and a diameter of 0.5-1.5 µm for *S. Epidermidis* [32,59]. Nevertheless, the size of the pores of the membranes is not the only determinant of the LRV and microfiltration efficiency recorded in **Table 6.3.** The ImageJ software test for estimating the maximal pore diameter of the bio-based specimens makes assumptions that the pores are cylindrical tubes. However, this is not the case with electrospun nonwoven materials in which the pores are interconnected as a bundle of tortuous tubes. This generates resistance to liquid movement, impeding bacterial invasion via the porous structure. Moreover, as previously stated, $AgTiO_2$ NPs are responsible for cell inactivation. Because the method employed to quantify the filtered cells only counts the number of living cells, those

deactivated were excluded from the filtration data. This explains why PG4 has a better microfiltration efficiency than P4, although P4 has a smaller pore size. This is consistent with the antibacterial results reported in the quantitative antimicrobial assay. Finally, our results show that our PG membranes, especially PG4 and PG5, had higher (≥ 99.9%) microfiltration efficiencies for both Gram-positive and Gram-negative bacteria.

6.3.3.2. Bacterial adhesion and anti-biofouling properties

Researchers have employed two ways for surface modification to reduce the biofouling potential of polymer membranes [60]. The first approach uses an anti-adhesion technique to reduce membrane biofouling [61]. Hydrophilic or polyelectrolyte materials can be added to the membrane surface to minimize bacterial adhesion to polymer membranes. For instance, hydrophilic compounds reduce the hydrophobic interactions between extracellular polymeric substances of the bio-foulants (bacteria) and membranes [62]. The second strategy involves an antibacterial technique that regulates membrane biofouling by applying biocides [61].

Following 18 h of incubation with *E. coli* and *S. Epidermidis*, the surfaces of the nanofibers were examined using SEM and CLSM **(Figure 6.4)** to obtain insight into the bacterial attachment on the electrospun membranes. The green fluorescence on the nanofibers' surfaces indicated a living bacterium cell, while the red fluorescence indicated a dead cell.

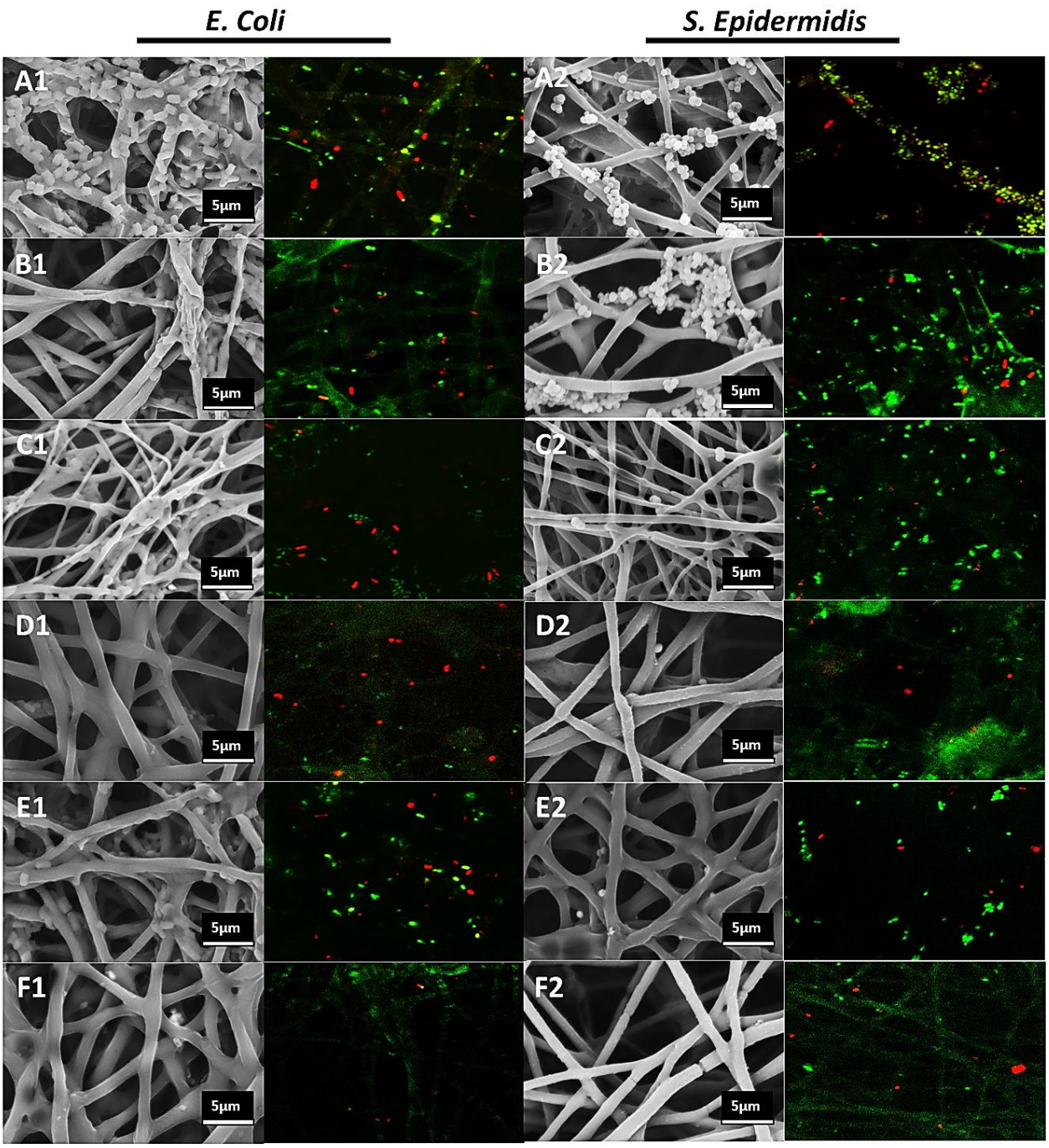

Figure 6.4: SEM and CLSM images of A) P0, B) PG0, C) PG3, D) PG4, E) P4, and F) PG5 membranes after being in contact with 1) *E. coli* and 2) *S. Epidermidis* cells.

SEM images detected large clusters of living *E. coli* and *S. Epidermidis* cells on the unloaded P0 and PG0 surfaces, showing significant growth of the extracellular matrix and a high level of biofilm formation. Corresponding CLSM images showed that the bacteria were stained

green, indicating the formation of healthy living bacterium cells on the P0 and PG0. In contrast, visual inspection revealed that most of the bacteria in $AgTiO_2$ NPs loaded nanofibers were dead. This indicates that the bacterial cells have been injured and become red due to penetration into their cell membranes. This was especially evident in PG4 and PG5, where the membranes displayed a distributed appearance, a notable decrease in the number of cells, and a significant reduction in biofilm. The bacterial cells turned red when the $AgTiO_2$ NPs content rose, indicating that they had been destroyed, showing the fouling-resistant property of the membranes. This suggests that $AgTiO_2$ NPs were responsible for killing bacteria, as previously stated.

Our findings show that blending PHB with gelatin may improve the membrane's anti-biofouling properties in addition to the antibacterial effect of $AgTiO_2$ NPs. By increasing the hydrophilicity of polymer membranes, hydrophilic PG electrospun nanofibers can potentially decrease membrane biofouling [63]. The WCA confirmed the decrease in hydrophobicity when gelatin was added. This explains the enhanced anti-biofouling property of PG4 against P4. Furthermore, by contact killing, the PG nanofibers loaded with $AgTiO_2$ NPs may lessen membrane biofouling caused by the antibacterial activity of $AgTiO_2$ NPs.

6.3.4. Biodegradability

The surge in demand for plastic materials is driving up the exploitation of fossil fuels, which poses a severe environmental hazard with implications for human health, ecosystem toxicity, and global warming. This situation has led to the requirement for new materials that can solve and provide sustainable solutions orthogonal to these immediate challenges.

To evaluate the biodegradation capacity of the nanofiber membranes, PG samples were buried in natural soil, and their morphological and weight variations were monitored over time **(Figures 6.5 and SI 6.3)**. It has been confirmed that PHB degrades naturally in soil [28], and it occurs in three steps, as previously reported [64]: from a high-molecular molecule to monomers and oligomers, the self-enzymatic breakdown of biomass generated during the first stage, and finally, from biomass to CO_2 and H_2O. The initial stage of degradation of the material is depicted in **Figure 6.5**, which shows changes in its structure. This phase is primarily characterized by the microbial activation and mechanical action of soil adhesion, as well as the onset of oxidative and hydrolytic action mediated by soil constituents and enzymes [65]. The fibers' microstructure underwent a substantial alteration after four weeks of exposure to natural soil **(Figure SI 6.3)**. The breakdown

of PG membranes occurred progressively over 8 weeks, with over 50% decomposition already evident by week 5. The pace at which the membrane broke down in soil was unaffected by the presence of gelatin. The primary cause of weight loss exceeding 50% after five weeks is the microbial breakdown of PHB in the soil [66].

The hydrophobicity of the nanofiber membrane makes it difficult for soil bacteria to survive and cling to the surface, which explains why P0 degrades slowly at first. However, it is speculated that microbial aggregation infiltrates from the membrane surface pores, causing direct contact with the inner PG nanofibers and accelerating the internal degradation of the polymer substrate, significantly increasing the degradation rate. Furthermore, investigations have shown that PG degraded quickly **(Figure SI 6.3)**, aided by its enhanced hydrophilicity, which promotes microbial aggregation. Microbial enzymes can break down PHB and gelatin molecules into smaller monomers or low-molecular-weight chemicals. Microorganisms can use these breakdown products to participate in organic cycling in soil, resulting in fast degradation and the formation of carbon dioxide and water [67]. The quick breakdown of PG could possibly be ascribed to the decrease in the crystallinity, as shown by the thermal analysis data.

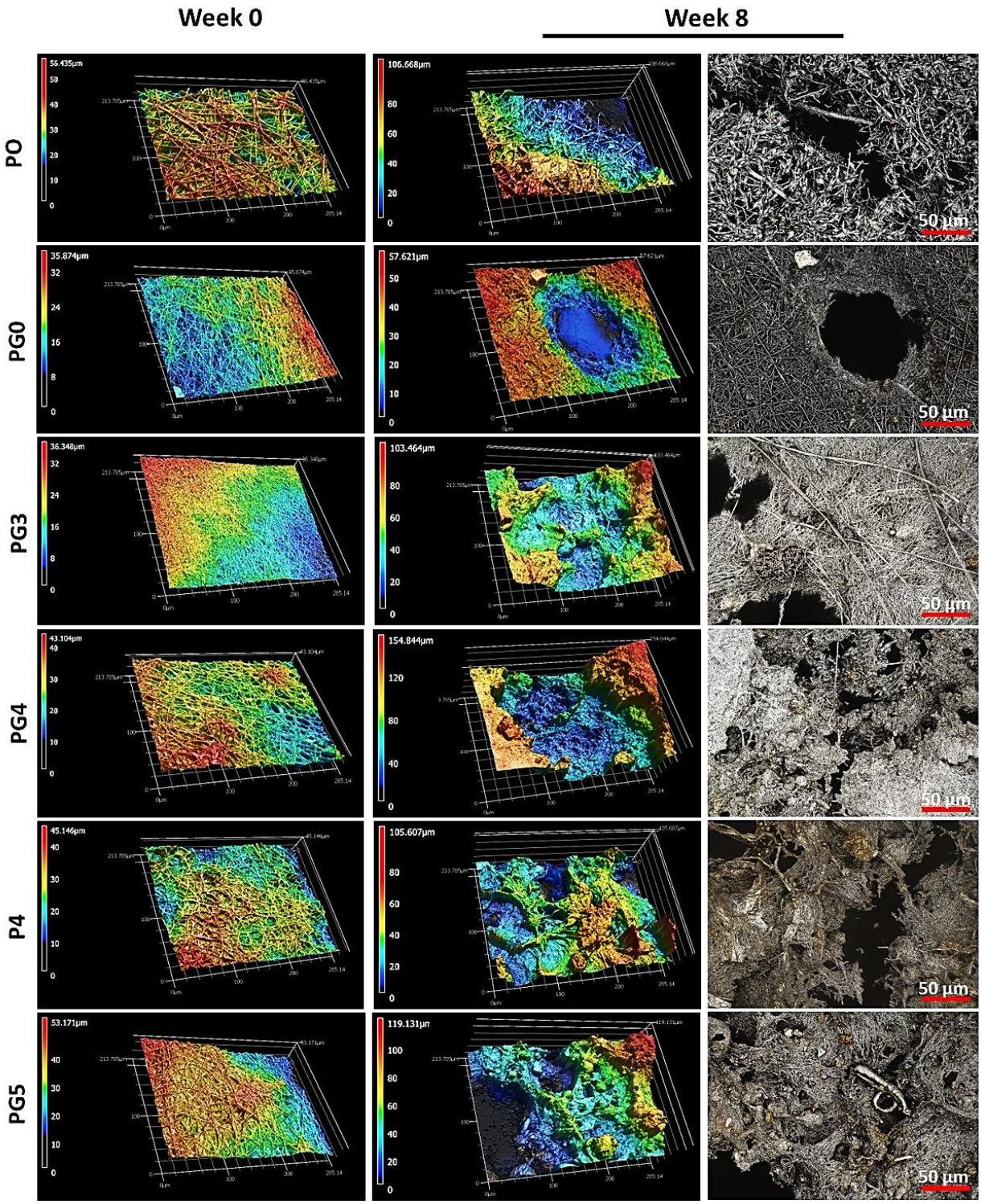

Figure 6.5: Confocal profiler 3D image and laser images of P0, PG0, PG3, PG4, P4, and PG5 membranes before and after 8 weeks of burial test.

Furthermore, it was shown that soil particles were included in the material's pores and structure (**Figure 6.5)**. This increase may be explained by adding soil particles to the material's surface, which could cause the membrane to retain more moisture or microbiological components than usual—a characteristic of the initial stages of soil degradation. It should be mentioned that there was a noticeable amount of sample embrittlement and fragmentation after 8 weeks of burial test. The existence and the size of membrane pores have a significant influence on biodegradation. Pores provide better microbial access, resulting in more pronounced enzymatic activity. As degradation advances, biofilms grow within the pores, which might clog smaller ones. Continuous microbial activity degrades the membrane structure, leading to fractures, pore expansion, and fragmentation (**Figure 6.5)**.

Moreover, as reported previously, including $AgTiO_2$ NPs did not inhibit the membranes' biodegradation [28]. Unlike previous investigations, introducing antimicrobial agents can slow or stop biodegradation. The soil burial experiment results show that PG membranes are biodegradable in soil, which perfectly aligns with the study's initial goal of preventing secondary contamination from antibacterial membranes. This study investigates a more sustainable, ecologically friendly environment with little environmental impact. Bio-based and biodegradable bioplastics PHB blended with gelatin can provide qualities similar to standard plastics while generating extra benefits due to their low carbon footprint.

6.4. Conclusion

Blended fibers, PHB, and gelatin loaded with $AgTiO_2$ NPs were electrospun with chloroform, dichloromethane, and acetic acid as co-solvents. The resulting fibers had a diameter ranging between 500 and 1000 nm. SEM, FTIR, wettability measurements, TGA and DSC studies, and tensile strength measurements confirmed the fabrication of the antibacterial nanofibers. It was discovered that gelatin decreased PHB's crystallinity, which affected wettability and enhanced the antibacterial effects due to the sustained antibacterial action of $AgTiO_2$ NPs against *E. Coli* and *S. Epidermidis*. Moreover, it was surprising that adding gelatin enhanced the fibers' tensile characteristics. It was also found that adding gelatin reduced the fibers' pore size, which improved the microfiltration efficiency. In addition, the biodegradation control was systematically elucidated with 99% soil biodegradation rates in eight weeks.

In summary, based on the findings of the characterizations, PG4 showed the highest level

of performance, including thermal, physical stability, and mechanical performance. It also exhibited an outstanding antibacterial and microfiltration efficiency of ≥ 99.99% against *E. Coli* and *S. Epidermidis* when exposed to LED light and good resistance to biofouling. The results showed that $AgTiO_2$ NPs are responsible for these antibacterial characteristics. Additional research may yield a deeper comprehension of the processes and effectiveness of bactericidal interaction. This could lead to the creation of novel antibacterial biomaterials that effectively inhibit the growth of biofilms, resulting in the creation of innovative approaches to the problems affecting human health and the environment today.

Funding Sources

Regards to Natural Sciences and Engineering Research Council of Canada (NSERC), l'Institut de recherche Robert-Sauvé en santé et en sécurité du travail (IRSST), Canada and le Centre de Recherche sur les Systèmes Polymères et Composites à Haute Performance (CREPEC) to financial support of this work.

6.5. References

1. Rosenthal VD, Bijie H, Maki DG, et al. International Nosocomial Infection Control Consortium (INICC) report, data summary of 36 countries, for 2004-2009. *American Journal of Infection Control*. 2012;40(5):396-407. doi:10.1016/j.ajic.2011.05.020

2. Imani SM, Ladouceur L, Marshall T, Maclachlan R, Soleymani L, Didar TF. Antimicrobial Nanomaterials and Coatings: Current Mechanisms and Future Perspectives to Control the Spread of Viruses Including SARS-CoV-2. *ACS Nano*. 2020;14(10):12341-12369. doi:10.1021/acsnano.0c05937

3. Venne C, Vu N-N, Ladhari S, Nguyen-Tri P. Innovations in Textile Technology Against Pathogenic Threats: A Review of the Recent Literature. Springer Nature Switzerland; 2024:67-99. doi: https://doi.org/10.1007/978-3-031-60255-9_6

4. Mah T-F, Pitts B, Pellock B, Walker GC, Stewart PS, O'Toole GA. A genetic basis for Pseudomonas aeruginosa biofilm antibiotic resistance. *Nature*. 2003/11/01 2003;426(6964):306-310. doi:10.1038/nature02122

5. Siedenbiedel F, Tiller JC. Antimicrobial Polymers in Solution and on Surfaces: Overview and Functional Principles. *Polymers*. 2012;4(1):46-71. doi:https://doi.org/10.3390/polym4010046

6. Andresen JA, Muir DCG, Ueno D, Darling CTR, Theobald N, Bester K. Emerging

pollutants in the North Sea in comparison to Lake Ontario, Canada, data. *Environmental Toxicology and Chemistry*. 2007;26. doi:10.1897/06-416r.1

7. Venne C, Vu N-N, Ladhari S, Saidi A, Barnabe S, Nguyen-Tri P. One-pot preparation of superhydrophobic polydimethylsiloxane-coated cotton via water/oil/water emulsion approach for enhanced resistance to chemical and bacterial adhesion. *Progress in Organic Coatings*. 2023/01/01/ 2023;174:107249. doi:https://doi.org/10.1016/j.porgcoat.2022.107249

8. Boisvert C, Vu N-N, Ladhari S, Polinarski MA, Brouillette F, Nguyen-Tri P. Preparation of Cotton Coated with ZnO-Ag Hybrid NPs for Photocatalytic Inactivation of Bacteria Under LED Light. Springer Nature Switzerland; 2024:49-65. doi:https://doi.org/10.1007/978-3-031-60255-9_5

9. Serwecińska L. Antimicrobials and Antibiotic-Resistant Bacteria: A Risk to the Environment and to Public Health. *Water*. 2020;12(12):3313. doi:https://doi.org/10.3390/w12123313

10. Mancuso G, Midiri A, Gerace E, Biondo C. Bacterial Antibiotic Resistance: The Most Critical Pathogens. *Pathogens*. Oct 12 2021;10(10). doi:10.3390/pathogens10101310

11. Doan TD, Vu N-N, Hoang TLG, Nguyen-Tri P. Metal-organic framework (MOF)-based materials for photocatalytic antibacterial applications. *Coordination Chemistry Reviews*. 2025/01/15/ 2025;523:216298. doi:https://doi.org/10.1016/j.ccr.2024.216298

12. Ladhari S, Vu N-N, Boisvert C, Saidi A, Nguyen-Tri P. Recent Development of Polyhydroxyalkanoates (PHA)-Based Materials for Antibacterial Applications: A Review. *ACS applied bio materials*. 03/13 2023;6. doi:10.1021/acsabm.3c00078

13. Thangavel K, Roshini T, Balaprakash V, Gowrisankar P, Sudha S, Mohan M. Structural, morphological and antibacterial properties of ZnO nanofibers fabricated by electrospinning technique. *Materials Today: Proceedings*. 2020/01/01/ 2020;33:2160-2166. doi:https://doi.org/10.1016/j.matpr.2020.03.241

14. Kegere J, Ouf A, Siam R, Mamdouh W. Fabrication of Poly(vinyl alcohol)/Chitosan/Bidens pilosa Composite Electrospun Nanofibers with Enhanced Antibacterial Activities. *ACS Omega*. May 31 2019;4(5):8778-8785. doi:10.1021/acsomega.9b00204

15. Castro-Mayorga JL, Fabra MJ, Cabedo L, Lagaron JM. On the Use of the Electrospinning Coating Technique to Produce Antimicrobial Polyhydroxyalkanoate Materials Containing In Situ-Stabilized Silver Nanoparticles. *Nanomaterials*. 2017;7(1):4. doi:10.3390/nano7010004

16. Kaur P, Bhola S, Kumar P, et al. Recent Development in Urban Polyhydroxyalkanoates Biorefineries. *ChemBioEng Reviews*. 2023;10(4):441-461. doi:https://doi.org/10.1002/cben.202200045

17. Shrivastav A, Kim H-Y, Kim Y-R. Advances in the Applications of Polyhydroxyalkanoate Nanoparticles for Novel Drug Delivery System. *BioMed Research International*. 2013;2013(1):581684. doi:https://doi.org/10.1155/2013/581684

18. Hassan MA, Amara AA, Abuelhamd AT, Haroun BM. Leucocytes show improvement growth on PHA polymer surface. *Pak J Pharm Sci*. 2010;23(3):332-336.

19. Silva IDdL, Andrade MFd, Caetano VF, Hallwass F, Brito AMSS, Vinhas GM. Development of active PHB/PEG antimicrobial films incorporating clove essential oil. *Polímeros*. 2020;30. doi:https://doi.org/10.1590/0104-1428.09319

20. Naderi P, Zarei M, Karbasi S, Salehi H. Evaluation of the effects of keratin on physical, mechanical and biological properties of poly (3-hydroxybutyrate) electrospun scaffold: Potential application in bone tissue engineering. *European Polymer Journal*. 2020/02/05/ 2020;124:109502. doi:https://doi.org/10.1016/j.eurpolymj.2020.109502

21. Alipal J, Mohd Pu'ad NAS, Lee TC, et al. A review of gelatin: Properties, sources, process, applications, and commercialisation. *Materials Today: Proceedings*. 2021/01/01/ 2021;42:240-250. doi:https://doi.org/10.1016/j.matpr.2020.12.922

22. Grande D, Ramier J, Versace DL, Renard E, Langlois V. Design of functionalized biodegradable PHA-based electrospun scaffolds meant for tissue engineering applications. *New Biotechnology*. 2017/07/25/ 2017;37:129-137. doi:https://doi.org/10.1016/j.nbt.2016.05.006

23. Pryadko AS, Botvin VV, Mukhortova YR, et al. Core-Shell Magnetoactive PHB/Gelatin/Magnetite Composite Electrospun Scaffolds for Biomedical Applications. *Polymers*. 2022;14(3):529. doi:https://doi.org/10.3390/polym14030529

24. Wu M, Sen A. Silver Nanoparticle Antimicrobials and Related Materials. 2012:3-45. doi:https://doi.org/10.1007/978-3-642-24428-5_1

25. Prakash J, Kumar P, Harris RA, et al. Synthesis, characterization and multifunctional properties of plasmonic Ag-TiO2 nanocomposites. *Nanotechnology*. Sep 2 2016;27(35):355707. doi:10.1088/0957-4484/27/35/355707

26. Jalali SAH, Allafchian AR, Banifatemi SS, Ashrafi Tamai I. The antibacterial properties of Ag/TiO2 nanoparticles embedded in silane sol–gel matrix. *Journal of the Taiwan Institute of*

Chemical Engineers. 2016/09/01/ 2016;66:357-362. doi:https://doi.org/10.1016/j.jtice.2016.06.011

27. Kędziora A, Speruda M, Krzyżewska E, Rybka J, Łukowiak A, Bugla-Płoskońska G. Similarities and Differences between Silver Ions and Silver in Nanoforms as Antibacterial Agents. *Int J Mol Sci*. 2018;19(2):444. doi:10.3390/ijms19020444

28. Ladhari S, Vu N-N, Boisvert C, et al. Biodegradable polyhydroxybutyrate microfiber membranes decorated with photoactive Ag-TiO2 nanoparticles for enhanced antibacterial and anti-biofouling activities. *Journal of Applied Polymer Science*. 2024 2024;n/a(n/a):e55660. doi:https://doi.org/10.1002/app.55660

29. Rodríguez-Tobías H, Morales G, Ledezma A, et al. Electrospinning and electrospraying techniques for designing novel antibacterial poly(3-hydroxybutyrate)/zinc oxide nanofibrous composites. *Journal of Materials Science*. 09/01 2016;51. doi:10.1007/s10853-016-0119-x

30. Bidone J, Melo APP, Bazzo GC, et al. Preparation and characterization of ibuprofen-loaded microspheres consisting of poly(3-hydroxybutyrate) and methoxy poly (ethylene glycol)-b-poly (D,L-lactide) blends or poly(3-hydroxybutyrate) and gelatin composites for controlled drug release. *Materials Science and Engineering: C*. 2009/03/01/ 2009;29(2):588-593. doi:https://doi.org/10.1016/j.msec.2008.10.016

31. Sanhueza C, Hermosilla J, Bugallo-Casal A, et al. One-step electrospun scaffold of dual-sized gelatin/poly-3-hydroxybutyrate nano/microfibers for skin regeneration in diabetic wound. *Materials Science and Engineering: C*. 2021/02/01/ 2021;119:111602. doi:https://doi.org/10.1016/j.msec.2020.111602

32. Bates IIC, Carrillo IBS, Germain H, Loranger É, Chabot B. Antibacterial electrospun chitosan-PEO/TEMPO-oxidized cellulose composite for water filtration. *Journal of Environmental Chemical Engineering*. 2021/10/01/ 2021;9(5):106204. doi:https://doi.org/10.1016/j.jece.2021.106204

33. Ren K, Wang Y, Sun T, Yue W, Zhang H. Electrospun PCL/gelatin composite nanofiber structures for effective guided bone regeneration membranes. *Materials Science and Engineering: C*. 2017/09/01/ 2017;78:324-332. doi:https://doi.org/10.1016/j.msec.2017.04.084

34. Gu SY, Wang Z-M, Ren J, Zhang C-Y. Electrospinning of gelatin and gelatin/poly(L-lactide) blend and its characteristics for wound dressing. *Materials Science and Engineering: C*. 08/01 2009;29:1822-1828. doi:10.1016/j.msec.2009.02.010

35. Hernández-Vargas J, Betzabe González-Campos J, Lara-Romero J, Ponce-Ortega JM. A Mathematical Programming Approach for the Optimal Synthesis of Nanofibers through Electrospinning Process. In: Klemeš JJ, Varbanov PS, Liew PY, eds. *Computer Aided Chemical Engineering*. Elsevier; 2014:1747-1752. doi:https://doi.org/10.1016/B978-0-444-63455-9.50126-4

36. Hohman M, Shin M, Rutledge G, Brenner M. Electrospinning and Electrically Forced Jets. II. Applications. *Physics of Fluids*. 08/01 2001;13. doi:10.1063/1.1384013

37. Schofield RM, Maciejewska BM, Dong S, et al. Driving fiber diameters to the limit: nanoparticle-induced diameter reductions in electrospun photoactive composite nanofibers for organic photovoltaics. *Advanced Composites and Hybrid Materials*. 2023/12/13 2023;6(6):229. doi:10.1007/s42114-023-00788-0

38. Heidari M, Bahrami SH, Ranjbar-Mohammadi M, Milan PB. Smart electrospun nanofibers containing PCL/gelatin/graphene oxide for application in nerve tissue engineering. *Materials Science and Engineering: C*. 2019/10/01/ 2019;103:109768. doi:https://doi.org/10.1016/j.msec.2019.109768

39. Castro Coelho S, Nogueiro Estevinho B, Rocha F. Encapsulation in food industry with emerging electrohydrodynamic techniques: Electrospinning and electrospraying – A review. *Food Chemistry*. 2021/03/01/ 2021;339:127850. doi:https://doi.org/10.1016/j.foodchem.2020.127850

40. Tijing LD, Ruelo MTG, Amarjargal A, et al. Antibacterial and superhydrophilic electrospun polyurethane nanocomposite fibers containing tourmaline nanoparticles. *Chemical Engineering Journal*. 2012/07/15/ 2012;197:41-48. doi:https://doi.org/10.1016/j.cej.2012.05.005

41. Gritsch L, Lovell C, Goldmann WH, Boccaccini AR. Fabrication and characterization of copper(II)-chitosan complexes as antibiotic-free antibacterial biomaterial. *Carbohydrate Polymers*. 2018/01/01/ 2018;179:370-378. doi:https://doi.org/10.1016/j.carbpol.2017.09.095

42. Mukherjee M, De S. Investigation of antifouling and disinfection potential of chitosan coated iron oxide-PAN hollow fiber membrane using Gram-positive and Gram-negative bacteria. *Materials Science and Engineering: C*. 2017/06/01/ 2017;75:133-148. doi:https://doi.org/10.1016/j.msec.2017.02.039

43. Gafri HFS, Zuki FM, Aroua MK, Hashim NA. Mechanism of bacterial adhesion on ultrafiltration membrane modified by natural antimicrobial polymers (chitosan) and combination with activated carbon (PAC). *Reviews in Chemical Engineering*. 2019;35(3):421-443.

doi:10.1515/revce-2017-0006

44. Muyonga J, Cole CGB, Duodu G. Fourier transform infrared (FTIR) spectroscopic study of acid soluble collagen and gelatin from skins and bones of young and adult Nile perch (Lates niloticus). *Food Chemistry*. 07/01 2004;86:325-332. doi:10.1016/j.foodchem.2003.09.038

45. Xu J, Guo B-H, Yang R, Wu Q, Chen G-Q, Zhang Z-M. In situ FTIR study on melting and crystallization of polyhydroxyalkanoates. *Polymer*. 2002;43(25):6893-6899. doi:10.1016/S0032-3861(02)00615-8

46. Shanesazzadeh E, Kadivar M, Fathi M. Production and characterization of hydrophilic and hydrophobic sunflower protein isolate nanofibers by electrospinning method. *International Journal of Biological Macromolecules*. 2018/11/01/ 2018;119:1-7. doi:https://doi.org/10.1016/j.ijbiomac.2018.07.132

47. Moon J, Jung U, Jung B, Park J. Improvement of Heat Transfer Properties through TiO2 Nanosphere Monolayer Embedded Polymers as Thermal Interface Materials. *Applied Sciences*. 2022;12(3):1348. doi:https://doi.org/10.3390/app12031348

48. Nagiah N, Madhavi L, Anitha R, Anandan C, Srinivasan NT, Sivagnanam UT. Development and characterization of coaxially electrospun gelatin coated poly (3-hydroxybutyric acid) thin films as potential scaffolds for skin regeneration. *Materials Science and Engineering: C*. 2013/10/01/ 2013;33(7):4444-4452. doi:https://doi.org/10.1016/j.msec.2013.06.042

49. Abdullah MF, Nuge T, Andriyana A, Ang BC, Muhamad F. Core–Shell Fibers: Design, Roles, and Controllable Release Strategies in Tissue Engineering and Drug Delivery. *Polymers*. 2019;11(12):2008. doi:https://doi.org/10.3390/polym11122008

50. Xu T, Yang H, Yang D, Yu Z-Z. Polylactic Acid Nanofiber Scaffold Decorated with Chitosan Islandlike Topography for Bone Tissue Engineering. *ACS Applied Materials & Interfaces*. 2017/06/28 2017;9(25):21094-21104. doi:10.1021/acsami.7b01176

51. Zhang D, Yu K, Hu X, Jiang A. Uniformly-aligned gelatin/polycaprolactone fibers promote proliferation in adipose-derived stem cells and have distinct effects on cardiac cell differentiation. *Int J Clin Exp Pathol*. 2021;14(6):680-692.

52. Doustgani A, Vasheghani-Farahani E, Soleimani M, Hashemi-Najafabadi S. Optimizing the mechanical properties of electrospun polycaprolactone and nanohydroxyapatite composite nanofibers. *Composites Part B: Engineering*. 2012/06/01/ 2012;43(4):1830-1836. doi:https://doi.org/10.1016/j.compositesb.2012.01.051

53. Pan Y, Xiong D, Chen X. Mechanical properties of nanohydroxyapatite reinforced poly (vinyl alcohol) gel composites as biomaterial. *Journal of Materials Science*. 2007;42(13):5129-5134. doi:https://doi.org/10.1007/s10853-006-1264-4

54. Samadian H, Salehi M, Farzamfar S, et al. In vitro and in vivo evaluation of electrospun cellulose acetate/gelatin/hydroxyapatite nanocomposite mats for wound dressing applications. Article. *Artificial Cells, Nanomedicine and Biotechnology*. 2018;46(sup1):964-974. doi:10.1080/21691401.2018.1439842

55. Guan G, Zhang L, Zhu J, Wu H, Li W, Sun Q. Antibacterial properties and mechanism of biopolymer-based films functionalized by CuO/ZnO nanoparticles against Escherichia coli and Staphylococcus aureus. *J Hazard Mater*. Jan 15 2021;402:123542. doi:10.1016/j.jhazmat.2020.123542

56. Bono N, Ponti F, Punta C, Candiani G. Effect of UV Irradiation and TiO2-Photocatalysis on Airborne Bacteria and Viruses: An Overview. *Materials*. 2021;14(5):1075. doi:10.3390/ma14051075

57. Siripatrawan U, Vitchayakitti W. Improving functional properties of chitosan films as active food packaging by incorporating with propolis. *Food Hydrocolloids*. 2016/12/01/ 2016;61:695-702. doi:https://doi.org/10.1016/j.foodhyd.2016.06.001

58. Epand RM, Walker C, Epand RF, Magarvey NA. Molecular mechanisms of membrane targeting antibiotics. *Biochimica et Biophysica Acta (BBA) - Biomembranes*. 2016/05/01/ 2016;1858(5):980-987. doi:https://doi.org/10.1016/j.bbamem.2015.10.018

59. Vuong C, Otto M. Staphylococcus epidermidis infections. *Microbes and Infection*. 2002/04/01/ 2002;4(4):481-489. doi:https://doi.org/10.1016/S1286-4579(02)01563-0

60. Kochkodan V, Hilal N. A comprehensive review on surface modified polymer membranes for biofouling mitigation. *Desalination*. 2015/01/15/ 2015;356:187-207. doi:https://doi.org/10.1016/j.desal.2014.09.015

61. Liu CX, Zhang DR, He Y, Zhao XS, Bai R. Modification of membrane surface for anti-biofouling performance: Effect of anti-adhesion and anti-bacteria approaches. *Journal of Membrane Science*. 2010/01/01/ 2010;346(1):121-130. doi:https://doi.org/10.1016/j.memsci.2009.09.028

62. Shi H, Xue L, Gao A, Fu Y, Zhou Q, Zhu L. Fouling-resistant and adhesion-resistant surface modification of dual layer PVDF hollow fiber membrane by dopamine and quaternary

polyethyleneimine. *Journal of Membrane Science*. 2016/01/15/ 2016;498:39-47. doi:https://doi.org/10.1016/j.memsci.2015.09.065

63. Wang X, Fang D, Yoon K, Hsiao BS, Chu B. High performance ultrafiltration composite membranes based on poly(vinyl alcohol) hydrogel coating on crosslinked nanofibrous poly(vinyl alcohol) scaffold. *Journal of Membrane Science*. 2006/07/05/ 2006;278(1):261-268. doi:https://doi.org/10.1016/j.memsci.2005.11.009

64. Gasparyan KG, Tyubaeva PM, Varyan IA, Vetcher AA, Popov AA. Assessing the Biodegradability of PHB-Based Materials with Different Surface Areas: A Comparative Study on Soil Exposure of Films and Electrospun Materials. *Polymers*. 2023;15(9):2042. doi:https://doi.org/10.3390/polym15092042

65. Mouhoubi R, Lasschuijt M, Ramon Carrasco S, Gojzewski H, Wurm FR. End-of-life biodegradation? how to assess the composting of polyesters in the lab and the field. *Waste Management*. 2022/12/01/ 2022;154:36-48. doi:https://doi.org/10.1016/j.wasman.2022.09.025

66. Weng K, Li F, Tanaka T, Zhou Y. Superhydrophobicity and biodegradability of silane-modified poly[(R)-3-hydroxybutyrate-co-(R)-3-hydroxyhexanoate] / deacetylated cellulose acetate composite nanofiber membrane. *Polymer Degradation and Stability*. 2024/09/01/ 2024;227:110862. doi:https://doi.org/10.1016/j.polymdegradstab.2024.110862

67. Ryan CA, Billington SL, Criddle CS. Biocomposite Fiber-Matrix Treatments that Enhance In-Service Performance Can Also Accelerate End-of-Life Fragmentation and Anaerobic Biodegradation to Methane. *Journal of Polymers and the Environment*. 2018/04/01 2018;26(4):1715-1726. doi:10.1007/s10924-017-1068-4

6.6. Supporting Information

The peak maximum or lowest of the calorimetric curves was used to determine the transition temperatures, and the degree of crystallinity was calculated from the normalized peak enthalpies from DSc analysis using the following formula:

$$Xm = (\Delta Hm, PHB - \Delta Hc, PHB) / \Delta H°m, PHB \times WPHB \quad \text{Equation 6.4}$$

Where W_{PHB} is the weight percentage of PHB in the films, $\Delta H_{m,\ PHB}$ is the apparent melting enthalpy of PHB, $\Delta H_{c,\ PHB}$ is the apparent heat of cold crystallization enthalpy of PHB, and $\Delta H°_{m,\ PHB}$ is the theoretical enthalpy value for a 100% crystalline sample (146 J/g) [1].

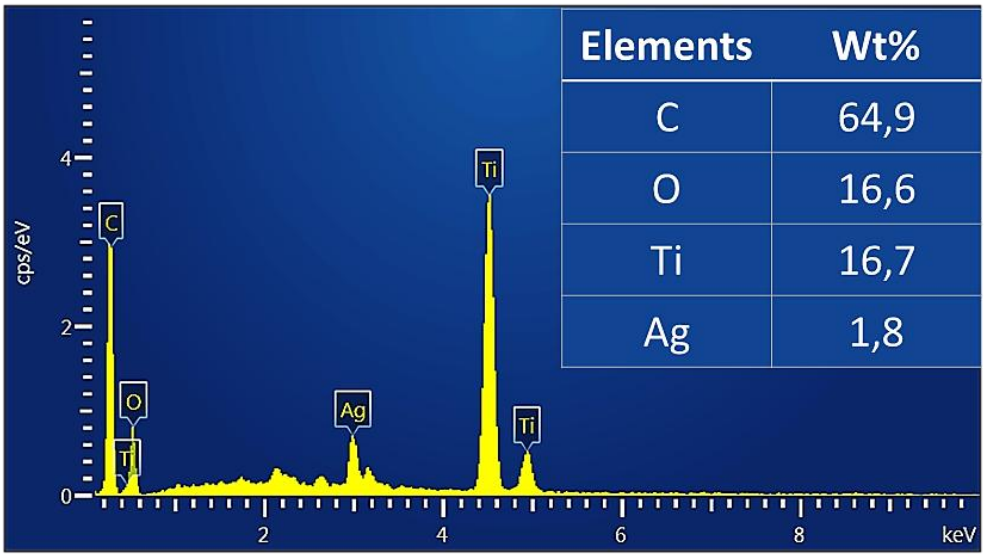

Figure SI. 6.1: Energy Dispersive Spectroscopy (EDS) mapping of PG5

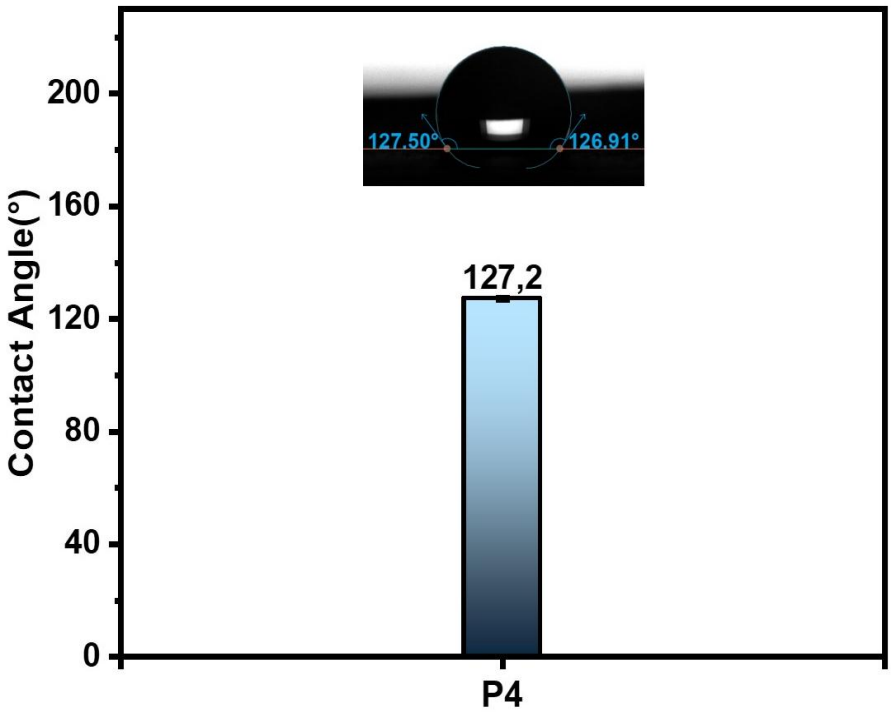

Figure SI. 6.2: Water contact angle (WCA) of P4

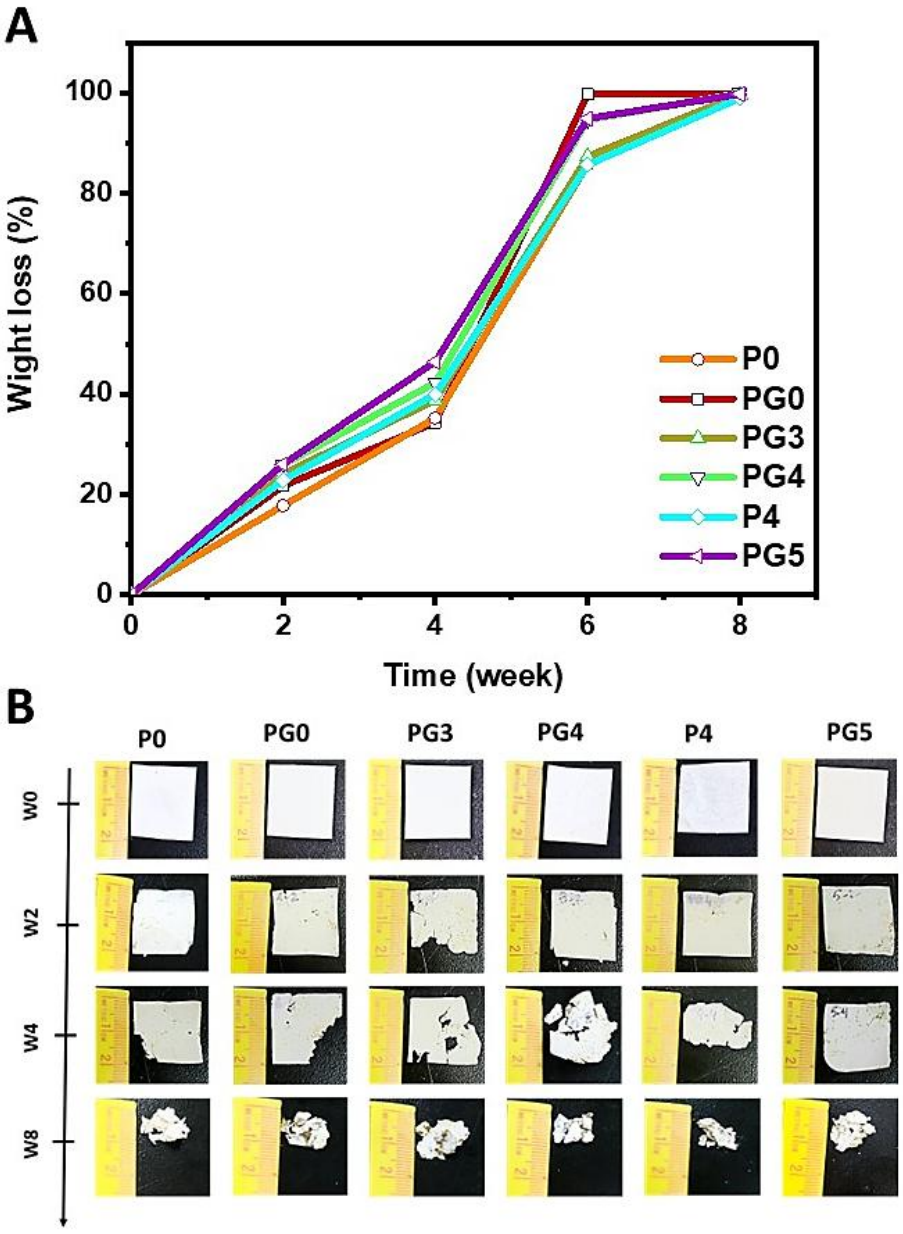

Figure SI. 6.3: Biodegradability test: A) Weight loss of P0, PG0, PG3, PG4, P4, and PG5 membranes after 2, 4, 6, and 8 weeks of burial test, (b) Photographs of P0, PG0, PG3, PG4, P4, and PG5 membranes before and after the soil burial test.

References

1. Gunaratne LMWK, Shanks RA. Multiple melting behaviour of poly(3-hydroxybutyrate-co-hydroxyvalerate) using step-scan DSC. *European Polymer Journal*. 2005/12/01/ 2005;41(12):2980-2988. doi:https://doi.org/10.1016/j.eurpolymj.2005.06.015

General conclusion and Future outlook

This chapter summarizes the thesis's work and highlights the efficiency of PHB-based materials for biodegradable applications and their advanced properties for destroying bacteria and preventing microbial contamination.

General conclusion

The study efficiently delineates the synthesis and characterization of innovative and multifunctional materials with integrated antibacterial, antifouling, and biodegradable properties, providing added advantages over conventional antimicrobial materials. Combining biopolymers with photoactive nanoparticles has introduced a new light-responsive antibacterial mechanism where the corrupted instance of reactive oxygen species is only generated through catalysis upon light irradiation. A new approach is a significant leap toward resolving critical problems of antibiotic resistance, surface bacterial contamination, and environmental pollution caused by non-biodegradable plastic waste.

This thesis outlines the advantages of employing photoactive Ag-doped TiO_2 and ZnO nano and microparticles to enhance the antibacterial and antifouling properties of polyhydroxybutyrate (PHB) biopolymer matrices. These materials exhibit effective antibacterial responses against the most common bacterial pathogens, such as *Escherichia coli* and *Staphylococcus epidermidis*, mainly when light is applied. The capabilities of these nanoparticles to generate ROS under light activation have set an energy-efficient, long-lasting route to bactericidal action, substantially surpassing chemical-based static antibacterial techniques.

This study contributes significantly to developing safer and environmentally sustainable materials for diverse applications, especially in packaging, where biodegradation and prevention of bacterial contamination are paramount to ensure safety. The synthesized green PHB films incorporated with ZnO exhibit high antibacterial activity and rapid degradation in soil (up to 99% within 10 weeks), making them suitable candidates for conventional plastic films, mediating the increasing environmental pollution crisis.

The combination of gelatin and PHB has improved the mechanical strength of the electrospun nanofiber membranes and exhibited resistance to biofouling, making them appropriate for demanding applications involving medical filtration. The enhanced biodegradability, bioactivity, and tensile strength demonstrate the versatility and functionality of these bio blends. For instance, the gradual degradation of the membranes over eight weeks demonstrates their great feasibility and environmentally friendly characteristics in minimizing their adverse effect on the environment after use.

Future outlook

These research perspectives open new frontiers in developing PHB-based materials, addressing pressing global challenges related to healthcare, environmental sustainability, and clean technologies. By exploring advanced functionalities, broadening material applications, and prioritizing ecological safety, these proposed directions build on current knowledge and align with the broader goals of innovation and sustainability. These future axes hold the potential to significantly impact various industries, from biomedical applications to packaging and environmental remediation, paving the way for the next generation of multifunctional, biodegradable materials.

The biodegradable and antibacterial materials field was also elevated by time-dependent demands, which focused on problems with non-biodegradable waste, antibiotic resistance, and bacterial contamination. As a result, it is now necessary to develop composites based on polyhydroxybutyrate (PHB) as a biocompatible and cost-effective substitute. Following on from earlier parts, a thorough research viewpoint will help investigate new directions for enhancing the commercialization, general applicability, and durability of PHB-based antimicrobial materials.

1) **Study of Material Degradation**

- Degradation with Carbon dioxide (CO_2) Control:

Future research could focus on measuring the degradation rate of these materials by monitoring CO_2 production as a key indicator of microbial activity. As microorganisms break down the biodegradable polymers, they consume oxygen and release CO_2, directly measuring the degradation process. This approach can quantify the rate and extent of degradation under controlled conditions. In addition, this method can also be applied to compare degradation rates in different environments, such as freshwater versus seawater, to evaluate their suitability for various environments.

- Molar Mass Changes:

Investigate the changes in molar mass of the polymers during degradation using techniques like gel permeation chromatography (GPC). This would help determine the rate of chain scission and the extent of degradation over time.

- Degradation in Different Environments:

Conduct systematic studies to evaluate the degradation behavior of the materials in various environments, such as soil, seawater, freshwater, and compost. This would provide insights into their performance under real-world conditions.

- Microbial Activity and Degradation:

Explore the role of microbial communities in the degradation process by analyzing the types of microorganisms involved and their enzymatic activities. This could be done using metagenomic analysis or enzyme assays.

2) Stability After Use

- Washing Effect:

Investigate the durability of the materials after repeated washing cycles to simulate real-world use in applications like medical textiles or reusable packaging. This would involve testing the retention of antibacterial properties and mechanical strength after washing.

- Friction Effect:

Study the impact of friction and wear on the materials, particularly for applications like filtration membranes or packaging films. This could involve abrasion tests to assess the loss of nanoparticles or changes in surface properties. For example, the friction resistance of PHB materials under mechanical stress can be tested to determine their durability in high-friction environments, such as conveyor belts in food packaging.

- Long-Term Stability:

Assess the long-term stability of the materials under different storage conditions (e.g., humidity, temperature, UV exposure) to ensure their performance over extended periods and to optimize storage conditions.

3) Use in Different Environments

- Acidic and Alkaline Conditions:

Evaluate the performance of the materials in acidic and alkaline environments to expand their applicability in industries like food processing, chemical storage, or wastewater treatment to assess their suitability for use in chemical-resistant applications.

- Saline and Marine Environments:

Explore the performance of the materials in saline or marine environments, which is particularly relevant for anti-biofouling applications in marine industries or aquaculture nets.

- Dynamic Environmental Conditions:

Study the materials under dynamic conditions, such as fluctuating pH, temperature, or light exposure, to simulate real-world scenarios. For example, evaluate PHB composites' antibacterial and degradation properties under alternating light-dark cycles to mimic day-night conditions in outdoor applications.

4) Advanced Characterization and Optimization

- Nanoparticle Release and Toxicity:

Investigate the release of nanoparticles from the materials during degradation or use and assess their potential toxicity to the environment and human health. This can be done using techniques like inductively coupled plasma mass spectrometry (ICP-MS) to quantify the release of metal ions (e.g., Ag^{+}, Zn^{2+}) over time.

- Cytotoxicity and Genotoxicity:

Evaluate the cytotoxicity and genotoxicity of released nanoparticles to human cells, particularly for materials used in medical applications. This can be done using in vitro assays, such as MTT assays for cell viability and comet assays for DNA damage.

- Long-Term Exposure Studies:

Conduct long-term exposure studies to understand the chronic effects of low concentrations of nanoparticles on organisms and ecosystems. This is important for assessing the potential risks associated with the prolonged use of these materials.

- Scalability and Industrial Production:

Explore the scalability of the material production process, including the feasibility of large-scale electrospinning and nanoparticle incorporation, by developing a pilot-scale production process to evaluate PHB composites' performance in real-world applications.

5) Exploration of New Applications

- Advanced Light-Sensitive Nanomaterials

These novel photoactive nanomaterials, including carbon quantum dots, perovskite nanocrystals, and well-lanthanide-doped particles, would be bioactive against bacteria in non-visible light conditions. These materials can be engineered to target particular wavelengths (i.e., visible but not UV or near-IR), making them more feasible than other materials. Moreover, these nanomaterials can enhance the photocatalytic activity of metal particles and reduce the levels of possible cytotoxicity.

- Smart Responsive Surfaces

Integrating pH-responsive polymers into the matrix can allow a membrane to release antimicrobials on demand. Modifying surfaces to be more hydrophobic or rough when bacteria attach is a further approach to prevent biofilm formation.

- Biohybrid Nanoparticles

Fabrication of biohybrid nanoparticles using bio-derived materials (chitosan, antimicrobial peptides, or plant-derived polyphenols) loaded into inorganic frameworks may improve antimicrobial activity and minimize toxicity. These particles can be used as dual-function agents, using their biological and inorganic characteristics for better antibacterials and antifouling activities to meet market demand for environmentally friendly, sustainable materials.

- Antiviral Properties

With growing concerns about viral contamination, especially during pandemics, extending the antimicrobial PHB-based composites to include antiviral properties would be valuable. Materials may be simulated by testing against viruses such as influenza, SARS-CoV-2, or

noroviruses. Antiviral agents, i.e., copper, silver ions, or any peptide in the PHB matrix, could provide the opportunity to design dual-functional membranes used in medical and personal protective equipment.

- Multifunctional Membranes for Water Purification

In addition to antibacterial and antifouling activity, PHB-based membranes can be employed to adsorb heavy metals or to degrade organic pollutants. Development of ternary filters based on functional additives embedded in the membrane, including zeolites, activated carbon, or catalytic enzymatic materials, may be possible to achieve environments producing affordable, high-quality filters without compromising their biodegradability.

- Antibiotic-Free Synergies

Combining biobased nanoparticles with non-antibiotic antimicrobial agents (i.e., essential oils, silver ions, or phenolics) can lead to materials that demonstrate enhanced antibacterial activity. This method can be used to reduce bacterial resistance and improve sustainability.

- 3D-Printed Functional Materials

The utilization of additive manufacturing (3D printing) of PHB-based reinforced composites would enable these materials to fabricate intricate structures for various applications, including custom-fit implants, high-performance filtration systems, or novel packaging concepts. This may include searching for and optimizing the printability of PHB and integrating antibacterial and biodegradable properties into such printed structures.

- Long-Term Environmental Assessment

The environmental consequences of candidate-based PHB products must be understood for sustained evolution. Detailed research into nanoparticles is critical for understanding their accumulation in soil, aquatic environments, and microbial communities. This provides explicit environmental assumptions for these materials. Cooperation with ecological scientists may be used to achieve a more complete analysis of the long-term performance of nanoparticle-filled PHB composites.

These approaches can offer novel pathways for PHB-based material synthesis to overcome the world's most significant challenges, including healthcare, environmental sustainability, and green technologies. They are often extended to a work of new functions, broader applications, and environmental feasibility. They are grounded in prior work and moving toward the next step in innovation and sustainability. In light of these future axes, there is great potential for directing various industries, ranging from biomedical fields to packaging and environmental treatments, resulting in the next generation of multifunctional biodegradable materials.

References

(1) Raja, R. K.; Nguyen-Tri, P.; Balasubramani, G.; Alagarsamy, A.; Hazir, S.; Ladhari, S.; Saidi, A.; Pugazhendhi, A.; Samy, A. A. SARS-CoV-2 and its new variants: a comprehensive review on nanotechnological application insights into potential approaches. *Applied Nanoscience* **2021**, 1-29. DOI: 10.1007/s13204-021-01900-w From NLM.

(2) Paras; Kumar, A. Anti-Bacterial and Anti-Viral Polymeric Coatings. *Reference Module in Materials Science and Materials Engineering* **2021**.

(3) Imani, S. M.; Ladouceur, L.; Marshall, T.; Maclachlan, R.; Soleymani, L.; Didar, T. F. Antimicrobial Nanomaterials and Coatings: Current Mechanisms and Future Perspectives to Control the Spread of Viruses Including SARS-CoV-2. *ACS Nano* **2020**, *14* (10), 12341-12369. DOI: 10.1021/acsnano.0c05937 PubMed. Balasubramaniam, B.; Prateek; Ranjan, S.; Saraf, M.; Kar, P.; Singh, S. P.; Thakur, V. K.; Singh, A.; Gupta, R. K. Antibacterial and Antiviral Functional Materials: Chemistry and Biological Activity toward Tackling COVID-19-like Pandemics. *ACS Pharmacology & Translational Science* **2021**, *4* (1), 8-54. DOI: 10.1021/acsptsci.0c00174. Pemmada, R.; Zhu, X.; Dash, M.; Zhou, Y.; Ramakrishna, S.; Peng, X.; Thomas, V.; Jain, S.; Nanda, H. S. Science-Based Strategies of Antiviral Coatings with Viricidal Properties for the COVID-19 Like Pandemics. *Materials (Basel)* **2020**, *13* (18), 4041. DOI: 10.3390/ma13184041 PubMed.

(4) Tiwari, A. A Guide to Antimicrobial Coatings. In *Paint and Coatings Industry*, 2020.

(5) Mah, T.-F.; Pitts, B.; Pellock, B.; Walker, G. C.; Stewart, P. S.; O'Toole, G. A. A genetic basis for Pseudomonas aeruginosa biofilm antibiotic resistance. *Nature* **2003**, *426* (6964), 306-310. DOI: 10.1038/nature02122.

(6) Gabriel, G. J.; Som, A.; Madkour, A. E.; Eren, T.; Tew, G. N. Infectious Disease: Connecting Innate Immunity to Biocidal Polymers. *Materials science & engineering. R, Reports : a review journal* **2007**, *57 1-6*, 28-64. Viazis, S.; Diez-Gonzalez, F. Enterohemorrhagic Escherichia coli. The Twentieth Century's Emerging Foodborne Pathogen: A Review. *Advances in Agronomy* **2011**, *111*, 1-50. Macedo, M. F.; Miller, A. Z.; Dionísio, A.; Saiz-Jimenez, C. Biodiversity of cyanobacteria and green algae on monuments in the Mediterranean Basin: an overview. *Microbiology (Reading)* **2009**, *155* (Pt 11), 3476-3490. DOI: 10.1099/mic.0.032508-0 From NLM.

(7) Siedenbiedel, F.; Tiller, J. C. Antimicrobial Polymers in Solution and on Surfaces: Overview and Functional Principles. *Polymers* **2012**, *4* (1), 46-71. DOI:

https://doi.org/10.3390/polym4010046.

(8) Andresen, J. A.; Muir, D. C. G.; Ueno, D.; Darling, C. T. R.; Theobald, N.; Bester, K. Emerging pollutants in the North Sea in comparison to Lake Ontario, Canada, data. *Environmental Toxicology and Chemistry* **2007**, *26*. DOI: 10.1897/06-416r.1.

(9) Vu, N.-N.; Venne, C.; Ladhari, S.; Saidi, A.; Moskovchenko, L.; Lai, T. T.; Xiao, Y.; Barnabe, S.; Barbeau, B.; Nguyen-Tri, P. Rapid Assessment of Biological Activity of Ag-Based Antiviral Coatings for the Treatment of Textile Fabrics Used in Protective Equipment Against Coronavirus. *ACS Applied Bio Materials* **2022**, *5* (7), 3405-3417. DOI: 10.1021/acsabm.2c00360.

(10) Tiller, J. C. Chapter 18 - Coatings for Prevention or Deactivation of Biological Contaminants. In *Developments in Surface Contamination and Cleaning (Second Edition)*, Kohli, R., Mittal, K. L. Eds.; William Andrew Publishing, 2008; pp 751-794.

(11) Tiller, J. C. Antimicrobial Surfaces. In *Bioactive Surfaces*, Börner, H. G., Lutz, J.-F. Eds.; Springer Berlin Heidelberg, 2011; pp 193-217. Venne, C.; Vu, N.-N.; Ladhari, S.; Saidi, A.; Barnabe, S.; Nguyen-Tri, P. One-pot preparation of superhydrophobic polydimethylsiloxane-coated cotton via water/oil/water emulsion approach for enhanced resistance to chemical and bacterial adhesion. *Progress in Organic Coatings* **2023**, *174*, 107249. DOI: https://doi.org/10.1016/j.porgcoat.2022.107249.

(12) Cornell, R. J.; Donaruma, L. G. 2-Methacryloxytropones. Intermediates for the Synthesis of Biologically Active Polymers. *Journal of Medicinal Chemistry* **1965**, *8* (3), 388-390. DOI: 10.1021/jm00327a025.

(13) Huang, K.-S.; Yang, C.-H.; Huang, S.-L.; Chen, C.-Y.; Lu, Y.-Y.; Lin, Y.-S. Recent Advances in Antimicrobial Polymers: A Mini-Review. *Int J Mol Sci* **2016**, *17* (9), 1578. DOI: 10.3390/ijms17091578 PubMed.

(14) Giourieva, V. S.; Papi, R.; Pantazaki, A. A. Polyhydroxyalkanoates Applications in Antimicrobial Agents Delivery and Wound Healing. *Biotechnological Applications of Polyhydroxyalkanoates* **2019**.

(15) Jiang, L.; Zhang, J. 7 - Biodegradable and Biobased Polymers. In *Applied Plastics Engineering Handbook (Second Edition)*, Kutz, M. Ed.; William Andrew Publishing, 2017; pp 127-143. Osswald, T. A.; García-Rodríguez, S. Chapter 1 History of Sustainable Bio-based Polymers. In *A Handbook of Applied Biopolymer Technology: Synthesis, Degradation and Applications*, The Royal Society of Chemistry, 2011; pp 1-21.

(16) Avérous, L.; Kalia, S. *Biodegradable and Biobased Polymers for Environmental and Biomedical Applications*; John Wiley & Sons, 2016. Beg, S.; Almalki, W. H.; Malik, A.; Farhan, M.; Aatif, M.; Rahman, Z.; Alruwaili, N. K.; Alrobaian, M.; Tarique, M.; Rahman, M. 3D printing for drug delivery and biomedical applications. *Drug Discovery Today* **2020**, *25* (9), 1668-1681. DOI: https://doi.org/10.1016/j.drudis.2020.07.007.

(17) Mehrpouya, M.; Vahabi, H.; Barletta, M.; Laheurte, P.; Langlois, V. Additive manufacturing of polyhydroxyalkanoates (PHAs) biopolymers: Materials, printing techniques, and applications. *Materials Science and Engineering: C* **2021**, *127*, 112216. DOI: https://doi.org/10.1016/j.msec.2021.112216.

(18) La Rosa, A. Life cycle assessment of biopolymers. In *Biopolymers and Biotech Admixtures for Eco-Efficient Construction Materials*, Elsevier, 2016; pp 57-78. Durkin, A.; Taptygin, I.; Kong, Q.; Gunam Resul, M. F. M.; Rehman, A.; Fernández, A. M. L.; Harvey, A. P.; Shah, N.; Guo, M. Scale-up and Sustainability Evaluation of Biopolymer Production from Citrus Waste Offering Carbon Capture and Utilisation Pathway. *ChemistryOpen* **2019**, *8* (6), 668-688. DOI: https://doi.org/10.1002/open.201900015.

(19) Elvers, D.; Song, C. H.; Steinbüchel, A.; Leker, J. Technology Trends in Biodegradable Polymers: Evidence from Patent Analysis. *Polymer Reviews* **2016**, *56* (4), 584-606. DOI: 10.1080/15583724.2015.1125918.

(20) Hazer, B.; Steinbüchel, A. Increased diversification of polyhydroxyalkanoates by modification reactions for industrial and medical applications. *Applied Microbiology and Biotechnology* **2007**, *74* (1), 1-12. DOI: 10.1007/s00253-006-0732-8.

(21) Yu, L.; Dean, K. M.; Li, L. Polymer blends and composites from renewable resources. *Progress in Polymer Science* **2006**, *31*, 576-602. Samrot, A. V.; Avinesh, R. B.; Sukeetha, S. D.; Senthilkumar, P. Accumulation of poly[(R)-3-hydroxyalkanoates] in Enterobacter cloacae SU-1 during growth with two different carbon sources in batch culture. *Appl Biochem Biotechnol* **2011**, *163* (1), 195-203. DOI: 10.1007/s12010-010-9028-7 PubMed. Samrot, A.; Bhakyalakshmi, M.; Raman, V.; Kuppa, S.; Ann Philip, S.; Tatipamula, J.; Pachiyappan, S. Optimization and Characterization of Poly[R]hydroxyalkanoates of Pseudomonas aeruginosa. *Biosciences, Biotechnology Research Asia* **2015**, *12*, 2133-2138. DOI: 10.13005/bbra/1883. Nisha, J. N.; Mudaliar, N.; Senthilkumar, P.; Narendrakumar; Samrot, A. V. Influence of substrate concentration in accumulation pattern of poly(R) hydroxyalkonoate in Pseudomonas putida SU-8. *African*

Journal of Microbiology Research **2012**, *6*. Senthilkumar, P.; Dawn, S. S.; Sree Samanvitha, K.; Sanjay Kumar, S.; Narendra Kumar, G.; Samrot, A. V. Optimization and characterization of poly[R]hydroxyalkanoate of Pseudomonas aeruginosa SU-1 to utilize in nanoparticle synthesis for curcumin delivery. *Biocatalysis and Agricultural Biotechnology* **2017**, *12*, 292-298. DOI: https://doi.org/10.1016/j.bcab.2017.10.019.

(22) Poirier, Y. Green chemistry yields a better plastic. *Nat Biotechnol* **1999**, *17* (10), 960-961. DOI: 10.1038/13652 From NLM. Anderson, A. J.; Dawes, E. A. Occurrence, metabolism, metabolic role, and industrial uses of bacterial polyhydroxyalkanoates. *Microbiol Rev* **1990**, *54* (4), 450-472. DOI: 10.1128/mr.54.4.450-472.1990 From NLM. de Waard, P.; van der Wal, H.; Huijberts, G. N. M.; Eggink, G. Heteronuclear NMR analysis of unsaturated fatty acids in poly(3-hydroxyalkanoates). Study of beta-oxidation in Pseudomonas putida. *The Journal of biological chemistry* **1993**, *268 1*, 315-319.

(23) Lee, S. Y. Bacterial polyhydroxyalkanoates. *Biotechnology and Bioengineering* **1996**, *49* (1), 1-14. DOI: https://doi.org/10.1002/(SICI)1097-0290(19960105)49:1<1::AID-BIT1>3.0.CO;2-P (acccessed 2020/11/28/04:49:26). From Wiley Online Library.

(24) Samrot, A. V.; Samanvitha, S. K.; Shobana, N.; Renitta, E. R.; Senthilkumar, P.; Kumar, S. S.; Abirami, S.; Dhiva, S.; Bavanilatha, M.; Prakash, P.; et al. The Synthesis, Characterization and Applications of Polyhydroxyalkanoates (PHAs) and PHA-Based Nanoparticles. *Polymers* **2021**, *13* (19), 3302. DOI: 10.3390/polym13193302 PubMed. Basnett, P.; Lukasiewicz, B.; Marcello, E.; Gura, H. K.; Knowles, J. C.; Roy, I. Production of a novel medium chain length poly(3-hydroxyalkanoate) using unprocessed biodiesel waste and its evaluation as a tissue engineering scaffold. *Microb Biotechnol* **2017**, *10* (6), 1384-1399. DOI: 10.1111/1751-7915.12782 PubMed.

(25) Embrandiri, A.; Kiyasudeen, K.; Rupani, P. F.; Ibrahim, M. Environmental Xenobiotics and Its Effects on Natural Ecosystem. 2016; pp 1-18.

(26) Loo, C.-Y.; Sudesh, K. Polyhydroxyalkanoates: Bio-based microbial plastics and their properties. 2007.

(27) Licciardello, G.; Catara, A. F.; Catara, V. Production of Polyhydroxyalkanoates and Extracellular Products Using Pseudomonas Corrugata and P. Mediterranea: A Review. *Bioengineering* **2019**, *6*.

(28) Han, J.; Qiu, Y.-Z.; Liu, D.-C.; Chen, G.-Q. Engineered Aeromonas hydrophila for enhanced production of poly(3-hydroxybutyrate-co-3-hydroxyhexanoate) with alterable monomers

composition. *FEMS Microbiology Letters* **2004**, *239* (1), 195-201. DOI: https://doi.org/10.1016/j.femsle.2004.08.044. Lee, S. H.; Oh, D. H.; Ahn, W. S.; Lee, Y.; Choi, J.-i.; Lee, S. Y. Production of poly(3-hydroxybutyrate-co-3-hydroxyhexanoate) by high-cell-density cultivation of Aeromonas hydrophila. *Biotechnology and Bioengineering* **2000**, *67* (2), 240-244. DOI: https://doi.org/10.1002/(SICI)1097-0290(20000120)67:2<240::AID-BIT14>3.0.CO;2-F.

(29) Wong, P.; Cheung, M. K.; Lo, W.-H.; Chua, H.; Yu, P. Investigation of the effects of the types of food waste utilized as carbon source on the molecular weight distributions and thermal properties of polyhydroxybutyrate produced by two strains of microorganisms. *e-Polymers* **2004**, *4*. DOI: 10.1515/epoly.2004.4.1.324. Yu, P. H.; Chua, H.; Huang, A. L.; Ho, K. P. Conversion of industrial food wastes by Alcaligenes latus into polyhydroxyalkanoates. *Appl Biochem Biotechnol* **1999**, *77-79*, 445-454. DOI: 10.1385/abab:78:1-3:445 From NLM.

(30) Lstrok; abużek, S.; Radecka, I. Biosynthesis of PHB tercopolymer by Bacillus cereus UW85. *Journal of Applied Microbiology* **2001**, *90* (3), 353-357. DOI: https://doi.org/10.1046/j.1365-2672.2001.01253.x. Yilmaz, M.; Beyatli, Y. Poly-β-hydroxybutyrate (PHB) production by a Bacillus cereus MS strain in sugarbeet molasses. *Zuckerindustrie* **2005**, *130*, 109-112. Valappil, S. P.; Peiris, D.; Langley, G. J.; Herniman, J. M.; Boccaccini, A. R.; Bucke, C.; Roy, I. Polyhydroxyalkanoate (PHA) biosynthesis from structurally unrelated carbon sources by a newly characterized Bacillus spp. *Journal of Biotechnology* **2007**, *127* (3), 475-487. DOI: https://doi.org/10.1016/j.jbiotec.2006.07.015.

(31) Althuri, A.; Mathew, J.; Sindhu, R.; Banerjee, R.; Pandey, A.; Binod, P. Microbial synthesis of poly-3-hydroxybutyrate and its application as targeted drug delivery vehicle. *Bioresource Technology* **2013**, *145*, 290-296, Article. DOI: 10.1016/j.biortech.2013.01.106 Scopus.

(32) Omar, S.; Rayes, A.; Eqaab, A.; Voß, I.; Steinbüchel, A. Optimization of Cell Growth and Poly(3-hydroxybutyrate) Accumulation on Date Syrup by a Bacillus megaterium Strain. *Biotechnology Letters* **2001**, *23*, 1119-1123. DOI: 10.1023/A:1010559800535. Gouda, M. K.; Swellam, A. E.; Omar, S. H. Production of PHB by a Bacillus megaterium strain using sugarcane molasses and corn steep liquor as sole carbon and nitrogen sources. *Microbiological Research* **2001**, *156* (3), 201-207. DOI: https://doi.org/10.1078/0944-5013-00104.

(33) Katırcıoğlu, H.; Aslım, B.; Yüksekdağ, Z. N.; Mercan, N.; Beyatlı, Y. Production of poly-β-hydroxybutyrate (PHB) and differentiation of putative Bacillus mutant strains by SDS-PAGE of total cell protein. *African Journal of Biotechnology* **2003**, *2* (6), 147-149. Shamala, T.;

Chandrashekar, A.; Vijayendra, S.; Kshama, L. Identification of polyhydroxyalkanoate (PHA)-producing Bacillus spp. using the polymerase chain reaction (PCR). *Journal of Applied Microbiology* **2003**, *94* (3), 369-374. Tajima, K.; Igari, T.; Nishimura, D.; Nakamura, M.; Satoh, Y.; Munekata, M. Isolation and characterization of Bacillus sp. INT005 accumulating polyhydroxyalkanoate (PHA) from gas field soil. *J Biosci Bioeng* **2003**, *95* (1), 77-81. DOI: 10.1016/s1389-1723(03)80152-4 From NLM. Yilmaz, M.; Soran, H.; Beyatli, Y. Determination of poly-β-hydroxybutyrate (PHB) production by some Bacillus spp. *World Journal of Microbiology and Biotechnology* **2005**, *21* (4), 565-566. DOI: 10.1007/s11274-004-3274-1. Full, T. D.; Jung, D. O.; Madigan, M. T. Production of poly-β-hydroxyalkanoates from soy molasses oligosaccharides by new, rapidly growing Bacillus species. *Letters in Applied Microbiology* **2006**, *43* (4), 377-384. DOI: https://doi.org/10.1111/j.1472-765X.2006.01981.x.

(34) Nakas, J.; Keenan, T.; Stipanovic, A.; Tanenbaum, S. Bioconversion of xylose and levulinic acid to polyhydroxyalkanoate (PHA) copolymers. In *ABSTRACTS OF PAPERS OF THE AMERICAN CHEMICAL SOCIETY*, 2004; AMER CHEMICAL SOC 1155 16TH ST, NW, WASHINGTON, DC 20036 USA: Vol. 227, pp U299-U299. Keenan, T. M.; Tanenbaum, S. W.; Stipanovic, A. J.; Nakas, J. P. Production and Characterization of Poly-β-hydroxyalkanoate Copolymers from Burkholderiacepacia Utilizing Xylose and Levulinic Acid. *Biotechnology Progress* **2004**, *20* (6), 1697-1704. DOI: https://doi.org/10.1021/bp049873d. Alias, Z.; Tan, I. K. Isolation of palm oil-utilising, polyhydroxyalkanoate (PHA)-producing bacteria by an enrichment technique. *Bioresour Technol* **2005**, *96* (11), 1229-1234. DOI: 10.1016/j.biortech.2004.10.012 From NLM. Celik, G.; Beyatli, Y.; Aslim, B. Determination of poly-beta-hydroxybutyrate (PHB) production in sugarbeet molasses by Pseudomonas cepacia G13 strain. *Zuckerindustrie* **2005**, *130* (3).

(35) Brämer, C. O.; Vandamme, P.; da Silva, L. F.; Gomez, J. G.; Steinbüchel, A. Polyhydroxyalkanoate-accumulating bacterium isolated from soil of a sugar-cane plantation in Brazil. *International Journal of Systematic and Evolutionary Microbiology* **2001**, *51* (5), 1709-1713. DOI: https://doi.org/10.1099/00207713-51-5-1709.

(36) Qi, Q.; Rehm, B. H. A. Polyhydroxybutyrate biosynthesis in Caulobacter crescentus: molecular characterization of the polyhydroxybutyrate synthase. *Microbiology* **2001**, *147* (12), 3353-3358. DOI: https://doi.org/10.1099/00221287-147-12-3353.

(37) Chee, J. Y.; Tan, Y.; Samian, R.; Sudesh, K. Isolation and Characterization of a Burkholderia

sp. USM (JCM15050) Capable of Producing Polyhydroxyalkanoate (PHA) from Triglycerides, Fatty Acids and Glycerols. *Journal of Polymers and the Environment* **2010**, *18*, 584-592. DOI: 10.1007/s10924-010-0204-1.

(38) Lee, W. H.; Azizan, M. N. M.; Sudesh, K. Effects of culture conditions on the composition of poly(3-hydroxybutyrate-co-4-hydroxybutyrate) synthesized by Comamonas acidovorans. *Polymer Degradation and Stability* **2004**, *84* (1), 129-134, Article. DOI: 10.1016/j.polymdegradstab.2003.10.003 Scopus.

(39) Thakor, N.; Trivedi, U.; Patel, K. C. Biosynthesis of medium chain length poly(3-hydroxyalkanoates) (mcl-PHAs) by Comamonas testosteroni during cultivation on vegetable oils. *Bioresour Technol* **2005**, *96* (17), 1843-1850. DOI: 10.1016/j.biortech.2005.01.030 From NLM.

(40) Yu, J.; Stahl, H. Microbial utilization and biopolyester synthesis of bagasse hydrolysates. *Bioresour Technol* **2008**, *99* (17), 8042-8048. DOI: 10.1016/j.biortech.2008.03.071 From NLM.

(41) Lee, W.-H.; Loo, C.-Y.; Nomura, C. T.; Sudesh, K. Biosynthesis of polyhydroxyalkanoate copolymers from mixtures of plant oils and 3-hydroxyvalerate precursors. *Bioresource Technology* **2008**, *99* (15), 6844-6851. DOI: https://doi.org/10.1016/j.biortech.2008.01.051.

(42) Cavalheiro, J. M. B. T.; de Almeida, M. C. M. D.; Grandfils, C.; da Fonseca, M. M. R. Poly(3-hydroxybutyrate) production by Cupriavidus necator using waste glycerol. *Process Biochemistry* **2009**, *44* (5), 509-515. DOI: https://doi.org/10.1016/j.procbio.2009.01.008.

(43) Mahishi, L. H.; Tripathi, G.; Rawal, S. K. Poly(3-hydroxybutyrate) (PHB) synthesis by recombinant Escherichia coli harbouring Streptomyces aureofaciens PHB biosynthesis genes: Effect of various carbon and nitrogen sources. *Microbiological Research* **2003**, *158* (1), 19-27. DOI: https://doi.org/10.1078/0944-5013-00161.

(44) Quillaguamán, J.; Hashim, S.; Bento, F.; Mattiasson, B.; Hatti-Kaul, R. Poly(β-hydroxybutyrate) production by a moderate halophile, Halomonas boliviensis LC1 using starch hydrolysate as substrate. *Journal of Applied Microbiology* **2005**, *99* (1), 151-157. DOI: https://doi.org/10.1111/j.1365-2672.2005.02589.x. Quillaguamán, J.; Delgado, O.; Mattiasson, B.; Hatti-Kaul, R. Poly(β-hydroxybutyrate) production by a moderate halophile, Halomonas boliviensis LC1. *Enzyme and Microbial Technology* **2006**, *38* (1), 148-154. DOI: https://doi.org/10.1016/j.enzmictec.2005.05.013.

(45) Bera, A.; Dubey, S.; Bhayani, K.; Mondal, D.; Mishra, S.; Ghosh, P. K. Microbial synthesis of polyhydroxyalkanoate using seaweed-derived crude levulinic acid as co-nutrient. *International*

Journal of Biological Macromolecules **2015**, *72*, 487-494, Article. DOI: 10.1016/j.ijbiomac.2014.08.037 Scopus.

(46) Mwamburi, S.; Mbatia, B.; Kasili, R.; Muge, E.; Noah, N. Production of polyhydroxyalkanoates by hydrocarbonaclastic bacteria. *AFRICAN JOURNAL OF BIOTECHNOLOGY* **2019**, *18*, 352-364. DOI: 10.5897/AJB2019.16763.

(47) James, B. W.; Mauchline, W. S.; Dennis, P. J.; Keevil, C. W.; Wait, R. Poly-3-hydroxybutyrate in Legionella pneumophila, an energy source for survival in low-nutrient environments. *Appl Environ Microbiol* **1999**, *65* (2), 822-827. DOI: 10.1128/aem.65.2.822-827.1999 From NLM.

(48) Cerrone, F.; Sánchez-Peinado, M. d. M.; Rodríguez-Díaz, M.; González-López, J.; Pozo, C. PHAs production by strains belonging to Massilia genus from starch. *Starch - Stärke* **2011**, *63* (4), 236-240. DOI: https://doi.org/10.1002/star.201000132.

(49) Wendlandt, K. D.; Geyer, W.; Mirschel, G.; Hemidi, F. A.-H. Possibilities for controlling a PHB accumulation process using various analytical methods. *Journal of Biotechnology* **2005**, *117* (1), 119-129. DOI: https://doi.org/10.1016/j.jbiotec.2005.01.007.

(50) Akar, A.; Akkaya, E. U.; Yesiladali, S. K.; Çelikyilmaz, G.; Çokgor, E. U.; Tamerler, C.; Orhon, D.; Çakar, Z. P. Accumulation of polyhydroxyalkanoates by Microlunatus phosphovorus under various growth conditions. *Journal of Industrial Microbiology and Biotechnology* **2006**, *33* (3), 215-220. DOI: 10.1007/s10295-004-0201-2 (acccessed 10/31/2022).

(51) Fernández, D.; Rodríguez, E.; Bassas, M.; Viñas, M.; Solanas, A. M.; Llorens, J.; Marqués, A. M.; Manresa, A. Agro-industrial oily wastes as substrates for PHA production by the new strain Pseudomonas aeruginosa NCIB 40045: Effect of culture conditions. *Biochemical Engineering Journal* **2005**, *26* (2), 159-167. DOI: https://doi.org/10.1016/j.bej.2005.04.022. Marsudi, S.; Unno, H.; Hori, K. Palm oil utilization for the simultaneous production of polyhydroxyalkanoates and rhamnolipids by Pseudomonas aeruginosa. *Appl Microbiol Biotechnol* **2008**, *78* (6), 955-961. DOI: 10.1007/s00253-008-1388-3 From NLM. Simon-Colin, C.; Raguénès, G.; Crassous, P.; Moppert, X.; Guezennec, J. A novel mcl-PHA produced on coprah oil by Pseudomonas guezennei biovar. tikehau, isolated from a "kopara" mat of French Polynesia. *Int J Biol Macromol* **2008**, *43* (2), 176-181. DOI: 10.1016/j.ijbiomac.2008.04.011 From NLM.

(52) Sandhya, M.; Aravind, J.; Kanmani, P. Production of polyhydroxyalkanoates from Ralstonia eutropha using paddy straw as cheap substrate. *International Journal of Environmental Science*

and Technology **2013**, *10* (1), 47-54. DOI: 10.1007/s13762-012-0070-6.

(53) Loo, C. Y.; Lee, W. H.; Tsuge, T.; Doi, Y.; Sudesh, K. Biosynthesis and characterization of poly(3-hydroxybutyrate-co-3- hydroxyhexanoate) from palm oil products in a Wautersia eutropha mutant. *Biotechnol Lett* **2005**, *27* (18), 1405-1410. DOI: 10.1007/s10529-005-0690-8 From NLM.

(54) Fonseca, G.; Antonio, R. Polyhydroxyalkanoates Production by Recombinant Escherichia coli Using Low Cost Substrate. *American Journal of Food Technology* **2007**, *2*, 12-20. DOI: 10.3923/ajft.2007.12.20.

(55) Saranya, V.; Shenbagarathai, R. Production and characterization of pha from recombinant E. coli harbouring phaC1 gene of indigenous Pseudomonas sp. LDC-5 using molasses. *Brazilian Journal of Microbiology* **2011**, *42* (3), 1109-1118, Article. DOI: 10.1590/S1517-83822011000300032 Scopus.

(56) Tsuge, T.; Yamamoto, T.; Yano, K.; Abe, H.; Doi, Y.; Taguchi, S. Evaluating the Ability of Polyhydroxyalkanoate Synthase Mutants to Produce P(3HB-co-3HA) from Soybean Oil. *Macromolecular Bioscience* **2009**, *9* (1), 71-78. DOI: https://doi.org/10.1002/mabi.200800118.

(57) Mercan, N.; Beyatli, Y. Production of poly-beta-hydroxybutyrate (PHB) by rhizobium meliloti, R-viciae and Bradyrhizobium japonicum with different carbon and nitrogen sources, and inexpensive substrates. *Zuckerindustrie* **2005**, *130* (5).

(58) Mukhopadhyay, M.; Patra, A.; Paul, A. K. Production of poly(3-hydroxybutyrate) and poly(3-hydroxybutyrate-co-3-hydroxyvalerate) by Rhodopseudomonas palustris SP5212. *World Journal of Microbiology and Biotechnology* **2005**, *21* (5), 765-769. DOI: 10.1007/s11274-004-5565-y.

(59) Shrivastav, A.; Mishra, S. K.; Shethia, B.; Pancha, I.; Jain, D.; Mishra, S. Isolation of promising bacterial strains from soil and marine environment for polyhydroxyalkanoates (PHAs) production utilizing Jatropha biodiesel byproduct. *International Journal of Biological Macromolecules* **2010**, *47* (2), 283-287, Article. DOI: 10.1016/j.ijbiomac.2010.04.007 Scopus.

(60) Jau, M.-H.; Yew, S.-P.; Toh, P. S. Y.; Chong, A. S. C.; Chu, W.-L.; Phang, S.-M.; Najimudin, N.; Sudesh, K. Biosynthesis and mobilization of poly(3-hydroxybutyrate) [P(3HB)] by Spirulina platensis. *International Journal of Biological Macromolecules* **2005**, *36* (3), 144-151. DOI: https://doi.org/10.1016/j.ijbiomac.2005.05.002.

(61) Wong, P. A.; Cheung, M. K.; Lo, W.-H.; Chua, H.; Yu, P. H. F. Investigation of the effects of the types of food waste utilized as carbon source on the molecular weight distributions and thermal properties of polyhydroxybutyrate produced by two strains of microorganisms. *e-Polymers* **2004**,

4 (1). Wong, P. A.; Cheung, M. K.; Lo, W.; Chua, H.; Yu, P. H. F. Effects of types of food waste as carbon source on the molecular weight distributions and thermal properties of the biopolymer (polyhydroxybutyrate) produced by two strains of microorganisms. *Materials Research Innovations* **2005**, *9* (1), 4-5.

(62) Loo, C.-Y.; Lee, W.-H.; Tsuge, T.; Doi, Y.; Sudesh, K. Biosynthesis and Characterization of Poly(3-hydroxybutyrate-co-3- hydroxyhexanoate) from Palm Oil Products in a Wautersia eutropha Mutant. *Biotechnology Letters* **2005**, *27* (18), 1405-1410. DOI: 10.1007/s10529-005-0690-8.

(63) Zinn, M.; Witholt, B.; Egli, T. Occurrence, synthesis and medical application of bacterial polyhydroxyalkanoate. *Advanced drug delivery reviews* **2001**, *53 1*, 5-21.

(64) Kamm, B.; Kamm, M. Principles of biorefineries. *Appl Microbiol Biotechnol* **2004**, *64* (2), 137-145. DOI: 10.1007/s00253-003-1537-7 From NLM. Devi, A.; Nachiyar, V.; Kaviyarasi, T.; Samrot, A. Characterization of polyhydroxybutyrate synthesized by Bacillus Cereus. *International Journal of Pharmacy and Pharmaceutical Sciences* **2015**, *7*, 140-144.

(65) Saratale, R. G.; Cho, S.-K.; Saratale, G. D.; Kadam, A. A.; Ghodake, G. S.; Kumar, M.; Bharagava, R. N.; Kumar, G.; Kim, D. S.; Mulla, S. I. A comprehensive overview and recent advances on polyhydroxyalkanoates (PHA) production using various organic waste streams. *Bioresource technology* **2021**, *325*, 124685.

(66) Puppi, D.; Pecorini, G.; Federica, C. Biomedical Processing of Polyhydroxyalkanoates. *Bioengineering* **2019**, *6*. DOI: 10.3390/bioengineering6040108.

(67) Wang, Y.; Yin, J.; Chen, G. Polyhydroxyalkanoates, challenges and opportunities. *Current opinion in biotechnology* **2014**, *30*, 59-65.

(68) Kalia, V. C.; Singh Patel, S. K.; Shanmugam, R.; Lee, J.-K. Polyhydroxyalkanoates: Trends and advances toward biotechnological applications. *Bioresource Technology* **2021**, *326*, 124737. DOI: https://doi.org/10.1016/j.biortech.2021.124737.

(69) Ray, S.; Kalia, V. C. Biomedical Applications of Polyhydroxyalkanoates. *Indian Journal of Microbiology* **2017**, *57* (3), 261-269. DOI: 10.1007/s12088-017-0651-7.

(70) Castellano, S.; Scarascia Mugnozza, G.; Russo, G.; Briassoulis, D.; Mistriotis, A.; Hemming, S.; Waaijenberg, D. Plastic nets in agriculture: A general review of types and applications. *Appl. Eng. Agric.* **2008**, *24* (6), 799-808.

(71) Guerrini, S.; Borreani, G.; Voojis, H. Biodegradable Materials in Agriculture: Case Histories

and Perspectives. In *Soil Degradable Bioplastics for a Sustainable Modern Agriculture*, Malinconico, M. Ed.; Springer Berlin Heidelberg, 2017; pp 35-65.

(72) Kaniuk, Ł.; Stachewicz, U. Development and Advantages of Biodegradable PHA Polymers Based on Electrospun PHBV Fibers for Tissue Engineering and Other Biomedical Applications. *ACS Biomaterials Science & Engineering* **2021**, *7* (12), 5339-5362. DOI: 10.1021/acsbiomaterials.1c00757.

(73) Kaniuk, Ł.; Krysiak, Z. J.; Metwally, S.; Stachewicz, U. Osteoblasts and fibroblasts attachment to poly(3-hydroxybutyric acid-co-3-hydrovaleric acid) (PHBV) film and electrospun scaffolds. *Mater Sci Eng C Mater Biol Appl* **2020**, *110*, 110668. DOI: 10.1016/j.msec.2020.110668 From NLM.

(74) Kaniuk, Ł.; Ferraris, S.; Spriano, S.; Luxbacher, T.; Krysiak, Z.; Berniak, K.; Zaszczynska, A.; Marzec, M. M.; Bernasik, A.; Sajkiewicz, P.; et al. Time-dependent effects on physicochemical and surface properties of PHBV fibers and films in relation to their interactions with fibroblasts. *Applied Surface Science* **2021**, *545*, 148983. DOI: https://doi.org/10.1016/j.apsusc.2021.148983. Chang, H. C.; Sun, T.; Sultana, N.; Lim, M. M.; Khan, T. H.; Ismail, A. F. Conductive PEDOT:PSS coated polylactide (PLA) and poly(3-hydroxybutyrate-co-3-hydroxyvalerate) (PHBV) electrospun membranes: Fabrication and characterization. *Materials Science and Engineering: C* **2016**, *61*, 396-410. DOI: https://doi.org/10.1016/j.msec.2015.12.074. Zine, R.; Sinha, M. Nanofibrous poly(3-hydroxybutyrate-co-3-hydroxyvalerate)/collagen/graphene oxide scaffolds for wound coverage. *Materials Science and Engineering: C* **2017**, *80*, 129-134. DOI: https://doi.org/10.1016/j.msec.2017.05.138.

(75) Amaro, L. F.; Correia, D. M.; Marques-Almeida, T.; Martins, P. M.; Pérez, L.; Vilas, J. L.; Botelho, G.; Lanceros-Méndez, S.; Ribeiro, C. Tailored Biodegradable and Electroactive Poly(Hydroxybutyrate-Co-Hydroxyvalerate) Based Morphologies for Tissue Engineering Applications. *Int J Mol Sci* **2018**, *19*. Tong, H.-w.; Wang, M.; Lu, W. W. Electrospun Poly(Hydroxybutyrate-co-Hydroxyvalerate) Fibrous Membranes Consisting of Parallel-Aligned Fibers or Cross-Aligned Fibers: Characterization and Biological Evaluation. *Journal of Biomaterials Science, Polymer Edition* **2011**, *22*, 2475 - 2497. Amaro, L.; Correia, D. M.; Martins, P. M.; Botelho, G.; Carabineiro, S. A. C.; Ribeiro, C.; Lanceros-Mendez, S. Morphology Dependence Degradation of Electro- and Magnetoactive Poly(3-hydroxybutyrate-co-hydroxyvalerate) for Tissue Engineering Applications. *Polymers* **2020**, *12* (4), 953. DOI:

10.3390/polym12040953 PubMed.

(76) Chang, H. M.; Wang, Z. H.; Luo, H. N.; Xu, M.; Ren, X. Y.; Zheng, G. X.; Wu, B. J.; Zhang, X. H.; Lu, X. Y.; Chen, F.; et al. Poly(3-hydroxybutyrate-co-3-hydroxyhexanoate)-based scaffolds for tissue engineering. *Braz J Med Biol Res* **2014**, *47* (7), 533-539. DOI: 10.1590/1414-431x20143930 PubMed. Wang, Y.; Bian, Y.; Wu, Q.; Chen, G. Evaluation of three-dimensional scaffolds prepared from poly(3-hydroxybutyrate-co-3-hydroxyhexanoate) for growth of allogeneic chondrocytes for cartilage repair in rabbits. *Biomaterials* **2008**, *29 19*, 2858-2868.

(77) Coltelli, M. B.; Panariello, L.; Morganti, P.; Danti, S.; Baroni, A.; Lazzeri, A.; Fusco, A.; Donnarumma, G. Skin-Compatible Biobased Beauty Masks Prepared by Extrusion. *J Funct Biomater* **2020**, *11* (2). DOI: 10.3390/jfb11020023 From NLM.

(78) Augustine, R.; Hasan, A.; Khanam, P. N.; Dalvi, Y.; Varghese, R.; Antony, A.; Unni, R.; N, S.; Al Moustafa, A.-E. Cerium Oxide Nanoparticle Incorporated Electrospun Poly(3-hydroxybutyrate- co -3-hydroxyvalerate) Membranes for Diabetic Wound Healing Applications. *ACS Biomaterials Science & Engineering* **2019**, *6*. DOI: 10.1021/acsbiomaterials.8b01352. Azimi, B.; Thomas, L.; Fusco, A.; Kalaoglu-Altan, O. I.; Basnett, P.; Cinelli, P.; De Clerck, K.; Roy, I.; Donnarumma, G.; Coltelli, M. B.; et al. Electrosprayed Chitin Nanofibril/Electrospun Polyhydroxyalkanoate Fiber Mesh as Functional Nonwoven for Skin Application. *J Funct Biomater* **2020**, *11* (3). DOI: 10.3390/jfb11030062 From NLM.

(79) Zhu, X. H.; Gan, S. K.; Wang, C. H.; Tong, Y. W. Proteins combination on PHBV microsphere scaffold to regulate Hep3B cells activity and functionality: a model of liver tissue engineering system. *J Biomed Mater Res A* **2007**, *83* (3), 606-616. DOI: 10.1002/jbm.a.31257 From NLM. Xin, H. Z.; Wang, C.-H.; Tong, Y. W. In vitro characterization of hepatocyte growth factor release from PHBV/PLGA microsphere scaffold. 2009.

(80) Chuah, J.-A.; Yamada, M.; Taguchi, S.; Sudesh, K.; Doi, Y.; Numata, K. Biosynthesis and characterization of polyhydroxyalkanoate containing 5-hydroxyvalerate units: Effects of 5HV units on biodegradability, cytotoxicity, mechanical and thermal properties. *Polymer Degradation and Stability* **2013**, *98*, 331-338. Gorodzha, S. N.; Muslimov, A. R.; Syromotina, D. S.; Timin, A. S.; Tcvetkov, N. Y.; Lepik, K. V.; Petrova, A. V.; Surmeneva, M. A.; Gorin, D. A.; Sukhorukov, G. B.; et al. A comparison study between electrospun polycaprolactone and piezoelectric poly(3-hydroxybutyrate-co-3-hydroxyvalerate) scaffolds for bone tissue engineering. *Colloids Surf B Biointerfaces* **2017**, *160*, 48-59. DOI: 10.1016/j.colsurfb.2017.09.004 From NLM. Zou, P.; Liu,

H.; Li, Y.; Huang, J.; Dai, Y. Surface dextran modified electrospun poly (3-hydroxybutyrate-co-3-hydroxyvalerate) (PHBV) fibrous scaffold promotes the proliferation of bone marrow-derived mesenchymal stem cells. *Materials Letters* **2016**, *179*, 109-113. Ribeiro-Samy, S.; Silva, N. A.; Correlo, V. M.; Fraga, J. S.; Pinto, L.; Teixeira-Castro, A.; Leite-Almeida, H.; Almeida, A.; Gimble, J. M.; Sousa, N.; et al. Development and characterization of a PHB-HV-based 3D scaffold for a tissue engineering and cell-therapy combinatorial approach for spinal cord injury regeneration. *Macromolecular bioscience* **2013**, *13 11*, 1576-1592. Rentsch, C.; Rentsch, B.; Breier, A.; Hofmann, A.; Manthey, S.; Scharnweber, D.; Biewener, A.; Zwipp, H. Evaluation of the osteogenic potential and vascularization of 3D poly(3)hydroxybutyrate scaffolds subcutaneously implanted in nude rats. *J Biomed Mater Res A* **2010**, *92* (1), 185-195. DOI: 10.1002/jbm.a.32314 From NLM.

(81) Verlinden, R. A.; Hill, D. J.; Kenward, M. A.; Williams, C. D.; Radecka, I. Bacterial synthesis of biodegradable polyhydroxyalkanoates. *J Appl Microbiol* **2007**, *102* (6), 1437-1449. DOI: 10.1111/j.1365-2672.2007.03335.x From NLM.

(82) Koller, M. Biodegradable and Biocompatible Polyhydroxy-alkanoates (PHA): Auspicious Microbial Macromolecules for Pharmaceutical and Therapeutic Applications. *Molecules* **2018**, *23* (2). DOI: 10.3390/molecules23020362 From NLM.

(83) Rodriguez-Contreras, A. Recent Advances in the Use of Polyhydroyalkanoates in Biomedicine. *Bioengineering (Basel)* **2019**, *6* (3). DOI: 10.3390/bioengineering6030082 From NLM.

(84) Harting, R.; Johnston, K. A.; Petersen, S. Correlating in vitro degradation and drug release kinetics of biopolymer-based drug delivery systems. *International Journal of Biobased Plastics* **2019**. Michalak, M.; Marek, A. A.; Zawadiak, J.; Kawalec, M.; Kurcok, P. Synthesis of PHB-based carrier for drug delivery systems with pH-controlled release. *European Polymer Journal* **2013**, *49* (12), 4149-4156. DOI: https://doi.org/10.1016/j.eurpolymj.2013.09.021. Romero, A. I.; Bermudez, J. M.; Villegas, M.; Dib Ashur, M. F.; Parentis, M. L.; Gonzo, E. E. Modeling of Progesterone Release from Poly(3-Hydroxybutyrate) (PHB) Membranes. *AAPS PharmSciTech* **2015**, *17*, 898-906. Raza, Z. A.; Abid, S.; Banat, I. M. Polyhydroxyalkanoates: Characteristics, production, recent developments and applications. *International Biodeterioration & Biodegradation* **2018**, *126*, 45-56.

(85) Augustine, R.; Hasan, A.; Dalvi, Y. B.; Rehman, S. R. U.; Varghese, R.; Unni, R. N.; Yalcin,

H. C.; Alfkey, R.; Thomas, S.; Al Moustafa, A.-E. Growth factor loaded in situ photocrosslinkable poly(3-hydroxybutyrate-co-3-hydroxyvalerate)/gelatin methacryloyl hybrid patch for diabetic wound healing. *Materials Science and Engineering: C* **2021**, *118*, 111519. DOI: https://doi.org/10.1016/j.msec.2020.111519.

(86) Parlane, N. A.; Gupta, S. K.; Rubio-Reyes, P.; Chen, S.; Gonzalez-Miro, M.; Wedlock, D. N.; Rehm, B. H. A. Self-Assembled Protein-Coated Polyhydroxyalkanoate Beads: Properties and Biomedical Applications. *ACS Biomaterials Science & Engineering* **2017**, *3* (12), 3043-3057. DOI: 10.1021/acsbiomaterials.6b00355.

(87) Augustine, R.; Hasan, A.; Patan, N. K.; Dalvi, Y. B.; Varghese, R.; Antony, A.; Unni, R. N.; Sandhyarani, N.; Moustafa, A.-E. A. Cerium Oxide Nanoparticle Incorporated Electrospun Poly(3-hydroxybutyrate-co-3-hydroxyvalerate) Membranes for Diabetic Wound Healing Applications. *ACS Biomaterials Science & Engineering* **2020**, *6* (1), 58-70. DOI: 10.1021/acsbiomaterials.8b01352.

(88) Nair, M. B.; Baranwal, G.; Vijayan, P.; Keyan, K. S.; Jayakumar, R. Composite hydrogel of chitosan–poly(hydroxybutyrate-co-valerate) with chondroitin sulfate nanoparticles for nucleus pulposus tissue engineering. *Colloids and Surfaces B: Biointerfaces* **2015**, *136*, 84-92. DOI: https://doi.org/10.1016/j.colsurfb.2015.08.026.

(89) Duan, B.; Wang, M. Selective laser sintering and its application in biomedical engineering. *MRS Bulletin* **2011**, *36* (12), 998-1005. DOI: 10.1557/mrs.2011.270 From Cambridge University Press Cambridge Core.

(90) Barouti, G.; Jaffredo, C. G.; Guillaume, S. M. Advances in drug delivery systems based on synthetic poly(hydroxybutyrate) (co)polymers. *Progress in Polymer Science* **2017**, *73*, 1-31.

(91) Sosnik, A.; Augustine, R. Challenges in oral drug delivery of antiretrovirals and the innovative strategies to overcome them. *Adv Drug Deliv Rev* **2016**, *103*, 105-120. DOI: 10.1016/j.addr.2015.12.022 From NLM.

(92) Herman, T. F.; Santos, C. First Pass Effect. In *StatPearls*, StatPearls Publishing
Copyright © 2022, StatPearls Publishing LLC., 2022.

(93) Wu, Y.-L.; Wang, H.; Qiu, Y.-K.; Liow, S. S.; Li, Z.; Loh, X. J. PHB-Based Gels as Delivery Agents of Chemotherapeutics for the Effective Shrinkage of Tumors. *Advanced Healthcare Materials* **2016**, *5* (20), 2679-2685. DOI: https://doi.org/10.1002/adhm.201600723. Liow, S. S.; Dou, Q.; Kai, D.; Li, Z.; Sugiarto, S.; Yu, C. Y. Y.; Kwok, R. T. K.; Chen, X.; Wu, Y.-L.; Ong, S.

T.; et al. Long-Term Real-Time In Vivo Drug Release Monitoring with AIE Thermogelling Polymer. *Small* **2017**, *13* (7), 1603404. DOI: https://doi.org/10.1002/smll.201603404. Li, Z.; Ye, E.; David; Lakshminarayanan, R.; Loh, X. J. Recent Advances of Using Hybrid Nanocarriers in Remotely Controlled Therapeutic Delivery. *Small* **2016**, *12 35*, 4782-4806. Li, Z.; Yang, J.; Loh, X. J. Polyhydroxyalkanoates: Opening doors for a sustainable future. *NPG Asia Materials* **2016**, *8*, e265. DOI: 10.1038/am.2016.48. Li, Z.; Lim, J. 22 - Biodegradable polyhydroxyalkanoates nanocarriers for drug delivery applications. In *Stimuli Responsive Polymeric Nanocarriers for Drug Delivery Applications, Volume 1*, Makhlouf, A. S. H., Abu-Thabit, N. Y. Eds.; Woodhead Publishing, 2018; pp 607-634.

(94) Hoffman, A. S. The origins and evolution of "controlled" drug delivery systems. *J Control Release* **2008**, *132* (3), 153-163. DOI: 10.1016/j.jconrel.2008.08.012 From NLM.

(95) Saidi, A.; Gauvin, C.; Ladhari, S.; Nguyen-Tri, P. Advanced Functional Materials for Intelligent Thermoregulation in Personal Protective Equipment. *Polymers* **2021**, *13* (21), 3711.

(96) Qtaishat, M.; Khayet, M.; Matsuura, T. Novel porous composite hydrophobic/hydrophilic polysulfone membranes for desalination by direct contact membrane distillation. *Journal of Membrane Science* **2009**, *341* (1), 139-148. DOI: https://doi.org/10.1016/j.memsci.2009.05.053.

(97) Im, J. S.; Yun, J.; Lim, Y.-M.; Kim, H. I.; Lee, Y.-S. Fluorination of electrospun hydrogel fibers for a controlled release drug delivery system. *Acta biomaterialia* **2010**, *6 1*, 102-109. Wei, D. W.; Wei, H.; Gauthier, A.; Song, J.; Jin, Y.; Xiao, H. Superhydrophobic modification of cellulose and cotton textiles: Methodologies and applications. 2020.

(98) Shrivastav, A. V.; Kim, H.-Y.; Kim, Y.-R. Advances in the Applications of Polyhydroxyalkanoate Nanoparticles for Novel Drug Delivery System. *BioMed Research International* **2013**, *2013*.

(99) Francis, L.; Meng, D.; Knowles, J. C.; Roy, I.; Boccaccini, A. R. Multi-functional P(3HB) microsphere/45S5 Bioglass®-based composite scaffolds for bone tissue engineering. *Acta Biomaterialia* **2010**, *6* (7), 2773-2786. DOI: https://doi.org/10.1016/j.actbio.2009.12.054.

(100) Xiong, Y.-C.; Yao, Y.-C.; Zhan, X.-Y.; Chen, G.-q. Application of Polyhydroxyalkanoates Nanoparticles as Intracellular Sustained Drug-Release Vectors. *Journal of Biomaterials Science, Polymer Edition* **2010**, *21*, 127 - 140.

(101) Artsis, M. I.; Bonartsev, A. P.; Iordanskii, A. L.; Bonartseva, G. A.; Zaikov, G. E. Biodegradation and Medical Application of Microbial Poly(3-hydroxybutyrate). *Molecular*

Crystals and Liquid Crystals **2008**, *523*, 21/[593] - 549/[621].

(102) Oka, C.; Ushimaru, K.; Horiishi, N.; Tsuge, T.; Kitamoto, Y. Heat generation of core-shell particles composed of biodegradable polymer and iron oxide. *Journal of the Magnetics Society of Japan* **2016**. DOI: 10.3379/msjmag.1605R009.

(103) Yao, Y. C.; Zhan, X. Y.; Zhang, J.; Zou, X. H.; Wang, Z. H.; Xiong, Y. C.; Chen, J.; Chen, G. Q. A specific drug targeting system based on polyhydroxyalkanoate granule binding protein PhaP fused with targeted cell ligands. *Biomaterials* **2008**, *29* (36), 4823-4830. DOI: 10.1016/j.biomaterials.2008.09.008 From NLM.

(104) Kwon, H.-S.; Jung, S.-G.; Kim, H.-Y.; Parker, S. A.; Batt, C. A.; Kim, Y.-R. A multi-functional polyhydroxybutyrate nanoparticle for theranostic applications. *Journal of Materials Chemistry B* **2014**, *2* (25), 3965-3971, 10.1039/C4TB00304G. DOI: 10.1039/C4TB00304G. Cheng, L.; Xiang, Q.; Liao, Y.; Zhang, H. CdS-Based photocatalysts. *Energy & Environmental Science* **2018**, *11* (6), 1362-1391, 10.1039/C7EE03640J. DOI: 10.1039/C7EE03640J.

(105) Waghmare, V. S.; Wadke, P. R.; Dyawanapelly, S.; Deshpande, A.; Jain, R. D.; Dandekar, P. P. Starch based nanofibrous scaffolds for wound healing applications. *Bioactive Materials* **2018**, *3*, 255 - 266.

(106) Findrik Balogová, A.; Hudák, R.; Tóth, T.; Schnitzer, M.; Feranc, J.; Bakoš, D.; Živčák, J. Determination of geometrical and viscoelastic properties of PLA/PHB samples made by additive manufacturing for urethral substitution. *Journal of Biotechnology* **2018**, *284*, 123-130. DOI: https://doi.org/10.1016/j.jbiotec.2018.08.019.

(107) Lizarraga-Valderrama, L. R.; Taylor, C. S.; Claeyssens, F.; Haycock, J. W.; Knowles, J. C.; Roy, I. Unidirectional neuronal cell growth and differentiation on aligned polyhydroxyalkanoate blend microfibres with varying diameters. *J Tissue Eng Regen Med* **2019**, *13* (9), 1581-1594. DOI: 10.1002/term.2911 PubMed.

(108) David, M. E.; Grigorescu, R.; Iancu, L.; Ion, R.-M.; Zaharia, C.; Ramona, A.-B. Methods of synthesis, properties and biomedical applications of polyhydroxyalkanoates: a review. *Journal of Biomaterials Science, Polymer Edition* **2019**, *30*, 1-18. DOI: 10.1080/09205063.2019.1605866. Butt, F. I.; Muhammad, N.; Hamid, A.; Moniruzzaman, M.; Sharif, F. Recent progress in the utilization of biosynthesized polyhydroxyalkanoates for biomedical applications - Review. *Int J Biol Macromol* **2018**, *120* (Pt A), 1294-1305. DOI: 10.1016/j.ijbiomac.2018.09.002 From NLM. Singh, A.; Srivastava, P. D. J.; Chandel, A.; Sharma, L.; Mallick, N.; Singh, S. Biomedical

Applications of Microbially Engineered Polyhydroxyalkanoates: an Insight into Recent Advances, Bottlenecks and Solutions (Full text available on https://rdcu.be/bg76M). *Applied Microbiology and Biotechnology* **2019**, *103*, 2007-2032. DOI: 10.1007/s00253-018-09604-y.

(109) Koller, M. Biodegradable and Biocompatible Polyhydroxy-alkanoates (PHA): Auspicious Microbial Macromolecules for Pharmaceutical and Therapeutic Applications. *Molecules (Basel, Switzerland)* **2018**, *23* (2), 362. DOI: 10.3390/molecules23020362 PubMed.

(110) Volova, T.; Shishatskaya, E.; Sevastianov, V.; Efremov, S.; Mogilnaya, O. Results of biomedical investigations of PHB and PHB/PHV fibers. *Biochemical Engineering Journal* **2003**, *16* (2), 125-133. DOI: https://doi.org/10.1016/S1369-703X(03)00038-X.

(111) Chen, G. Q.; Wu, Q. The application of polyhydroxyalkanoates as tissue engineering materials. *Biomaterials* **2005**, *26* (33), 6565-6578. DOI: 10.1016/j.biomaterials.2005.04.036 From NLM.

(112) Doyle, C.; Tanner, E. T.; Bonfield, W. In vitro and in vivo evaluation of polyhydroxybutyrate and of polyhydroxybutyrate reinforced with hydroxyapatite. *Biomaterials* **1991**, *12* (9), 841-847. DOI: 10.1016/0142-9612(91)90072-i From NLM.

(113) Jost, V.; Kopitzky, R. Blending of Polyhydroxybutyrate-co-valerate with Polylactic Acid for Packaging Applications – Reflections on Miscibility and Effects on the Mechanical and Barrier Properties. *Chemical and Biochemical Engineering Quarterly* **2015**, *29*, 221-246.

(114) Anjana; Raturi, G.; Shree, S.; Sharma, A.; Panesar, P. S.; Goswami, S. Recent approaches for enhanced production of microbial polyhydroxybutyrate: Preparation of biocomposites and applications. *International Journal of Biological Macromolecules* **2021**, *182*, 1650-1669. DOI: https://doi.org/10.1016/j.ijbiomac.2021.05.037.

(115) Baidurah, S.; Kubo, Y.; Ishida, Y.; Yamane, T. Direct determination of poly(3-hydroxybutyrate) accumulated in bacteria by thermally assisted hydrolysis and methylation-gas chromatography in the presence of organic alkali. *Pure and Applied Chemistry* **2018**, *90* (6), 1011-1017. DOI: doi:10.1515/pac-2017-0905. Sen, K. Y.; Hussin, M. H.; Baidurah, S. Biosynthesis of poly(3-hydroxybutyrate) (PHB) by Cupriavidus necator from various pretreated molasses as carbon source. *Biocatalysis and Agricultural Biotechnology* **2019**.

(116) Front matter. In *Biodegradable Polymers for Industrial Applications*, Smith, R. Ed.; Woodhead Publishing, 2005; pp i-iii.

(117) Koller, M. Poly(hydroxyalkanoates) for Food Packaging: Application and Attempts towards

Implementation. *Applied Food Technology and Biotechnology* **2014**, *1*, 1-13.

(118) Vandewijngaarden, J.; Murariu, M.; Dubois, P.; Carleer, R.; Yperman, J.; Adriaensens, P.; Schreurs, S.; Lepot, N.; Peeters, R.; Buntinx, M. Gas Permeability Properties of Poly(3-hydroxybutyrate-co-3-hydroxyhexanoate). *Journal of Polymers and the Environment* **2014**, *22*, 501-507.

(119) Pantani, R.; Turng, L.-S. Manufacturing of advanced biodegradable polymeric components. *Journal of Applied Polymer Science* **2015**, *132* (48). DOI: https://doi.org/10.1002/app.42889. Rydz, J.; Musioł, M.; Zawidlak-Węgrzyńska, B.; Sikorska, W. Present and Future of Biodegradable Polymers for Food Packaging Applications. 2018. Shishatskaya, E. I.; Volova, T. G. A comparative investigation of biodegradable polyhydroxyalkanoate films as matrices for in vitro cell cultures. *J Mater Sci Mater Med* **2004**, *15* (8), 915-923. DOI: 10.1023/B:JMSM.0000036280.98763.c1 From NLM. Zhao, X.; Ji, K.; Kurt, K.; Cornish, K.; Vodovotz, Y. Optimal mechanical properties of biodegradable natural rubber-toughened PHBV bioplastics intended for food packaging applications. *Food Packaging and Shelf Life* **2019**. Meléndez-Rodríguez, B.; Castro-Mayorga, J. L.; Reis, M. A. M.; Sammon, C.; Cabedo, L.; Torres-Giner, S.; Lagarón, J. M. Preparation and Characterization of Electrospun Food Biopackaging Films of Poly(3-hydroxybutyrate-co-3-hydroxyvalerate) Derived From Fruit Pulp Biowaste. *Frontiers in Sustainable Food Systems* **2018**.

(120) Torres-Giner, S.; Hilliou, L.; Melendez-Rodriguez, B.; Figueroa-Lopez, K. J.; Madalena, D.; Cabedo, L.; Covas, J. A.; Vicente, A. A.; Lagaron, J. M. Melt processability, characterization, and antibacterial activity of compression-molded green composite sheets made of poly(3-hydroxybutyrate-co-3-hydroxyvalerate) reinforced with coconut fibers impregnated with oregano essential oil. *Food Packaging and Shelf Life* **2018**, *17*, 39-49. DOI: https://doi.org/10.1016/j.fpsl.2018.05.002.

(121) Boey, J. Y.; Mohamad, L.; Khok, Y. S.; Tay, G. S.; Baidurah, S. A Review of the Applications and Biodegradation of Polyhydroxyalkanoates and Poly(lactic acid) and Its Composites. *Polymers* **2021**, *13*.

(122) Eraslan, K.; Aversa, C.; Nofar, M.; Barletta, M.; Gisario, A.; Salehiyan, R.; Goksu, Y. A. Poly(3-hydroxybutyrate-co-3-hydroxyhexanoate) (PHBH): Synthesis, properties, and applications - A review. *European Polymer Journal* **2022**, *167*, 111044. DOI: https://doi.org/10.1016/j.eurpolymj.2022.111044.

(123) Zare, M.; Namratha, K.; Ilyas, S.; Hezam, A.; Mathur, S.; Byrappa, K. Smart Fortified PHB-

CS Biopolymer with ZnO-Ag Nanocomposites for Enhanced Shelf Life of Food Packaging. *ACS applied materials & interfaces* **2019**.

(124) Castro-Mayorga, J. L.; Fabra, M. J.; Cabedo, L.; Lagarón, J. M. On the Use of the Electrospinning Coating Technique to Produce Antimicrobial Polyhydroxyalkanoate Materials Containing In Situ-Stabilized Silver Nanoparticles. *Nanomaterials* **2016**, *7*. DOI: 10.3390/nano7010004.

(125) Ibrahim, M. I.; Alsafadi, D.; Alamry, K. A.; Hussein, M. A. Properties and Applications of Poly(3-hydroxybutyrate-co-3-hydroxyvalerate) Biocomposites. *Journal of Polymers and the Environment* **2020**, *29*, 1010 - 1030.

(126) Panaitescu, D. M.; Ionita, E. R.; Nicolae, C. A.; Gabor, A. R.; Ionita, M. D.; Trusca, R.; Lixandru, B. E.; Codita, I.; Dinescu, G. Poly(3-hydroxybutyrate) Modified by Nanocellulose and Plasma Treatment for Packaging Applications. *Polymers (Basel)* **2018**, *10* (11). DOI: 10.3390/polym10111249 From NLM.

(127) Díez-Pascual, A. M.; Díez-Vicente, A. L. Poly(3-hydroxybutyrate)/ZnO bionanocomposites with improved mechanical, barrier and antibacterial properties. *Int J Mol Sci* **2014**, *15* (6), 10950-10973. DOI: 10.3390/ijms150610950 From NLM.

(128) Lugoloobi, I.; Li, X.; Zhang, Y.; Mao, Z.; Wang, B.; Sui, X.; Feng, X. Fabrication of lignin/poly(3-hydroxybutyrate) nanocomposites with enhanced properties via a Pickering emulsion approach. *International Journal of Biological Macromolecules* **2020**, *165*, 3078-3087. DOI: https://doi.org/10.1016/j.ijbiomac.2020.10.156.

(129) Manikandan, N. A.; Pakshirajan, K.; Pugazhenthi, G. Preparation and characterization of environmentally safe and highly biodegradable microbial polyhydroxybutyrate (PHB) based graphene nanocomposites for potential food packaging applications. *International Journal of Biological Macromolecules* **2020**, *154*, 866-877. DOI: https://doi.org/10.1016/j.ijbiomac.2020.03.084.

(130) Rogovina, S.; Zhorina, L.; Gatin, A.; Prut, E.; Kuznetsova, O.; Yakhina, A.; Olkhov, A.; Samoylov, N.; Grishin, M.; Iordanskii, A.; et al. Biodegradable Polylactide–Poly(3-Hydroxybutyrate) Compositions Obtained via Blending under Shear Deformations and Electrospinning: Characterization and Environmental Application. *Polymers* **2020**, *12* (5), 1088.

(131) Tănase, E. E.; Popa, M. E.; Râpă, M.; Popa, O. PHB/Cellulose Fibers Based Materials: Physical, Mechanical and Barrier Properties. *Agriculture and Agricultural Science Procedia* **2015**,

6, 608-615. DOI: https://doi.org/10.1016/j.aaspro.2015.08.099.

(132) Le, T. D.; Phasupan, P.; Visaruthaphong, K.; Chouwatat, P.; Thi Thu, V.; Nguyen, L. T. Development of an antimicrobial photodynamic poly(3-hydroxybutyrate-co-3-hydroxyvalerate) packaging film for food preservation. *Food Packaging and Shelf Life* **2021**, *30*, 100749. DOI: https://doi.org/10.1016/j.fpsl.2021.100749.

(133) Costa, M. J.; Pastrana, L. M.; Teixeira, J. A.; Sillankorva, S. M.; Cerqueira, M. A. Characterization of PHBV films loaded with FO1 bacteriophage using polyvinyl alcohol-based nanofibers and coatings: A comparative study. *Innovative Food Science & Emerging Technologies* **2021**, *69*, 102646. DOI: https://doi.org/10.1016/j.ifset.2021.102646.

(134) Castro-Mayorga, J. L.; Fabra, M. J.; Pourrahimi, A. M.; Olsson, R. T.; Lagaron, J. M. The impact of zinc oxide particle morphology as an antimicrobial and when incorporated in poly(3-hydroxybutyrate-co-3-hydroxyvalerate) films for food packaging and food contact surfaces applications. *Food and Bioproducts Processing* **2017**, *101*, 32-44. DOI: https://doi.org/10.1016/j.fbp.2016.10.007.

(135) Râpă, M.; Stefan, M.; Popa, P. A.; Toloman, D.; Leostean, C.; Borodi, G.; Vodnar, D. C.; Wrona, M.; Salafranca, J.; Nerín, C.; et al. Electrospun Nanosystems Based on PHBV and ZnO for Ecological Food Packaging. *Polymers (Basel)* **2021**, *13* (13). DOI: 10.3390/polym13132123 From NLM.

(136) Gouvêa, R. F.; Del Aguila, E. M.; Paschoalin, V. M. F.; Andrade, C. T. Extruded hybrids based on poly(3-hydroxybutyrate-co-3-hydroxyvalerate) and reduced graphene oxide composite for active food packaging. *Food Packaging and Shelf Life* **2018**, *16*, 77-85. DOI: https://doi.org/10.1016/j.fpsl.2018.02.002.

(137) Castro-Mayorga, J. L.; Fabra, M. J.; Lagaron, J. M. Stabilized nanosilver based antimicrobial poly(3-hydroxybutyrate-co-3-hydroxyvalerate) nanocomposites of interest in active food packaging. *Innovative Food Science & Emerging Technologies* **2016**, *33*, 524-533. DOI: https://doi.org/10.1016/j.ifset.2015.10.019.

(138) Yu, H.-Y.; Qin, Z.-Y.; Sun, B.; Yang, X.-G.; Yao, J.-M. Reinforcement of transparent poly(3-hydroxybutyrate-co-3-hydroxyvalerate) by incorporation of functionalized carbon nanotubes as a novel bionanocomposite for food packaging. *Composites Science and Technology* **2014**, *94*, 96-104. DOI: https://doi.org/10.1016/j.compscitech.2014.01.018.

(139) Melendez-Rodriguez, B.; M'Bengue, M.-S.; Torres-Giner, S.; Cabedo, L.; Prieto, C.;

Lagaron, J. M. Barrier biopaper multilayers obtained by impregnation of electrospun poly(3-hydroxybutyrate-co-3-hydroxyvalerate) with protein and polysaccharide hydrocolloids. *Carbohydrate Polymer Technologies and Applications* **2021**, *2*, 100150. DOI: https://doi.org/10.1016/j.carpta.2021.100150.

(140) Martínez-Abad, A.; González-Ausejo, J.; Lagarón, J. M.; Cabedo, L. Biodegradable poly(3-hydroxybutyrate-co-3-hydroxyvalerate)/thermoplastic polyurethane blends with improved mechanical and barrier performance. *Polymer Degradation and Stability* **2016**, *132*, 52-61. DOI: https://doi.org/10.1016/j.polymdegradstab.2016.03.039.

(141) Chikh, A.; Benhamida, A.; Kaci, M.; Pillin, I.; Bruzaud, S. Synergistic effect of compatibilizer and sepiolite on the morphology of poly(3-hydroxybutyrate-co-3-hydroxyvalerate)/poly(butylene succinate) blends. *Polymer Testing* **2016**, *53*, 19-28. DOI: https://doi.org/10.1016/j.polymertesting.2016.05.008.

(142) Gigante, V.; Seggiani, M.; Cinelli, P.; Signori, F.; Vania, A.; Navarini, L.; Amato, G.; Lazzeri, A. Utilization of coffee silverskin in the production of Poly(3-hydroxybutyrate-co-3-hydroxyvalerate) biopolymer-based thermoplastic biocomposites for food contact applications. *Composites Part A: Applied Science and Manufacturing* **2021**, *140*, 106172. DOI: https://doi.org/10.1016/j.compositesa.2020.106172.

(143) Malmir, S.; Montero, B.; Rico, M.; Barral, L.; Bouza, R.; Farrag, Y. Effects of poly (3-hydroxybutyrate-co-3-hydroxyvalerate) microparticles on morphological, mechanical, thermal, and barrier properties in thermoplastic potato starch films. *Carbohydrate Polymers* **2018**, *194*, 357-364. DOI: https://doi.org/10.1016/j.carbpol.2018.04.056.

(144) Varghese, S. A.; Pulikkalparambil, H.; Rangappa, S. M.; Siengchin, S.; Parameswaranpillai, J. Novel biodegradable polymer films based on poly(3-hydroxybutyrate-co-3-hydroxyvalerate) and Ceiba pentandra natural fibers for packaging applications. *Food Packaging and Shelf Life* **2020**, *25*, 100538. DOI: https://doi.org/10.1016/j.fpsl.2020.100538.

(145) Kovalcik, A.; Machovsky, M.; Kozakova, Z.; Koller, M. Designing packaging materials with viscoelastic and gas barrier properties by optimized processing of poly(3-hydroxybutyrate-co-3-hydroxyvalerate) with lignin. *Reactive and Functional Polymers* **2015**, *94*, 25-34. DOI: https://doi.org/10.1016/j.reactfunctpolym.2015.07.001.

(146) Pal, A. K.; Wu, F.; Misra, M.; Mohanty, A. K. Reactive extrusion of sustainable PHBV/PBAT-based nanocomposite films with organically modified nanoclay for packaging

applications: Compression moulding vs. cast film extrusion. *Composites Part B: Engineering* **2020**, *198*, 108141. DOI: https://doi.org/10.1016/j.compositesb.2020.108141.

(147) Vandewijngaarden, J.; Wauters, R.; Murariu, M.; Dubois, P.; Carleer, R.; Yperman, J.; D'Haen, J.; Ruttens, B.; Schreurs, S.; Lepot, N.; et al. Poly(3-hydroxybutyrate-co-3-hydroxyhexanoate)/Organomodified Montmorillonite Nanocomposites for Potential Food Packaging Applications. *Journal of Polymers and the Environment* **2016**, *24*. DOI: 10.1007/s10924-016-0751-1.

(148) Díez-Pascual, A. M. Effect of Graphene Oxide on the Properties of Poly(3-Hydroxybutyrate-co-3-Hydroxyhexanoate). *Polymers (Basel)* **2021**, *13* (14). DOI: 10.3390/polym13142233 From NLM.

(149) Correa, J. P.; Molina, V.; Sanchez, M.; Kainz, C.; Eisenberg, P.; Massani, M. B. Improving ham shelf life with a polyhydroxybutyrate/polycaprolactone biodegradable film activated with nisin. *Food Packaging and Shelf Life* **2017**, *11*, 31-39. DOI: https://doi.org/10.1016/j.fpsl.2016.11.004.

(150) Garcia-Garcia, D.; Lopez-Martinez, J.; Balart, R.; Strömberg, E.; Moriana, R. Reinforcing capability of cellulose nanocrystals obtained from pine cones in a biodegradable poly(3-hydroxybutyrate)/poly(ε-caprolactone) (PHB/PCL) thermoplastic blend. *European Polymer Journal* **2018**, *104*, 10-18. DOI: https://doi.org/10.1016/j.eurpolymj.2018.04.036.

(151) Yang, S.; Miao, Q.; Huang, Y.; Jian, P.; Wang, X.; Tu, M. Preparation of cinnamaldehyde-loaded polyhydroxyalkanoate/chitosan porous microspheres with adjustable controlled-release property and its application in fruit preservation. *Food Packaging and Shelf Life* **2020**, *26*, 100596. DOI: https://doi.org/10.1016/j.fpsl.2020.100596.

(152) Iglesias Montes, M. L.; Cyras, V. P.; Manfredi, L. B.; Pettarín, V.; Fasce, L. A. Fracture evaluation of plasticized polylactic acid / poly (3-HYDROXYBUTYRATE) blends for commodities replacement in packaging applications. *Polymer Testing* **2020**, *84*, 106375. DOI: https://doi.org/10.1016/j.polymertesting.2020.106375.

(153) Siracusa, V.; Karpova, S.; Olkhov, A.; Zhulkina, A.; Kosenko, R.; Iordanskii, A. Gas Transport Phenomena and Polymer Dynamics in PHB/PLA Blend Films as Potential Packaging Materials. *Polymers* **2020**, *12* (3), 647.

(154) Arrieta, M. P.; Samper, M. D.; López, J.; Jiménez, A. Combined Effect of Poly(hydroxybutyrate) and Plasticizers on Polylactic acid Properties for Film Intended for Food

Packaging. *Journal of Polymers and the Environment* **2014**, *22* (4), 460-470. DOI: 10.1007/s10924-014-0654-y.

(155) Hoffmann, R.; Morais, D. D. S.; Braz, C. J. F.; Haag, K.; Wellen, R. M. R.; Canedo, E. L.; de Carvalho, L. H.; Koschek, K. Impact of the natural filler babassu on the processing and properties of PBAT/PHB films. *Composites Part A: Applied Science and Manufacturing* **2019**, *124*, 105472. DOI: https://doi.org/10.1016/j.compositesa.2019.105472.

(156) Ambekar, R. S.; Kandasubramanian, B. Advancements in nanofibers for wound dressing: A review. *European Polymer Journal* **2019**.

(157) Wang, X.; Hsiao, B. S. Electrospun nanofiber membranes. *Current opinion in chemical engineering* **2016**, *12*, 62-81.

(158) Hamdan, N.; Yamin, A.; Hamid, S. A.; Khodir, W. K. W. A.; Guarino, V. Functionalized Antimicrobial Nanofibers: Design Criteria and Recent Advances. *Journal of functional biomaterials* **2021**, *12* (4), 59. DOI: 10.3390/jfb12040059 PubMed.

(159) Rai, M.; Yadav, A.; Gade, A. Silver nanoparticles as a new generation of antimicrobials. *Biotechnol Adv* **2009**, *27* (1), 76-83. DOI: 10.1016/j.biotechadv.2008.09.002 From NLM. Abrigo, M.; McArthur, S. L.; Kingshott, P. Electrospun nanofibers as dressings for chronic wound care: advances, challenges, and future prospects. *Macromol Biosci* **2014**, *14* (6), 772-792. DOI: 10.1002/mabi.201300561 From NLM. Cheng, G.; Dai, J.; Dai, J.; Wang, H.; Chen, S.; liu, Y.; Liu, X.; Li, X.; Zhou, X.; Deng, H.; et al. Extracellular matrix imitation utilizing nanofibers-embedded biomimetic scaffolds for facilitating cartilage regeneration. *Chemical Engineering Journal* **2021**, *410*, 128379. DOI: https://doi.org/10.1016/j.cej.2020.128379. Hu, F.; Zhang, X.; Liu, H.; Xu, P.; Doulathunnisa; Teng, G.; Xiao, Z. Neuronally differentiated adipose-derived stem cells and aligned PHBV nanofiber nerve scaffolds promote sciatic nerve regeneration. *Biochemical and Biophysical Research Communications* **2017**, *489* (2), 171-178. DOI: https://doi.org/10.1016/j.bbrc.2017.05.119.

(160) Liu, X.-F.; Zhang, J.; Liu, J.-J.; Zhou, Q.-H.; Liu, Z.; Hu, P.-Y.; Yuan, Z.; Ramakrishna, S.; Yang, D.-P.; Long, Y.-Z. Bifunctional CuS composite nanofibers via in situ electrospinning for outdoor rapid hemostasis and simultaneous ablating superbug. *Chemical Engineering Journal* **2020**, *401*, 126096. DOI: https://doi.org/10.1016/j.cej.2020.126096. Xie, X.; Li, D.; Chen, Y.; Shen, Y.; Yu, F.; Wang, W.; Yuan, Z.; Morsi, Y.; Wu, J.; Mo, X. Conjugate Electrospun 3D Gelatin Nanofiber Sponge for Rapid Hemostasis. *Adv Healthc Mater* **2021**, *10* (20), e2100918. DOI:

10.1002/adhm.202100918 From NLM.

(161) Schoeller, J.; Itel, F.; Wuertz-Kozak, K.; Gaiser, S.; Luisier, N.; Hegemann, D.; Ferguson, S. J.; Fortunato, G.; Rossi, R. M. pH-Responsive Chitosan/Alginate Polyelectrolyte Complexes on Electrospun PLGA Nanofibers for Controlled Drug Release. *Nanomaterials (Basel)* **2021**, *11* (7). DOI: 10.3390/nano11071850 From NLM. Udomluck, N.; Lee, H.; Hong, S.; Lee, S.-H.; Park, H. Surface functionalization of dual growth factor on hydroxyapatite-coated nanofibers for bone tissue engineering. *Applied Surface Science* **2020**, *520*, 146311. Kowalczyk, T. Functional Micro- and Nanofibers Obtained by Nonwoven Post-Modification. *Polymers* **2020**, *12* (5), 1087.

(162) Keshvardoostchokami, M.; Majidi, S. S.; Huo, P.; Ramachandran, R.; Chen, M.; Liu, B. Electrospun Nanofibers of Natural and Synthetic Polymers as Artificial Extracellular Matrix for Tissue Engineering. *Nanomaterials* **2020**, *11*.

(163) Zhong, X.; Li, R.; Wang, Z.; Wang, W.; Yu, D. Eco-fabrication of antibacterial nanofibrous membrane with high moisture permeability from wasted wool fabrics. *Waste management* **2019**, *102*, 404-411. Al-Enizi, A. M.; Zagho, M. M.; Elzatahry, A. A. Polymer-Based Electrospun Nanofibers for Biomedical Applications. *Nanomaterials* **2018**, *8*.

(164) Ferraris, S.; Guarino, V.; Cochis, A.; Varesano, A.; Cruz Maya, I.; Vineis, C.; Rimondini, L.; Spriano, S. Aligned keratin submicrometric-fibers for fibroblasts guidance onto nanogrooved titanium surfaces for transmucosal implants. *Materials Letters* **2018**, *229*, 1-4. DOI: https://doi.org/10.1016/j.matlet.2018.06.103.

(165) Jingcheng, L.; Reddy, V.; Jayathilaka, W. A. D. M.; Chinnappan, A.; Ramakrishna, S.; Ghosh, R. Intelligent Polymers, Fibers and Applications. *Polymers* **2021**, *13*, 1427. DOI: 10.3390/polym13091427. Castro Coelho, S.; Nogueiro Estevinho, B.; Rocha, F. Encapsulation in food industry with emerging electrohydrodynamic techniques: Electrospinning and electrospraying - A review. *Food Chem* **2021**, *339*, 127850. DOI: 10.1016/j.foodchem.2020.127850 From NLM.

(166) Li, D.; Xia, Y. Electrospinning of Nanofibers: Reinventing the Wheel? *Advanced Materials* **2004**, *16* (14), 1151-1170. DOI: https://doi.org/10.1002/adma.200400719.

(167) Zhou, F.; Gong, R. H. Manufacturing technologies of polymeric nanofibres and nanofibre yarns. *Polymer International* **2008**, *57*, 837-845.

(168) Xue, J.; Wu, T.; Dai, Y.; Xia, Y. Electrospinning and Electrospun Nanofibers: Methods, Materials, and Applications. *Chem Rev* **2019**, *119* (8), 5298-5415. DOI: 10.1021/acs.chemrev.8b00593 PubMed.

(169) Feng, L.; Li, S.; Li, H.; Zhai, J.; Song, Y.; Jiang, L.; Zhu, D. Super-hydrophobic surface of aligned polyacrylonitrile nanofibers. *Angew Chem Int Ed Engl* **2002**, *41* (7), 1221-1223. DOI: 10.1002/1521-3773(20020402)41:7<1221::aid-anie1221>3.0.co;2-g From NLM.

(170) Huie, J. C. Guided molecular self-assembly: a review of recent efforts. *Smart Materials and Structures* **2003**, *12* (2), 264-271. DOI: 10.1088/0964-1726/12/2/315. Faul, C. F. J.; Antonietti, M. Ionic Self-Assembly: Facile Synthesis of Supramolecular Materials. *Advanced Materials* **2003**, *15*.

(171) Tucker, N.; Stanger, J.; Staiger, M. P.; Razzaq, H. A. A.; Hofman, K. The History of the Science and Technology of Electrospinning from 1600 to 1995. *Journal of Engineered Fibers and Fabrics* **2012**, *7*.

(172) Teo, W. E.; Ramakrishna, S. A review on electrospinning design and nanofibre assemblies. *Nanotechnology* **2006**, *17* (14), R89-r106. DOI: 10.1088/0957-4484/17/14/r01 From NLM. Burger, C.; Hsiao, B.; Chu, B. Nanofibrous Materials and Their Applications. *Annu. Rev. Mater. Res* **2006**, *36*, 333-368. DOI: 10.1146/annurev.matsci.36.011205.123537.

(173) Ding, J.; Zhang, J.; Li, J.; Li, D.; Xiao, C.; Xiao, H.; Yang, H.; Zhuang, X.; Chen, X. Electrospun polymer biomaterials. *Progress in Polymer Science* **2019**, *90*, 1-34. DOI: https://doi.org/10.1016/j.progpolymsci.2019.01.002. Xue, J.; Wu, T.; Dai, Y.; Xia, Y. Electrospinning and Electrospun Nanofibers: Methods, Materials, and Applications. *Chem Rev* **2019**, *119* (8), 5298-5415. DOI: 10.1021/acs.chemrev.8b00593 From NLM.

(174) Cheng, H.; Yang, X.; Che, X.; Yang, M.; Zhai, G. Biomedical application and controlled drug release of electrospun fibrous materials. *Mater Sci Eng C Mater Biol Appl* **2018**, *90*, 750-763. DOI: 10.1016/j.msec.2018.05.007 From NLM.

(175) Martínez-Pérez, C. A. Electrospinning: A promising technique for drug delivery systems. *REVIEWS ON ADVANCED MATERIALS SCIENCE* **2020**, *59* (1), 441-454. DOI: doi:10.1515/rams-2020-0041.

(176) Liu, M.; Duan, X.-P.; Li, Y.-M.; Yang, D.-P.; Long, Y.-Z. Electrospun nanofibers for wound healing. *Materials Science and Engineering: C* **2017**, *76*, 1413-1423. DOI: https://doi.org/10.1016/j.msec.2017.03.034.

(177) Chen, D.; Narayanan, N.; Federici, E.; Yang, Z.; Zuo, X.; Gao, J.; Fang, F.; Deng, M.; Campanella, O. H.; Jones, O. G. Electrospinning Induced Orientation of Protein Fibrils. *Biomacromolecules* **2020**, *21* (7), 2772-2785. DOI: 10.1021/acs.biomac.0c00500 From NLM.

(178) Ding, J.; Zhang, J.; Li, J.; Li, D.; Xiao, C.; Xiao, H.; Yang, H.; Zhuang, X.; Chen, X.

Electrospun polymer biomaterials. *Progress in Polymer Science* **2019**.

(179) Szewczyk, P. K.; Stachewicz, U. The impact of relative humidity on electrospun polymer fibers: From structural changes to fiber morphology. *Advances in colloid and interface science* **2020**, *286*, 102315.

(180) Ura, D.; Berniak, K.; Stachewicz, U. Critical length reinforcement in core-shell electrospun fibers using composite strategies. *Composites Science and Technology* **2021**, *211*, 108867. DOI: 10.1016/j.compscitech.2021.108867.

(181) Zaarour, B.; Liu, W. Enhanced piezoelectric performance of electrospun PVDF nanofibers by regulating the solvent systems. *Journal of Engineered Fibers and Fabrics* **2022**, *17*, 15589250221125437. DOI: 10.1177/15589250221125437.

(182) Volova, T. G.; Goncharov, D. V.; Sukovatyi, A.; Shabanov, A. V.; Nikolaeva, E. D.; Shishatskaya, E. I. Electrospinning of polyhydroxyalkanoate fibrous scaffolds: effects on electrospinning parameters on structure and properties. *Journal of Biomaterials Science, Polymer Edition* **2014**, *25*, 370 - 393.

(183) Sadik, T.; Massardier, V.; Becquart, F.; Taha, M. Polyolefins/Poly(3-hydroxybutyrate-co-hydroxyvalerate) blends compatibilization: Morphology, rheological, and mechanical properties. *Journal of Applied Polymer Science* **2013**, *127* (2), 1148-1156. DOI: https://doi.org/10.1002/app.37957.

(184) Sombatmankhong, K.; Sanchavanakit, N.; Pavasant, P.; Supaphol, P. Bone scaffolds from electrospun fiber mats of poly(3-hydroxybutyrate), poly(3-hydroxybutyrate-co-3-hydroxyvalerate) and their blend. *Polymer* **2007**, *48* (5), 1419-1427. DOI: https://doi.org/10.1016/j.polymer.2007.01.014.

(185) Tong, H.-w.; Wang, M.; Lu, W. W. Electrospinning and Evaluation of PHBV-Based Tissue Engineering Scaffolds with Different Fibre Diameters, Surface Topography and Compositions. *Journal of Biomaterials Science, Polymer Edition* **2012**, *23*, 779 - 806.

(186) Ying, T. H.; Ishii, D.; Mahara, A.; Murakami, S.; Yamaoka, T.; Sudesh, K.; Samian, R.; Fujita, M.; Maeda, M.; Iwata, T. Scaffolds from electrospun polyhydroxyalkanoate copolymers: Fabrication, characterization, bioabsorption and tissue response. *Biomaterials* **2008**, *29* (10), 1307-1317. DOI: https://doi.org/10.1016/j.biomaterials.2007.11.031.

(187) Gao, Y.; Truong, Y. B.; Zhu, Y.; Kyratzis, I. L. Electrospun antibacterial nanofibers: Production, activity, and in vivo applications. *Journal of Applied Polymer Science* **2014**, *131*, 9041-

9053.

(188) Ryšánek, P.; Malý, M.; Čapková, P.; Kormunda, M.; Kolská, Z.; Gryndler, M.; Novák, O.; Hocelíková, L.; Bystrianský, L.; Munzarová, M. Antibacterial modification of nylon-6 nanofibers: structure, properties and antibacterial activity. *Journal of Polymer Research* **2017**, *24* (11), 208. DOI: 10.1007/s10965-017-1365-6.

(189) Anselme, K.; Davidson, P.; Popa, A. M.; Giazzon, M.; Liley, M.; Ploux, L. The interaction of cells and bacteria with surfaces structured at the nanometre scale. *Acta Biomater* **2010**, *6* (10), 3824-3846. DOI: 10.1016/j.actbio.2010.04.001 From NLM. Kurtz, I. S.; Schiffman, J. D. Current and Emerging Approaches to Engineer Antibacterial and Antifouling Electrospun Nanofibers. *Materials (Basel)* **2018**, *11* (7), 1059. DOI: 10.3390/ma11071059 PubMed.

(190) Patanaik, A.; Jacobs, V.; Anandjiwala, R. D. Performance evaluation of electrospun nanofibrous membrane. *Journal of Membrane Science* **2010**, *352*, 136-142.

(191) Nicosia, A.; Gieparda, W.; Foksowicz-Flaczyk, J.; Walentowska, J.; Wesołek, D.; Vazquez, B.; Prodi, F.; Belosi, F. Air filtration and antimicrobial capabilities of electrospun PLA/PHB containing ionic liquid. *Separation and Purification Technology* **2015**, *154*, 154-160. DOI: https://doi.org/10.1016/j.seppur.2015.09.037.

(192) Bartczak, Z.; Galeski, A. Mechanical Properties of Polymer Blends. 2014. Liu, S.; Li, C.; Wu, H.; Guo, S. Novel Structure to Improve Mechanical Properties of Polymer Blends: Multilayered Ribbons. *Industrial & Engineering Chemistry Research* **2020**, *59*, 20221-20231.

(193) Fernandes, J. G.; Correia, D. M.; Botelho, G.; Padrão, J.; Dourado, F.; Ribeiro, C.; Lanceros-Méndez, S.; Sencadas, V. PHB-PEO electrospun fiber membranes containing chlorhexidine for drug delivery applications. *Polymer Testing* **2014**, *34*, 64-71. DOI: https://doi.org/10.1016/j.polymertesting.2013.12.007.

(194) Soleymani Eil Bakhtiari, S.; Karbasi, S.; Toloue, E. B. Modified poly(3-hydroxybutyrate)-based scaffolds in tissue engineering applications: A review. *International Journal of Biological Macromolecules* **2021**, *166*, 986-998. DOI: https://doi.org/10.1016/j.ijbiomac.2020.10.255.

(195) Sadat-Shojai, M.; Khorasani, M.-T.; Jamshidi, A. A new strategy for fabrication of bone scaffolds using electrospun nano-HAp/PHB fibers and protein hydrogels. *Chemical Engineering Journal* **2016**, *289*, 38-47. DOI: https://doi.org/10.1016/j.cej.2015.12.079.

(196) Vigneswari, S.; Chai, J. M.; Kamarudin, K. H.; Amirul, A.-A. A.; Focarete, M. L.; Ramakrishna, S. Elucidating the Surface Functionality of Biomimetic RGD Peptides Immobilized

on Nano-P(3HB-co-4HB) for H9c2 Myoblast Cell Proliferation. *Frontiers in Bioengineering and Biotechnology* **2020**, *8*, Original Research. DOI: 10.3389/fbioe.2020.567693.

(197) Spasova, M.; Stoilova, O.; Manolova, N.; Rashkov, I.; Naydenov, M. Electrospun Eco-Friendly Materials Based on Poly(3-hydroxybutyrate) (PHB) and TiO2 with Antifungal Activity Prospective for Esca Treatment. *Polymers* **2020**, *12* (6). DOI: 10.3390/polym12061384.

(198) Sanhueza, C.; Hermosilla, J.; Bugallo-Casal, A.; Da Silva-Candal, A.; Taboada, C.; Millán, R.; Concheiro, A.; Alvarez-Lorenzo, C.; Acevedo, F. One-step electrospun scaffold of dual-sized gelatin/poly-3-hydroxybutyrate nano/microfibers for skin regeneration in diabetic wound. *Materials Science and Engineering: C* **2021**, *119*, 111602. DOI: https://doi.org/10.1016/j.msec.2020.111602.

(199) Mousavi Khaneghah, A.; Hashemi, S. M. B.; Limbo, S. Antimicrobial agents and packaging systems in antimicrobial active food packaging: An overview of approaches and interactions. *Food and Bioproducts Processing* **2018**.

(200) Mlalila, N.; Hilonga, A.; Swai, H.; Devlieghere, F.; Ragaert, P. Antimicrobial packaging based on starch, poly(3-hydroxybutyrate) and poly(lactic-co-glycolide) materials and application challenges. *Trends in Food Science & Technology* **2018**, *74*, 1-11. DOI: https://doi.org/10.1016/j.tifs.2018.01.015.

(201) Panaitescu, D. M.; Ionita, E. R.; Nicolae, C.-A.; Gabor, A. R.; Ionita, M. D.; Trusca, R.; Lixandru, B.-E.; Codita, I.; Dinescu, G. Poly(3-hydroxybutyrate) Modified by Nanocellulose and Plasma Treatment for Packaging Applications. *Polymers* **2018**, *10* (11), 1249.

(202) Díez-Pascual, A. M.; Díez-Vicente, A. L. Poly(3-hydroxybutyrate)/ZnO bionanocomposites with improved mechanical, barrier and antibacterial properties. In *Int J Mol Sci*, 2014; Vol. 15, pp 10950-10973.

(203) Díez-Pascual, A. M.; Díez-Vicente, A. L. ZnO-reinforced poly(3-hydroxybutyrate-co-3-hydroxyvalerate) bionanocomposites with antimicrobial function for food packaging. *ACS Appl Mater Interfaces* **2014**, *6* (12), 9822-9834. DOI: 10.1021/am502261e From NLM.

(204) Nemani, K.; Annavarapu, R. K.; Mohammadian, B.; Raiyan, A.; Heil, J.; Haque, M.; Abdelaal, A.; Sojoudi, H. Surface Modification: Surface Modification of Polymers: Methods and Applications (Adv. Mater. Interfaces 24/2018). *Advanced Materials Interfaces* **2018**, *5*. DOI: 10.1002/admi.201870121.

(205) Wang, Y.; Lu, L.; Zheng, Y.; Chen, X. Improvement in hydrophilicity of PHBV films by

plasma treatment. *Journal of biomedical materials research. Part A* **2006**, *76 3*, 589-595.

(206) Maslakci, N. N.; Ulusoy, S.; Oksuz, A. U. Investigation of the effects of plasma-treated chitosan electrospun fibers onto biofilm formation. *Sensors and Actuators B: Chemical* **2017**, *246*, 887-895. DOI: https://doi.org/10.1016/j.snb.2017.02.089.

(207) Cui, H.; Bai, M.; Lin, L. Plasma-treated poly(ethylene oxide) nanofibers containing tea tree oil/beta-cyclodextrin inclusion complex for antibacterial packaging. *Carbohydr Polym* **2018**, *179*, 360-369. DOI: 10.1016/j.carbpol.2017.10.011 From NLM.

(208) Surucu, S.; Masur, K.; Sasmazel, H. T.; Woedtke, T. v.; Weltmann, K.-D. Atmospheric plasma surface modifications of electrospun PCL/chitosan/PCL hybrid scaffolds by nozzle type plasma jets for usage of cell cultivation. *Applied Surface Science* **2016**, *385*, 400-409.

(209) Slepička, P.; Malá, Z.; Rimpelová, S.; Švorčík, V. Antibacterial properties of modified biodegradable PHB non-woven fabric. *Mater Sci Eng C Mater Biol Appl* **2016**, *65*, 364-368. DOI: 10.1016/j.msec.2016.04.052 From NLM.

(210) Chang, C.-K.; Wang, H.-M. D.; Lan, J. C.-W. Investigation and Characterization of Plasma-Treated Poly(3-hydroxybutyrate) and Poly(3-hydroxybutyrate-co-3-hydroxyvalerate) Biopolymers for an In Vitro Cellular Study of Mouse Adipose-Derived Stem Cells. *Polymers* **2018**, *10* (4), 355. Karahaliloğlu, Z.; Demirbilek, M.; Şam, M.; Erol-Demirbilek, M.; Sağlam, N.; Denkbaş, E. B. Plasma polymerization-modified bacterial polyhydroxybutyrate nanofibrillar scaffolds. *Journal of Applied Polymer Science* **2012**, *128*, 1904-1912. Zhang, J.; Kasuya, K.-i.; Takemura, A.; Isogai, A.; Iwata, T. Properties and enzymatic degradation of poly(acrylic acid) grafted polyhydroxyalkanoate films by plasma-initiated polymerization. *Polymer Degradation and Stability* **2013**, *98*, 1458-1464. Slepičková Kasálková, N.; Slepička, P.; Sajdl, P.; Švorčík, V. Surface changes of biopolymers PHB and PLLA induced by Ar+ plasma treatment and wet etching. *Nuclear Instruments and Methods in Physics Research Section B: Beam Interactions with Materials and Atoms* **2014**, *332*, 63-67. DOI: https://doi.org/10.1016/j.nimb.2014.02.031.

(211) Slepička, P.; Malá, Z.; Rimpelová, S.; Švorčík, V. Antibacterial properties of modified biodegradable PHB non-woven fabric. *Materials Science and Engineering: C* **2016**, *65*, 364-368. DOI: 10.1016/j.msec.2016.04.052 (acccessed 2021/07/21/17:40:26). From DOI.org (Crossref). Mirmohammadi, S. A.; Khorasani, M. T.; Mirzadeh, H.; Irani, S. Investigation of Plasma Treatment on Poly(3-hydroxybutyrate) Film Surface: Characterization and Invitro Assay. *Polymer-Plastics Technology and Engineering* **2012**, *51* (13), 1319-1326. DOI:

10.1080/03602559.2012.701365. Aflori, M. Embedding silver nanoparticles at PHB surfaces by means of combined plasma and chemical treatments. *Revue Roumaine de Chimie* **2016**, *61*, 405-409.

(212) Guarino, V.; Khodir, W. K. W. A.; Ambrosio, L. Biodegradable Microparticles and Nanoparticles by Electrospraying Techniques. *Journal of Applied Biomaterials & Functional Materials* **2012**, *10* (3), 191-196. DOI: 10.5301/jabfm.2012.10369.

(213) Guarino, V.; Altobelli, R.; Cirillo, V.; Cummaro, A.; Ambrosio, L. Additive electrospraying: A route to process electrospun scaffolds for controlled molecular release. *Polymers for Advanced Technologies* **2015**, *26* (12), 1359-1369.

(214) Hamdan, N.; Yamin, A.; Hamid, S. A.; Khodir, W. K.; Guarino, V. Functionalized Antimicrobial Nanofibers: Design Criteria and Recent Advances. *Journal of Functional Biomaterials* **2021**, *12* (4). DOI: 10.3390/jfb12040059.

(215) Arkoun, M.; Daigle, F.; Heuzey, M. C.; Ajji, A. Mechanism of Action of Electrospun Chitosan-Based Nanofibers against Meat Spoilage and Pathogenic Bacteria. *Molecules* **2017**, *22* (4). DOI: 10.3390/molecules22040585 From NLM.

(216) Shahini Shams Abadi, M.; Mirzaei, E.; Bazargani, A.; Gholipour, A.; Heidari, H.; Hadi, N. Antibacterial activity and mechanism of action of chitosan nanofibers against toxigenic Clostridioides (Clostridium) difficile Isolates. *Ann Ig* **2020**, *32* (1), 72-80. DOI: 10.7416/ai.2020.2332 From NLM.

(217) Sundaramurthi, D.; Krishnan, U. m.; Sethuraman, S. Electrospun Nanofibers as Scaffolds for Skin Tissue Engineering. *Polymer Reviews* **2014**, *54*, 348 - 376.

(218) Gupta, A.; Landis, R. F.; Rotello, V. M. Nanoparticle-Based Antimicrobials: Surface Functionality is Critical. *F1000Research* **2016**, *5*.

(219) Sengupta, I.; Bhattacharya, P.; Talukdar, M.; Neogi, S.; Pal, S. K.; Chakraborty, S. Bactericidal effect of graphene oxide and reduced graphene oxide: Influence of shape of bacteria. *Colloid and Interface Science Communications* **2019**.

(220) Gupta, A.; Mumtaz, S.; Li, C. H.; Hussain, I.; Rotello, V. M. Combatting antibiotic-resistant bacteria using nanomaterials. *Chem Soc Rev* **2019**, *48* (2), 415-427. DOI: 10.1039/c7cs00748e From NLM.

(221) Zhao, Y.; Tian, Y.; Cui, Y.; Liu, W.; Ma, W.; Jiang, X. Small molecule-capped gold nanoparticles as potent antibacterial agents that target Gram-negative bacteria. *Journal of the*

American Chemical Society **2010**, *132 35*, 12349-12356.

(222) Ang, J. Y.; Ezike, E.; Asmar, B. I. Antibacterial resistance. *Indian J Pediatr* **2004**, *71* (3), 229-239. DOI: 10.1007/bf02724275 From NLM.

(223) Ventola, C. L. The antibiotic resistance crisis: part 1: causes and threats. *P T* **2015**, *40* (4), 277-283. PubMed.

(224) Gupta, A.; Landis, R. F.; Li, C.-H.; Schnurr, M.; Das, R.; Lee, Y.-W.; Yazdani, M.; Liu, Y.; Kozlova, A.; Rotello, V. M. Engineered Polymer Nanoparticles with Unprecedented Antimicrobial Efficacy and Therapeutic Indices against Multidrug-Resistant Bacteria and Biofilms. *Journal of the American Chemical Society* **2018**, *140* (38), 12137-12143. DOI: 10.1021/jacs.8b06961.

(225) Slavin, Y. N.; Asnis, J.; Häfeli, U. O.; Bach, H. Metal nanoparticles: understanding the mechanisms behind antibacterial activity. *Journal of Nanobiotechnology* **2017**, *15* (1), 65. DOI: 10.1186/s12951-017-0308-z.

(226) Naskar, A.; Kim, K. S. Nanomaterials as Delivery Vehicles and Components of New Strategies to Combat Bacterial Infections: Advantages and Limitations. *Microorganisms* **2019**, *7* (9). DOI: 10.3390/microorganisms7090356 From NLM. Vallet-Regí, M.; González, B.; Izquierdo-Barba, I. Nanomaterials as Promising Alternative in the Infection Treatment. *Int J Mol Sci* **2019**, *20*.

(227) Grumezescu, A. M. *Engineering of Nanobiomaterials: Applications of Nanobiomaterials*; 2016. Khezerlou, A.; Alizadeh-Sani, M.; Azizi-Lalabadi, M.; Ehsani, A. Nanoparticles and their antimicrobial properties against pathogens including bacteria, fungi, parasites and viruses. *Microbial pathogenesis* **2018**, *123*, 505-526.

(228) Miller, K. P.; Wang, L.; Benicewicz, B. C.; Decho, A. W. Inorganic Nanoparticles Engineered to Attack Bacteria. *ChemInform* **2015**, *46*.

(229) Celebioglu, A.; Topuz, F.; Yildiz, Z.; Uyar, T. One-step green synthesis of antibacterial silver nanoparticles embedded in electrospun cyclodextrin nanofibers. *Carbohydrate polymers* **2019**, *207*, 471-479. Jatoi, A. W.; Kim, I. S.; Ni, Q. Q. Cellulose acetate nanofibers embedded with AgNPs anchored TiO(2) nanoparticles for long term excellent antibacterial applications. *Carbohydr Polym* **2019**, *207*, 640-649. DOI: 10.1016/j.carbpol.2018.12.029 From NLM. Phan, D.-N.; Rebia, R. A.; Saito, Y.; Kharaghani, D.; Khatri, M.; Tanaka, T.; Lee, H.; Kim, I. S. Zinc oxide nanoparticles attached to polyacrylonitrile nanofibers with hinokitiol as gluing agent for synergistic antibacterial activities and effective dye removal. *Journal of Industrial and Engineering*

Chemistry **2020**, *85*, 258-268. Sekar, A. D.; Kumar, V.; Muthukumar, H.; Gopinath, P.; Matheswaran, M. Electrospinning of Fe-doped ZnO nanoparticles incorporated polyvinyl alcohol nanofibers for its antibacterial treatment and cytotoxic studies. *European Polymer Journal* **2019**, *118*, 27-35. DOI: https://doi.org/10.1016/j.eurpolymj.2019.05.038. Tsai, Y.-H.; Yang, Y.-N.; Ho, Y.-C.; Tsai, M.-L.; Mi, F.-L. Drug release and antioxidant/antibacterial activities of silymarin-zein nanoparticle/bacterial cellulose nanofiber composite films. *Carbohydrate Polymers* **2018**, *180*, 286-296. DOI: https://doi.org/10.1016/j.carbpol.2017.09.100.

(230) Min, M.; Shi, Y.; Ma, H.; Huang, H. L.; Shi, J.; Chen, X.; Liu, Y.; Wang, L. Polymer-Nanoparticle Composites Composed of Poly(3-hydroxybutyrate-co-3-hydroxyvalerate) and Coated Silver Nanoparticles. *Journal of Macromolecular Science, Part B* **2015**, *54*, 411 - 423. Busolo, M. A.; Lagarón, J. M. Antimicrobial biocomposites of melt-compounded polylactide films containing silver-based engineered clays. *Journal of Plastic Film & Sheeting* **2013**, *29*, 290 - 305. Martínez-Abad, A.; Lagarón, J. M.; Ocio, M. J. Characterization of transparent silver loaded poly(l-lactide) films produced by melt-compounding for the sustained release of antimicrobial silver ions in food applications. *Food Control* **2014**, *43*, 238-244.

(231) Adam, S. Thermal Degradation Behavior of Poly(3 Hydroxybutyrate)/Sepiolite Nanocomposites. 2015. Fortunati, E.; Peltzer, M.; Armentano, I.; Jiménez, A.; Kenny, J. M. Combined effects of cellulose nanocrystals and silver nanoparticles on the barrier and migration properties of PLA nano-biocomposites. *Journal of Food Engineering* **2013**, *118* (1), 117-124. DOI: https://doi.org/10.1016/j.jfoodeng.2013.03.025.

(232) Yu, H.; Sun, B.; Zhang, D.; Chen, G.; Yang, X.; Yao, J. Reinforcement of biodegradable poly(3-hydroxybutyrate-co-3-hydroxyvalerate) with cellulose nanocrystal/silver nanohybrids as bifunctional nanofillers. *Journal of Materials Chemistry B* **2014**, *2* (48), 8479-8489, 10.1039/C4TB01372G. DOI: 10.1039/C4TB01372G.

(233) Castro-Mayorga, J. L.; Martínez-Abad, A.; Fabra, M. F.; Lagarón, J. M.; Ocio, M. J.; Sánchez, G. Silver-Based Antibacterial and Virucide Biopolymers. 2016.

(234) Duran, N.; Seabra, A.; Lima, R. Cytotoxicity and Genotoxicity of Biogenically Synthesized Silver Nanoparticles. 2014; pp 245-263.

(235) Liz, R. G. d.; Simard, J.-C.; Leonardi, L. B. A.; Girard, D. Silver nanoparticles rapidly induce atypical human neutrophil cell death by a process involving inflammatory caspases and reactive oxygen species and induce neutrophil extracellular traps release upon cell adhesion. *International*

immunopharmacology **2015**, *28 1*, 616-625.

(236) Składanowski, M.; Golinska, P.; Rudnicka, K.; Dahm, H.; Rai, M. Evaluation of cytotoxicity, immune compatibility and antibacterial activity of biogenic silver nanoparticles. *Med Microbiol Immunol* **2016**, *205* (6), 603-613. DOI: 10.1007/s00430-016-0477-7 From NLM.

(237) Salama, H. E.; Saad, G. R.; Sabaa, M. W. Synthesis, characterization and antimicrobial activity of biguanidinylated chitosan-g-poly[(R)-3-hydroxybutyrate]. *International journal of biological macromolecules* **2017**, *101*, 438-447.

(238) Chairuangkitti, P.; Lawanprasert, S.; Roytrakul, S.; Aueviriyavit, S.; Phummiratch, D.; Kulthong, K.; Chanvorachote, P.; Maniratanachote, R. Silver nanoparticles induce toxicity in A549 cells via ROS-dependent and ROS-independent pathways. *Toxicology in Vitro* **2013**, *27* (1), 330-338. DOI: https://doi.org/10.1016/j.tiv.2012.08.021.

(239) Munteanu, B. S.; Aytac, Z.; Pricope, G. M.; Uyar, T.; Vasile, C. Polylactic acid (PLA)/Silver-NP/VitaminE bionanocomposite electrospun nanofibers with antibacterial and antioxidant activity. *Journal of Nanoparticle Research* **2014**, *16*, 1-12.

(240) Martínez-Abad, A.; Sánchez, G.; Lagarón, J. M.; Ocio, M. J. Influence of speciation in the release profiles and antimicrobial performance of electrospun ethylene vinyl alcohol copolymer (EVOH) fibers containing ionic silver ions and silver nanoparticles. *Colloid and Polymer Science* **2012**, *291*, 1381-1392.

(241) Jeon, H. J.; Kim, J. S.; Kim, T. G.; Kim, J.-H.; Yu, W. R.; Youk, J. H. Preparation of poly(ε-caprolactone)-based polyurethane nanofibers containing silver nanoparticles. *Applied Surface Science* **2008**, *254*, 5886-5890.

(242) Rujitanaroj, P.-o.; Pimpha, N.; Supaphol, P. Preparation, characterization, and antibacterial properties of electrospun polyacrylonitrile fibrous membranes containing silver nanoparticles. *Journal of Applied Polymer Science* **2010**, *116*, 1967-1976.

(243) Jeong, S. H.; Yeo, S. Y.; Yi, S. C. The effect of filler particle size on the antibacterial properties of compounded polymer/silver fibers. *Journal of Materials Science* **2005**, *40*, 5407-5411.

(244) Chae, W.-P.; Xing, Z.-C.; Kim, Y. J.; Sang, H.-S.; Huh, M.-w.; Kang, I. K. Fabrication and Biocompatibility of Rutin-containing PHBV Nanofibrous Scaffolds. *Polymer-korea* **2011**, *35*, 210-215. Min, M.; Shi, Y. Y.; Chen, X. X.; Shi, J.; Ma, H.; Huang, H. L.; Wang, L. Preparation and Characteristics of Electrospun Silver-Containing PHBV Ultrafine Fiber. *Applied Mechanics and*

Materials **2014**, *548-549*, 34 - 37.

(245) Fei, P.; Shi, Y.; Zhou, M.; Cai, J.; Tang, S.; Xiong, H. Effects of nano-TiO2 on the properties and structures of starch/poly(ε-caprolactone) composites. *Journal of Applied Polymer Science* **2013**, *130*, 4129-4136. Mirjalili, B. B. F.; Bamoniri, A.; Akbari, A.; Taghavinia, N. Nano-TiO2: An eco-friendly and re-usable catalyst for the synthesis of 14-Aryl or alkyl-14H-dibenzo[a,j]xanthenes. *Journal of the Iranian Chemical Society* **2011**, *8*, S129-S134.

(246) Maurya, A.; Chauhan, P. Synthesis and characterization of sol–gel derived PVA-titanium dioxide (TiO2) nanocomposite. *Polymer Bulletin* **2011**, *68*, 961-972. Chou, P. M.; Mariatti, M.; Zulkifli, A.; Sreekantan, S. Evaluation of the flexural properties and bioactivity of bioresorbable PLLA/PBSL/CNT and PLLA/PBSL/TiO2 nanocomposites. *Composites Part B: Engineering* **2012**, *43* (3), 1374-1381. DOI: https://doi.org/10.1016/j.compositesb.2011.11.023. Shi, H.; Magaye, R.; Castranova, V.; Zhao, J. Titanium dioxide nanoparticles: a review of current toxicological data. *Part Fibre Toxicol* **2013**, *10*, 15. DOI: 10.1186/1743-8977-10-15 From NLM.

(247) Zolfi, M.; Khodaiyan, F.; Mousavi, M.; Hashemi, M. Development and characterization of the kefiran-whey protein isolate-TiO2 nanocomposite films. *International journal of biological macromolecules* **2014**, *65*, 340-345.

(248) O'Regan, B. C.; Grätzel, M. A low-cost, high-efficiency solar cell based on dye-sensitized colloidal TiO2 films. *Nature* **1991**, *353*, 737-740.

(249) Wood, A.; Giersig, M.; Mulvaney, P. Fermi Level Equilibration in Quantum Dot−Metal Nanojunctions†. *Journal of Physical Chemistry B* **2001**, *105*, 8810-8815.

(250) Tada, H.; Ishida, T.; Takao, A.; Ito, S. Drastic enhancement of TiO2-photocatalyzed reduction of nitrobenzene by loading Ag clusters. *Langmuir : the ACS journal of surfaces and colloids* **2004**, *20 19*, 7898-7900.

(251) Mofokeng, J. P.; Luyt, A. S. Morphology and thermal degradation studies of melt-mixed PLA/PHBV biodegradable polymer blend nanocomposites with TiO2 as filler. *Journal of Applied Polymer Science* **2015**, *132*.

(252) Josset, S.; Keller, N.; Lett, M. C.; Ledoux, M. J.; Keller, V. Numeration Methods for Targeting Photoactive Materials in the UV-A Photocatalytic Removal of Microorganisms. *ChemInform* **2008**, *39*.

(253) Kubacka, A.; Diez, M. S.; Rojo, D.; Bargiela, R.; Ciordia, S.; Zapico, I.; Albar, J. P.; Barbas, C.; Martins dos Santos, V. A. P.; Fernández-García, M.; et al. Understanding the antimicrobial

mechanism of TiO2-based nanocomposite films in a pathogenic bacterium. *Scientific Reports* **2014**, *4* (1), 4134. DOI: 10.1038/srep04134.

(254) Hamming, L. M.; Qiao, R.; Messersmith, P. B.; Catherine Brinson, L. Effects of dispersion and interfacial modification on the macroscale properties of TiO2 polymer–matrix nanocomposites. *Composites Science and Technology* **2009**, *69* (11), 1880-1886. DOI: https://doi.org/10.1016/j.compscitech.2009.04.005. Luan, J.; Wang, S.; Hu, Z.; Zhang, L. Synthesis Techniques, Properties and Applications of Polymer Nanocomposites. *Current Organic Synthesis* **2012**, *9*, 114-136. Kubacka, A.; Ferrer, M.; Cerrada, M.; Serrano, C.; Nchez-Chaves, M.; Fernández-García, M.; Andre, A.; Jiménez Riobóo, R.; Ndez-Martín, F.; Fernández-García, M. Boosting TiO2-anatase antimicrobial activity: Polymer-oxide thin films. *Applied Catalysis B Environmental* **2009**, *89*, 441-449. DOI: 10.1016/j.apcatb.2009.01.002. Kubacka, A.; Ferrer, M.; Fernández-García, M. Kinetics of photocatalytic disinfection in TiO2-containing polymer thin films: UV and visible light performances. *Applied Catalysis B-environmental* **2012**, *121*, 230-238.

(255) Matsunaga, T.; Tomoda, R.; Nakajima, T.; Wake, H. Photoelectrochemical sterilization of microbial cells by semiconductor powders. *Fems Microbiology Letters* **1985**, *29*, 211-214.

(256) Foster, H. A.; Ditta, I. B.; Varghese, S.; Steele, A. Photocatalytic disinfection using titanium dioxide: spectrum and mechanism of antimicrobial activity. *Appl Microbiol Biotechnol* **2011**, *90* (6), 1847-1868. DOI: 10.1007/s00253-011-3213-7 From NLM. Alrousan, D.; Polo-López, M. I.; Dunlop, P. S. M.; Fernández-Ibáñez, P.; Byrne, J. A. Solar photocatalytic disinfection of water with immobilised titanium dioxide in re-circulating flow CPC reactors. *Applied Catalysis B-environmental* **2012**, *128*, 126-134.

(257) Mukherjee, A.; I, M.; Tc, P.; Chandrasekaran, N. Antimicrobial activity of aluminium oxide nanoparticles for potential clinical applications. Vol. 1; 2011; pp 245-251.

(258) Allahverdiyev, A. M.; Abamor, E. S.; Bagirova, M.; Rafailovich, M. Antimicrobial effects of TiO(2) and Ag(2)O nanoparticles against drug-resistant bacteria and leishmania parasites. *Future Microbiol* **2011**, *6* (8), 933-940. DOI: 10.2217/fmb.11.78 From NLM.

(259) Cho, M.; Chung, H.; Choi, W.; Yoon, J. Linear correlation between inactivation of E. coli and OH radical concentration in TiO2 photocatalytic disinfection. *Water Res* **2004**, *38* (4), 1069-1077. DOI: 10.1016/j.watres.2003.10.029 From NLM.

(260) Haider, A.; Jameel, Z. N.; Al-Hussaini, I. Review on: Titanium Dioxide Applications. *Energy Procedia* **2019**, *157*, 17-29. DOI: 10.1016/j.egypro.2018.11.159.

(261) Alrousan, D. M. A.; Dunlop, P. S. M.; McMurray, T. A.; Byrne, J. A. Photocatalytic inactivation of E. coli in surface water using immobilised nanoparticle TiO2 films. *Water Research* **2009**, *43* (1), 47-54. DOI: https://doi.org/10.1016/j.watres.2008.10.015. Brunet, L.; Lyon, D. Y.; Hotze, E. M.; Alvarez, P. J. J.; Wiesner, M. R. Comparative Photoactivity and Antibacterial Properties of C60 Fullerenes and Titanium Dioxide Nanoparticles. *Environmental Science & Technology* **2009**, *43* (12), 4355-4360. DOI: 10.1021/es803093t.

(262) Mitoraj, D.; Jańczyk, A.; Strus, M.; Kisch, H.; Stochel, G.; Heczko, P. B.; Macyk, W. Visible light inactivation of bacteria and fungi by modified titanium dioxide. *Photochemical & Photobiological Sciences* **2007**, *6* (6), 642-648, 10.1039/B617043A. DOI: 10.1039/B617043A. Cabeen, M. T.; Jacobs-Wagner, C. Bacterial cell shape. *Nature Reviews Microbiology* **2005**, *3* (8), 601-610. DOI: 10.1038/nrmicro1205.

(263) Roberts, I. S. THE BIOCHEMISTRY AND GENETICS OF CAPSULAR POLYSACCHARIDE PRODUCTION IN BACTERIA. *Annu. Rev. Microbiol.* **1996**, *50* (1), 285-315. DOI: 10.1146/annurev.micro.50.1.285.

(264) Scott, J. R.; Barnett, T. C. Surface Proteins of Gram-Positive Bacteria and How They Get There. *Annu. Rev. Microbiol.* **2006**, *60* (1), 397-423. DOI: 10.1146/annurev.micro.60.080805.142256.

(265) Shi, J.; Li, J.; Wang, Y.; Yang Zhang, C. TiO2-based Nanosystem for Cancer Therapy and Antimicrobial Treatment: A Review. *Chemical Engineering Journal* **2021**.

(266) Lee, K.; Lee, S. Multifunctionality of poly(vinyl alcohol) nanofiber webs containing titanium dioxide. *Journal of Applied Polymer Science* **2012**, *124* (5), 4038-4046. DOI: https://doi.org/10.1002/app.34929.

(267) Korina, E.; Stoilova, O.; Manolova, N.; Rashkov, I. Polymer fibers with magnetic core decorated with titanium dioxide prospective for photocatalytic water treatment. *Journal of environmental chemical engineering* **2018**, *6*, 2075-2084.

(268) Korina, E.; Stoilova, O.; Manolova, N.; Rashkov, I. Multifunctional Hybrid Materials From Poly(3-Hydroxybutyrate), TiO 2 Nanoparticles, and Chitosan Oligomers by Combining Electrospinning/Electrospraying and Impregnation. *Macromolecular bioscience* **2013**, *13*. DOI: 10.1002/mabi.201200410.

(269) Braga, N. F.; Vital, D. A.; Guerrini, L. M.; Lemes, A. P.; Formaggio, D. M. D.; Tada, D. B.; Arantes, T. M.; Cristovan, F. H. PHBV-TiO(2) mats prepared by electrospinning technique:

Physico-chemical properties and cytocompatibility. *Biopolymers* **2018**, *109* (5), e23120. DOI: 10.1002/bip.23120 From NLM.

(270) Yew, S.-P.; Tang, H. Y.; Sudesh, K. Photocatalytic activity and biodegradation of polyhydroxybutyrate films containing titanium dioxide. *Polymer Degradation and Stability* **2006**, *91*, 1800-1807.

(271) Zablotsky, D.; Segal, I.; Zablotskaya, A.; Mairov, M.; Nguyen, T. A. Antimicrobial activity of hybrid organic–inorganic core–shell magnetic nanocomposites. 2021; pp 501-527.

(272) Nguyen Tri, P.; Nguyen, T. A.; Nguyen, T. H.; Carriere, P. Chapter 7 - Antibacterial Behavior of Hybrid Nanoparticles. In *Noble Metal-Metal Oxide Hybrid Nanoparticles*, Mohapatra, S., Nguyen, T. A., Nguyen-Tri, P. Eds.; Woodhead Publishing, 2019; pp 141-155.

(273) Wang, Z.; Wang, X.; Wang, Y.; Zhu, Y.; Liu, X.; Zhou, Q. NanoZnO-modified titanium implants for enhanced anti-bacterial activity, osteogenesis and corrosion resistance. *J Nanobiotechnology* **2021**, *19* (1), 353. DOI: 10.1186/s12951-021-01099-6 From NLM.

(274) Jaworek, A.; Krupa, A.; Lackowski, M.; Sobczyk, A. T.; Czech, T.; Ramakrishna, S.; Sundarrajan, S.; Pliszka, D. Nanocomposite fabric formation by electrospinning and electrospraying technologies. *Journal of Electrostatics* **2009**, *67* (2), 435-438. DOI: https://doi.org/10.1016/j.elstat.2008.12.019.

(275) Korina, E.; Stoilova, O.; Manolova, N.; Rashkov, I. Multifunctional Hybrid Materials From Poly(3-Hydroxybutyrate), TiO2 Nanoparticles, and Chitosan Oligomers by Combining Electrospinning/Electrospraying and Impregnation. *Macromolecular Bioscience* **2013**, *13* (6), 707-716. DOI: https://doi.org/10.1002/mabi.201200410.

List of publications and presentations

Publications

12. **Safa Ladhari**, N.N.Vu, J. Vallée Bastien, B.V. Tran, T.H. Nguyen, A. Saidia, S. Barnabe, and P. Nguyen-tri, "*Mechanical and antimicrobial properties of green and photoactive $AgTiO_2$/ polyhydroxybutyrate (PHB) electrospun membranes*" in press, Polymer Engineering & Science, 2024

11. **Safa Ladhari**, N.N.Vu, A. Saidia, A.A. Assadi, and P. Nguyen-tri, "*A green synthesis route of ZnO/polyhydroxybutyrate composites with antibacterial and biodegradable properties*" in press, Polymer Engineering & Science, 2024

10. C. Boisvert, N.N. Vu, **Safa Ladhari**, M.A. Polinarski, F. Brouillette and P. Nguyen-Tri, "*Preparation of Cotton Coated with ZnO-Ag Hybrid NPs for Photocatalytic Inactivation of Bacteria Under LED Light*", Springer Nature Switzerland; 2024.

9. C. Venne, N.N. Vu, **Safa Ladhari** and P. Nguyen-Tri, "*Innovations in Textile Technology Against Pathogenic Threats: A Review of the Recent Literature*", Springer Nature Switzerland; 2024.

8. J. Vallée-Bastien, B.V. Tran, **Safa Ladhari**, N.N. Vu and P. Nguyen-Tri, "*Synthesis of Antimicrobial and Biodegradable Polyhydroxybutyrate Films Embedded with Zinc Oxide NPs by Casting Method*", Springer Nature Switzerland; 2024.

7. M.A. Polinarski, N.N. Vu, **Safa Ladhari**, C. Boisvert, S. Barnabé, J.B. Wenzel, H.J. Alves and Phuong Nguyen-Tri, "In-situ growth of Ag nanoparticles embedded in chitosan coating for potent antimicrobial activity", Materials Today Communications; 2024.

6. **Safa Ladhari**, N.N. Vu, C. Boisvert, M.A. Polinarski, C.Venne, A. Saidi, S, Barnabe, and P. Nguyen-Tri, "*Biodegradable polyhydroxybutyrate microfiber membranes decorated with Ag-TiO_2 nanoparticles for enhanced antibacterial and anti-biofouling activities*", Journal of Applied Polymer Science, 2024.

5. **Safa Ladhari**, N.N. Vu, C. Boisvert, A. Saidi, and P. Nguyen-Tri "*Recent Development of Polyhydroxyalkanoates (PHA)-Based Materials for Antibacterial Applications: A Review*", ACS Applied Bio Materials, 2023.

4. C. Venne, N.N. Vu, **Safa Ladhari**, A. Saidi, S. Barnabe, P. Nguyen-Tri, "*One-pot preparation of superhydrophobic polydimethylsiloxane-coated cotton via water/oil/water emulsion approach for enhanced resistance to chemical and bacterial adhesion*", Progress in Organic Coatings, 2023.

3. N.N. Vu, C. Venne, **Safa Ladhari**, A. Saidi, L. Moskovchenko, T. Lai, Y. Xiao, S. Barnabe, B. Barbeau and P. Nguyen-Tri, "*Rapid assessment of biological activity of Ag-based antiviral coatings for the treatment of textile fabrics used in protective equipment against coronavirus*". ACS Applied Bio Materials, 2022.

2. A. Saidi, C. Gauvin, **Safa Ladhari** and P. Nguyen-Tri, "*Advanced Functional Materials for Intelligent Thermoregulation in Personal Protective Equipment*", Polymers, 2021.

1. K. Raja, P. Nguyen-Tri, G. Balasubramani, A. Alagarsamy, S. Hazir, **S. Ladhari**, S. Rtimi, A. Saidi, A. Pugazhendhi, "*SARS-CoV-2 and its new variants: a comprehensive review on nanotechnological application insights into potential approaches*", Applied Nanoscience, 2021

Presentations

7. **Safa Ladhari**, A. Saidi, and P. Nguyen-Tri, "*Synthesis of antimicrobial and biodegradable electrospun Polyhydroxybutyrate films coated with $AgTiO_2$ nanoparticles for personal protective equipment*", **Poster presentation**, CQMF **2023**, UQTR, Canada. **(4th price).**

6. **Safa Ladhari**, A. Saidi, and P. Nguyen-Tri, "*Synthesis of antimicrobial and biodegradable electrospun Polyhydroxybutyrate films coated with $AgTiO_2$ nanoparticles for personal protective equipment*", **Poster presentation,** CREPEC **2023**, Université ETS, Canada.

5. J. Vallée-Bastien, B.V. Tran, **Safa Ladhari**, N.N. Vu and P. Nguyen-Tri, "*Préparation de films de polyhydroxybutyrate (PHB) incorporant des nanoparticules de ZnO synthétiques vertes pour des activités antibactériennes puissantes*", **Poster presentation,** CREPEC **2023,** Université ETS, Canada. **(2nd price).**

4. **Safa Ladhari**, A. Saidi, and P. Nguyen-Tri, "*Évaluation de l'activité biologique des nouveaux matériaux textile antimicrobiens et biodégradables pour les équipements de protection*", M2EBA **2023**, online. **Price: Best presentation of the conference.**

3. **Safa Ladhari**, A. Saidi, and P. Nguyen-Tri, "*Évaluation de l'activité biologique des nouveaux matériaux textile antimicrobiens et biodégradables pour les équipements de protection*", M2EBA **2022**, online.

2. **Safa Ladhari**, A. Saidi, and P. Nguyen-Tri, "*Évaluation de l'activité biologique des nouveaux matériaux textile antimicrobiens et biodégradables pour les équipements de protection*", **2022** ACFAS Congrès, online.

1. **Safa Ladhari**, A. Saidi, and P. Nguyen-Tri, "*Antiviral and biodegradable nonwoven textiles for the protection against SARS-CoV-2 (COVID-19)*", M.I.S.S Duong Lab **2022**, online, **Poster presentation**, **(2nd price).**

Other activities

- UQTR Student delegate on the Graduate Program Committee for Physics, Energy, and Materials Sciences (CPCS-PSEM) for **2023-2024**.

- Analytical chemistry lecturer at UQTR, **September-December 2023**

- UQTR student delegate on research center for high-performance polymer and composite systems (CREPEC) for **2022-2024**.